



**AALBORG UNIVERSITY**  
DENMARK

**Aalborg Universitet**

## **Numerical Modelling Approaches for Sediment Transport in Sewer Systems**

Mark, Ole

*Publication date:*  
1995

*Document Version*  
Publisher's PDF, also known as Version of record

[Link to publication from Aalborg University](#)

*Citation for published version (APA):*

Mark, O. (1995). *Numerical Modelling Approaches for Sediment Transport in Sewer Systems*. The Hydraulics and Coastal Engineering Group, Dept. of Civil Engineering, Aalborg University. Series paper No. 10

### **General rights**

Copyright and moral rights for the publications made accessible in the public portal are retained by the authors and/or other copyright owners and it is a condition of accessing publications that users recognise and abide by the legal requirements associated with these rights.

- ? Users may download and print one copy of any publication from the public portal for the purpose of private study or research.
- ? You may not further distribute the material or use it for any profit-making activity or commercial gain
- ? You may freely distribute the URL identifying the publication in the public portal ?

### **Take down policy**

If you believe that this document breaches copyright please contact us at [vbn@aub.aau.dk](mailto:vbn@aub.aau.dk) providing details, and we will remove access to the work immediately and investigate your claim.

Hydraulics & Coastal Engineering Laboratory  
Department of Civil Engineering  
Aalborg University  
Sohngaardsholmsvej 57  
DK-9000 Aalborg, Denmark

ISSN 0909-4296  
Series Paper No. 10

---

NUMERICAL MODELLING APPROACHES  
FOR SEDIMENT TRANSPORT  
IN SEWER SYSTEMS

by

OLE MARK

May 1995

## PREFACE

This thesis is submitted as part of a Nordic Industrial Foundation research study and as part of the requirements for the degree of Ph.D. The thesis together with a Technical Reference Manual: "MOUSE TRAP Technical Reference Version 1.00", and a User Manual: "MOUSE TRAP User Manual Version 1.00", constitute the basis for the defence of the Ph.D.

The outcome of the Ph.D. study is the present Ph.D thesis, seven scientific papers and a mathematical modelling system for the transport of sediments and dissolved matter on the surface of the catchment and in sewer systems with a User Manual and a Technical Reference Manual. The specifications for the surface model were derived in cooperation with the MOUSE TRAP project, where especially Dr. Gilbert Svensson, Chalmers University of Technology made a large contribution. The modelling system is the first deterministic system for the transport processes in sewers. As the complete modelling system itself is quite large and complex and data are not available for validation of large parts of the system, this thesis deals with only some of the modelling aspects of the sediment transport processes in sewer systems, ie:

- a description of the transport processes in sewer systems
- an evaluation of the applicability of the existing sediment transport formulations for rivers to the sediment transport processes in sewer systems
- an evaluation of the applicability of the advection-dispersion equations to the description of the transport of dissolved matter and sediments transported in the mode of wash load in sewer systems

The Ph.D study has been carried out at the Department of Civil Engineering, Aalborg University, Denmark and VBB-Viak, Sweden. The study is funded by the Nordic Industrial Foundation and the Swedish Water and Waste Water Works Association. The study was guided by Prof. Torben Larsen, Aalborg University, Denmark, Dr. Johan Larsson, VBB-Viak, Sweden, Dr. Sven Lyngfelt, Chalmers University of Technology, Sweden and Dr. Kim Wium Olesen, Danish Hydraulic Institute, Denmark.

I would like to thank my supervisors together with Chief Engineer Karsten Havnø and Henrik Garsdal, Danish Hydraulic Institute for many fruitful discussions on the topic. I would also like to thank the Nordic Industrial Foundation and the Swedish Water and Waste Water Works Association for the financial support of the study. Comments on the text by Dr. Gustavo Perrusquía, Chalmers University of Technology were very useful. Finally my sincerest thanks to Sarah Brierley and Birgitte Helwich for the proofreading.

May 1995

  
Ole Mark

# CONTENTS

## LIST OF SYMBOLS

## ABSTRACT

## SAMMENFATNING

## SAMMANFATTNING

<b>1</b>	<b>INTRODUCTION</b> .....	<b>1-1</b>
<b>2</b>	<b>GOALS AND OBJECTIVES</b> .....	<b>2-1</b>
<b>3</b>	<b>SUMMARY OF DEVELOPED MATHEMATICAL MODELS</b> .....	<b>3-1</b>
3.1	The Surface Model .....	3-2
3.1.1	Accumulation of Particles on the Catchment .....	3-2
3.1.2	Wash-off of Particles by Rainfall .....	3-2
3.1.3	The Gully Pot Module .....	3-3
3.2	The Advection-Dispersion Model .....	3-3
3.3	The Sediment Transport Models .....	3-3
3.3.1	The Non-Cohesive Sediment Transport Model .....	3-4
3.3.2	The Sediment Transport Model based on the Advection-Dispersion Equations	3-4
3.4	Verification of the Modelling System .....	3-5
3.5	Validation of the Modelling System .....	3-5
3.6	Examples of Application of the Modelling System .....	3-5
<b>4</b>	<b>A QUALITATIVE DISCUSSION OF THE TRANSPORT PROCESSES IN SEWERS</b> .....	<b>4-1</b>
4.1	Classification and Characteristics of Sediments in Sewers .....	4-1
4.2	The Sources of Sediments in Sewer Systems .....	4-2
4.3	The Sources of Dissolved Substances in Sewer Systems .....	4-3
4.3.1	Dissolved Substances in the Surface Runoff .....	4-3
4.3.2	Build up of Dissolved Substances in Gully Pots .....	4-3
4.3.3	Infiltration into the Sewer System .....	4-4
4.3.4	Waste water .....	4-4
4.4	The Characteristics of Sediment Transport in Sewers .....	4-4
4.4.1	Sediment Transport with Limited Supply of Sediments .....	4-5
4.4.2	The First Foul Flush .....	4-5
4.4.3	The Mode of Sediment Transport in Sewer Systems .....	4-6
4.4.4	The Bed Load Transport .....	4-7

4.4.5	The Suspended Load Transport . . . . .	4-7
4.4.6	The Wash Load Transport . . . . .	4-8
4.5	Transport Mechanics of Sediments in Sewers . . . . .	4-8
4.5.1	The Critical Bed Shear Stress for Non-Cohesive Sediment . . . . .	4-8
4.5.2	The Critical Bed Shear Stress for Non-Uniform Non-Cohesive Sediment . . . . .	4-9
4.5.3	The Critical Bed Shear Stress for a Pipe without Sediment Deposits . . . . .	4-9
4.5.4	The Critical Bed Shear Stress for Adhesive Sediment . . . . .	4-10
4.5.5	Erosion and Deposition of Sediment in Sewers . . . . .	4-10
4.5.6	Sediment Transport in Ancillary Structures . . . . .	4-11
<b>5</b>	<b>FLOW RESISTANCE IN SEWERS . . . . .</b>	<b>5-1</b>
5.1	Description of the Shear Stress in Sewers . . . . .	5-1
5.1.1	The Side Wall Elimination . . . . .	5-2
5.1.2	Verification of the Side Wall Elimination . . . . .	5-2
5.2	Comparison of Predicted Bed Resistance with Measured Data . . . . .	5-5
5.2.1	The Ackers-White Model . . . . .	5-6
5.2.2	The Engelund-Hansen Model . . . . .	5-7
5.2.3	The Engelund-Fredsøe Model . . . . .	5-8
5.2.4	The van Rijn Model . . . . .	5-10
5.3	Comments on the Prediction of the Bed Shear Stress . . . . .	5-13
<b>6</b>	<b>SEDIMENT TRANSPORT IN SEWERS . . . . .</b>	<b>6-1</b>
6.1	Selection of a Sediment Transport Formula for Sewers . . . . .	6-1
6.1.1	The Bed Load Mode of Transport . . . . .	6-2
6.1.2	The Suspended Load Mode of Transport . . . . .	6-3
6.1.3	The Wash Load Mode of Transport . . . . .	6-7
6.2	Comparison of Predicted Sediment Transport Rates with Measured Data . . . . .	6-9
6.2.1	Characteristics of the Sediment Transport Formulae . . . . .	6-11
6.2.2	The Ackers-White Theory . . . . .	6-13
6.2.3	The Engelund-Hansen Theory . . . . .	6-15
6.2.4	The Engelund-Fredsøe Theory . . . . .	6-18
6.2.5	The van Rijn Theory . . . . .	6-21
6.3	Comments on the Performance of the Sediment Transport Formulae . . . . .	6-23
<b>7</b>	<b>A DISCUSSION OF THE ADVECTION-DISPERSION MODEL . . . . .</b>	<b>7-1</b>
7.1	The Applicability of the Advection-Dispersion Scheme to Sewers . . . . .	7-1
7.1.1	The Continuity Equation for the Transport of Dissolved Substances . . . . .	7-2
7.1.2	The Advection-Dispersion Equation . . . . .	7-2
7.1.3	Dispersion in Sewer Systems . . . . .	7-3
7.1.4	Solution of the Advection-Dispersion Equation at Structures and Manholes . . . . .	7-4
7.2	The Advection-Dispersion Scheme . . . . .	7-7
7.2.1	The Accuracy of the Numerical Scheme . . . . .	7-9

7.3	Test of the Applicability of the Advection-Dispersion Scheme to Sewers . .	7-11
7.3.1	Test of Propagation for Pure Advection with a Courant number = 1.0 . . .	7-11
7.3.2	Propagation Test for Pure Advection through a Single Pipe . . . . .	7-14
7.3.3	Propagation Test for Pure Advection through Multiple Pipes . . . . .	7-16
7.3.4	Verification of the Mass Balance . . . . .	7-17
7.3.5	Mass Balance Test for a Peak routed through Multiple Pipes . . . . .	7-19
7.3.6	Mixing Test for three Pipes flowing into a Manhole . . . . .	7-19
7.4	Summary of the Test of the Applicability of the Advection-Dispersion Scheme to Sewers . . . . .	7-21
<b>8</b>	<b>DESCRIPTION OF THE SEDIMENT TRANSPORT MODELS . . . . .</b>	<b>8-1</b>
8.1	Modelling of Non-Cohesive Sediments in Sewers . . . . .	8-1
8.1.1	Sediment Transport at Structures . . . . .	8-1
8.1.2	Sediment Transport through a Pump . . . . .	8-5
8.2	Special Formulations for Modelling of Sediment Transport in Sewers . . . . .	8-5
8.2.1	The Critical Bed Shear Stress for Non-Uniform Non-Cohesive Sediments . . .	8-5
8.2.2	The Critical Bed Shear Stress for a Pipe with Negligible Sediment Deposits .	8-6
8.2.3	The Critical Bed Shear Stress for a Pipe with a Thin Layer of Sediment . . . .	8-6
8.2.4	The Critical Bed Shear Stress for Adhesive Sediments . . . . .	8-6
8.2.5	The Sediment Transport in a Pipe without Sediment Deposits . . . . .	8-7
8.2.6	Sediment Transport in Pipes with a Thin Layer of Sediment . . . . .	8-8
8.3	The Non-Cohesive Sediment Transport Scheme . . . . .	8-9
8.3.1	Characteristics of the Non-Cohesive Sediment Transport Scheme . . . . .	8-10
8.3.2	The Boundary Conditions for the Continuity Equation for Bed Sediment . . .	8-12
8.3.3	The Stability of the Preissmann Scheme Applied to the Continuity Equation for Bed Sediment . . . . .	8-12
8.4	Test of the Applicability of the Sediment Transport Scheme to Sewers . . . .	8-16
8.4.1	Test of Sediment Transport Formulae . . . . .	8-16
8.4.2	Test of the Mass Balance for Non-Cohesive Sediment . . . . .	8-17
8.4.3	Test of the Interaction between the Hydrodynamic Model and the Sediment transport Model . . . . .	8-18
8.4.4	Propagation Test for a Sand Wave . . . . .	8-18
8.5	Summary of Modelling of Non-Cohesive Sediments in Sewers . . . . .	8-22
<b>9</b>	<b>AN EXAMPLE OF AN APPLICATION OF THE ADVECTION-DISPERSION MODEL . . . . .</b>	<b>9-1</b>
9.1	Application of the Advection-Dispersion Model . . . . .	9-1
9.2	The Dispersion Processes in Sewer Systems. . . . .	9-4
9.3	The Dispersion from Manholes. . . . .	9-5

<b>10</b>	<b>AN EXAMPLE OF AN APPLICATION OF THE SEDIMENT TRANSPORT MODEL</b> .....	10-1
10.1	The Rya catchment, Gothenburg, Sweden .....	10-1
10.2	The Ljubljana catchment, Slovenia .....	10-8
10.2.1	Evaluation of the Erosion/Deposition Pattern in the A2 Collector .....	10-10
10.2.1	Simulation of the Development of the Sediment Deposits with an Initial Sediment Depth of 1 cm and no Sediment Supply .....	10-10
10.2.3	Prediction of Locations with Sediment Deposits in the Ljubljana Sewer System .....	10-13
10.2.4	Simulation of the Development of the Sediment Deposits without any Initial Sediment Deposits and a Time Varying Sediment Supply .....	10-10
10.2.5	Effects From Sediment Deposits on the Hydraulic Capacity of the Ljubljana Sewer System .....	10-16
<b>11</b>	<b>CONCLUSION</b> .....	11-1
11.1	Summary of Goals and Objectives .....	11-1
11.2	The Selected Modelling Approach .....	11-1
11.3	Résumé of Results Achieved .....	11-2
11.3.1	The Hydraulic Capacity of Pipes with Sediment Deposits .....	11-2
11.3.2	The Bed Shear Stress .....	11-2
11.3.3	The Sediment Transport .....	11-3
11.3.4	Application of the Advection-Dispersion Model .....	11-5
11.3.5	Application of the Sediment Transport Model .....	11-5
11.3.6	Verification of the Modelling System .....	11-6
11.4	Recommendations for further Work .....	11-6
11.4.1	The Bed Shear Stress .....	11-6
11.4.2	The Sediment Transport .....	11-7
11.4.3	Basins, Structures and Pumps .....	11-7
<b>12</b>	<b>REFERENCES</b> .....	12-1

**APPENDICES**

**APPENDIX A VERIFICATION OF THE SEDIMENT PROCESSES IN THE SURFACE MODEL . . . . . A-1**

**APPENDIX B VERIFICATION OF THE TRANSPORT PROCESSES IN THE ADVECTION-DISPERSION MODEL . . . . . B-1**

**APPENDIX C VERIFICATION OF THE SEDIMENT TRANSPORT PROCESSES IN THE SEDIMENT TRANSPORT MODEL . . . . . C-1**

**APPENDIX D SENSITIVITY ANALYSIS OF THE INFLUENCE OF THE CRITERION FOR THE INITIATION OF MOTION ON THE SEDIMENT TRANSPORT . . . . . D-1**



## LIST OF SYMBOLS

a	thickness of the bed layer,
A	flow area,
A	critical flow mobility number in Ackers and White model,
$A_s$	fraction of surface area covered with sediment,
c	concentration, arbitrary unit,
c1	constant in equation (6.4),
$c_a$	reference concentration for the van Rijn formula,
$c_b$	concentration of suspended sediment at the bed,
C	model parameter in the Ackers and White Model,
C	the Chezy coefficient,
CN	concentration in a node,
$C_r$	Courant number,
$C_{rb}$	Courant number for the sediment transport,
$C_s$	source/sink concentration
d	grain diameter,
$d_i$	representative grain size in class i,
$d_{med}$	representative grain size of total population,
$d_n$	grain diameter for which n% of the sample is finer,
dx	distance between two grid points,
D	pipe diameter,
D	dispersion coefficient,
$D_{gr}$	dimensionless grain diameter,
$D_r$	coefficient for rainfall generated detachment,
$D_*$	particle number,
E	sediment trap efficiency,
f	friction factor,
F	Froude number,
F	factor for the suspended load in the van Rijn formula,
$F_D$	drag force,
$F_{gr}$	general mobility parameter,
g	acceleration due to gravity ( $9.81 \text{ m/s}^2$ ),
$G_{gr}$	general transport parameter,
i	time step,
$i_r$	rainfall intensity,
$i_d$	rainfall intensity constant (25.4 mm/h),
I	slope of the energy line,
j	grid point number,
k	the wave number,
k1	calibration constant, Equation (8-3),
k2	calibration constant, Equation (8-3),
kk	number of connecting pipes,
$k_s$	equivalent sand roughness,
$k_x$	dimensionless dispersion coefficient,

K	linear decay coefficient,
K	dimensionless variable, Equation (8-2),
K <sub>i</sub>	calibration constant, Equation (8-1),
K <sub>N</sub>	linear decay coefficient for a node,
L	length of the catchment,
m	model parameter in Ackers and White model,
M	mass,
M	Manning number,
M <sub>bed</sub>	Manning number for the sediment bed ,
M <sub>pipe</sub>	Manning number for the pipe,
n	time level,
n	model parameter in Ackers and White model,
n	calibration factor for basins,
n <sub>i</sub>	calibration constant, Equation (8-1),
p	the wet perimeter,
p	probability for particles to move,
Pe	Peclet number,
q	flow discharge per unit width,
q <sub>s</sub>	suspended sediment transport,
Q	flow discharge,
Q <sub>full</sub>	flow discharge of full running pipe,
Q <sub>pipe</sub>	flow discharge in a pipe,
r	constant in Table 6.1,
R	hydraulic radius,
R <sub>b</sub>	hydraulic radius related to the bed,
s	relative density of sediment,
s <sub>n</sub> <sup>j</sup>	is the sediment transport rate per unit width,
S	sediment transport,
t	time,
t	thickness of the sediment bed,
T	transport rate,
u	mean flow velocity,
u <sub>r</sub>	friction velocity,
V <sub>fine particles</sub>	average transport velocity of the fine sediment particles, (m/s)
V	volume,
V <sub>N</sub>	volume of a node,
V <sub>sr</sub>	sediment volume detached by the rain per unit of time,
w	fall velocity,
W	width of the flow,
W	width of the catchment,
x	coordinate in flow direction,
X	sediment transport, mass flux per unit mass flow rate,
y	distance above bed level,
Y	water depth,
Z	the Rouse number,
$\alpha$	ratio between suspended transport in a open channel and suspended transport in a full running a pipe,
$\beta$	factor for the non-uniform distribution of the flow over the depth, equation (6-7),

$\beta$	dynamic friction coefficient, Appendix C,
$\epsilon$	is the porosity of the sediment,
$\epsilon_s$	sediment diffusion coefficient,
$\psi$	space centring coefficient ( $0.5 \leq \psi \leq 1$ ),
$\kappa$	von Karman constant, ( $\kappa \approx 0.41$ ),
$\lambda_b$	linear concentration related to $c_b$ ,
$\nu$	kinematic viscosity,
$\rho$	fluid density,
$\theta$	dimensionless bed shear stress,
$\theta_c$	critical dimensionless bed shear stress,
$\theta_{ci}$	critical dimensionless bed shear stress for class i,
$\theta_{bot}$	critical dimensionless bed shear stress at the bottom of the sediment bed,
$\theta_{top}$	critical dimensionless bed shear stress at the top of the sediment bed,
$\theta'$	dimensionless skin friction,
$\theta''$	dimensionless form friction,
$\theta$	time centring coefficient ( $0.5 \leq \theta \leq 1$ ),
$\tau$	bed shear stress,
$\tau_c$	critical bed shear stress,
$\tau'$	skin friction,
$\tau''$	form drag,
$\gamma$	specific gravity of water,
$\mu$	dimensionless variable, Equation (8-2),
$\mu_1$	calibration constant, Equation (8-3),
$\mu_2$	calibration constant, Equation (8-3),
$\sigma$	dimensionless variable, Equation (8-2),
$\sigma_1$	calibration constant, Equation (8-3),
$\sigma_2$	calibration constant, Equation (8-3),
$\Phi$	dimensionless sediment transport rate,
$\Phi_b$	dimensionless bed load sediment transport rate,
$\Phi_s$	dimensionless suspended sediment load transport rate,
$\Phi_t$	dimensionless total sediment transport rate,

## ABSTRACT

A study of the sediment transport processes in sewers has been carried out. Based on this study a mathematical modelling system has been developed to describe the transport processes of sediments and dissolved matter in sewer systems. The modelling system consists of three sub-models which constitute the basic modelling system necessary to give a description of the most dominant physical transport processes concerning particles and dissolved matter in sewer systems:

- a **surface model** for the description of the build-up and the wash-off of sediment particles on catchment surfaces
- an **advection-dispersion model** for the description of the transport of dissolved substances and fine sediments in suspension in sewer systems.
- a **sediment transport model** with a movable bed for the description of the non-cohesive sediment transport in sewer systems.

These three models have been implemented into the already existing MOUSE system. The MOUSE system is a deterministic modelling system, which solves the full St. Venant equations for both part full and surcharged pipes in looped sewer systems. The surface model is a lumped conceptual model which runs in parallel with the surface runoff models in MOUSE. The advection-dispersion and the sediment transport models are based on implicit finite difference schemes and are coupled directly to the hydrodynamic pipe model in MOUSE. The advection-dispersion model can describe the transport of dissolved matter and the transport of the fine sediments in suspension. The sediment transport model can describe the transport of non-uniform, non-cohesive sediments. The transport of non-cohesive sediments is modelled by solution of the continuity equation for bed sediments. Four of the most common sediment transport theories are implemented for the description of the non-cohesive sediment transport.

The capability of the advection-dispersion model to predict the transport times for dissolved matter in sewer systems has been validated against field data from a gravity sewer. From the validation of the advection-dispersion model it can be concluded that the model can be used to predict the transport times for dissolved matter in sewer systems flowing part full.

The capability of the sediment transport theories to predict the bed resistance from sediment deposits and the sediment transport in sewer systems with stationary flow and transport has been validated against laboratory data. From the validation of the sediment transport model it can be concluded that the model can be used to predict the hydraulic capacity and the bed load transport of sediments in sewer pipes under laboratory conditions. Field measurements and further laboratory experiments with suspended load transport and graded sediments are needed in order to evaluate the full applicability of the model to sewer systems.

## SAMMENFATNING

Denne rapport er resultatet af et studie af sediment transportprocesserne i afløbssystemer. Baseret på dette studie er der udviklet en matematisk model til at beskrive transportprocesserne for partikulære sedimenter og opløst stof i afløbssystemer. Den matematiske model består af tre del-modeller som udgør det nødvendige modelgrundlag for en beskrivelse af de vigtigste fysiske transportprocesser for transport af partikler og opløst stof i afløbssystemer:

- en **overflademodel** til beskrivelse af opbygning og afvaskning af partikulært sediment på befæstede overfladearealer,
- en **advektions-dispersionsmodel** til beskrivelse af transporten af opløst stof i afløbssystemet.
- en **sedimenttransportmodel** med en bevægelig bund til beskrivelse af sedimenttransporten i afløbssystemet,

Disse tre modeller er implementeret i det eksisterende MOUSE system, der er et fuldt deterministisk model kompleks, som løser St. Venants ligninger for både delvis fyldte og fuldtløbende afløbssystemer. Overflademodellen er en arealintegreret, konceptuel model som afvikles parallelt med de eksisterende hydrauliske overflademodeller i MOUSE. Advektions-dispersions- og sedimenttransport-modellerne er baseret på implicite finitte differensskemaer, og de er direkte koblet til den hydrodynamiske rørmodel i MOUSE. Transporten af kohæsive sedimenter og opløst stof bliver modelleret ved at løse advektions-dispersionsligningen. Sedimenttransportmodellen beskriver transporten af både uensformige kohæsive og ikke kohæsive sedimenter. Transporten af ikke-kohæsive sedimenter bliver modelleret ved at løse kontinuitetsligningen for sedimenttransport. Fire af de mest almindelige sedimenttransportformler er implementeret til beskrivelsen af den ikke-kohæsive sedimenttransport.

Advektions-dispersions modellens evne til at forudsige transporttiden for opløst stof i afløbssystemer er valideret mod feltdata fra et afløbssystem i Dronninglund, Danmark. Ud fra valideringen af advektions-dispersions modellen kan det konkluderes, at modellen kan bruges til at forudsige transporttiden for opløst stof i delvis fyldte ledninger i afløbssystemer.

Sedimenttransport-modellens evne til at forudsige bundforskydningsspændinger fra sedimentaflejring samt sedimenttransporten i afløbssystemer med stationære hydrauliske forhold er valideret mod data fra laboratorieforsøg. Ud fra valideringen af sedimenttransport-modellen kan det konkluderes, at modellen kan bruges til at forudsige den hydrauliske kapacitet og sedimenttransporten i rør under laboratorieforhold. Feltmålinger og yderligere laboratorieforsøg med uensformige sedimenter og sediment i suspensionstransport er nødvendige for at evaluere modellens fulde anvendelighed i afløbssystemer.

## SAMMANFATTNING

Denna rapport är resultatet av en undersökning som gjorts av sedimenttransportprocesserna i avloppssystem. Med denna undersökning som grund har en matematisk modell utvecklats för att beskriva transportprocesserna för partikulära sediment och upplösta ämnen i avloppssystem. Den matematiska modellen består av tre delmodeller som utgör de nödvändiga modellförutsättningarna för att beskriva de viktigaste fysiska transportprocesserna för transport av partiklar och upplösta ämnen i avloppssystem.

- **en ytavrinningsmodell** för beskrivning av uppbyggnad och avspolning av partikulärt sediment på hårdgjorda ytor.
- **en advektions-dispersionsmodell** för beskrivning av transporten av upplösta ämnen i avloppssystemet.
- **en sedimenttransportmodell** med ett rörligt sedimentdjup för beskrivning av sedimenttransporten i avloppssystemet.

Dessa tre modeller är implementerade i det existerande MOUSE systemet, som är ett komplett deterministiskt modellpaket som löser St. Venants ekvationer för både delvis och helt fyllda avloppssystem. Ytavrinningsmodellen är en areaintegrerad, avrinningsmodell som körs parallellt med de existerande hydrauliska modellerna i MOUSE. Advektions-dispersions- och sedimenttransport-modellerna baserar sig på implicita finita differensscheman, och är direkt kopplade till den hydrodynamiska rörmodellen i MOUSE. Transporten av kohesiva sediment och upplösta ämnen modelleras genom att lösa advektions-dispersionsekvationen. Sedimenttransportmodellen beskriver transporten av både olikformiga och icke-kohesiva sediment. Transporten av icke-kohesiva sediment modelleras genom att lösa kontinuitets-ekvationen för sedimenttransport. Fyra av de vanligaste formlerna för sedimenttransport är implementerade i beskrivningen av den icke-kohesiva sedimenttransporten.

Advektions-dispersionsmodellens förmåga att förutsäga transporttiden för upplösta ämnen i avloppssystem har verifierats mot fältdata från ett avloppssystem i Dronninglund, Danmark. Verifieringen av advektions-dispersionsmodellen bekräftar att modellen kan användas till att förutsäga transporttiden för upplösta ämnen i delvis fyllda rörledningar i avloppssystem.

Sedimenttransportmodellens förmåga att förutsäga bäddmotståndet från sedimentavlagringar samt sedimenttransporten i avloppssystem med stationära hydrauliska förhållanden har verifierats mot data från laborieförsök. Verifieringen av sedimenttransportmodellen bekräftar att modellen kan användas för att förutsäga den hydrauliska kapaciteten och sedimenttransporten i ett rör under laborieförhållanden. Fältmätningar och ytterligare laborieförsök med olikformiga sediment och sediment som transporteras i suspension är nödvändiga för att utvärdera modellens användbarhet i verkliga avloppssystem.

## INTRODUCTION

Combined sewers and storm sewer overflows have a well recognised effect on the hydraulic conditions, morphological regime and water quality in receiving waters. Today many sewer systems need to be renovated and at the same time there is an increasing interest in reducing the amount of polluted water spilling out of the sewer system during heavy rain. When the performance of a sewer system is evaluated the impact from the sewer system on the receiving waters and the sewage treatment plant must be taken into consideration. The efficiency of the sewage treatment plant and the impact on the receiving waters depend strongly on both the quantity and the quality of the sewage. The existing mathematical models for sewer systems describe well the hydraulic conditions in pipes without sediment deposits, but the hydraulic capacity of a pipe depends strongly on whether or not sediment deposits are present. Furthermore, pollutants are carried through the sewer system both attached to the sediments and as dissolved matter in the water phase. These phenomena must be taken into consideration when the overall performance of the sewer system is evaluated.

In order to avoid flooding the sediment deposits which reduce the hydraulic capacity have to be removed at high maintenance costs and expensive retention basins are built to reduce the combined sewer overflows. Feasible ways to improve the performance of the sewer system are to rehabilitate the sewer system or to establish regulation strategies for rain storms. In the analyses of the optimum (re-)design or regulation strategy it is necessary to describe the actual conditions in the sewer system as accurately as possible. Hence, there is a need for knowledge concerning the temporal and spatial variation of the sediments and the pollutants in the sewer system. This interest in a better description and understanding of the transport mechanisms in sewers has induced a wish to model the physical transport processes in the sewer system. In this study a deterministic modelling system has been developed for the transport processes of sediments and dissolved matter in sewers. The modelling system can describe:

- the build-up and wash-off of sediments and dissolved pollutants in catchments
- the hydraulic conditions due to sediment deposits
- the dynamic changes of the sediment deposits in pipes
- the sediment transport and the transport of dissolved pollutants
- the effect of retention basins and control strategies on the transport of sediments and pollutants in the combined sewer overflows
- the temperature and concentrations at the sewage treatment plant.

## 2 GOALS AND OBJECTIVES

The objective of the present study is to collect and analyse the available knowledge concerning sediments and dissolved matter in sewers and from this basis to establish a modelling system for the transport of sediments and dissolved matter from the source to the combined sewer overflow and the sewage treatment plant. The outcome of the study is presented in the form of a Ph.D thesis dealing with the theoretical aspects of modelling of sediment in sewers, a Technical Reference Manual: "MOUSE TRAP Technical Reference Version 1.00" which contains the mathematical background for the modelling system, and an user manual for the modelling system: "MOUSE TRAP User Manual Version 1.00".

The modelling system includes a description of the transport of sediments and dissolved matter in sewer systems together with a formulation of the accumulation and erosion of sediment on catchment surfaces. A formulation of the transport of sediments and dissolved matter through the most common hydraulic structures in the sewer system is also included. The modelling system is directly coupled to the hydrodynamic model in the MOUSE system, which ensures that the system has an accurate hydrodynamic basis. The following issues are described in detail within the study:

- analyses of the sewer as a transport medium for sediments and dissolved matter
- the critical bed shear stress for different types of sediment
- the hydraulic resistance for different types of sediments
- the reduction in flow capacity due to sediment deposits
- transport processes for non-cohesive sediments, fine particles and dissolved matter
- deposition, erosion and resuspension of sediments.

The applicability of the modelling system to model the processes related to the sediment transport in sewer systems should be evaluated against theoretical tests and against field data from a real sewer system.

At present, no detailed models exist and very limited knowledge and few field data are available on sediments in sewers. In the process of collecting the state of the art theory, building and applying the models it will become evident where further research is needed to improve the understanding and the description of the transport processes in sewer systems.



### 3

## SUMMARY OF DEVELOPED MATHEMATICAL MODELS

During the present study the state of the art theories concerning the sediment transport processes in sewer systems have been collected. The theories have been analysed and based on these analyses a mathematical modelling system for the transport processes in sewers has been developed. Finally, the performance of the modelling system has been evaluated based on theoretical tests and field data. The modelling system consists of three models:

- a surface model
- an advection-dispersion model for the transport of dissolved matter and fine sediments in suspension
- a sediment transport model with a movable bed

The surface model describes the build-up and the wash-off of sediment particles from surface areas. The advection-dispersion model describes the transport processes of fine sediments and dissolved matter in the pipe system. The sediment transport model describes the sediment transport and the resistance in the sewer system due to sediment deposits. A sketch of the model structure is shown in Figure 3.1. The arrows in Figure 3.1 indicate the direction of the data exchange between the models. The modelling system is built into the MOUSE package (Lindberg et al. 1986 and 1989). In the process of developing the models well established DHI software libraries for the building of input menus, presentation of output data, solution of matrices, etc have been used together with knowledge gained by the author during the time he was responsible for maintaining the hydrodynamic model in MOUSE and in the process of developing the one dimensional morphological model in MIKE 11. Without these software libraries and this knowledge it would not have been possible to complete the study within the planned timetable.

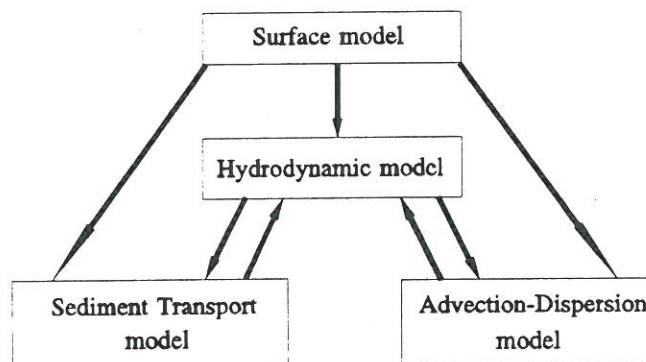


Figure 3.1. A sketch of the model structure

## **3.1 The Surface Model**

The surface model consists of three modules:

- a module for the description of the accumulation of particles on the catchment
- a module for the routing of the wash-off by overland flow
- a gully pot module for the description of build-up and wash-out of dissolved pollutants in gully pots

These models are described in more detail below.

### **3.1.1 Accumulation of Particles on the Catchment**

During dry weather periods the fine particles accumulate on the surface of the catchment. The most common formulations of the problem are to assume that the build-up is a linear or an exponential function of time (Huber and Dickinson, 1988). Both build-up formulations have been implemented in the model.

### **3.1.2 Wash-off of Particles by Rainfall**

The wash-off of sediment particles during a rain event can be divided into two processes; the erosion by rain drops and the erosion by overland flow. Only the erosion by rain drops is taken into account in the model as this process is considered to be the most important in urban catchments (Svensson, 1987).

The erosion by rain drops is governed by several parameters. The most important factors are: rainfall intensity, rainfall height and duration, rain drop size, catchment topography, particle characteristics and vegetation. However, parameters such as rain drop size and rain fall height are rarely available so a simpler approximation is adopted in the model. This approximation states that the rain drop erosion is a function of the rainfall intensity and a detachment rate (Svensson, 1987).

The sediment transport is divided into a fine and a coarse fraction. The fine sediment fraction is transported in the mode of wash load. The transport of this fraction is not limited by the transport capacity of the overland flow but the transport is limited by the availability of the fine sediments. The fine fraction builds up during dry weather periods. The coarse sediments on the surface is transported in the mode of bed load and suspended load. Hence, the coarse sediment is limited by the transport capacity of the overland flow, but it is not limited in supply. The transport capacity is calculated as the sum of the transport capacity for bed load and suspended load calculated from the van Rijn sediment transport formulae (van Rijn, 1984a and 1984b).

### 3.1.3 The Gully Pot Module

Gully pots are a significant source for pollutants, (Butler et al., 1994 and Morrison et al., 1994). During dry weather dissolved pollutants build-up in the gully pots and they are washed-out from the gully pots during storm conditions. The gully pot module is an optional lumped module which serves as a link between the surface and the hydrodynamic model. The function of the gully pot module is to include a description of the release of polluted water from gully pots which under some circumstances contribute significantly to a first foul flush. Few data exist on the build-up of dissolved substances in gully pots. Based on the data from the UK (Crabtree et al., 1993) a linear build-up function was chosen. During rain storms the incoming water is assumed to mix instantaneously with the liquid in the gully pot.

## 3.2 The Advection-Dispersion Model

The advection-dispersion model is based on the one dimensional transport equations for dissolved material. The equations are solved by use of an implicit finite difference scheme which is fully time and space centred in order to minimise the numerical dispersion. The advection-dispersion equation reflects two transport mechanisms:

- the convective transport with the mean flow velocity
- the dispersive transport due to concentration gradients in the water

The main assumptions of the advection-dispersion model are:

- the considered substance is completely mixed over the cross-sections. This implies that a source/sink term is considered to mix instantaneously over the cross-section
- the substance is conservative or subject to a first order reaction (linear decay)
- Fick's diffusion laws can be applied, ie the dispersive transport is proportional to the concentration gradient

Special formulations based on a local continuity equation were developed to describe the transport at manholes and auxiliary structures. The advection-dispersion model is discussed in detail in Chapter 7.

## 3.3 The Sediment Transport Models

Two sediment transport models are implemented in the modelling system:

- a non-cohesive, movable bed (morphological) sediment transport model
- a sediment transport model based on the advection-dispersion equation

Both models run in parallel with the hydrodynamic module in the MOUSE package and it is possible to run the two sediment transport models in conjunction, ie some

sediment fractions can be transported as wash load, while other sediment fractions are transported in the mode of bed load and suspended load.

Special formulations have been developed for the critical bed shear stress and the sediment transport for pipes with a thin layer of sediments.

### **3.3.1 The Non-Cohesive Sediment Transport Model**

This type of sediment transport model describes the sediments transported in the mode of bed load and suspended load. The movable bed model solves the continuity equation for sediment by use of a Preissmann implicit finite difference scheme. The model can simulate the dynamic development of graded non-cohesive sediment deposits and provides feedback to the hydrodynamic component due to the change in flow area and the change in resistance due to the sediment deposits, eg with dunes, in the pipes. Four different sediment transport formulae are implemented in the model:

- Ackers - White (Ackers and White, 1973)
- Engelund - Hansen (Engelund and Hansen, 1967)
- Engelund - Fredsøe (Fredsøe, 1984)
- van Rijn (van Rijn, 1984a, 1984b)

The Ackers-White and the Engelund-Hansen models calculate the total load, whereas the Engelund-Fredsøe and the van Rijn models calculate the bed load and the suspended load separately. The formulation of the transport of graded sediment is included in order to describe the wide range of sediment characteristics found in a sewer system (Laplace, 1991). The formulation for graded sediment differs in two ways from the formulation for uniform sediment. First the critical bed shear stress is modified by applying Egiazaroff's correction factor (Egiazaroff, 1965), in order to take into account the shielding of smaller particles by larger particles. Secondly the total sediment transport is calculated as the sum of the sediment transport multiplied by the percentage of availability for each sediment fraction.

### **3.3.2 The Sediment Transport Model based on the Advection-Dispersion Equations**

This type of sediment transport model describes the sediments transported in the mode of wash load; hence it is applicable for the transport of sediments carried in suspension at a velocity close to the flow velocity. The model is based on the advection-dispersion equations, ie the sediment transport depends on the upstream erosion/deposition and the local hydraulic conditions. The erosion of the sediments is based on a description of an erodibility constant together with the bed shear stress (Ariathurai et al., 1971). The deposition is modelled as a sink term, which is calculated from the fall velocity, the concentration, the mean settling depth and the bed shear stress. The sediment transport models are discussed in more detail in Chapter 8.

### **3.4 Verification of the Modelling System**

The verification of the modelling system consists of an evaluation of the capability of the modelling system to reproduce known analytical solutions.

The verifications of the surface model, the sediment transport model and the advection-dispersion model were focused on the mass balance and the transport times in the models. The surface model is not discussed further in this report. More information concerning the verification of this model is included in Appendix A. The verification of the advection-dispersion and the sediment transport models are presented in Chapters 7 and 8 and also in Appendices B and C. Further, the implementation of the Einstein Sidewall Elimination Procedure for the prediction of the reduction in hydraulic capacity due to sediment deposits in the pipes has been verified, see Chapter 5.

### **3.5 Validation of the Modelling System**

The validation of the modelling system consists of an evaluation of the capability of the modelling system to reproduce field or laboratory data.

A few aspects of the sediment transport modelling system have been validated against laboratory data from the Chalmers University of Technology, Sweden, Newcastle University, UK, and HR Wallingford, UK. The validation was carried out for the prediction of the bed resistance from the sediment deposits and the prediction of the sediment transport by the non-cohesive sediment transport formulae (see Chapters 5 and 6).

At present, studies are undertaken to make a further validation of the modelling system, eg an evaluation of the description in the advection-dispersion model for the mixing of pollutants in manholes is currently carried out at Sheffield University, (O'Brien and Mark, 1995).

### **3.6 Examples of Application of the Modelling System**

The sediment model has been applied with uniform sediments to make preliminary analyses of the sediment transport the Rya sewage treatment plant in Gothenburg, Sweden. The purpose of this application is to evaluate the capability of the sediment transport model to reproduce the transport of sediments to the Rya sewage treatment plant during a storm, see Chapter 10.

The sediment transport model the a movable bed has been used to predict the locations with sediment deposits in the sewer system of Ljubljana, Slovenia. The results, in terms of locations with sediment deposits, are compared with field data from the sewer system in Ljubljana. Further, the model is used to predict the effect of the removal of the sediment deposits on the combined sewer overflows, see Chapter 10.

The advection-dispersion model has been setup for a gravity sewer flowing part full in Dronninglund, Denmark (Garsdal et al., 1994). The purpose of this application was to show the capability of the model to reproduce the transport of dissolved matter, see Chapter 9.

## 4 A QUALITATIVE DISCUSSION OF THE TRANSPORT PROCESSES IN SEWERS

A long tradition exists for studying sediment transport in rivers, where the transport processes and the characteristics of the sediment are well described. However, with respect to pipes the criteria for self cleansing conditions and slurry transport have been studied while studies in the field of sediment transport in sewers with sediment deposits is quite new. The first workshop on sediment in sewers was held in Brussels in 1991 (Verbanck et al., 1992). At this workshop it was concluded that there is no well established terminology within the area of sediment transport in sewers. As many similarities exist between the sediment transport processes in sewers and rivers, the terminology for sediment transport in rivers has been adopted in the present study. There is an overlap between processes in sewer systems and rivers, since large sewers with a deposited sediment bed in principle act as small rivers/flumes, hence the transport processes are the same within this range of flow conditions.

In the field of sediment transport in sewers very few laboratory studies have been carried out within the range of flow conditions which are found in sewers during storm conditions. In addition very few field measurements are available. Sediment characteristics in sewers cover a much wider range than the sediments in rivers and the sediments in sewers often have cohesive properties where chemical and biological processes have a dominant role. Furthermore, sewers differ from rivers in three important ways; sewers have rigid boundaries, and they often have a limited amount of sediments and the sediment transport in sewers depends on the supply of sediments from the surface to the sewer system. The following section describes some of the characteristics of the transport processes in sewer systems.

### 4.1 Classification and Characteristics of Sediments in Sewers

The characteristics of sediments found in sewers cover a wide range. Grain sizes vary from particles with a size of a few  $\mu\text{m}$  up to the size of boulders, the density of the sediments varies from below  $1000 \text{ kg/m}^3$  to  $2650 \text{ kg/m}^3$  and the sediments may exhibit "cohesive like"<sup>1</sup> properties (eg Verbanck, 1992). Further, sediments in sewers may aggregate or disaggregate due to the biological and chemical processes. A description of these processes is beyond the scope of this study. A general classification of sewer sediments was proposed by Crabtree (1988). The classification is based on a comprehensive data collection programme carried out in the UK. The sediments are divided into five categories based on visual appearance and

---

<sup>1</sup> The term "cohesive like" is a frequently used term within sewer sediment terminology. The reason for the term "cohesive like" is that the sediment has cohesive properties, but the properties differ significantly from cohesive sediments found eg in coastal estuaries. The sediments in sewers are adhesive, ie they stick together, but the grain sizes vary from silt to gravel. Further, the adhesiveness originates from biological and chemical processes in the waste water which are far from understood.

location within a sewer system together with the physical and chemical characteristics of the sediment:

- Type A coarse, predominantly granular mineral material found in the invert of pipes
- Type B similar in composition to type A but concreted by the addition of mineral cements, fats and tars
- Type C mobile, fine grained, largely organic sludge found in quiescent zones
- Type D organic pipe wall slimes and zoogloal biofilm
- Type E fine grained organic and mineral deposits found in storage tanks

In general, the Type A, Type B and Type E sediment deposits affect the hydraulic performance of the sewer system and the Type A and the Type C deposit are considered to be the significant sources of the pollutants in sewers. The Type C deposits may contribute to a first foul flush and the Type A sediment deposits may cause high pollutant loading if they are eroded during a storm. Ashley et al. (1993) reported from a sewer system in Dundee, UK, that Type A sediment was most commonly found, Type C sediment was found as a thin layer of largely organic sludge on top of type A sediment. The Type B sediment was rarely found in the system and the Type D sediment, the organic pipe wall slimes, was mostly found on the pipe walls at dry weather flow levels.

## 4.2 The Sources of Sediments in Sewer Systems

Most of the Type A and Type B sediments are eroded from the surface and they are transported to the sewer system through the gully pots by overland flow during rain storms (Crabtree, 1988). Most of the material originates from:

- winter gritting
- wash off from pervious surfaces
- wash off from impervious surfaces
- construction works
- materials from road surfaces
- waste water

The Type C and Type E sediments originate from waste water, domestic sewage and the wash-off from pervious and impervious surfaces. The Type D sediment builds up due to biological processes in the sewer system (Crabtree, 1988).



## 4.3 The Sources of Dissolved Substances in Sewer Systems

Dissolved substances in sewers originate from several sources. These are:

- surface runoff
- build up in gully pots during dry weather
- infiltration
- waste water

The sources are described below in more detail.

### 4.3.1 Dissolved Substances in Surface Runoff

Dissolved substances in surface runoff consist of two components:

- dissolved substances in the precipitation
- wash off from the surface

Precipitation is far from clean. As it passes through the atmosphere there is an uptake of substances such as nutrients, organic material, solids, metals and pesticides. Kluesener and Lee (1974) found higher levels of ammonia in precipitation than in runoff from residential areas, and they found that nitrate in the precipitation in some urban areas accounted for 20-90 % of the nitrate in the storm water runoff. The remaining part of the dissolved substances in the surface runoff comes from the erosion of sediments on the catchment surface.

### 4.3.2 Build up of Dissolved Substances in Gully Pots

The purpose of a gully pot is to trap particles to prevent them from entering the pipe system and to prevent the release of odour from the pipe system. During dry weather flow dissolved pollutants, eg BOD/COD or ammonia, accumulate in the gully pot liquid due to biological and chemical processes. The rate of build up depends on the following elements:

- the type of pollutant
- the biological and chemical conditions in the gully pot
- the temperature

During rain storms the gully pot liquid mixes with the incoming rain water and the polluted water is discharged into the sewer system. Under some circumstances these phenomena contribute significantly to the first foul flush (Butler et al. 1994). The first foul flush is discussed later in this chapter (Section 4.4.2).

### **4.3.3 Infiltration into the Sewer System**

The infiltration is often assumed to be clean due to its origin in the soil layers. The infiltration originates from three sources:

- antecedent precipitation
- frozen residual moisture
- ground water

In general, few data are available concerning the concentrations of dissolved pollutants in the water infiltrating the sewer system. If data were available on the water quality of the ground water or an infiltration study had been carried out, the concentrations of the water infiltrating the sewer system could be estimated. The infiltration is usually assumed to be much cleaner than the precipitation as the water is filtered by the soil.

### **4.3.4 Waste water**

The waste water originates from the human activity in the catchment. The sources of waste water are:

- residential areas
- commercial areas
- industrial areas

The waste water carries pollutants either in terms of organic material or chemical substances. Typical the waste water is characterised by the amount of biological oxygen demand, BOD, or the chemical oxygen demand, COD, per person living in the catchment. The concentrations of the dissolved substances in the waste water depend strongly on the local conditions, eg land use type, number of inhabitants in the catchment and type of industry. The concentrations in the waste water will typically vary on an hourly and daily basis and even a yearly variation may be observed at some locations.

## **4.4 The Characteristics of Sediment Transport in Sewers**

In sewers various transport phenomena may take place at the same time, ie both transport of dissolved matter and transport of sediments. Hence, when sediment transport is modelled in sewer systems, it is very important to apply models which describe the dominant physical processes of interest, and especially to note the similarities and differences between the assumptions in the model and the characteristics of the transport process.

Investigations on the sediment transport in sewer systems have shown that there is often a diurnal cycle in the sediment transport which follows the domestic use of water (Ristenpart and Uhl, 1993). They found that during low flow conditions at night, sediment is deposited and re-eroded during the first peak flow in the morning.

Further, a long term cycle exists with an accumulation of material during dry weather periods and wash-out of sediments during rain storms. After a long dry weather period the water in the sewers may have very high concentrations of sediments and dissolved matter.

#### **4.4.1 Sediment Transport with Limited Supply of Sediment**

There is quite often or even always a limited supply of sediments in sewer systems as the sewer systems are usually designed to be self cleansing, ie the sediment transport during a storm will usually be much less than the sediment transport capacity of the flow in the pipe system. During such flow conditions the sediment deposits in the pipes may be partly or totally eroded and the traditional sediment transport formulations for rivers break down as these assume an unlimited supply of sediments from the alluvial sediment bed.

If the transport mode is bed load and a limited supply of sediment is present, isolated dunes form on the invert of the pipe. These migrate through the system at a higher velocity and with a smaller dune height and length compared to a dune under similar flow conditions in a pipe with a continuous sediment bed. Such dunes have been observed at Delft University (Kleijwegt, 1992a), and at Chalmers University of Technology (Perrusquía, 1992). Both report that such dunes increase the flow resistance.

At present, no exact theory exists for the incorporation of the flow resistance and the sediment transport from isolated dunes in rigid pipes. The modelling of sediment transport and the critical bed shear stress in pipes, where the sediment depth is less than the height of an equilibrium dune, are discussed further in Chapter 8 and in the Technical Reference Manual pp. ST 63-64.

#### **4.4.2 The First Foul Flush**

The first foul flush is a term used for the description of the very high concentrations of sediment and dissolved matter found in the rising stage of the first peak flow during rain storms. The first foul flush is caused by rapid erosion of the fluid sediment layer, typically Type C sediments, and the wash out of dissolved substances built up in gully pots during dry weather periods. An understanding of these flushes is important in order to investigate which components of the water are discharged to the receiving waters and which are transported to the sewage treatment plant. In this way the performance of the sewer system can be assessed with respect to the transport of pollutants, especially the performance of the combined sewer overflows. Whether a phenomenon called the first foul flush exists or not, is still a subject of debate but more recent research (Ashley et al., 1993; Ichiki et al., 1993), indicate the presence of such a phenomenon. The factors which determine whether a first foul flush is observed are:

- catchment characteristics
- the layout of the sewer system
- time since the last rain
- time of the year
- the location of the observation point in the sewer system

It is hard to say whether a first foul flush will be present in a specific sewer system. If the sewer system operates under self cleansing conditions the sediment is not likely to deposit and hence a first foul flush will not be present. However, if there are sources of the sediments in the catchment, if it is possible for the sediments to build up in the gully pots and the pipe system and if it is a long time since the system was last flushed by a heavy rain storm, then a first foul flush will probably be present.

#### 4.4.3 The Mode of Sediment Transport in Sewer Systems

There is still discussion as to which transport processes actually take place in sewer systems, (Ashley et al., 1993; Verbanck, 1993). The current debate concerns whether or not a heavy-fluid layer (also termed *fluid sediment*) exists. The heavy-fluid layer is characterised by a dense suspension moving along the bed. Further, there is doubt concerning whether this layer, if it exists, is a continuous layer or a discontinuous layer and whether the layer can be described by conventional bed load theory. As insufficient information exists about this layer, no special considerations were taken to describe it within this study. For simplicity, the sediment transport modes in sewers are, as in rivers, split into three transport modes. A qualitative description of the transport modes is given below:

- bed load
- suspended load
- wash load

The bed load and the suspended load is termed "bed material" in river engineering. The bed material consists typically of non-cohesive sediment, eg sand, Type A sediment. The sediment transported as wash load are typically fine organic material, ie Type E sediment. The common non-cohesive sediment transport formulae for rivers only include bed load and suspended load, and not the wash load (Engelund and Hansen, 1967; Fredsøe and Deigaard, 1992).

The mode of transport of a particle in a sewer system depends on the particle characteristics and the hydraulic conditions. A sketch of the transport mode as a function of the fall velocity and the flow velocity is shown in Figure 4.1. It can be seen that a particle which during dry weather flow conditions is transported as bed load may be transported as suspended load or even as wash load during storm conditions, ie transported with the mean flow velocity without significant interaction with the bed. When the sediment is transported as wash load during these high flow rates the transport is determined by the upstream conditions and a space and a time lag may exist between the sediment transport and the local flow conditions.

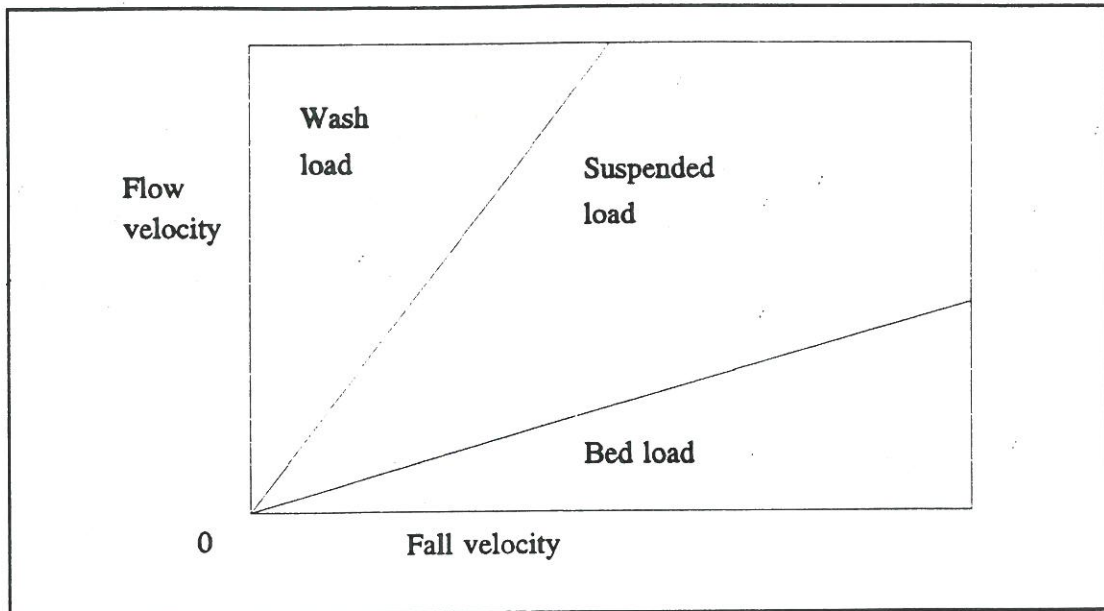


Figure 4.1. Sketch of the transport modes for sediment as a function of the fall velocity and the flow velocity.

#### 4.4.4 The Bed Load Transport

The bed load consists of those particles which move in almost continuous contact with the bed during the transport, eg by rolling, jumping or sliding. If sufficient sediment is present in the pipe, the bed load transport will often form dunes or other bed forms (Engelund and Hansen, 1967), hence bed load transport can increase the bed resistance in a pipe. The bed load deposits during the dry weather flow conditions, and the deposit decreases the hydraulic capacity of the pipe by both reducing the flow area and increasing the bed resistance of the pipe. The bed load is a function of the local hydraulic conditions and the most important parameter in the description of the bed load is the effective bed shear acting on the sand surface. Bed load can be modelled by use of conventional non-cohesive sediment transport formulae, eg van Rijn or Engelund-Fredsoe. Sediment transported as bed load transport is typically Type A sediment.

#### 4.4.5 The Suspended Load Transport

The suspended load is transported without continuous contact with the bed, but it is part of the erosion/deposition process in the sewer. A particle is transported in the mode of suspended load when the turbulent eddies have large vertical velocity components. The suspended load is a function of the local flow conditions and the composition of the bed material. The suspended load can be modelled by use of conventional non-cohesive sediment transport equations, eg van Rijn or Engelund-Fredsoe. Sediment transported as suspended load is typically the same type of sediment as transported as bed load, ie Type A sediment.

#### **4.4.6 The Wash Load Transport**

The wash load consists of fine sediment transported in suspension. The difference between the wash load and the suspended load is that the exchange between the bed material and the wash load is generally small while the suspended load takes part in the erosion and deposition of the sediment deposits in the pipes. Hence, the wash load is in general not important with respect to the hydraulic resistance and the morphological changes in the sewer system. However, the sediment transported as wash load typically has attached pollutants and these must be modelled in order to evaluate the overall performance of the sewer system with respect to pollutants. The wash load often has a very small fall velocity compared to the mean velocity of the flow, hence the wash load transport is a function of both the upstream and the local flow conditions. Due to the small fall velocity the wash load typically has a more or less uniform vertical concentration distribution. As the common non-cohesive sediment transport formulae do not include the transport of wash load, the transport of wash load has to be described otherwise, eg by use of the advection-dispersion equations. The sediment transported in the mode of wash load is typically Type C sediment, but also Type A sediment with a small grain size may be transported as wash load during storm situations.

#### **4.5 Transport Mechanics of Sediments in Sewers**

The modelling of the transport mechanics in sewers is complex as continuous formulations eg for the critical bed shear stress, have to be made for a range of pipes; eg from pipes without sediment deposits to pipes with a deposited sediment bed. Further, the erosion rates of the sediment deposits have to be adjusted due to the limited amount of sediment in the pipes. In the present study mathematical descriptions have been developed for the sediment transport processes in the range from pipes without sediment deposits to pipes with a full deposited sediment bed.

##### **4.5.1 The Critical Bed Shear Stress for Non-Cohesive Sediment**

The critical bed shear stress is a very important parameter which describes whether the sediment can be eroded or not. Hence, the transport of sediment in pipes begins when the critical bed shear stress is exceeded. In some sewers, eg storm sewers where the sediments may be non-cohesive, the critical bed shear stress can be found from the Shields criterion (Shields, 1936). Based on a dimensional analysis Shields analysed a single grain resting in a uniform sediment deposit. In the analysis it was assumed that a particle would start to move for a given ratio between the driving forces and the stabilising forces. The driving forces acting on a sediment particle resting on a plane bed are the drag force and the lift force. The stabilising forces are the gravity force and the frictional force. The sediment grains start to move when the driving forces exceed the stabilising forces. The critical bed shear stress was found to be a function of the grain Reynold number. A curve fit for critical bed shear stress as a function of the Reynold number by van Rijn (1984a) can be seen in the Technical Reference Manual p ST 9.

#### 4.5.2 The Critical Bed Shear Stress for Non-Uniform Non-Cohesive Sediment

The critical bed shear stress for non-uniform sediment differs from that for a uniform sediment as there is a larger exposure of the larger particles and the smaller particles are sheltered by the larger particles. Further, mutual interference may exist between particles of different size, resulting in a larger stabilizing force.

In rivers, the critical bed shear stress for non-uniform, non-cohesive sediments can be found for instance by use of Egiazaroff's correction factor (Egiazaroff, 1965). This description is based on the reduction in drag force on a single particle from the sheltering of particles with a different size. The same description is adopted in the present version of the modelling system as no experiments have yet been carried out to investigate the bed shear stress in pipes with graded sediment. For the mathematical description of the modified critical bed shear stress see the Technical Reference Manual p ST 70.

#### 4.5.3 The Critical Bed Shear Stress for a Pipe without Sediment Deposits

The critical bed shear stress for a sand grain on a rigid bed differs from the critical bed shear stress obtained by Shields curve for a deposited bed. A single grain is exposed to a larger drag force and a smaller stabilising force. Hence, the critical bed shear stress for a single grain is less than the critical bed shear stress for a grain resting in a uniform sediment deposit. Novak and Nalluri (1984) carried out experiments to determine the threshold value for the initiation of motion for a single sand grain and multiple sand grains in a pipe without sediment deposits. The results showed that the critical bed shear stress was smaller than that predicted by Shields (1936). They also found that the critical bed shear stress was increased when multiple grains lay on the bottom of the pipe, but it was still less than the critical bed shear stress predicted by Shields (1936). A consequence of these findings is that in order to avoid deposition when sediment moves on a sediment bed a larger bed shear stress is needed compared to the sediment movement on a rigid bed.

To obtain a mathematical description of the critical bed shear stress for a pipe without sediment deposits an analogy is made between the critical bed shear stress for a sand grain in a rigid pipe and the critical bed shear stress for non-uniform non-cohesive sediment. The critical bed shear stress is always a function of the balance between the driving and the stabilising forces on a single particle, ie the critical bed shear stress is a function of the distance between the individual grains in the pipe (Novak and Nalluri, 1984) and a function of the grain size compared to the equivalent grain roughness of the pipe. Hence, if the ratio of the particle diameter to the equivalent grain size of the pipe decreases then the critical bed shear stress will increase due to sheltering effects from the roughness of the pipe. If the distance between the particles in the pipe is larger than approximately six times the grain diameter then the grains will act as individual particles, as the sheltering no longer exists. If the distance between the particles decreases, the critical bed shear stress increases due to the sheltering from other grains. This reduces drag force on the individual grain. In the present sediment transport model Egiazaroff's correction factor (Egiazaroff, 1965) has been used to describe the critical bed shear stress for

a for a pipe without sediment deposits. For further information on the modelling of the critical bed shear stress in pipes without sediment deposits, see Section 8.2.2.

#### 4.5.4 The Critical Bed Shear Stress for Adhesive Sediment

The sediment in combined sewers may exhibit cohesive properties ie adhesion exists between the individual grains. Field experiments have shown that sediment deposits with cohesive properties may have a much higher critical bed shear stress than the critical bed shear stress for non-cohesive sediment. In the Dundee interceptor sewer the typical critical bed shear stress for cohesive sediment was found to be up to 25 N/m<sup>2</sup> (Ashley et al., 1992), the critical bed shear stress was measured by using a cruciform applied stress rheometry. In the same catchment critical bed shear stresses has been measured to values as high as 2650 N/m<sup>2</sup> (Ashley, 1993).

Experiments carried out with artificial cohesive sediments at Newcastle University have shown that sediments with cohesive properties erode at a higher bed shear stress than non-cohesive sediment (Nalluri and Alvarez, 1990). The critical bed shear stress for the artificial cohesive sediment was in the order of 2.5-7 N/m<sup>2</sup>. The erosion of the sediment took place as a discontinuous process where large portions of the sediment were eroded instantaneously. When the sediment eroded, it was observed that the sediment moved within the same transport mode as non-cohesive sediment, but there is some doubt as to whether this is the case for real sewers (Nalluri and Alvarez, 1990). Very few laboratory and field data exist concerning the development of cohesive properties of sediment in sewers, hence a very limited knowledge is presently available concerning the processes which generate the adhesive properties and the time scale for the build up of the critical bed shear stress.

Ashley (1993) also reported that a correlation exists between the liquid content of the sediment deposit and the shear strength. Data on the liquid content of the sediment deposits are rarely available so the critical bed shear stress is described as a function of the erosion depth of the sediment deposit in the pipes. This approach is chosen as the sediment in estuaries has a variation in the critical bed shear stress as a function of the sediment depth due to the consolidation process, and this approach is in correspondence with the observations by Ashley (1993). Further information on the mathematical description of the critical bed shear stress as a function of the sediment depth is given in Section 8.2.4 and in the Technical Reference Manual p. ST 62.

#### 4.5.5 Erosion and Deposition of Sediment in Sewers

The sediments start to move when the critical bed shear stress is exceeded, but this does not mean that erosion necessarily takes place. The sediment transport continuity equation can be applied for a stretch of the sewer system to predict whether sediment deposits erode. If the inflow flux of sediment is equal to the outflow flux then no erosion/deposition of sediment takes place, ie the bed level may not change even for quite large bed shear stresses and sediment transport rates. If the inflow flux of



sediment is smaller than the outflow flux erosion occurs and if the inflow flux of sediment is larger than the outflow flux deposition occurs.

The description of erosion and deposition patterns for non-cohesive sediments in the transport modes of bed load and suspended load are typically modelled by use of the continuity equation for sediment transport, as described above.

The description of the erosion and deposition pattern for cohesive sediments transported as wash load is typically modelled by use of an erosion and a deposition rate in the advection-dispersion equations. The erosion is described as a source and the deposition is described as a sink based on the fall velocity of the particles. In sewers the erosion rate has to be restricted by the fact that only a limited amount of sediment is available. For the mathematical descriptions of erosion and deposition of cohesive sediment, see the Technical Reference Manual p. ST 74.

#### 4.5.6 Sediment Transport in Ancillary Structures

No general description exists for the sediments transported through hydraulic structures. Further, the structures have different functions in the sewer system, ie some structures are designed for self-cleansing conditions while others are designed to trap the sediment. The structures can be divided into three groups depending on the function of the structure in the sewer system:

- manholes/junctions
- overflow structures
- tanks/retention basins

Little is yet known of the sediment transport through manholes, but as the level of turbulence is high in manholes it is generally assumed that the sediment does not deposit in the manholes. Deposition may however take place during time of surcharge when the retention time of the flow in the manhole is sufficiently long to allow the sediment to deposit (Crabtree et al. 1991).

The performance of overflow weirs and swirl separators is in general well known on an individual basis, eg Sørensen (1991). As no general formulation exists for these structures the individual characteristics of the overflow structures must be taken into account to describe the sediment transport.

Tanks often play an important part in the (re-)design of sewer systems. The descriptions of the movement and deposition of sediments in tanks/retention basins are important as the design of the tank may be aimed at containing the self-cleansing conditions and/or to be operated as a storage facility. However, tanks have individual design and the flow pattern in the tank is often 2-D or 3-D, which makes a detailed modelling of these structures very complex.

In this study simple formulations have been adopted for the description of the transport through hydraulic structures. The formulations can to a large extent be modified to suit the individual structure, consequently no detailed individual

modelling of the structures is carried out. For further information on the modelling of the sediment transport through structures see Section 8.1.1 and the Technical Reference Manual pp. ST 58-62.

## 5 FLOW RESISTANCE IN SEWERS

The calculation of the flow resistance from sediment deposits is important as the sediment deposits both reduce the flow area and may increase the flow resistance in the pipe. This may significantly reduce the flow capacity of a pipe and hence cause flooding. Furthermore it is important to have a good estimate of the bed shear stress for the prediction of the sediment transport, ie if a large scatter is present in the prediction of the bed shear stress this scatter will also be present in the prediction of the sediment transport.

The calculation of the flow resistance in sewers is far more complex for sewers with sediment at the pipe invert compared to a river or a sewer without sediment deposits. This is because one part of the hydraulic resistance in the sewer originates from the pipe wall and another part originates from the sediment on the bottom of the sewer. Additionally, the resistance from the sediment deposition comprises two components. One part originates from the grain friction and the other part originates from the expansion loss behind the bed forms. The configuration of the bed forms is determined by the sediment transport and the hydrodynamics.

The principal sources of roughness in sewers are:

- the resistance from the pipe material itself
- the resistance from the sediment grains
- the resistance from bed forms in the pipe
- other factors: aging effects, structural failure, biological growth

The resistance from the pipe and the resistance from the sand grain can be described with standard hydraulic theory. The resistance from the bed forms can be described by sediment transport formulae. The description of the resistance from the other factors is beyond the scope of this study.

### 5.1 Description of the Shear Stress in Sewers

The description of the flow in a pipe with a sediment bed is complicated by the fact that the roughness of the pipe wall and the roughness from the sediment bed differ. The sediment bed itself, will typically have a higher resistance than the pipe wall, ie sediment deposits increase the average resistance in the pipe. The resistance from the sediment deposits increases further if bed forms are present.

### 5.1.1 The Side Wall Elimination

One way to determine the shear stress on the sediment bed in a sewer or to find the total resistance to the flow when the hydraulic conditions and the characteristics of the sediment layer are known, is to apply a side wall elimination procedure. The side wall elimination is based upon the assumptions of Einstein (1942) or Vanoni and Brooks (1957). The former used the Manning equation and the latter the Darcy-Weisbach equation. The Einstein side wall elimination procedure is used in the present modelling system. The basic assumptions of the Einstein side wall elimination procedure are:

- the cross-section area can be divided into sub-areas each of which is connected to a part of the wetted perimeter
- the mean velocity is the same for all sub-areas

Einstein used these assumptions to separate the resistance from the channel sides and the bottom in channel flow. A definition sketch of a sewer with sediment is shown in Figure 5.1.

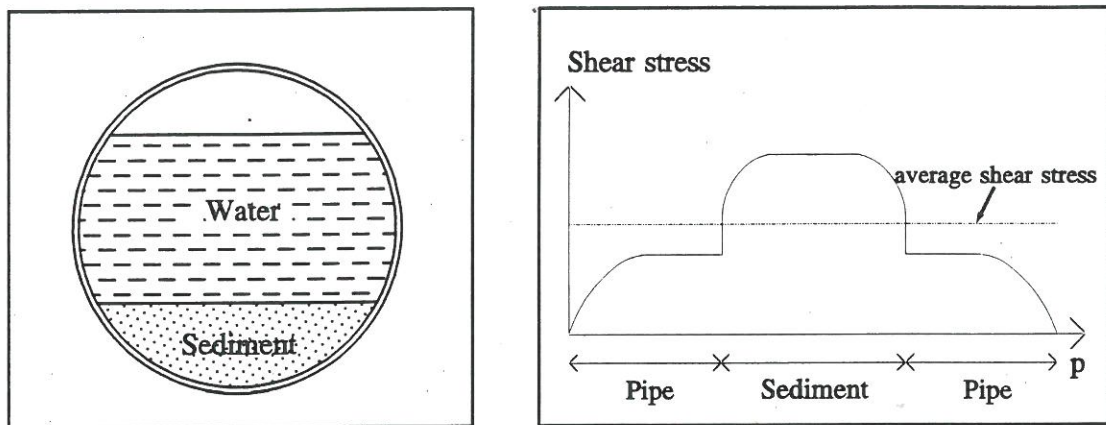


Figure 5.1. Sketch of a part full pipe with a sediment bed together with a sketch of the boundary shear stress along the wet perimeter,  $p$ , of the pipe. Modified after Perrusquía et al. (1994).

### 5.1.2 Verification of the Side Wall Elimination

At present, the side wall elimination procedure by Einstein (1942), has been successfully applied to sewers flowing part full (Perrusquía et al., 1986). The experiments at Chalmers University of Technology were carried out in a 23 m long, 225 mm circular concrete pipe. The pipe was constructed from 1 m long sections joined by rubber rings. The slope of the pipe was 0.1 %, the sand had a grain size of 2.5 mm and the sediment bed was without dunes. The roughness of the pipe was found from the experiments without sediment deposits to be represented by the Manning number as:  $M_{\text{pipe}} = 97.1 \text{ m}^{1/3}/\text{s}$  and the roughness of the sediment bed was found by a test of different roughness predictors to be two times the grain diameter, ie  $M_{\text{bed}} = 61.5 \text{ m}^{1/3}/\text{s}$ . The measured data, the rating curves calculated from the

Einstein side wall elimination procedure and the points on the rating curve calculated by the modelling system can be seen in Figure 5.2. It can be seen that there is a good agreement between the measured data and the simulated rating curves.

Additional investigations on the range of the applicability of the side elimination procedure for sewers have been carried out by Perrusquía et al., (1994). These investigations revealed that the difference between the side wall elimination procedure and a numerical turbulence model, the PHOENICS model, for prediction of the boundary shear stress is of the order 5 %. Hence, the accuracy of side wall elimination procedure is sufficient for one dimensional modelling of sewer systems.

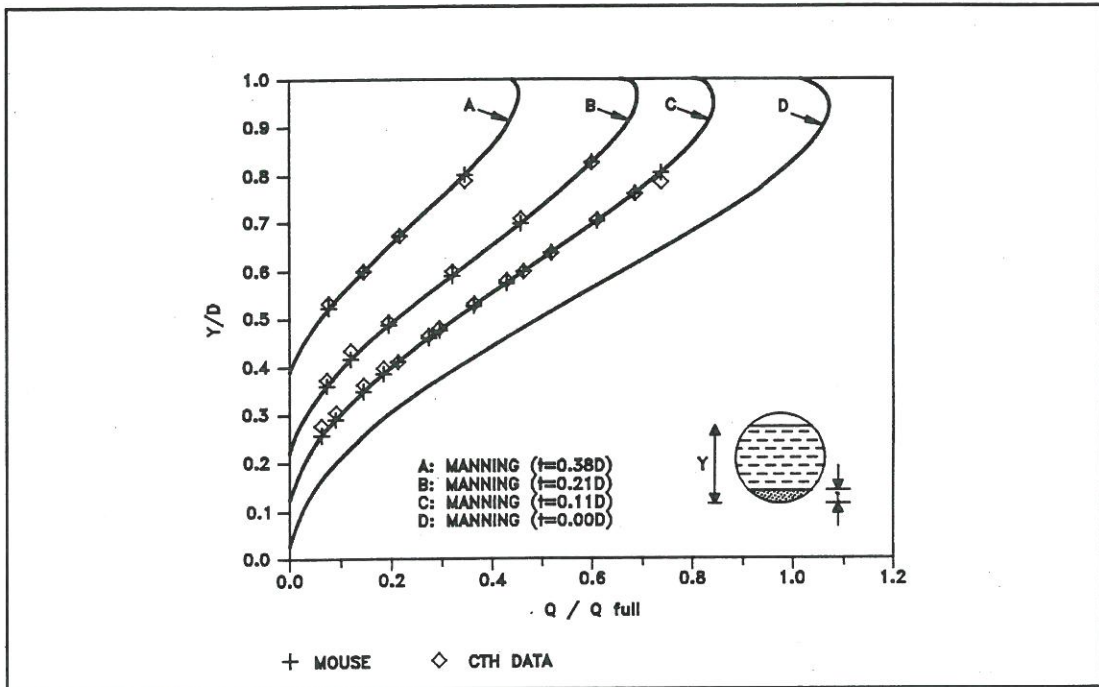
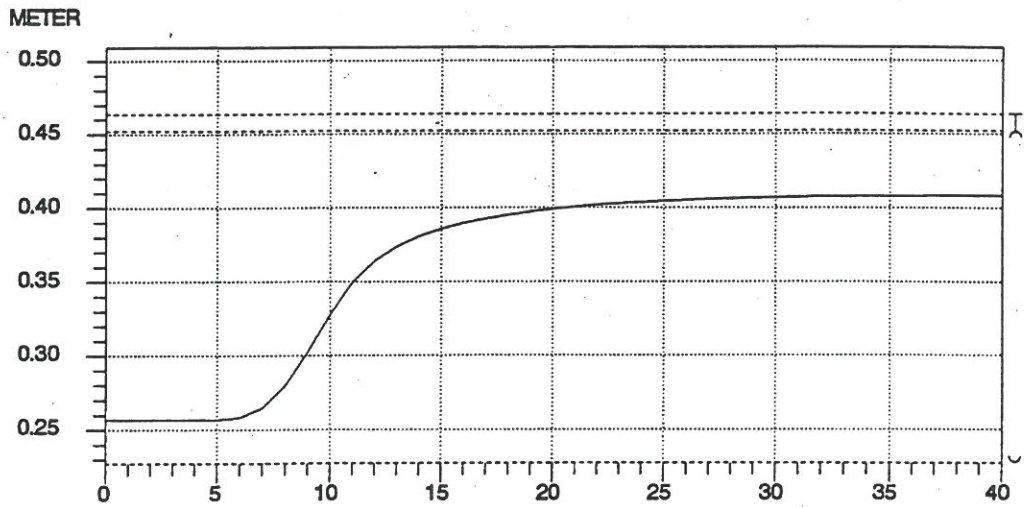


Figure 5.2. The side wall elimination theory together with simulations from the present modelling system, MOUSE, and the measurements from Chalmers University of Technology, CTH data, (Perrusquía, 1992).

In order to visualise the effect from sediment deposits on the average Manning number, the average Manning number is plotted as a function of the water depth, see Figure 5.3. From the Figure 5.3 it can be seen how the average Manning number, found by use of the side wall elimination procedure, changes as a function of the water depth. For small water depths the Manning number is approximately equal to the Manning number from the sediment bed and for large water depths the Manning number approaches the Manning number for the pipe. It can be seen that there is a difference of approx 50 % between the Manning number for low flow and pipe full flow conditions. This means that numerical models for the hydrodynamics in sewers cannot be calibrated satisfactory for both low flow and pipe full conditions if sediment deposits are present and this variation of the Manning number not is taken into account.

WATER LEVEL BRANCHES 1 - 2 273 METER



Manning number, 1 -- 2 273 METER

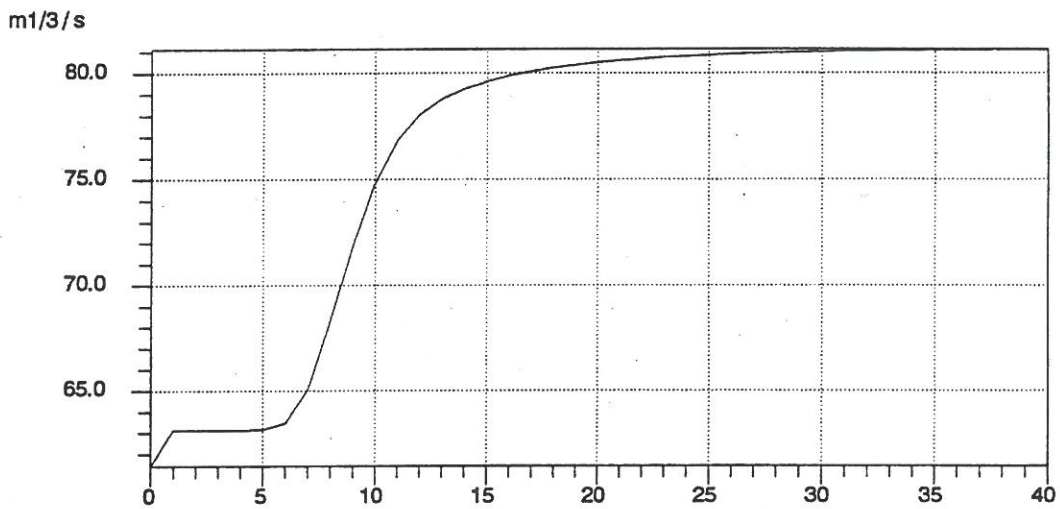


Figure 5.3. The water depth and the average Manning number as a function of time in a pipe with a sediment deposit, pipe diameter=0.225 m,  $M_{pipe}=97$ ,  $M_{bed}=61.5$ . The invert of the pipe is at level 0.23 meter.

## 5.2 Comparison of Predicted Bed Resistance with Measured Data

The calculated bed shear stresses from the experiments at Chalmers University of Technology are in general small compared to the bed shear stresses which may be observed during storm conditions in a sewer system. The observed<sup>1</sup> bed shear stress in the experiments at Chalmers University of Technology for a pipe flowing part-full has been compared to the bed shear stress predicted by the Ackers-White, the Engelund-Hansen, the Engelund-Fredsoe and the van Rijn model. The input to the formulae for the prediction of the bed shear stress are the sediment properties together with the hydraulic parameters measured in the laboratory, ie grain size, density of the sand, water depth and the discharge, etc. The general parameter used in this section to describe the bed shear stress is the dimensionless bed shear stress,  $\theta$ , defined as:

$$\theta = \frac{\tau}{\gamma (s-1) d} \quad (5-1)$$

where

$\tau$  is the bed shear stress  
 $s$  is the relative density of the sediment  
 $\gamma$  is the specific gravity of water  
 $d$  is the grain diameter

In order to evaluate the importance of the resistance from bed forms compared to the grain friction in sewer systems, the grain friction was calculated by the van Rijn model as this model divides the total bed shear stress into the grain friction and the friction from bed forms. The equations are given in the Technical Reference Manual pp. ST 54-57. The calculated grain shear stress was plotted together with the observed bed shear stress, see Figure 5.4. It can be seen from Figure 5.4 that the grain shear stress gives a good estimate of the total bed shear stress for very small bed shear stresses when no bed forms are present. When the bed shear stress increases the calculated grain shear stress significantly underestimates the bed shear stress as the importance of the resistance from the bed forms increases. In the experiment with the highest bed shear stresses, the total bed shear stress is of the order of 3-10 times larger than the grain shear stress. Hence, the resistance from the bed forms must be taken into account in order to describe the total bed shear stress in a pipe with non-cohesive sediment deposits.

---

<sup>1</sup> The term observed bed resistance covers the fact that the bed resistance was calculated by use of the side wall elimination procedure from observed water levels, pipe slope, etc.

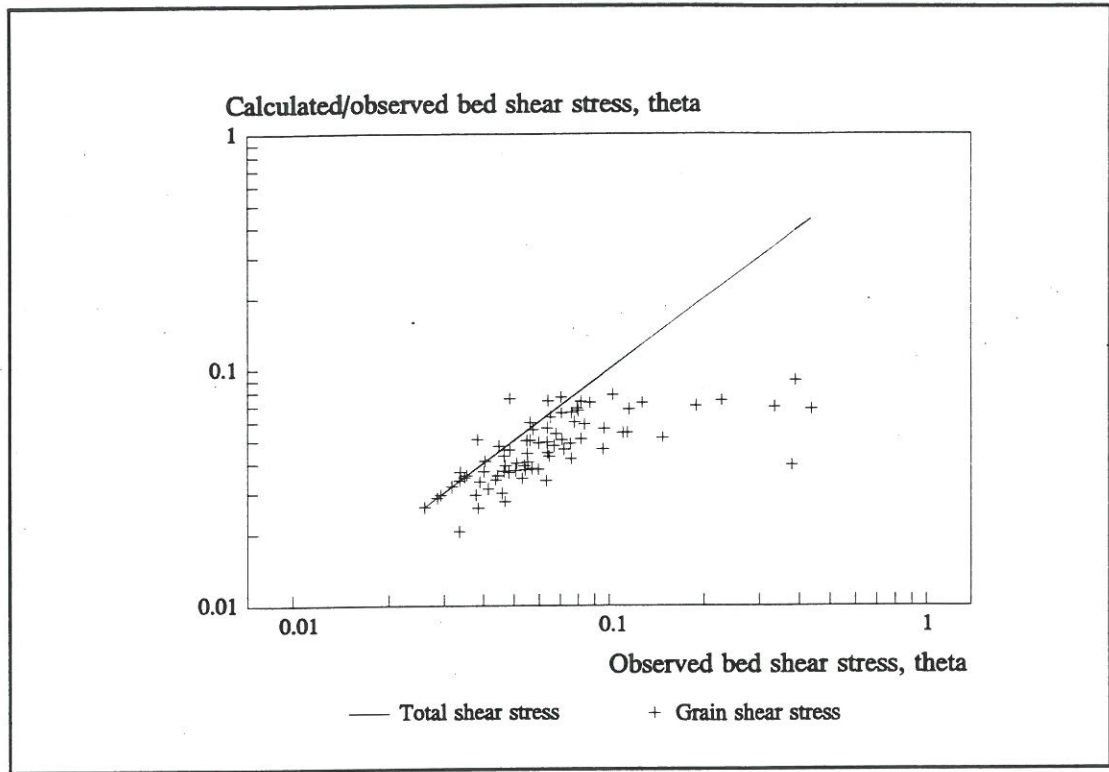


Figure 5.4. The grain friction and the total bed shear stress plotted against the observed bed shear stress. Experimental data from (Perrusquía, 1992).

### 5.2.1 The Ackers-White Model

The prediction of the bed resistance according to White et al. (1979), is an extension to the original Ackers-White model. The method is an iterative procedure and is described in the Technical Reference Manual pp. ST 22-24. In general the model performs well but it overestimates the dimensionless bed shear stress,  $\theta$ , by a factor of 2-3 for bed shear stress in the range 0.06-0.1. The comparison between the dimensionless bed shear stress observed in the experiments and the dimensionless bed shear stress predicted by the Ackers-White model can be seen in Figure 5.5.



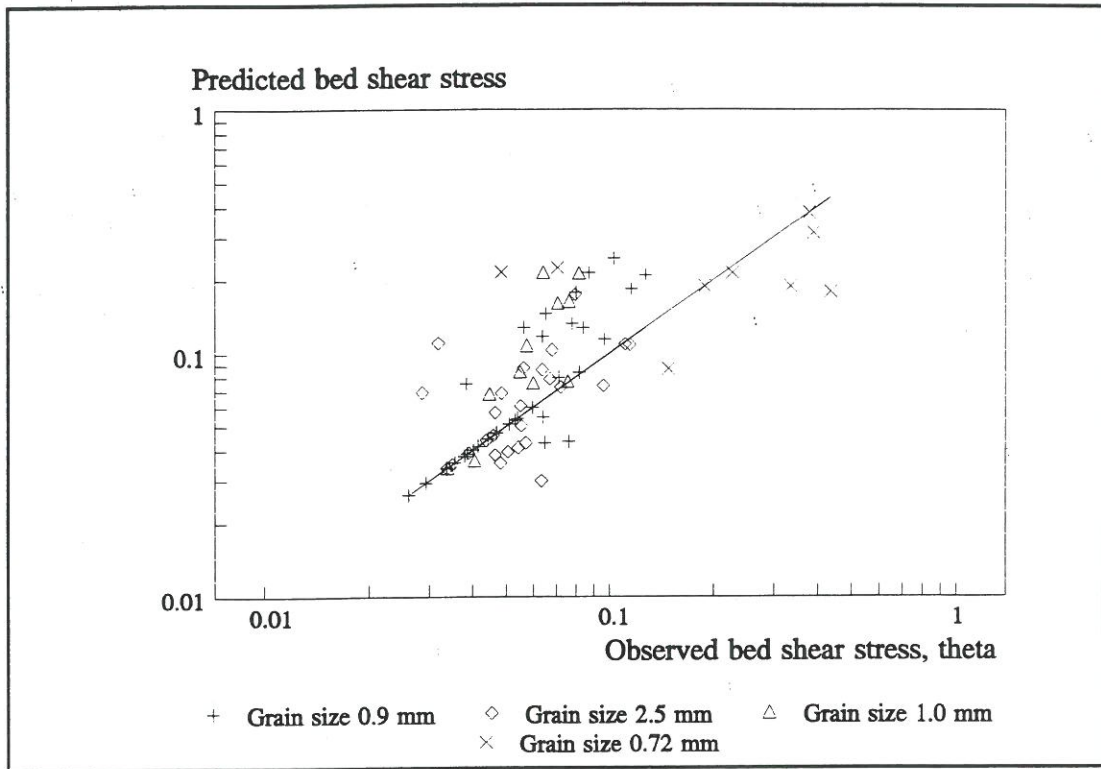


Figure 5.5. Comparison of the dimensionless bed shear stress observed in the experimental data with the dimensionless bed shear stress predicted by the Ackers-White model. Data from Perrusquía (1992).

### 5.2.2 The Engelund-Hansen Model

The prediction of the bed shear stress in the Engelund-Hansen model is based on an empirical relation between the bed shear stress and the skin friction, the  $\theta$ - $\theta'$  relation. The equations for the prediction of the bed resistance are given in the Technical Reference Manual pp. ST 24-30. The model gives a good estimate of the small bed shear stresses, but the model has a tendency to underestimate the large bed shear stresses. The comparison between the dimensionless bed shear stress,  $\theta$ , calculated from the experiments and the dimensionless bed shear stress predicted by the Engelund-Hansen model can be seen in Figure 5.6.

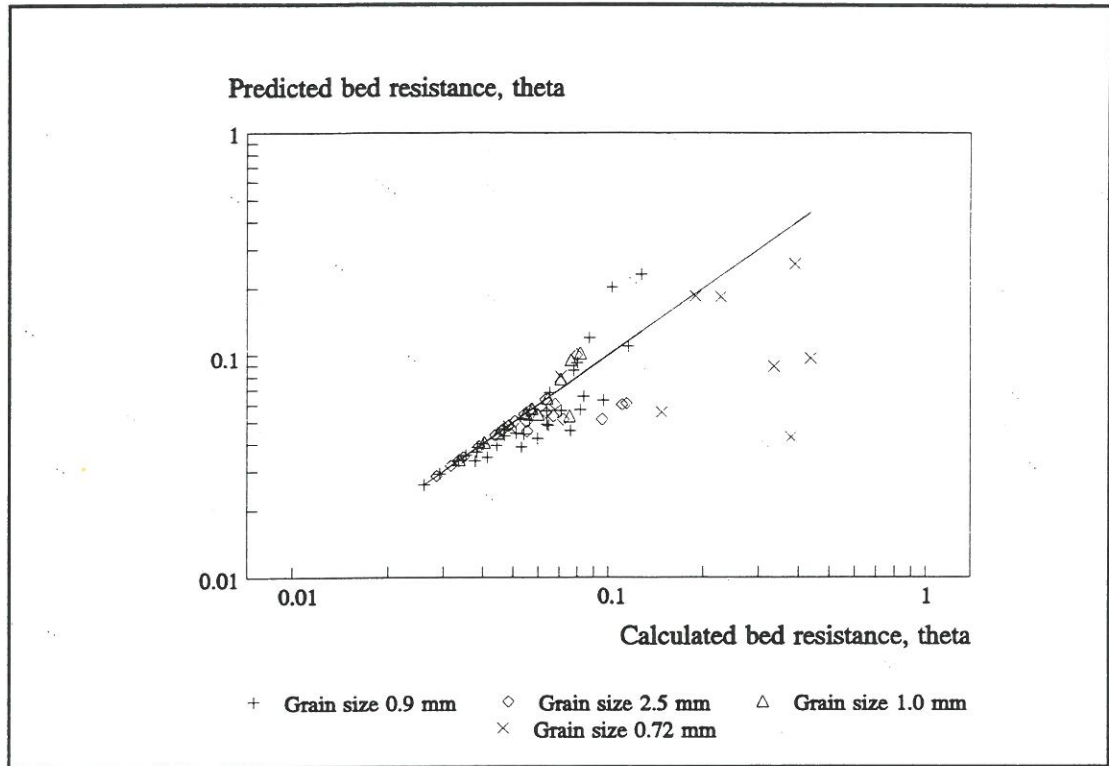


Figure 5.6. Comparison of the dimensionless bed shear stress calculated from the experimental data (Perrusquía, 1992) with the dimensionless bed shear stress predicted by the Engelund-Hansen model.

### 5.2.3 The Engelund-Fredsoe Model

The prediction of the bed shear stress in the Engelund-Fredsoe model is based on the  $\theta-\theta'$  relation and a calculation of the bed form dimensions. The equations for the prediction of the bed resistance are given in the Technical Reference Manual pp. ST 34-46. In general the model overestimates the bed form height and underestimates the bed form length for the 0.9 and the 1.0 mm grain fractions, see Figure 5.7 and 5.8. This may be the reason why the model overestimates the dimensionless bed shear stress for these grain fractions, as the bed shear stress is proportional to the bed form height to the power two and the bed form length to the power minus one (Fredsoe, 1984). The model performs well with no bias for the estimation of the small dimensionless bed shear stresses,  $\theta$ , (0.03-0.1), but for higher bed shear stresses a larger scatter is present in the predicted dimensionless bed shear stresses. The comparison between the dimensionless bed shear stress,  $\theta$ , and the dimensionless bed shear stress predicted by the Engelund-Fredsoe model can be seen in Figure 5.9.

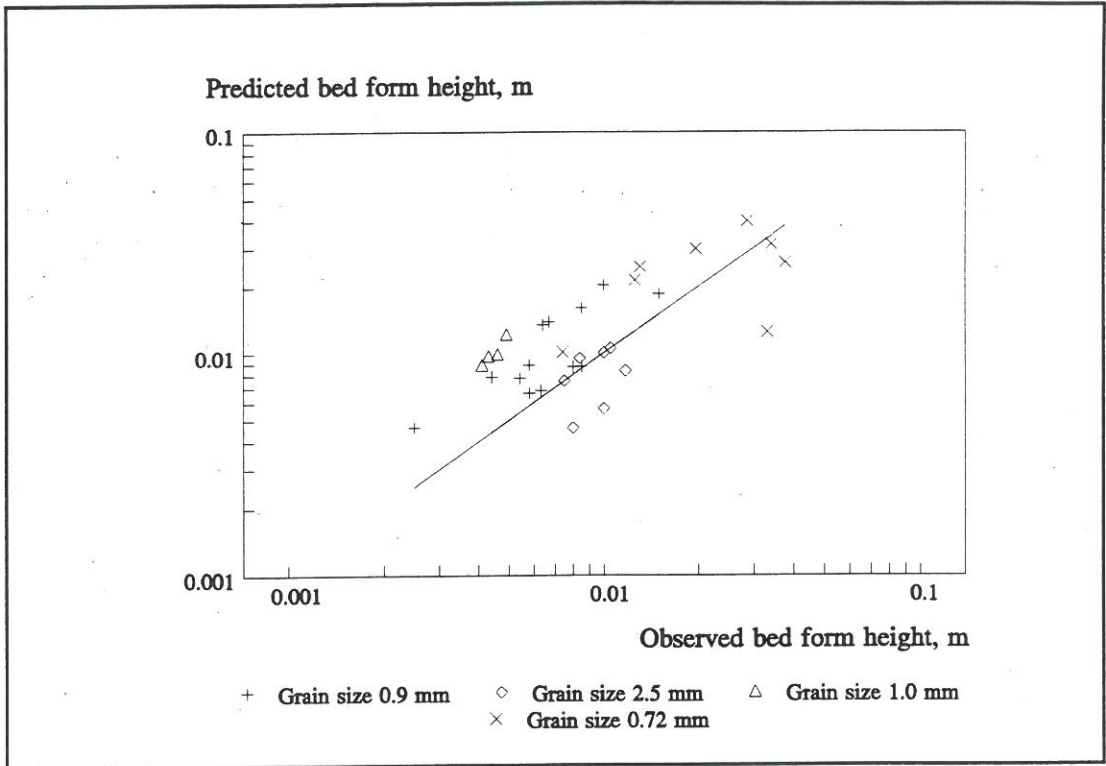


Figure 5.7. Comparison of the observed bed form height with the bed form height predicted by the Engelund-Fredsøe model. Experimental data from (Perrusquía, 1992).

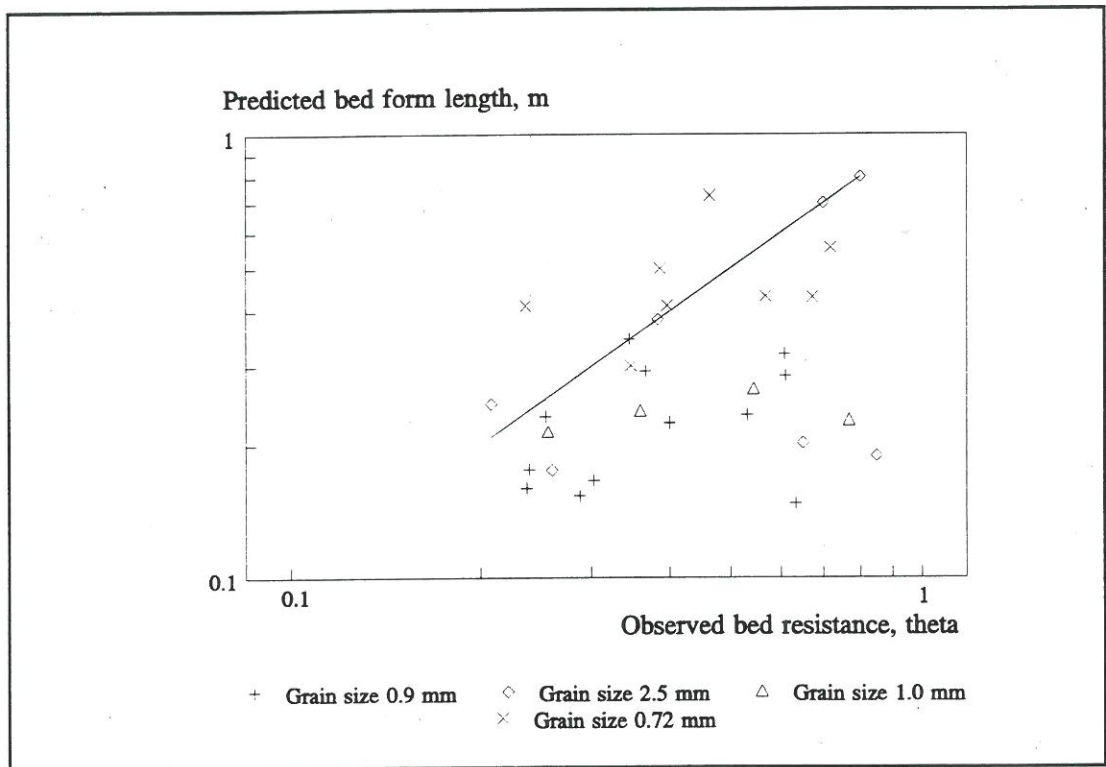


Figure 5.8. Comparison of the observed bed form length with the bed form length predicted by the Engelund-Fredsøe model. Experimental data from (Perrusquía, 1992).

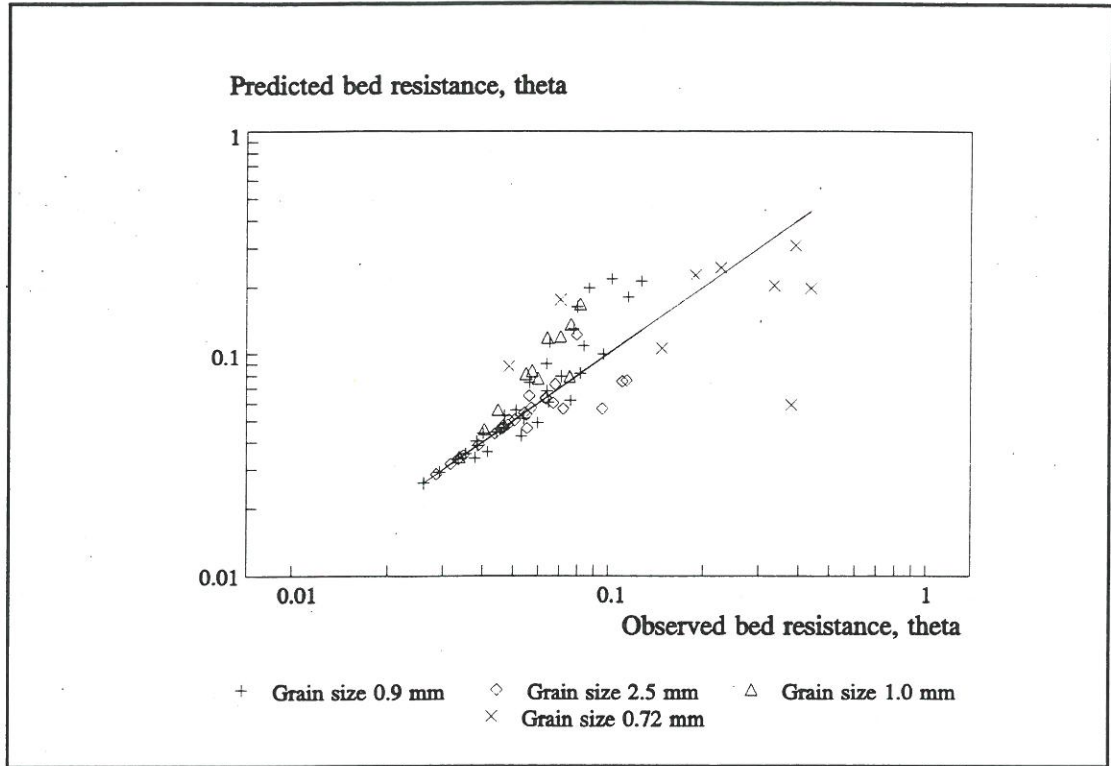


Figure 5.9. Comparison of the dimensionless bed shear stress observed in the experimental data with the dimensionless bed shear stress predicted by the Engelund-Fredsoe model. Experimental data from (Perrusquia, 1992).

#### 5.2.4 The van Rijn Model

The van Rijn model calculates the bed shear stress from the height and the length of the bed forms. The formulae for the bed form dimensions are given in the Technical Reference Manual pp. ST 54-57. The comparison between the observed bed form dimensions and calculated bed form dimensions can be seen in Figure 5.10 and 5.11. The comparison between the dimensionless bed shear stress calculated from the experiments and the dimensionless bed shear stress predicted by the van Rijn model can be seen in Figure 5.12.

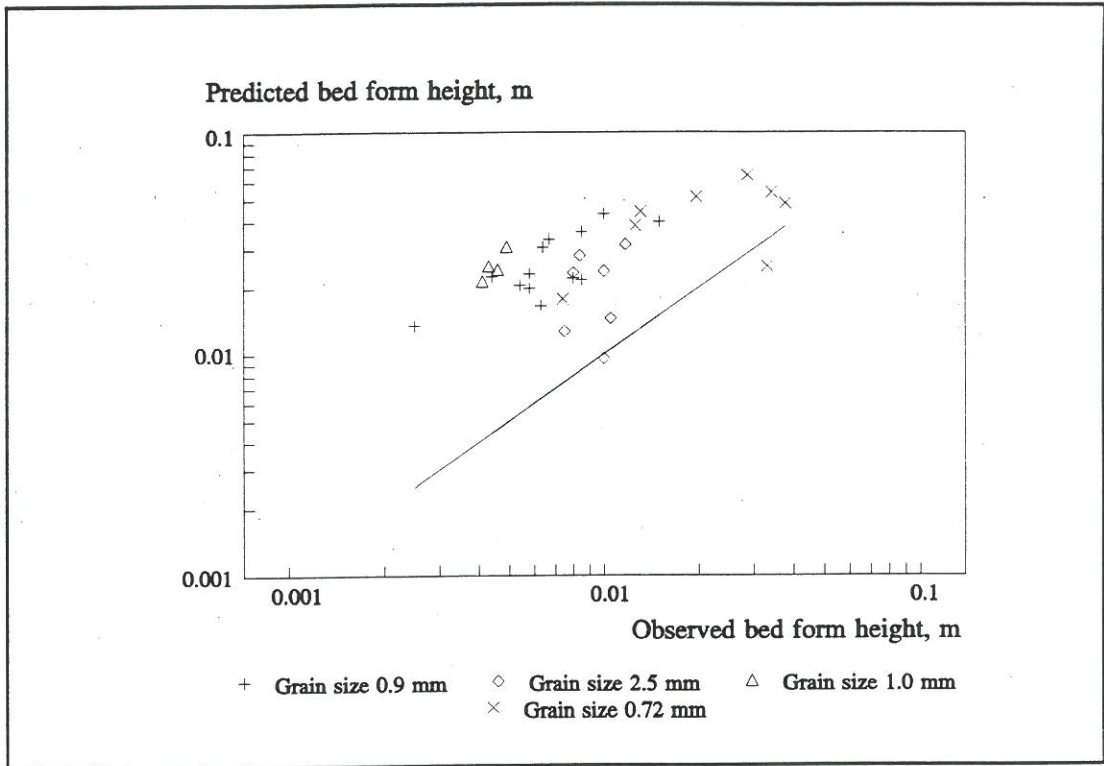


Figure 5.10. Comparison of the observed bed form height with the bed form height predicted by the van Rijn model. Experimental data from (Perrusquía, 1992).

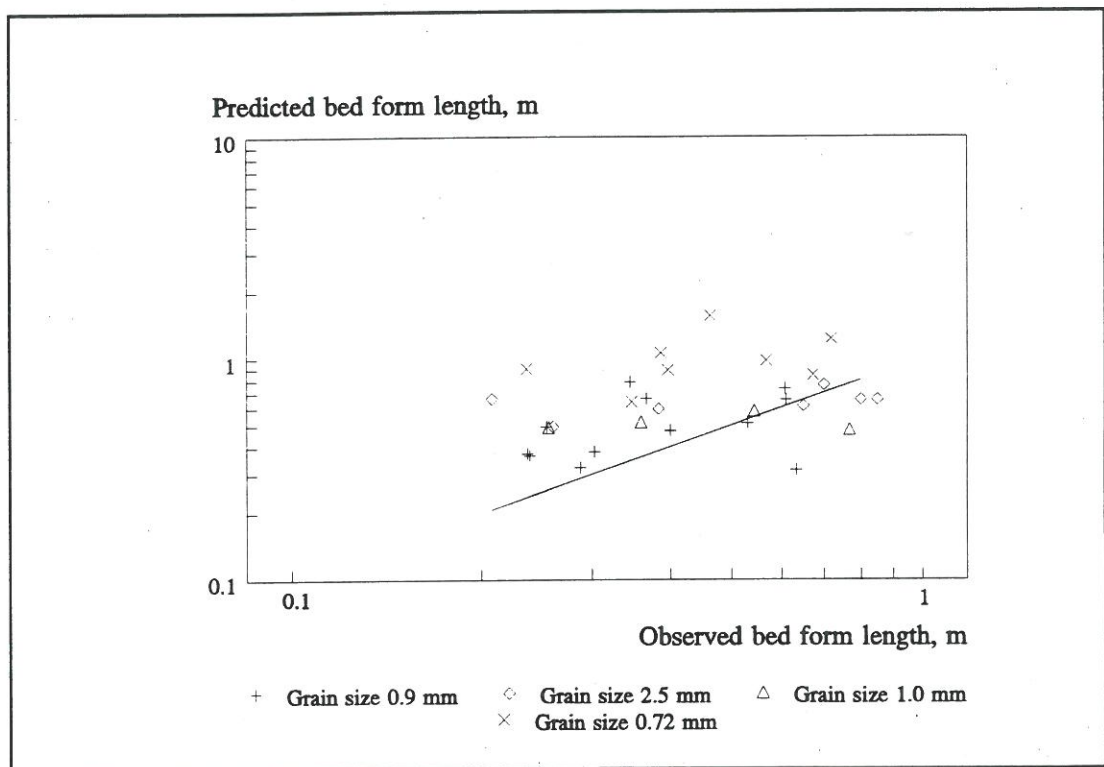


Figure 5.11. Comparison of the observed bed form length with the bed form length predicted by the van Rijn model. Experimental data from (Perrusquía, 1992).

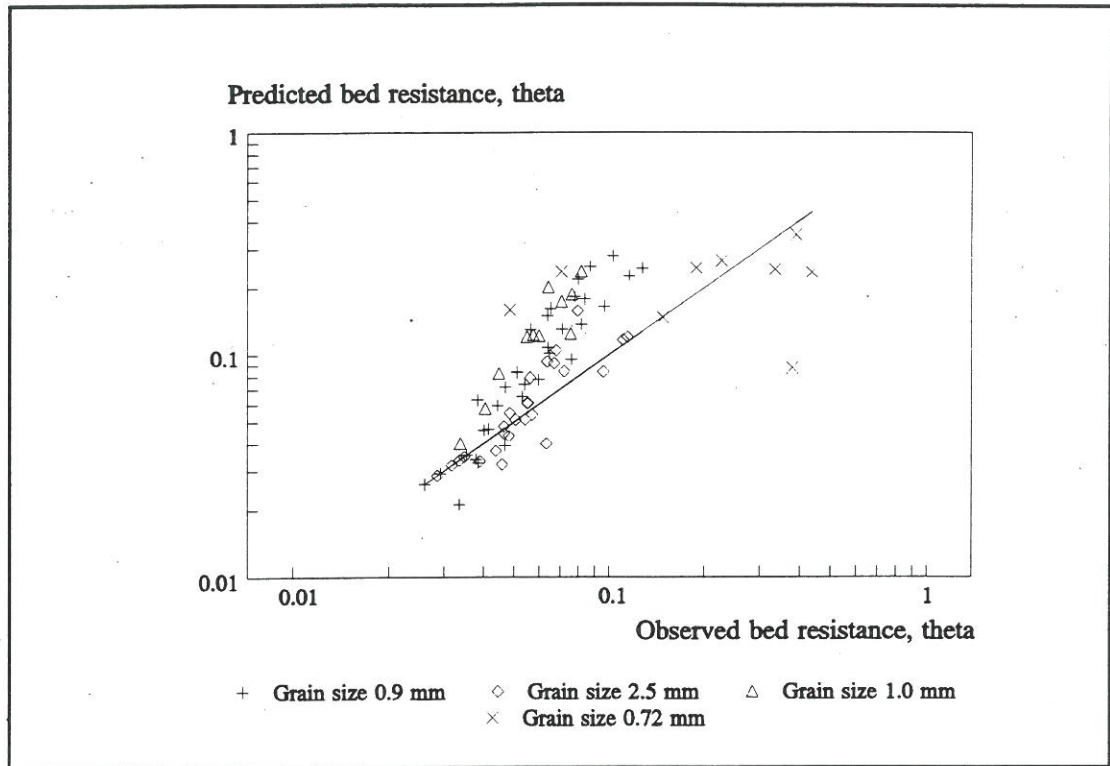


Figure 5.12. Comparison of the observed dimensionless bed shear stress with the dimensionless bed shear stress predicted by the van Rijn model. Experimental data from (Perrusquia, 1992).

The total bed resistance predicted by the van Rijn formulae is good except for dimensionless bed shear stresses in the range of 0.05-0.1, where the model overestimates the resistance by a factor of 2-3. A large scatter is present in the prediction of the bed form dimensions, but in general the van Rijn model overestimates the bed form height and the bed form length. The height of the bed forms calculated by the van Rijn formulae is a function of the same parameters as used in the calculation of the sediment transport, which again is a function of the critical bed shear stress. As the sediment transport predicted by the van Rijn model is very sensitive within the range of flow conditions in the experiments, a large scatter is expected in the prediction of the bed form height. For the sensitivity analysis on the sediment transport, see Appendix D. Furthermore, the water depth in a sewer system with sediment deposits is different from the water depth in a river with the same sediments and bed configurations as one part of the resistance in sewers originates from the pipe and another part from the sediment bed. In the van Rijn formulae the length of the bed form is only a function of the water depth. This basic assumption is probably too simple for sewer systems as a unique relation between the water depth and the bed shear stress does not exist, eg due to back water effects and the fact that the resistance originates both the pipe wall and the sediment bed. Hence, deviations between the predicted and the observed bed resistance can be expected as uncertainties exist in the prediction of both the bed form height and length, and the bed resistance is a function of the bed form dimensions.

### 5.3 Comments on the Prediction of the Bed Shear Stress

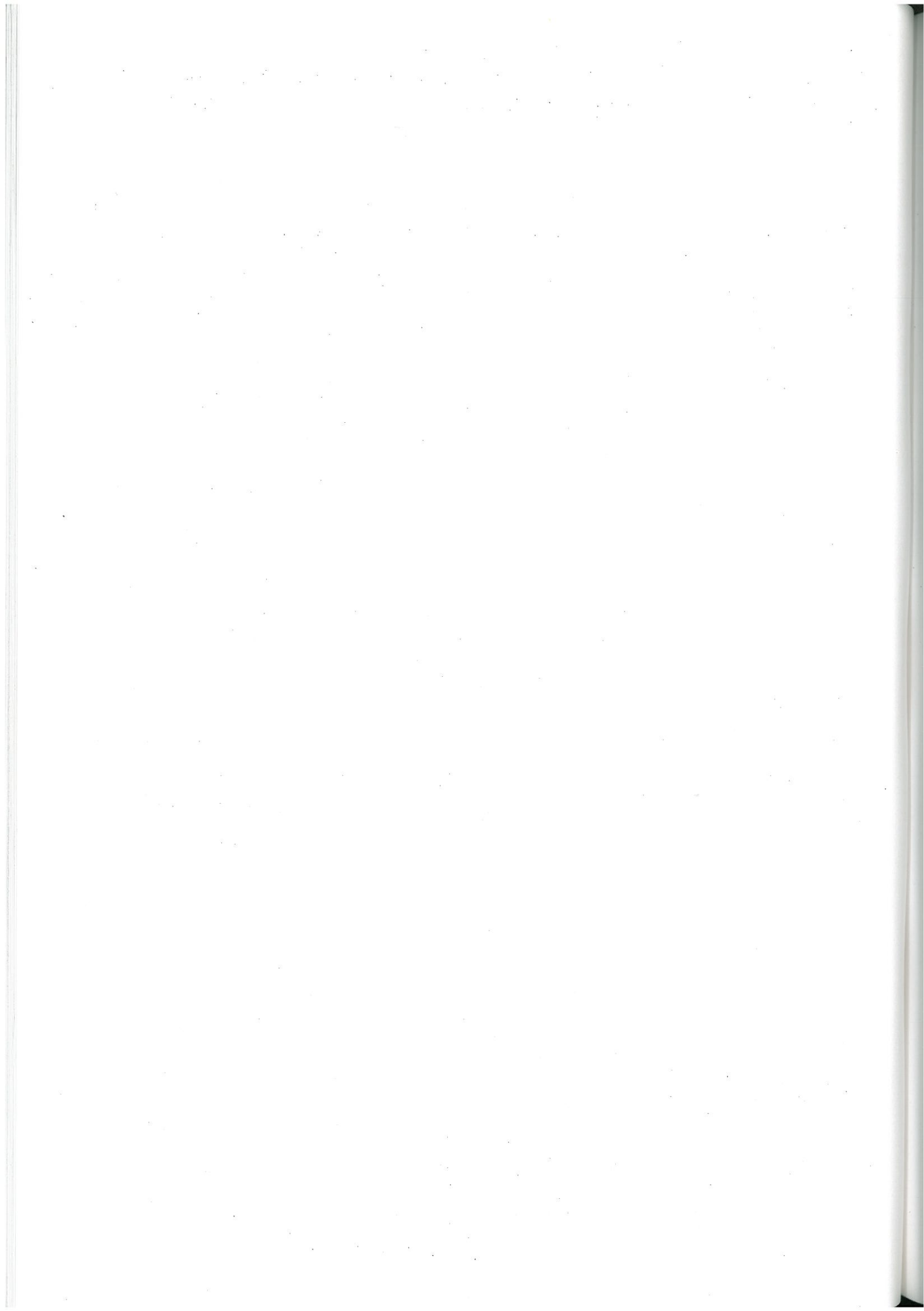
Today, insufficient data are available to evaluate the existing methods for prediction of the bed form dimensions and the bed resistance in full flowing pipes, but data are available for an evaluation of the bed shear stress in pipes flowing part full, (Perrusquía, 1992). In order to estimate the bed shear stress from non-cohesive sediment deposits in sewer systems, it was found that it is necessary to describe the resistance from both the grain and the bed forms, as the grain shear stress underestimates the total bed shear stress, and the total bed shear stress may be 3-10 times the grain shear stress.

The side wall elimination procedure can be used to predict the average bed shear stress for a pipe flowing part full with a sediment deposit. However, as the experiments at Chalmers University of Technology by Perrusquía et al. (1986) and Perrusquía (1992) were all carried out with a free surface, the side wall elimination procedure and the prediction of the bed shear stress still have to be validated against data for full flowing pipes.

The Engelund-Fredsøe model gives a fair estimate of the total bed resistance. The Engelund-Hansen model gives good estimates of the bed resistance for small bed shear stresses but it underestimates the bed shear stress for high bed shear stresses. The Ackers-White and the van Rijn models both give fair estimates of the bed shear stress, except for dimensionless bed shear stresses in the range of 0.06 - 0.1, where they overestimate the bed shear stress. All the models can be used with care to evaluate the extra resistance from bed forms in sewer systems. It is important to have a good estimate of the bed shear stress in order to give a good prediction of the sediment transport. This is because if a large scatter is present in the prediction of the bed shear stress a large scatter must be expected in the sediment transport models, as the computation of the sediment transport uses the predicted bed shear stress, eg the Engelund-Hansen and the Engelund-Fredsøe models.

The water depth is a typical parameter in the formulations for the prediction of the bed shear stress, eg the van Rijn model states that the bed form length is 7.3 times the water depth. As the flow conditions are determined from the resistance from the pipe walls and the sediment bed, a unique relationship cannot exist between the water depth and the dune length in sewers with sediment deposits even though such a relationship may exist in rivers with uniform shear flow. Hence, a better description can probably be obtained if the water depth is substituted from the formulae for the prediction of the bed resistance. Unfortunately, insufficient knowledge is available to do this at present. However, some of the uncertainties in the prediction of the bed shear stress are levelled out when the average shear stress to the flow is found by use of the side wall elimination procedure.

Experiments carried out at Delft University (Kleijwegt, 1992b) with non-cohesive sediment deposits in full flowing pipes also showed the development of bed forms. Nevertheless, the formulations for the formation of bed forms in full flowing pipes probably need some further considerations as the interaction between the free surface and the dunes does not exist in full flowing pipes. This interaction is indirectly assumed in the sediment transport formulae which commonly are used for prediction of the bed resistance in rivers, eg Engelund-Fredsøe (1984) and van Rijn (1984c).





## 6 SEDIMENT TRANSPORT IN SEWERS

The sediment transport processes in rivers and in sewers with a deposited sediment bed are basically the same. Many data are available concerning the sediment transport in rivers and flumes with an "infinite" layer of sediment in the flume, but very few data are available on sediment transport in circular pipes, except for slurry transport in suspension. When the sediment transport in sewers is investigated each mode of sediment transport has to be evaluated with respect to the special conditions in sewer systems. If the mode of sediment transport is bed load then the particles are transported due to the drag force, proportional to the bed shear stress, acting on the grains. At present it is not possible to say whether scale effects exist for the bed resistance (the bed form dimensions) and the bed load transport in sewers. As a small pipe and a pipe with a thin layer of sediment not are similar to a river, it may be expected that the sediment transport formulae have to be adjusted for small pipes. But if the scale effects are negligible and the bed shear stress can be found, then the results from experiments with bed load transport in ordinary flumes are directly applicable to sewers.

A general problem is that very few studies have been carried out within the range of flow conditions which exist in sewers, hence little knowledge is available concerning the influence from the pipe walls and the concentration profile on the sediment transport. Furthermore, sewers very rarely have an unlimited supply of sediments and their sediments often have cohesive properties. At present, insufficient data exist to develop specific sediment transport formulae for sewers. However, it is assumed that sediment transport formulae for large pipes approximate sediment transport formulations for rivers as large sewers in principle act as small rivers/flumes. Hence, the sediment transport formulae for sewers should be an extension of the existing, well proven sediment transport formulations for rivers with special considerations if the pipe is very small, the layer of sediment in the pipe is thin or the pipe is running full.

### 6.1 Selection of a Sediment Transport Formula for Sewers

So far there is no reliable sediment transport formula which is valid for all ranges of natural flow conditions, (Correia et al. 1992). Hence, when a sediment transport formula is applied to a river/channel and in particular to a sewer system it is important that the formula is applicable to the transport mode, and it should have been validated for the flow conditions and the sediment characteristics, eg particle size and density, in the study. Further, it is very important to be aware of the assumptions and the limitations of the formula.

The selection of a sediment transport formula for a specific study of the sediment transport in a sewer system depends on the sediment characteristics and the flow characteristics including the level of turbulence in the flow. During dry weather flow, the non-cohesive sediment in the sewer system will typically be transported as

bed load transport. During storm situations some of the sediments will be transported as bed load but most sediment will be transported in suspension, depending on the flow and the sediment characteristics. The sediment in suspension is either transported as suspended load which from time to time is in contact with the bed or it is transported as wash load, ie advection transport with the flow velocity.

If the phenomenon studied is characterized by small flow velocities and the sediment has a high density,  $1.8 \text{ kg/m}^3 - 2.65 \text{ kg/m}^3$ , ie the sediment has a high fall velocity, then it has been shown by eg Nalluri and El-Zaemey (1993) and Perrusquía (1992) that the sediment transport can be modelled by use of a bed load formula for non-cohesive sediment, eg Fredsøe (1984), van Rijn (1984a), Novak and Nalluri (1975), or Perrusquía (1992).

If high flow velocities exist and the sediment has a high fall velocity then it is necessary to use a sediment transport formula for non-cohesive sediments which describes both bed load transport and suspended load transport, eg Ackers-White (1973), Engelund-Hansen (1967), Engelund-Fredsøe (1984) or van Rijn (1984a and 1984b).

If high velocities exist and the sediment has a small density  $1000 \text{ kg/m}^3 - 1500 \text{ kg/m}^3$ , ie the sediment has a small fall velocity, the sediment transport must be described as suspended transport by use of an advection model including a description for erosion and deposition, as the sediment transport locally is a function of both the local flow and the upstream conditions.

If more sediment transport formulae are applicable to a transport mode then these formulae should be evaluated against measurements, and a sensitivity analysis carried out for each formula. The sediment transport formula which gives the best fit and which is the least sensitive within the range of the flow conditions and sediment characteristics in the study data should be selected.

### 6.1.1 The Bed Load Mode of Transport

The difference between a sewer and a river is that in a sewer the shear stress is derived from both the pipe and the sediment bed while the shear stress in a river is more or less only determined by the sediment bed. One way to determine the shear stress on the sediment bed in a sewer is to apply a side wall elimination procedure<sup>1</sup>. Once a side wall elimination procedure has been applied to find the bed shear stress then there is no difference between computation of the bed load transport taking place in a wide pipe with a sediment deposit and that taking place in a flume/river.

---

<sup>1</sup> For further information on the side wall elimination procedure, see Chapter 5.

### 6.1.2 The Suspended Load Mode of Transport

The traditional sediment transport formulations for suspended load transport in rivers are based on the assumption of a logarithmic velocity profile. The velocity profile in sewers changes from a logarithmic velocity profile similar to that in rivers when the pipe is flowing part full to a double logarithmic velocity profile when the pipe is flowing full. Examples of the two types of velocity profile can be seen in Figure 6.1 and 6.2. The suspended load is traditionally calculated as the integral over the cross-section area of the concentration multiplied by the velocity, ie:

$$q_s = \int_A u(x,y) \cdot c(x,y) da \quad (6-1)$$

where

- $q_s$  is the suspended sediment transport, (m<sup>3</sup>/s)
- $u(x,y)$  is the velocity, (m/s)
- $c(x,y)$  is the concentration, arbitrary unit (-)
- $A$  is the flow area, (m<sup>2</sup>)
- $x$  is the horizontal coordinate, (m)
- $y$  is the vertical coordinate, (m)

Little research has yet been carried out concerning the variation of the concentration profile over the cross-section in sewers. Investigations of the concentration profile have been carried out for sewers flowing part full (Ashley et al., 1992; Ristenpart et al., 1994 and Verbanck, 1994). These investigations have shown that a variation exists in the concentration profile and Ristenpart et al. (1994) found a good agreement between the variation in concentration along the centre line in a the sewer and the classical Rouse concentration profile. In rivers the computation of the suspended load is usually based on the following differential equation, reflecting an equilibrium distribution of suspended load:

$$\epsilon_s \frac{dc}{dy} + wc = 0 \quad (6-2)$$

where

- $\epsilon_s$  is the sediment diffusion coefficient (m<sup>2</sup>/s)
- $c$  is the concentration, (-)
- $w$  is the fall velocity, (m/s)

In wide rivers it is usually assumed that the sediment diffusion coefficient,  $\epsilon_s$ , is approximately equal to the eddy viscosity,  $\epsilon$ , ie:

$$\epsilon_s = \epsilon = \kappa u_f y \left(1 - \frac{y}{Y}\right) \quad (6-3)$$

$$\epsilon_s = \epsilon = \kappa u_f y \left(1 - \frac{y}{Y}\right) \quad (6-3)$$

where

$\kappa$  is the von Karman constant, ( $\kappa \approx 0.41$ )  
 $u_f$  is the friction velocity, (m/s)  
 $Y$  is the water depth in the river or in the pipe, (m)

This gives concentration profiles according to the Rouse profile:

$$c = c1 \cdot \left(\frac{Y-y}{y}\right)^Z \quad (6-4)$$

where

$Z = w/(\kappa u_f)$  is the Rouse number  
 $c1$  is a constant

The constant,  $c1$ , can be found when the concentration is known at a reference level, ie this is the boundary condition for the differential equation. The expression in equation (6-4) is from Rouse (1939), and it has been experimentally verified by Vanoni (1946).

According to Ristenpart et al. (1994) it can be assumed that the concentration profiles are the same along the middle of a pipe as in a river, thus the change in suspended transport,  $\alpha$ , from the change in velocity profile in the middle of a full running pipe can be evaluated as:

$$\alpha = \frac{\int_0^Y u(y)_{river} \cdot c(y) dy}{\int_0^Y u(y)_{sewer} \cdot c(y) dy} \quad (6-5)$$

The integral in equation (6-5) has been evaluated for the following data:

water depth,	1 m
pipe diameter	1 m
Chezy no.	40 m <sup>1/2</sup> /s
mean velocity	0.6 m/s

The velocity profiles for the pipe and the river are shown in Figure 6.1 and 6.2. The concentration profile for a Rouse number,  $Z = 0.5$ , can be seen in Figure 6.3 and

the result of the evaluation of the integral is shown in Figure 6.4. From Figure 6.4 it can be seen that the suspended load transport is the same in rivers and sewers for small Rouse numbers, which corresponds to a uniform distribution of the concentration profile over the water depth. Similarly it can be seen from the figure that for large Rouse numbers suspended load transport calculated based on river formulations should be multiplied by a factor of 1.4 in order to give the suspended load transport in a pipe. However, it should be noted that this factor probably changes when the suspended load is calculated over the full cross-section of the sewer by use of the integral given in Equation (6-1). In the implemented sediment transport models it is possible to multiply the bed load, the suspended load or the total sediment transport by a factor in order to calibrate the sediment transport model, hence it is possible to calibrate the implemented formulae to the flow conditions in full running sewers.

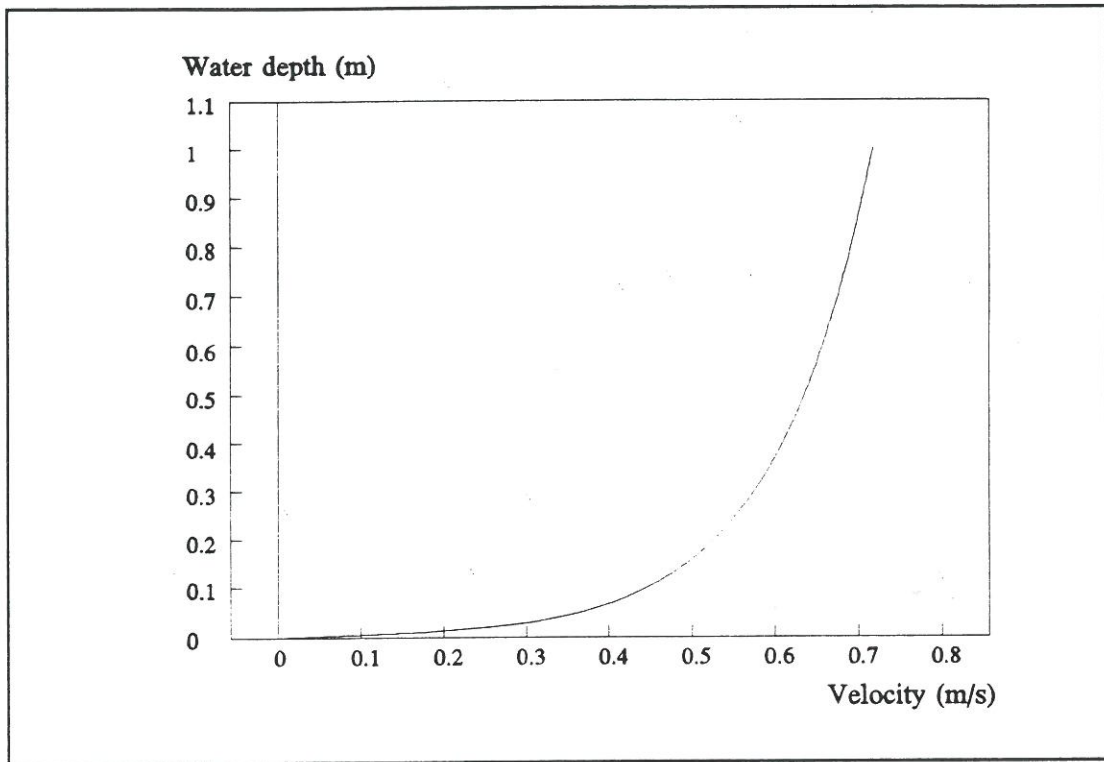


Figure 6.1. The velocity profile in a river. Water depth = 1 m and Chezy no. =  $40 \text{ m}^{1/2}/\text{s}$ .

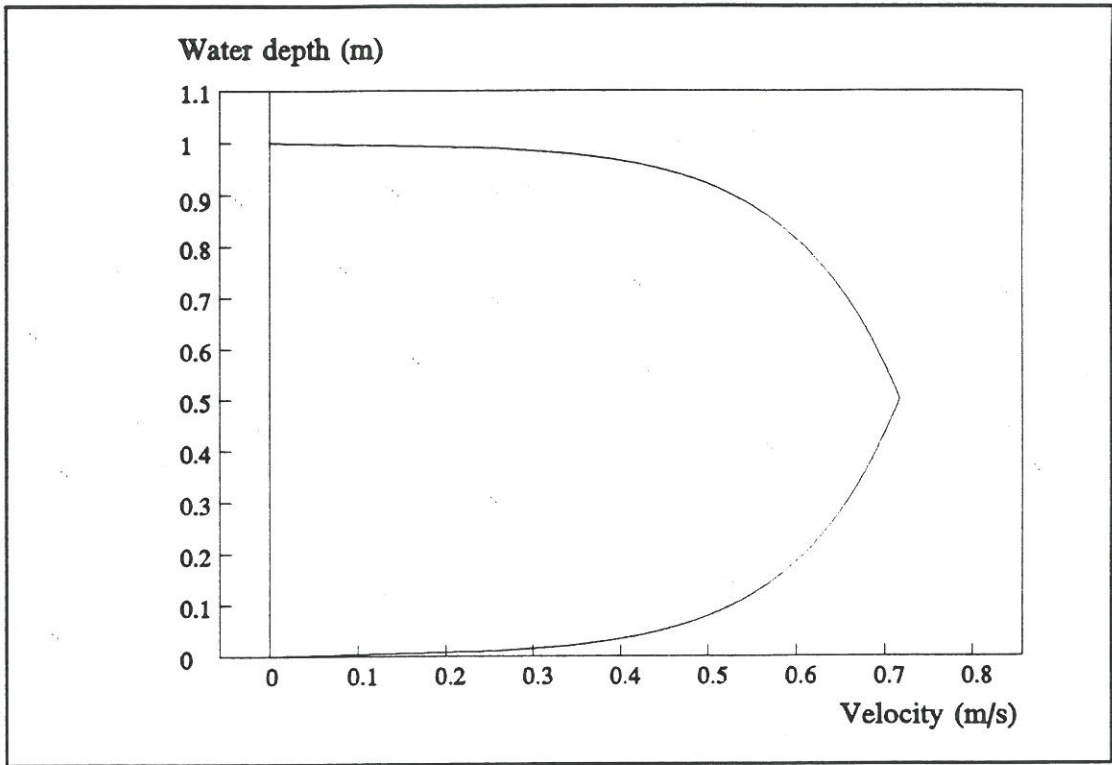


Figure 6.2. The velocity profile in a pipe. Water depth = 1 m, Chezy no. =  $40 \text{ m}^{1/2}/\text{s}$  and pipe diameter = 1 m.

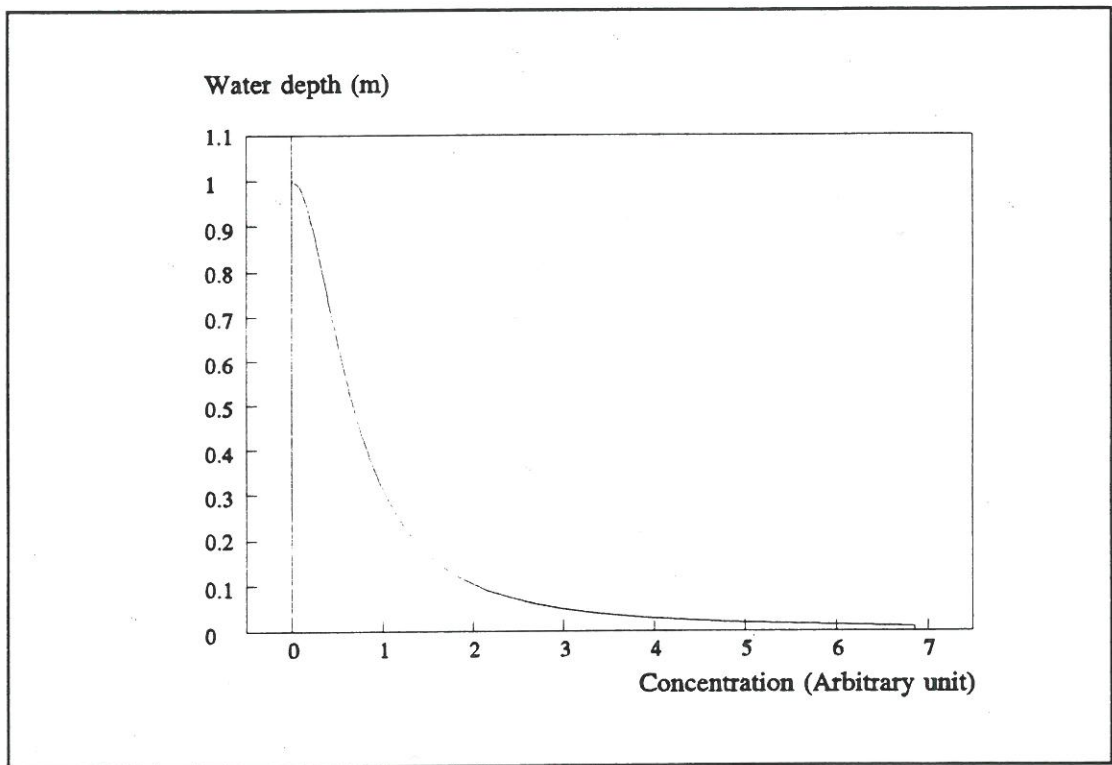


Figure 6.3. The concentration profile for a Rouse number,  $Z = 0.5$ .

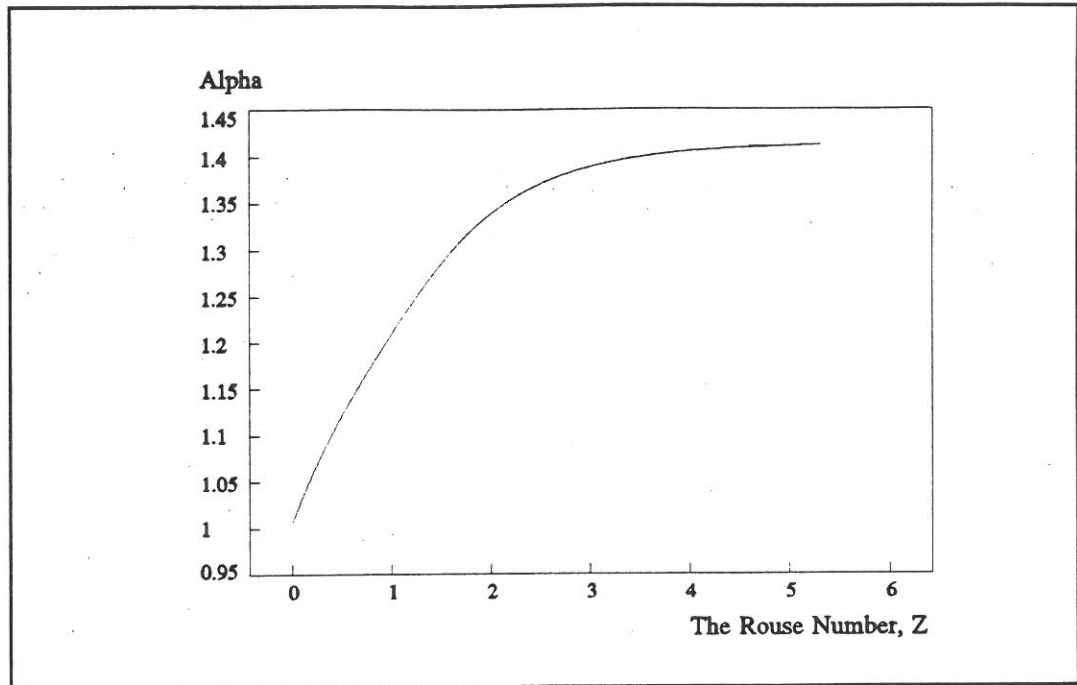


Figure 6.4. The change in suspended transport,  $\alpha$ , from the change in velocity profile for a river and a sewer as a function of the Rouse number. Velocity = 0.6 m/s, Chezy no. =  $40 \text{ m}^{1/2}/\text{s}$  and water depth = 1.0 m.

### 6.1.3 The Wash Load Transport

No major difference should be expected between the transport formulations for sewers and rivers if the wash load has a uniform concentration profile. However, referring to the discussion on the "heavy-fluid layer" in Section 4.4.3, this may not always be the case in sewers. If large gradients are present in the concentration profile the description of the transport of fine particles has to be modified. The transport of the fine particles will then take place with a smaller velocity than the mean flow velocity. The average velocity of the fine particles is a function of the local flow velocity and the local concentration, it can be calculated as:

$$v_{\text{fine particles}} = \frac{\int_0^A u(x,y) \cdot c(x,y) \, da}{\int_0^A c(x,y) \, da} \quad (6-6)$$

where

A is the flow area, ( $\text{m}^2$ )  
 $v_{\text{fine particles}}$  is the average transport velocity of the fine sediment particles, (m/s)

A factor,  $\beta$ , which relates the average flow velocity to the average transport velocity of the fine sediments can now be defined as:

$$q_s = \beta \bar{C} \bar{u} A \quad (6-7)$$

where

- $q_s$  is the suspended sediment transport, ( $m^3/s$ )
- $\beta$  is the factor for the non-uniform distribution of the concentration over the depth
- $\bar{C}$  is the mean concentration, (arbitrary unit)
- $\bar{u}$  is the mean flow velocity, ( $m/s$ )
- $A$  is the flow area, ( $m^2$ )

The average transport velocity for the fine sediments as a function of the Rouse Number is shown in Figure 6.5. From Figure 6.5 it can be seen that the average transport velocity of fine particles decreases as the concentration profile becomes non-uniform, i.e. the advection-dispersion equations have a transport velocity which is too high for this phenomenon in sewer systems.

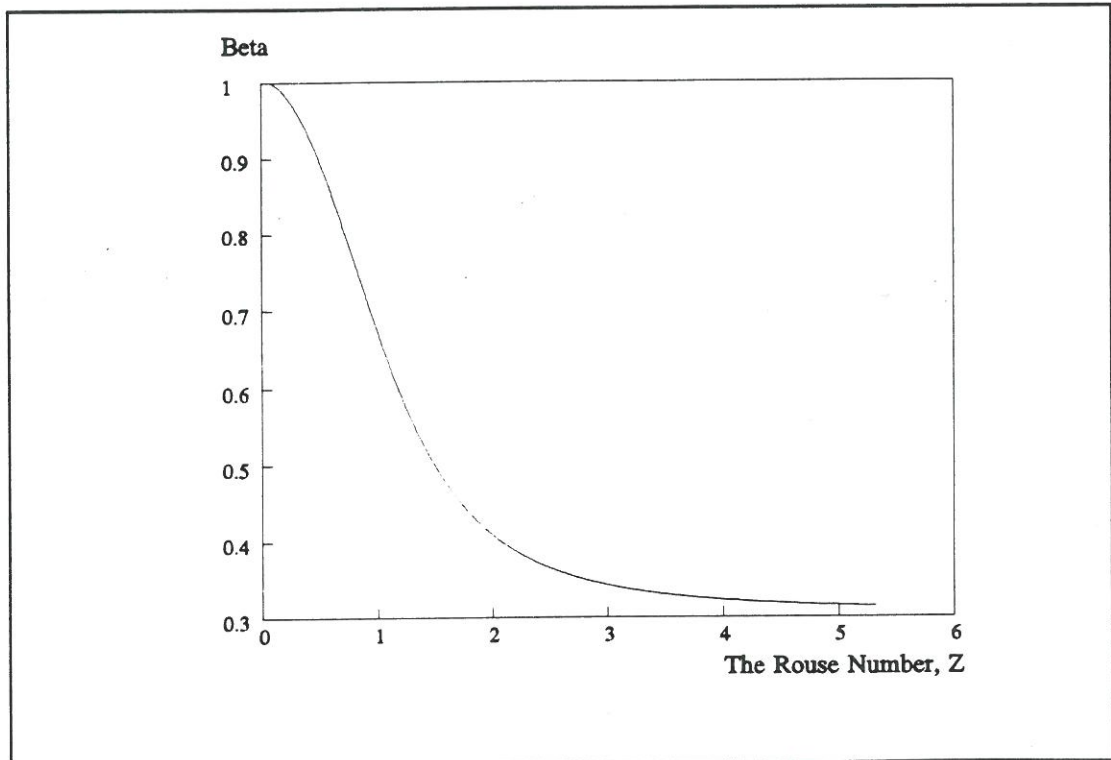


Figure 6.5. The change in average transport velocity,  $\beta$ , for fine sediments in a sewer as a function of the Rouse number. Mean flow velocity = 0.6 m/s, Chezy no. = 40  $m^{1/2}/s$  and water depth = 1.0 m.



The advection-dispersion equations can be modified to describe the transport of fine sediments with a non-uniform distribution of the concentration over the water depth. The modification consists of an introduction of the average transport velocity of the fine sediment by use of the constant,  $\beta$ , defined in Equation (6-7), multiplied with the average flow velocity. If the advection-dispersion equation has to be modified according to:

$$\frac{\partial(AC)}{\partial t} + \frac{\partial(\beta QC)}{\partial x} - \frac{\partial}{\partial x} \left( AD \frac{\partial C}{\partial x} \right) = C_s \cdot q \quad (6-8)$$

where

$\beta$	is the factor for the non-uniform distribution of the concentration over the depth
$C$	is the concentration (arbitrary unit)
$A$	is the area of the cross-section ( $m^2$ )
$C_s$	is the source/sink concentration
$q$	is the lateral inflow ( $m^2/s$ )
$x$	is the space coordinate (m)
$t$	is the time coordinate (s)

Very little is yet known of the concentration distribution over the cross-section in sewers and there is still discussion as to whether or not a heavy-fluid layer exists and the physical characteristics of such a layer, if the layer exists. Due to these causes and due to time constraints in the present study, it was decided not to implement a description of this phenomenon in the present modelling system.

## 6.2 Comparison of Predicted Sediment Transport Rates with Measured Data

Available laboratory experiments mostly concern the bed load transport in sewers, as it is possible to make controlled laboratory experiments for this mode of transport. The typical layout of an experiment for the measurement of bed load is a flume/pipe with a sediment trap. Very few laboratory experiments have been carried out to measure the suspended sediment transport in pipes. This is because it is more difficult to measure suspended load transport in the laboratory as it is necessary to measure a vertical profile of the sediment concentration over the cross-section in order to determine the sediment transport. However, it is possible to measure suspended load transport in the laboratory and this may be one of the areas to study in the future.

Experiments with bed load in pipes have been carried out at Chalmers University of Technology, Sweden, Newcastle University, UK and Hydraulic Research Ltd., Wallingford, UK (Perrusquía 1990, 1991, 1992). These experiments have been used to evaluate the capability of the implemented sediment transport formulae to predict

to evaluate the capability of the implemented sediment transport formulae to predict the sediment transport in pipes. These experiments are quite valuable as they are specific for bed load transport in sewers, even though they only cover a part of the range of flow conditions in the sewer systems. The layout of the experiments is described in Chapter 5. The grain sizes in the experiments were 0.72 mm, 0.9 mm, 1.0 mm and 2.5 mm and the pipe slopes were up to 0.6 %. The experiments cover a range of the dimensionless bed shear stress from the critical bed shear stress up to 0.14. The transport process in these studies is bed load, ie the experiments only cover dry weather periods. As the sediment transport theories by Engelund-Fredsoe and van Rijn split the transport into bed load and suspended load, only the transport formulation for bed load can be evaluated by use of these experimental data.

A comparison between the sediment transport and the bed shear stress from the laboratory experiments (Perrusquía 1990, 1991, 1992) and the maximum sediment transport capacity and the maximum bed shear stress simulated in a real sewer system during a storm in November 1992 has been carried out, see Figure 6.6. The sewer system is located at the Rya sewage treatment plant in Gothenburg, Sweden. In Figure 6.6 it can be seen that the simulated dimensionless bed shear stress for a real sewer system is of the order of 100 times larger than the dimensionless bed shear stress observed in the laboratory. Furthermore, there is a factor of 10.000 between the sediment transport measured in the laboratory and the simulated sediment transport capacity for the Rya system. The simulated sediment transport capacity of 1 m<sup>3</sup>/s is not realistic in a sewer system due to the limited supply of sediment in sewers. A more realistic sediment transport would be in the order of 0.0001-0.001 m<sup>3</sup>/s.

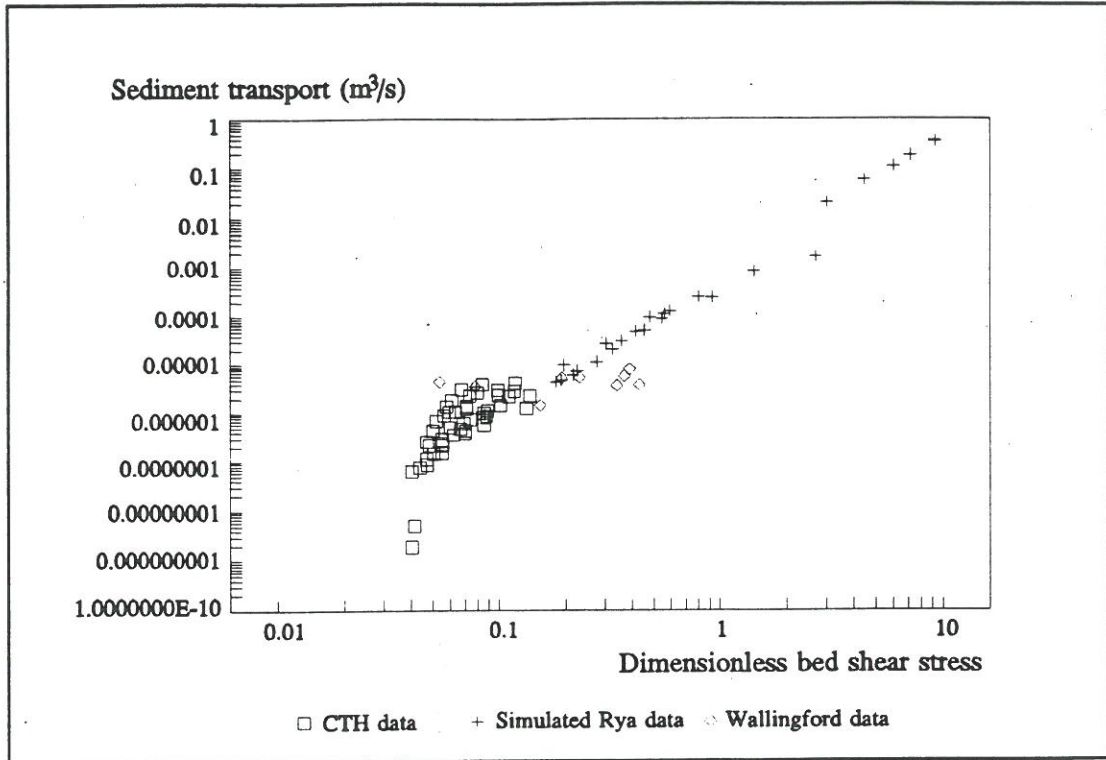


Figure 6.6. The measured sediment transport by Perrusquía (1991), shown as CTH and Wallingford data, plotted together with the maximum simulated sediment transport capacity in the Rya sewer system. The sediment transport is plotted against the measured dimensionless bed shear stress (Perrusquía, 1991) and the simulated dimensionless bed shear stress in the Rya sewer system.

The maximum recorded sediment transport at the Rya, sewage treatment plant during the storm was in the order of  $0.001 \text{ m}^3/\text{s}$  for both the fine and the coarse sediment, which is much less than the simulated transport capacity. Hence, the simulation indicates that if non-cohesive sediment is present in the pipes then most of the time during this storm in November 1992, there is too little sediment present in the pipes to apply the sediment transport formulations directly without modifications. For further information on the application of the sediment transport model, see Chapter 10.

### 6.2.1 Characteristics of the Sediment Transport Formulae

The sediment transport formulae of Ackers-White, Engelund-Fredsoe, and van Rijn, all describe the bed load as a function of the criteria for the initiation of motion. The Engelund-Fredsoe and the van Rijn theories give the bed load as a function of the critical bed shear stress from Shields (1936), whilst the Ackers-White theory gives the bed load as a function of the mobility parameter "a". The bed shear stress in the experiments by Perrusquía (1990, 1991, 1992) is close to the critical dimensionless bed shear stress, of the order of 0.03-0.05, and there is an uncertainty of approx. 20% in the critical bed shear stress defined by Shields curve, see Raudkivi (1990). Hence, quite large deviations can be expected between the measured and the predicted sediment transport.

A linear regression analysis was carried out between the measurements by Perrusquía (1991), and the sediment transport rates predicted by the four implemented sediment transport formulations. The correlation coefficient for the sediment transport formulations can be seen in Table 1. It can be seen that there is a good correlation for all the theories between the predicted and the measured sediment transport rates. The performance for the theories was evaluated based on the performance index by Van Rijn (1984a). The performance index,  $r$ , is the percentage of data within the discrepancy range:

$0.5 * \text{observed transport} < \text{computed transport} < 2 * \text{observed transport}$ , or:

$$0.5 < \frac{\text{Bed load}_{\text{computed}}}{\text{Bed load}_{\text{measured}}} < 2 \quad (6-6)$$

A common mode of calibration in sediment transport modelling is to multiply the sediment transport formula by a constant factor (Ammentorp et al., 1992). The determination of the optimum calibration factor is an iterative procedure based on a systematic elimination of the data outside the discrepancy range. A calibration of the sediment transport formulae was carried out and the performance of the formulae was improved significantly. The performance of the formulae with and without calibration can be seen in Table 6.1.

	Correlation coefficient	Performance without calibration %	Calibration factor	Performance with calibration %
Ackers-White	0.87	7 %	1.5	57 %
Engelund-Hansen <sup>1</sup>	0.72	32 %	2.0	84 %
Engelund-Hansen <sup>2</sup>	0.76	23 %	3.2	82 %
Engelund-Fredsøe <sup>1</sup>	0.77	66 %	0.7	78 %
Engelund-Fredsøe <sup>2</sup>	0.89	72 %	0.8	81 %
van Rijn <sup>3</sup>	0.73	55 %	1.0	55 %
van Rijn <sup>4</sup>	0.80	76 %	0.8	80 %
van Rijn <sup>5</sup>	0.91	10 %	3.8	76 %

<sup>1</sup> without prediction of the bed shear stress

<sup>2</sup> with prediction of the bed shear stress

<sup>3</sup> all grain fractions

<sup>4</sup> all grain fractions except the 2.5 mm grain fraction

<sup>5</sup> only the 2.5 mm grain fraction

Table 6.1. Correlation coefficient from the linear regression analysis and scores (percentage) of predicted bed load in the discrepancy range  $0.5 < r < 2$ .

Based on 600 data sets Van Rijn (1984a) found the following performance,  $r$ , for various bed load transport formulae:

Ackers-White	: 77%
Engelund-Hansen	: 76%
van Rijn	: 77%
Meyer-Peter and Müller	: 58%
Engelund-Fredsoe	: This theory was not evaluated by van Rijn

It should be noted that van Rijn just has a performance of 77% for his own bed load transport formula. A comparison between the predicted and the measured sediment transport rates is discussed for each theory in more detail below. In the following paragraphs only the cases where transport was predicted by the various sediment transport formulae have been presented in the plots as predicted sediment transport versus measured sediment transport.

### 6.2.2 The Ackers-White Theory

The Ackers-White theory predicts that sediment transport takes place in 52 out of 66 experiments where transport was measured. There is a good correlation between the measured and predicted sediment transport. The Ackers-White theory generally underestimates the sediment transport, except for the 0.72 mm grain size. The theory predicts 47 % of the data is within the range 0.5-2.0 times the measured sediment transport. By applying a calibration factor of 1.5, the performance of the theory increases to 57 %. This is a low performance rate compared to the performance rate of 77 % reported by van Rijn (1984a). There is no systematic variation with grain size or pipe slope in the agreement between the measured and the simulated sediment transport. The deviation between the measured and the predicted data is, as expected, large for the small sediment transport rates. The comparison between the measured and the predicted sediment transport can be seen in Figure 6.7.

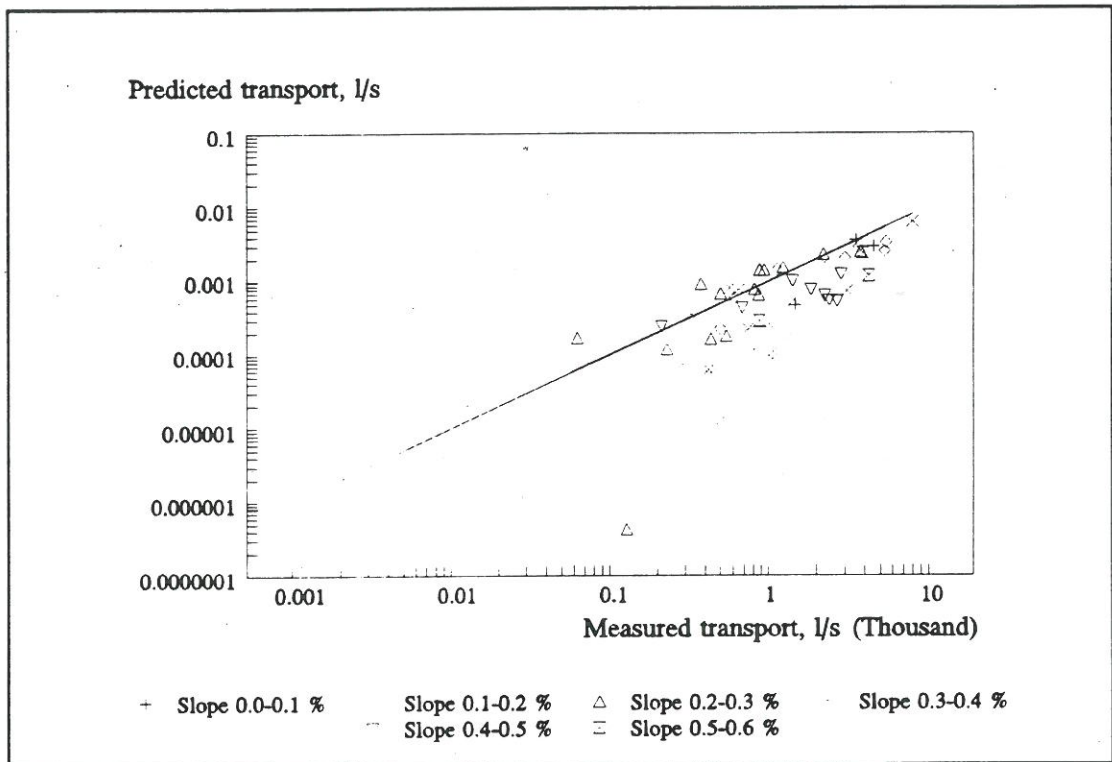
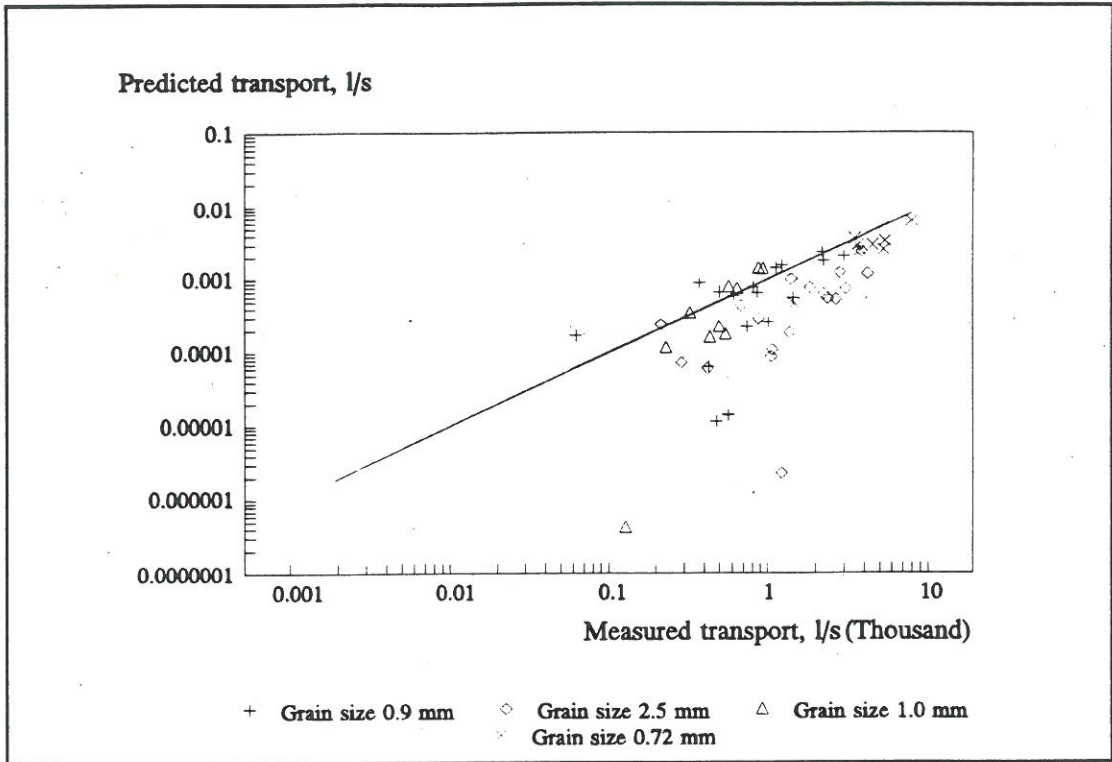


Figure 6.7. Predicted sediment transport versus measured transport for the Ackers-White theory for a range of grain sizes and pipe slopes (top figure with different grain sizes, bottom figure with different pipe slopes). Experimental data from Perrusquía (1992).

### 6.2.3 The Engelund-Hansen Theory

The Engelund-Hansen theory has an option for prediction of the bed shear stress based on the hydraulic conditions. The calculation of the sediment transport was carried out with the observed bed shear stress and with the bed shear stress predicted by the Engelund-Hansen theory.

#### Without Prediction of the Bed Shear Stress

The Engelund-Hansen theory, without prediction of the bed shear stress, predicts that sediment transport takes place in 65 out of 66 experiments where transport was measured. In general the theory underestimates the sediment transport, but the transport rates predicted by the theory follow the tendency of the experimental data very well. The theory underestimates the sediment transport for all the grain sizes and all pipe slopes. The theory predicts 32% of the data is within the range 0.5-2.0 times the measured sediment transport, which is a very low score. It can be seen from Figure 6.8 that there is no deviation in the quality of the prediction of the sediment transport with pipe slope or grain size.

By applying a calibration factor of 2.0 the performance of the theory increases to 84%, see Figure 6.10. This is a good performance rate, and it is better than the performance rate of 76 % reported by van Rijn (1984a).

#### With Prediction of the Bed Shear Stress

The Engelund-Hansen theory with prediction of the bed shear stress predicts that sediment transport takes place in 57 out of 66 experiments where transport was measured. In general the theory still underestimates the sediment transport, but performance of the theory has improved for the highest sediment transport rates. The theory has a low score, it predicts 23% of the data is within the range 0.5-2.0 times the measured sediment transport. The performance can be improved by use of a calibration factor of 3.2. The performance then increases to 82% which is a good score. It can be seen from Figure 6.9 that there is no deviation in the quality of the prediction of the sediment transport with pipe slope or grain size.

The reason that the Engelund-Hansen theory, both with and without prediction of the bed shear stress, underestimates the sediment transport is probably due to the fact that the formula is developed to predict total transport, and it is not a pure bed load formula. The authors state in the paper (Engelund and Hansen, 1967) that if a bed load formula is required then the transport rate should be proportional to  $\theta^2$ , (the sediment transport rate in the Engelund-Hansen formula is proportional to  $\theta^{2\frac{1}{2}}$ ).

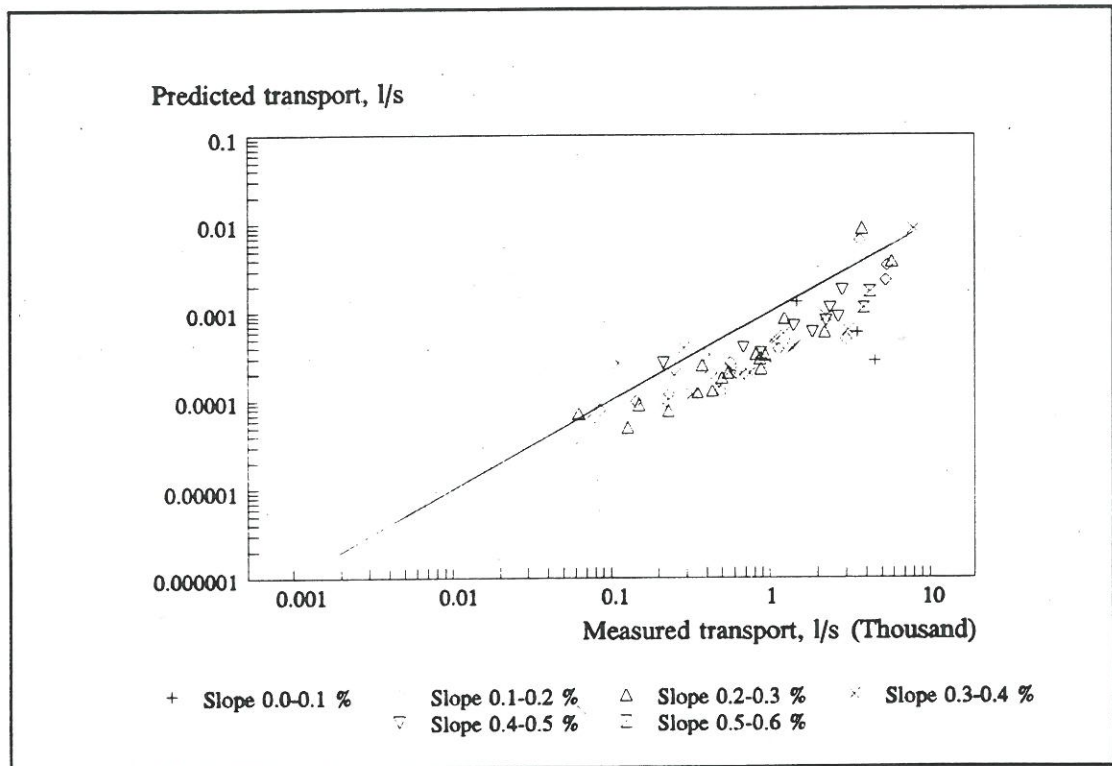
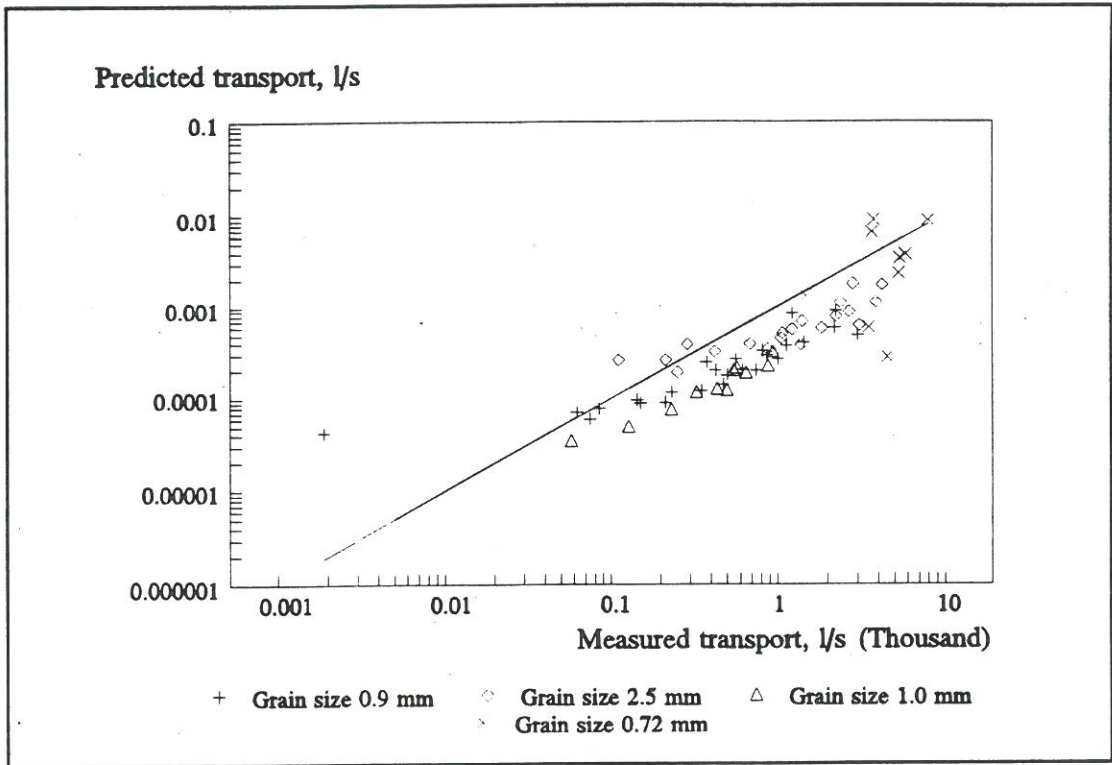


Figure 6.8. Predicted sediment transport versus measured transport for the Engelund-Hansen theory without prediction of the bed shear stress, for a range of grain sizes and pipe slopes (top figure with different grain sizes, bottom figure with different pipe slopes). Experimental data from Perrusquía (1992).



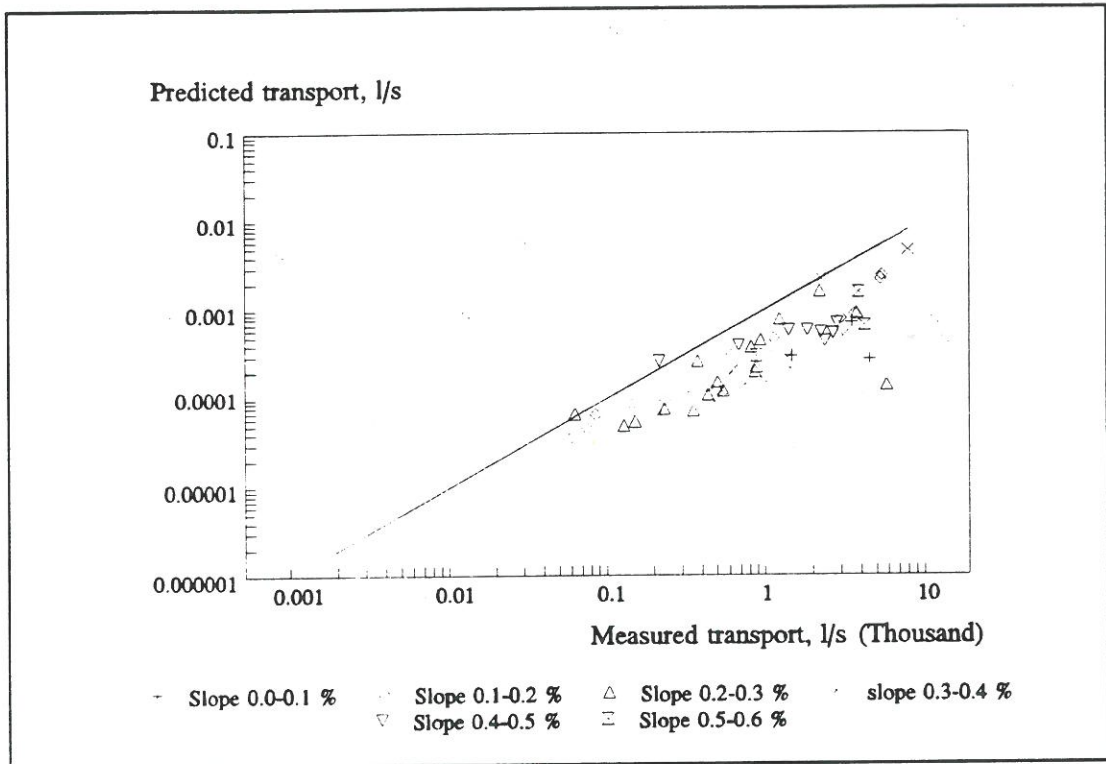
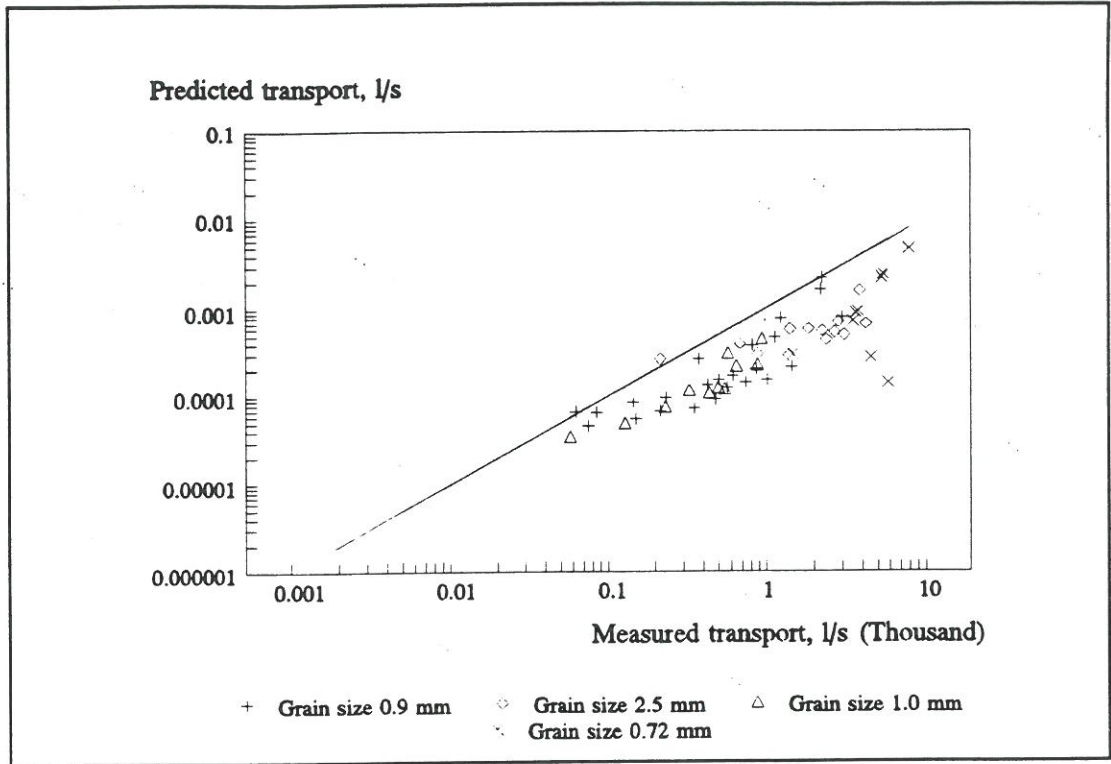


Figure 6.9. Predicted sediment transport versus measured transport for the Engelund-Hansen theory with prediction of the bed shear stress, for a range of grain sizes and the pipe slopes (top figure with different grain sizes, bottom figure with different pipe slopes). Experimental data from Perrusquía (1992).

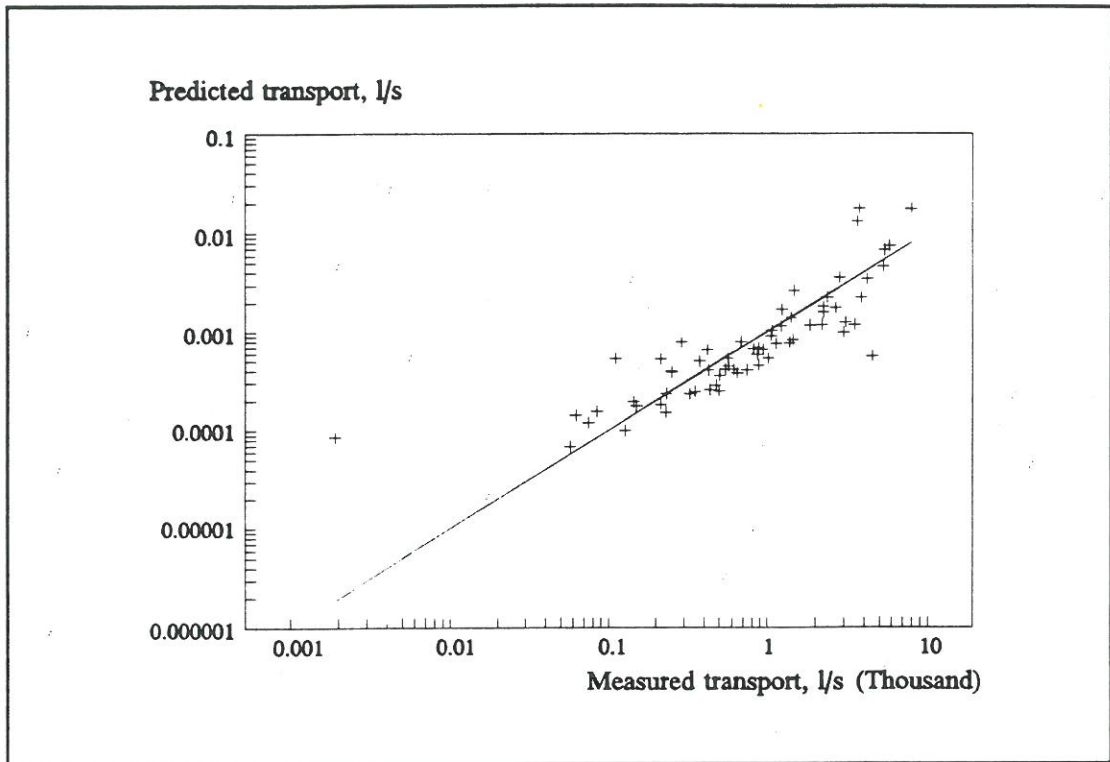


Figure 6.10. Comparison between the measured data and the Engelund-Hansen formula multiplied by a factor of 2.0, without prediction of the bed shear stress. Experimental data from Perrusquía (1992).

#### 6.2.4 The Engelund-Fredsoe Theory

The Engelund-Fredsoe theory has, as with the Engelund-Hansen theory, an option for calculation of the sediment transport with and without prediction of the bed shear stress. The sediment transport has been calculated with both options. The performance of the Engelund-Fredsoe theory was not evaluated by van Rijn (1984a).

##### Without prediction of the bed shear stress

The Engelund-Fredsoe theory without prediction of the bed shear stress predicts that sediment transport takes place in 65 out of 66 experiments where transport was measured. In general, the Engelund-Fredsoe theory without prediction of the bed shear stress gives a fair estimate of the sediment transport. The theory has a tendency to slightly overestimate the sediment transport for small sediment transport rates. The theory has a good performance rate as it predicts that 66 % of the data is within the range 0.5-2.0 times the measured sediment transport. By applying a calibration factor of 0.7 the performance increases to 78 %. No dependency on slope or grain size can be observed in the deviation between the measured and the simulated sediment transport. The comparison between the measured and the predicted sediment transport can be seen in Figure 6.11.

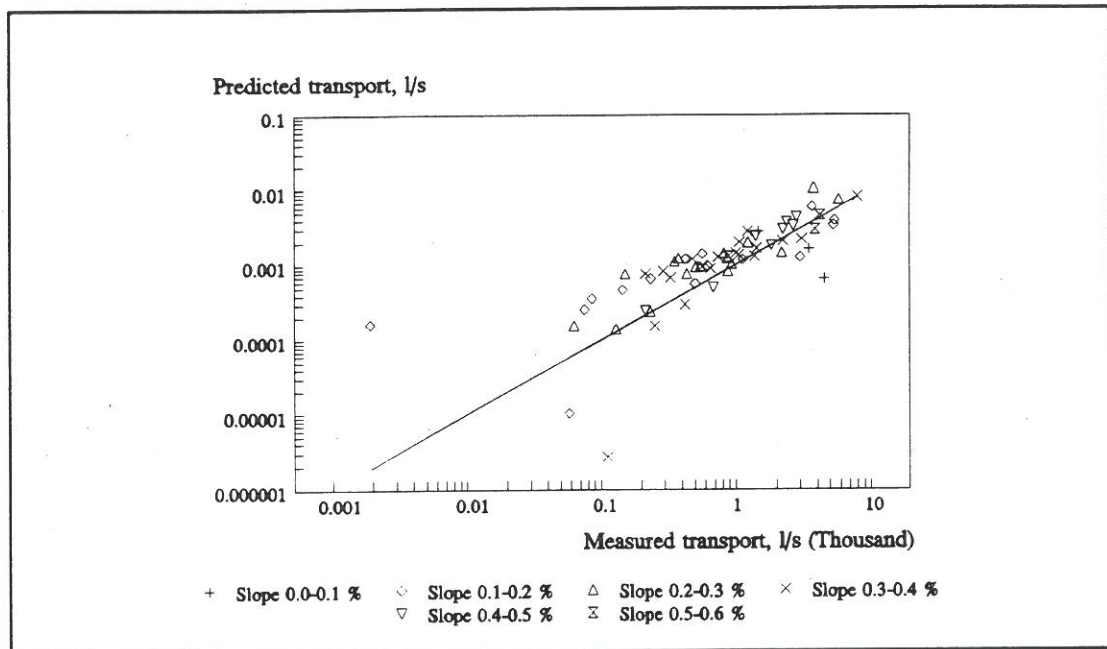
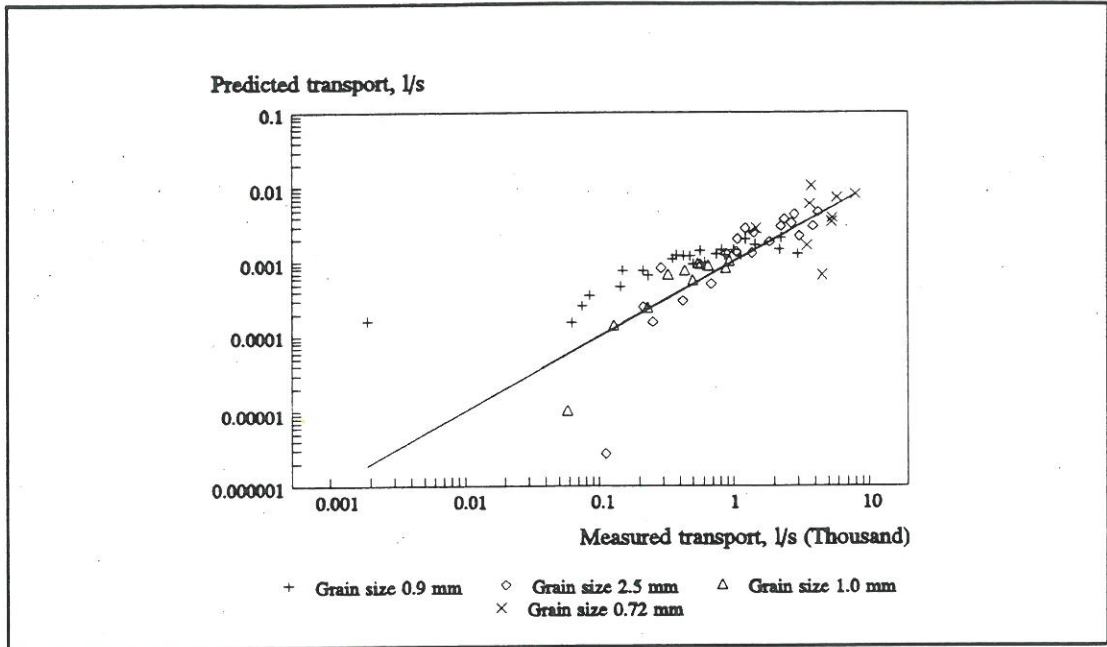


Figure 6.11. Predicted sediment transport (bed load) versus measured transport for the Engelund-Fredsoe theory without prediction of the bed shear stress, for a range of grain sizes and pipe slopes (top figure with different grain sizes, bottom figure with different pipe slopes). Experimental data from Perrusquia (1992).

### With prediction of the bed shear stress

The Engelund-Fredsoe theory with prediction of the bed shear stress predicts that sediment transport takes place in 57 out of 66 experiments where transport was measured. The theory with prediction of the bed shear stress gives a better estimate of the small sediment transport rates than the theory without prediction of the bed

shear stress, but the deviation between the measured and the predicted transport is slightly higher for the high sediment transport rates. The performance of the theory is 72 % without calibration and 81 % with a calibration factor of 0.8. The comparison between the measured and the predicted sediment transport can be seen in Figure 6.12.

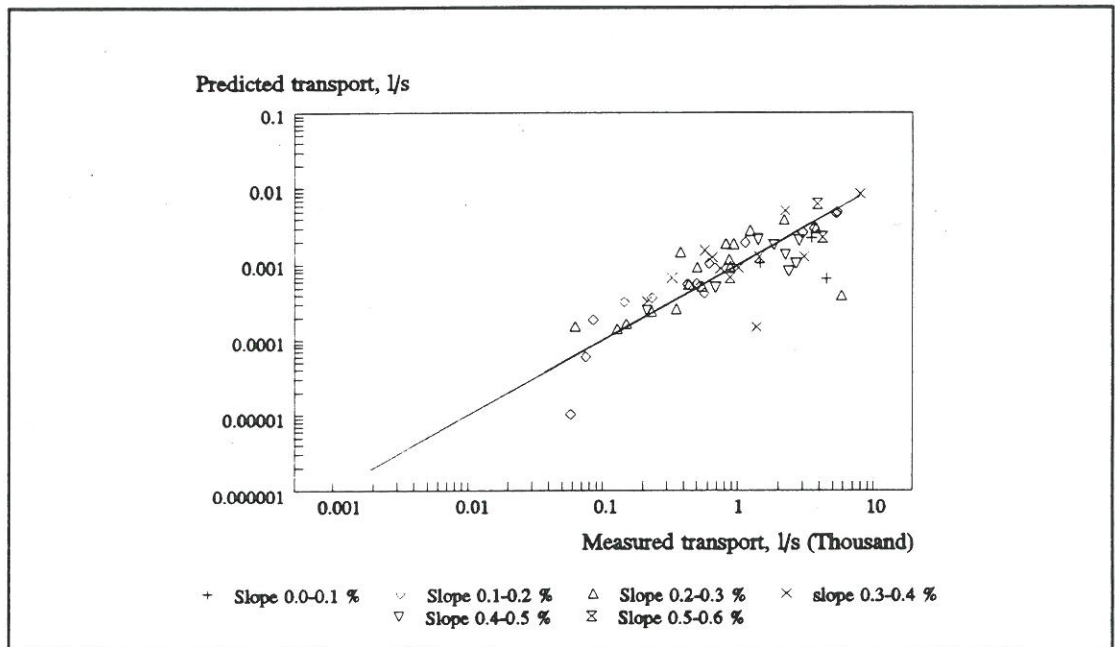
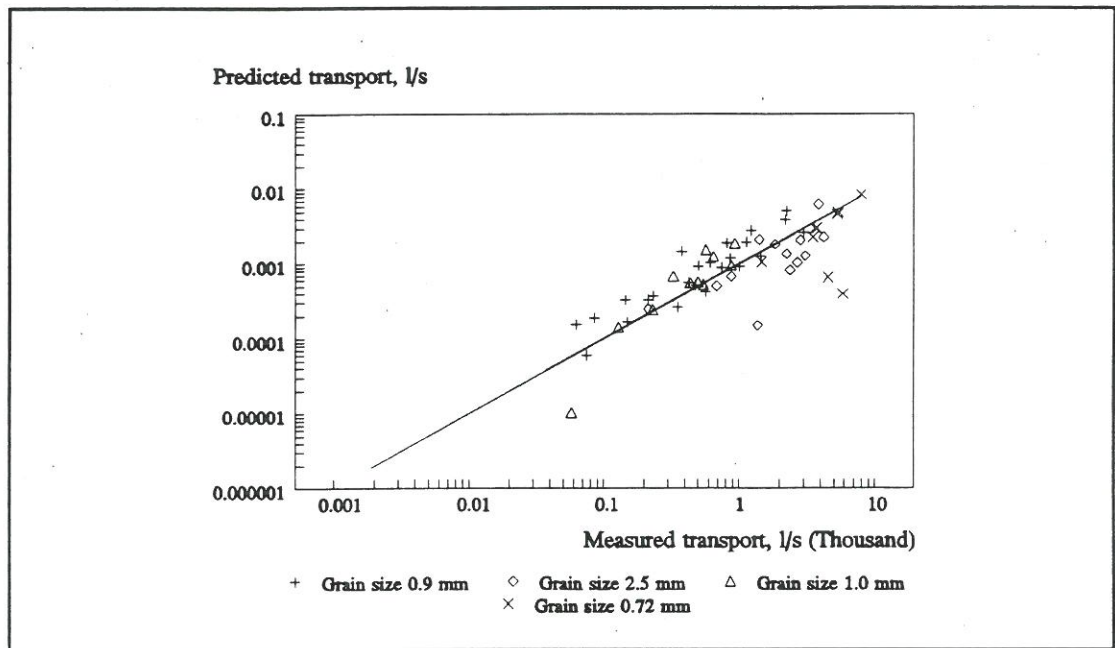


Figure 6.12. Predicted sediment transport (bed load) versus measured transport for the Engelund-Fredsoe theory with prediction of the bed shear stress, for a range of grain sizes and pipe slopes (top figure with different grain sizes, bottom figure with different pipe slopes). Experimental data from Perrusquia (1992).

### 6.2.5 The van Rijn Theory

The van Rijn theory predicts that sediment transport takes place in all 66 experiments where transport was measured. The van Rijn theory gives good estimates of the sediment transport for the 0.72, 0.9 and 1.0 mm grain size and small pipe slopes. The theory gives a poor prediction of the sediment transport for large pipe slopes (0.5% - 0.6%) and the 2.5 mm grain size. Based on these data it is not possible to say exactly whether it is the high slopes, the grain diameter or a poor estimation of the critical bed shear stress which causes the deviations for the 2.5 mm grain size, but it is probably due to the grain size, as van Rijn in the original paper (van Rijn, 1984a) states that the theory is validated for grain sizes in the range 200  $\mu\text{m}$  - 2000  $\mu\text{m}$ , hence the experiments with a grain size of 2.5 mm is beyond the range where the theory has been verified by van Rijn (1984a). The overall performance of the theory is 55%, and it can not be improved by calibration. If the 2.5 mm grain fraction is taken out of the data set, then the performance of the theory increases to 76%, which is nearly the same as reported by van Rijn (1984a). By application of a calibration factor of 0.8, the performance is increased to 80%. The comparison between the measured and the predicted sediment transport can be seen in Figure 6.13. The performance of the 2.5 mm grain fraction alone, is as low as 10%. By use of a calibration factor of 3.8, the performance of the sediment transport formula for this fraction is increased significantly, to 76%.

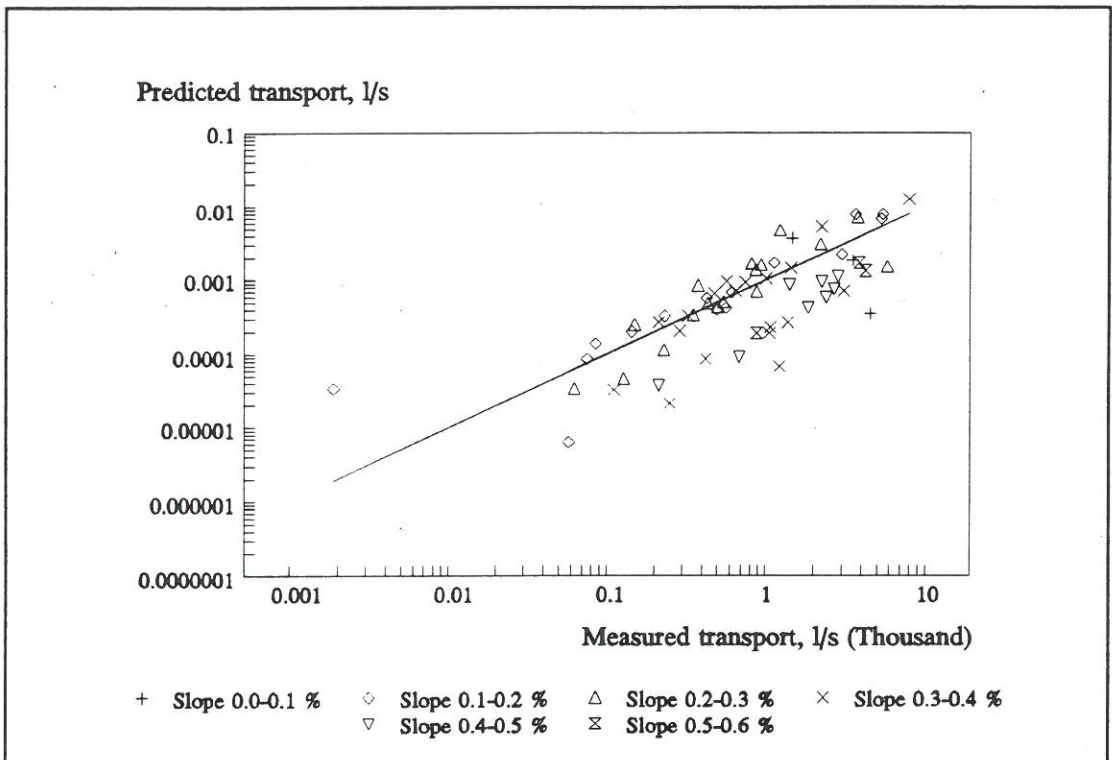
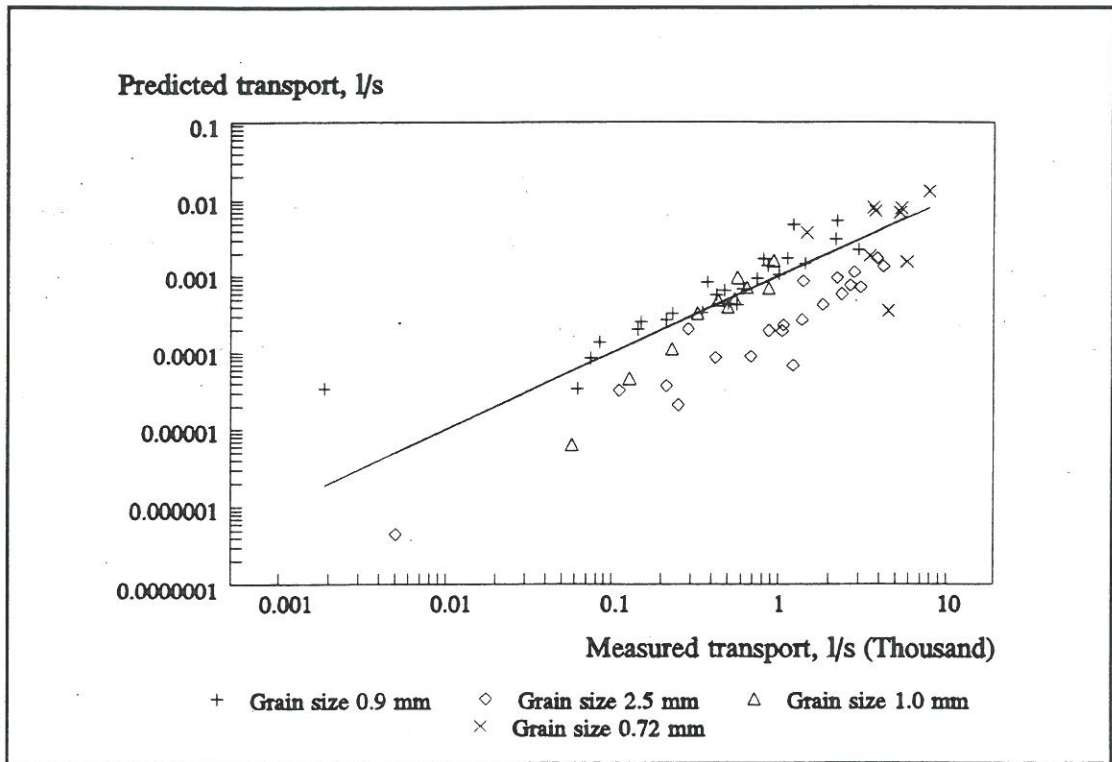


Figure 6.13. Predicted sediment transport (bed load) versus measured transport for the van Rijn theory for a range of grain sizes and pipe slopes (top figure with different grain sizes, bottom figure with different pipe slopes). Experimental data from Perrusquía (1992).

### 6.3 Comments on the Performance of the Sediment Transport Formulae

The experimental data from Perrusquía (1991) were tested against Ackers-White, the Engelund-Hansen, the total Engelund-Fredsøe and the total van Rijn theory including the formulations for both bed load and suspended load. Both the Engelund-Fredsøe and the van Rijn theories predicted only bed load transport and no suspended load, which is in agreement with the observations in the laboratory. The experiments represent bed load transport at small bed shear stresses and with small sediment transport rates. Hence, only the bed load formulations of the Engelund-Fredsøe and the van Rijn formulae could be evaluated. It must be expected that these suspended load formulations must be modified in order to be applicable without calibration to full running sewers.

As there is a large uncertainty in the criteria for the initiation of motion (Raudkivi, 1990) it cannot be expected that the theories predict transport in all the cases where transport was measured, as the experimental data are close to the point for the initiation of motion. Only the van Rijn theory predicted sediment transport in all the cases where transport was measured in the experiments. The Engelund-Hansen and the Engelund-Fredsøe theories predicted no sediment transport in 1 out of 66 cases without prediction of the bed shear stress, and 9 out of 66 cases with prediction of the bed shear stress. The Ackers-White theory predicted no transport in 13 out of the 66 experiments.

The sediment transport formulae by Ackers-White, Engelund-Fredsøe and van Rijn all describe the transport as a function of their criteria for the initiation of motion. However, there is an uncertainty of up to 20% on the criterion for initiation of motion and the dimensionless bed shear stress in the experiments are in the order of 1-3 times the critical bed shear stress. In addition the bed load is mainly a function of the skin friction, thus deviations in the sediment transport rates predicted by the sediment transport theory may be expected.

A sensitivity analysis was carried out, see Appendix D, which showed that the Ackers-White and the van Rijn theories are very sensitive to a reduction of 10% in their criteria for the initiation of motion. The Engelund-Fredsøe theory is less sensitive to a 10% decrease in the critical bed shear stress. The sediment transport rates predicted by the Engelund-Hansen theory are independent of the critical bed shear stress. Hence, the capability of the theories to predict the sediment transport rates cannot be expected to be as good as reported by van Rijn as the experimental data are very close to the critical bed shear stress and the sediment transport is very sensitive at this point. Furthermore, there is a large scatter in the prediction of the bed shear stress for all the implemented theories, ie the theories which can predict the bed shear stress for the calculation of sediment transport (Engelund-Hansen and Engelund-Fredsøe) will predict sediment transport rates with a large uncertainty as the sediment transport rate is dependent on the bed shear stress. This can be seen from the fact that the theories with prediction of the bed shear stress perform less

well than when they predict the sediment transport rate from the observed bed shear stress. Hence, it is important to have a good estimate of the bed shear stress in order to predict the sediment transport rate.

The van Rijn theory (without the 2.5 mm grain size) and the Engelund-Fredsøe theory perform well without calibration. The reason that the van Rijn formula does not perform very well for grain sizes larger than 2.5 mm may be due to the fact that only sediments with a grain size up to 2.0 mm were used for the derivation of this formula. When all the theories were calibrated (the Engelund-Hansen theory without prediction of the bed shear stress, the van Rijn theory (without the 2.5 mm grain size) and the Engelund-Fredsøe theory with and without prediction of the bed shear stress), they gave a performance of 76% or more. Hence, these sediment transport theories perform equally well for the prediction of sediment transport in pipes and in flumes/streams. It can be concluded that the conventional sediment transport theories for rivers can be used to predict the bed load transport in pipes, but large deviations in the transport, especially for the small sediment transport rates, must be expected due to the uncertainty in the criteria for the initiation of motion. It must be recommended that before a sediment transport theory is applied to predict the sediment transport in a pipe it must be validated against measured data.

For a further validation of the applicability of these sediment transport formulae to sewers, it is recommended to compare these to other experiments on sediment transport in pipes, with different flow pattern and pipes material, eg the experiments by Kleijwegt (1992). Such a comparison has not been carried out in the present study due to time constraints.

Laboratory experiments with higher bed shear stresses and higher sediment transport rates are required in order to evaluate how the sediment transport theories perform under storm conditions, when the pipes are running full and suspended load is present. Further, field measurements of sediment transport in sewer systems covering wide ranges of pipe sizes and flow velocities are needed for both dry weather and storm conditions in order to validate/modify the existing sediment transport theories to the conditions in sewer systems.



## 7 A DISCUSSION OF THE ADVECTION-DISPERSION MODEL

The transport of dissolved pollutants and fine sediments is based on a numerical solution of the advection-dispersion equations. The numerical modelling of the advection-dispersion equations is based on a finite difference scheme. In this chapter the advection-dispersion equations are described for their application to sewer systems. In addition the accuracy of the numerical finite difference scheme in the modelling system is discussed together with an evaluation of the applicability of the scheme to sewer systems. Further, the special modelling approaches for conditions in sewers are discussed.

### 7.1 The Applicability of the Advection-Dispersion Scheme to Sewers

The transport of dissolved substances is traditionally described by the advection-dispersion equation. These equations describe the one dimensional transport for the conservation of mass of dissolved material. The advection-dispersion equation needs input from a hydrodynamic model in terms of water levels and discharges. The hydrodynamic basis of the advection-dispersion model is the hydrodynamic model in MOUSE. This model solves the full St. Venant equations for looped systems with free surface flow or pressurized flow. The hydrodynamic model is described in the "MOUSE User's Guide & Technical Reference". The main assumptions of the one dimensional advection-dispersion equations are:

- the considered substance is completely mixed over the water column. This implies that a source/sink term is considered to mix instantaneously
- the substance is considered to be conservative or subject to a first order decay
- Fick's diffusion law can be applied, ie the dispersive transport is proportional to the gradient of the concentration

If the flow passes rapidly through the sewer system, the decay will seldom be important. Many of the dissolved substances/pollutants can be modelled as conservative or with a first order decay.

### 7.1.1 The Continuity Equation for the Transport of Dissolved Substances

The one-dimensional vertically integrated equation for the conservation of mass of a substance in solution is given:

$$\frac{\partial(AC)}{\partial t} + \frac{\partial T}{\partial x} = -A \cdot K \cdot C + C_s \cdot q \quad (7-1)$$

where

C	is the concentration (arbitrary unit)
A	is the area of the cross-section (m <sup>2</sup> )
T	is the transport
K	is the linear decay coefficient (s <sup>-1</sup> )
C <sub>s</sub>	is the source/sink concentration
q	is the lateral inflow (m <sup>2</sup> /s)
x	is the space coordinate (m)
t	is the time coordinate (s)

### 7.1.2 The Advection-Dispersion Equation

The advection-dispersion equation reflects two transport mechanisms:

- the convective transport of the dissolved substances with the mean flow velocity
- the dispersive transport due to concentration gradients of the dissolved substance in the water

The one dimensional vertically integrated equation for the conservation of mass of a substance in solution, ie the one dimensional advection-dispersion equation reads:

$$\frac{\partial(AC)}{\partial t} + \frac{\partial(QC)}{\partial x} - \frac{\partial}{\partial x} \left( AD \frac{\partial C}{\partial x} \right) = -A \cdot K \cdot C + C_c \cdot q \quad (7-2)$$

In equation (7-2) the dispersion coefficient is constant. In the present numerical model it has been selected to implement a general description of the dispersion coefficient. The dispersion coefficient is determined as a function of the mean flow velocity:

$$D = a \cdot |u|^b \quad (7-3)$$

where u is the mean velocity (m/s) and a, b are calibration constants.

The dispersion coefficient can be set to a constant by selecting: b = 0.0.

### 7.1.3 Dispersion in Sewer Systems

The dispersion again reflects several phenomena, ie molecular diffusion, turbulent diffusion and the effect from the non uniform velocity distribution over the cross-section. The two first mentioned diffusion processes are rather insignificant compared to the effect from the non uniform velocity distribution. The dispersion coefficient for the turbulent flow in a full running pipe was found through theoretical analyses by Taylor (1954):

$$k_x = \frac{D}{u_f \cdot R} = 20.2 \quad (7-4)$$

where

$k_x$  is the dimensionless dispersion coefficient  
 $D$  is the dispersion coefficient ( $m^2/s$ )  
 $u_f$  is the friction velocity ( $m/s$ )  
 $R$  is the hydraulic radius ( $m$ )

Equation (7-4) can be obtained from the general formulation in equation (7-3) by selecting:

$$a = 20.2 \frac{\sqrt{g}}{M} R^{5/6} \quad \text{and} \quad b = 1 \quad (7-5)$$

The theoretical analysis by Taylor was verified against experimental data. The effect of the dispersion in a pipe eg a 1 metre circular pipe with a slope of  $1.0E-2$  the dispersion coefficient,  $D$ , can be evaluated as:

$$D = 20.2 \cdot \sqrt{gRI} \cdot R = \quad (7-6)$$
$$20.2 \sqrt{9.81 \cdot 0.25 \cdot 1.0E-2} \cdot 0.25 = 0.8 m^2/s$$

This value of the dispersion coefficient is in the same order of magnitude as the dispersion coefficient ( $D = 1.5 m^2/s$ ) found for the Dronninglund gravity sewer, see Chapter 9. If gradients are present in the distribution of the concentration the over the cross-section, eg for cohesive sediment, larger dispersion coefficients must be anticipated.

#### 7.1.4 Solution of the Advection-Dispersion Equation at Structures and Manholes

The solution of the advection-dispersion equation has to be modified at hydraulic structures in sewer systems. The general way to describe the transport at a hydraulic structure is to setup a local continuity equation. Further, special cases exist where the local continuity equation has to be modified, eg when free flow into a manhole is present. The modifications to the advection-dispersion equation are described below.

##### Manholes

The effect of the dispersion term is probably small for sewer systems with high flow velocities, but it becomes important in systems with small gradients and backwater effects, eg in the Netherlands. In sewer systems, the manholes are a significant source for dispersion in sewer systems but today very limited knowledge is available concerning the mixing at manholes. At present, experiments are being carried out concerning the dispersion in manholes at Sheffield University (O'Brien, 1993 and Guymer and O'Brien, 1994). So far only preliminary results have been presented. The results indicate that the dispersion may be overestimated by assuming full mixing in the manholes. A method to reduce this overestimation of the dispersion in the system is to reduce the dispersion coefficient in the pipes.

The transport across a manhole is modelled by assuming that the incoming volume of water mixes instantaneously with the water in the manhole. This assumption is obviously rather simple and may not always be fulfilled, eg when the manhole is surcharged. A better description of the dispersion in a manhole can probably be achieved by describing the mixing process in a manhole by use of the theory from aggravated dead zones (Pedersen, 1977) together with the jet theory for the transport through the manhole (eg Pedersen and Mark, 1989).

In the model the local continuity equation which is applied at a manhole yields:

$$\frac{\partial(V_N C_N)}{\partial t} + \sum_{i=1}^{i=kk} T = -V_N \cdot C_N \cdot K_N \quad (7-7)$$

where

$V_N$	is the volume of the structure ( $m^3/s$ )
$C_N$	is the concentration in the node
$T$	is the transport into the node ( $kg/s$ )
$K_N$	is the decay constant for the node
$kk$	is the number of connecting pipes

The continuity equation for the water flow to and from a hydraulic structure can be given as:

$$\frac{\partial V_N}{\partial t} + \sum_{i=1}^{i=kk} Q = 0 \quad (7-8)$$

where

$Q$  is the discharge in the connecting branches ( $\text{m}^3/\text{s}$ ).

The continuity equation for a structure in the advection-dispersion model, equation (7-7), can be rearranged by use of the continuity equation for water, equation (7-8), and the full equation for a manhole now yields:

$$V_N \frac{\partial C_N}{\partial t} - C_N \sum_{i=1}^{i=kk} Q + \sum_{i=1}^{i=kk} T = -V_N \cdot C_N \cdot K_N \quad (7-9)$$

### Free Flow into a Structure

When free flow into a structure occurs, ie the water level at the structure is lower than the water level in the inlet pipe, the concentration in the pipe is independent of the concentration at the structure. Hence, the dispersion term in the formulation of the transport is neglected, ie the transport is pure advection, see Figure 7.1. The transport into a structure with free inflow is formulated as:

$$T = Q \cdot C \quad (7-10)$$

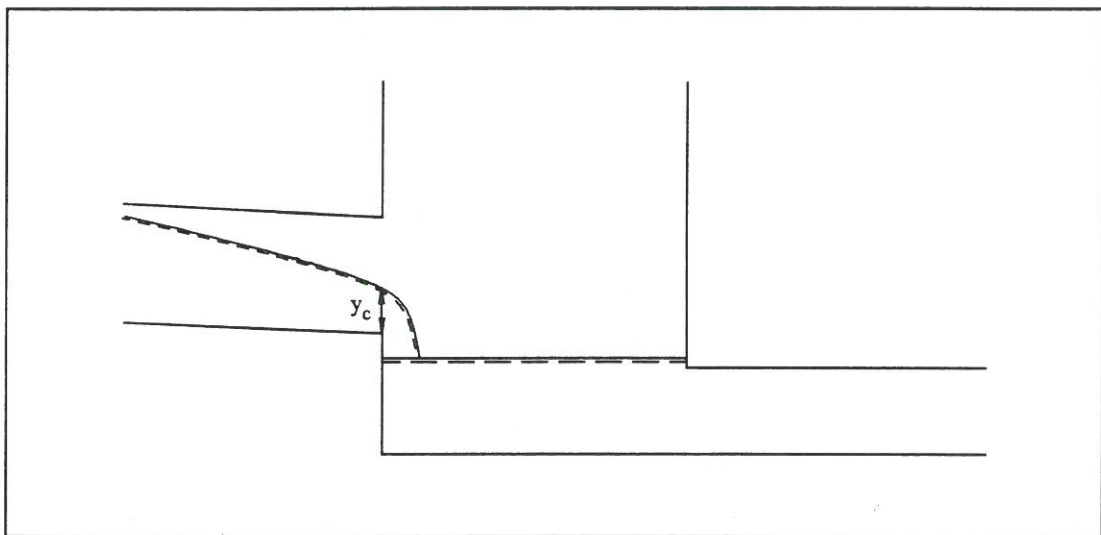


Figure 7.1. Sketch of a situation with free inflow to a manhole.

### No Outflow from a Structure to a Pipe

This condition occurs when the water level at the structure is lower than the bottom invert of the outlet pipe, eg when several pipes leave the structure at different elevations, see Figure 7.2. When such a situation arises a modified local continuity equation is applied in which the transport into the outlet pipe is described by:

$$T = Q_{pipe} \cdot C_N \quad (7-11)$$

where

$Q_{pipe}$  is the discharge at the first grid point in the outlet pipe, ( $m^3/s$ )

In reality the discharge in the outlet pipe ought to be zero. However, due to the stability of the numerical scheme in the hydrodynamic model a minimum water depth of 2% of the pipe diameter (maximum 2 cm) will always be present in the pipes. Hence, a small discharge will always be present in the outlet pipe. This minimum depth has no influence of the mass balance, but a dilution of the dissolved substance will take place.

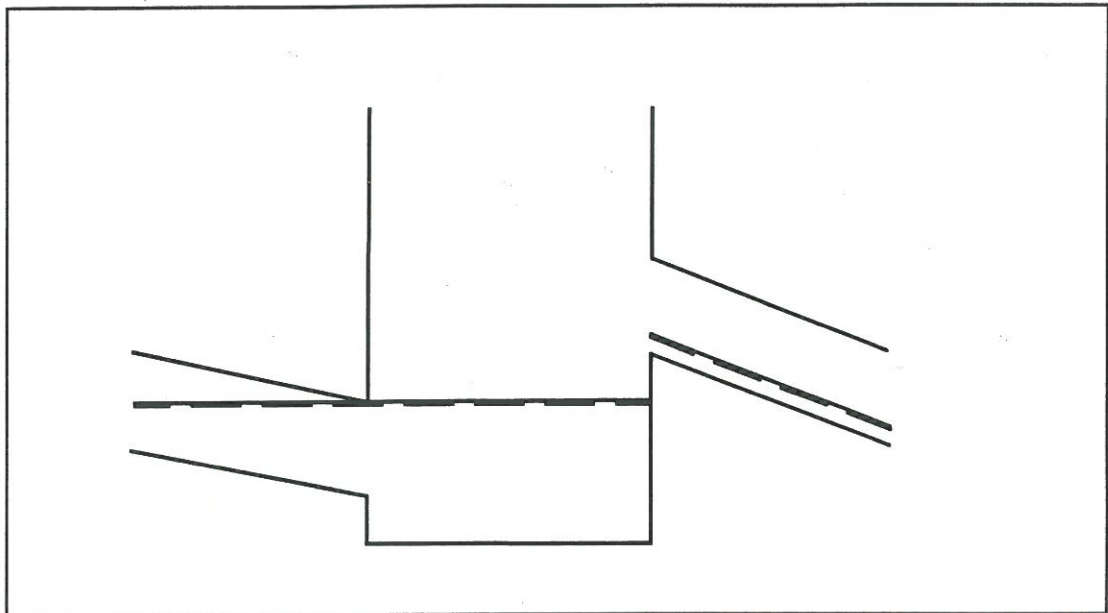


Figure 7.2. Sketch of a situation in MOUSE with no flow from the manhole to the outlet pipe.

### Formulation of the Transport of Dissolved Substances in a Pump

The dissolved substance is routed through the pump with no time lag between the structure with the pump and the destination node. The pumped mass,  $q_p \cdot c_s$ , is added to the source term of the continuity equation at the destination node.

## Formulation of the Transport of Dissolved Substances over Weirs

The transport past a weir is routed directly between the weir and the structure to which the weir is spilling. The mass flowing past the weir,  $q_s \cdot c_s$ , is added to the source term of the continuity equation at the destination node.

### 7.2 The Advection-Dispersion Scheme

The advection-dispersion equation is solved using an implicit finite-difference scheme which is centred in time and space in order to avoid numerical dispersion. The concentrations are defined in each grid point, ie non-staggered. A third order correction term has been evaluated for the advection-dispersion equation by use of Taylor expansions. The correction term has been included in order to eliminate the third order truncation error. A sketch of the numerical scheme is shown in Figure 7.3.

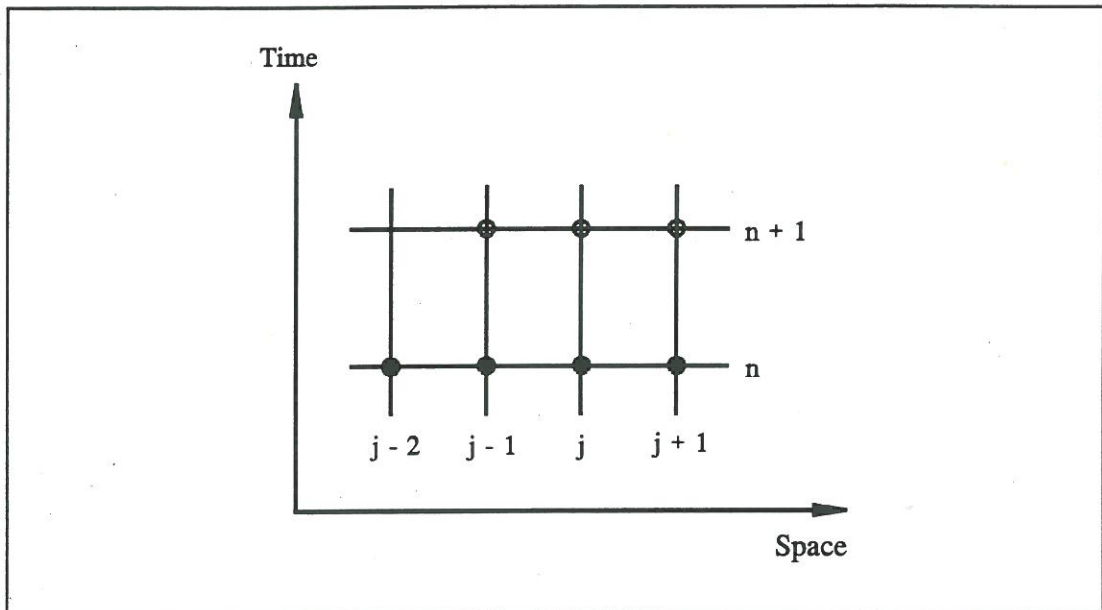


Figure 7.3. The numerical scheme for the advection-dispersion model.

The two equations considered are the continuity equation and the advection-dispersion equation. The continuity equation is given in equation (7-1). A sketch of the transport of dissolved substances through a small element of water is shown in Figure 7.4.

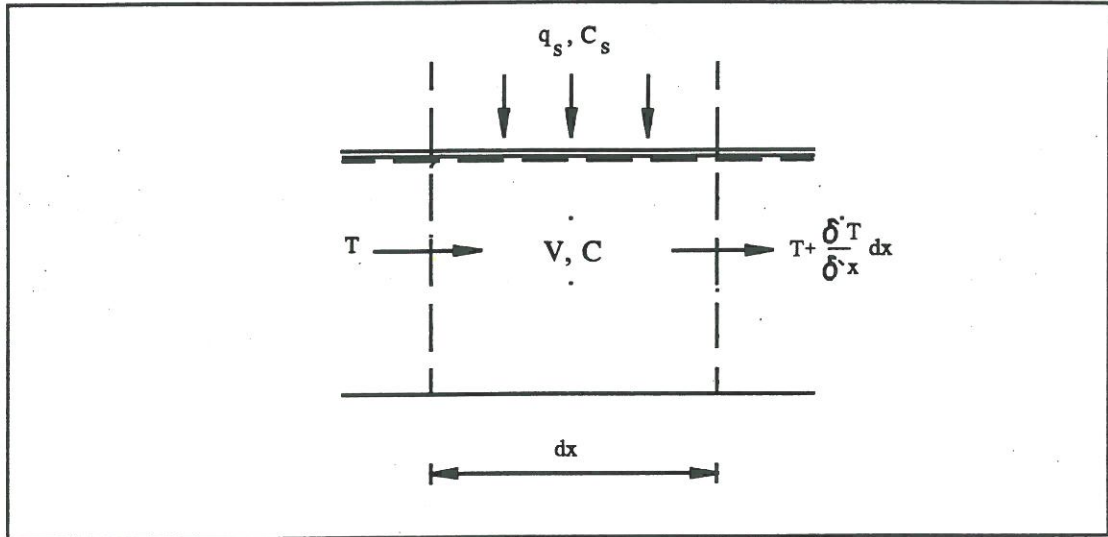


Figure 7.4. Sketch of the transport of dissolved substances through a small element of water.

The continuity equation for dissolved substance can be written in discrete form as:

$$\frac{(V_j C_j)^{n+1} - (V_j C_j)^n}{\Delta t} + T_{j+1/2}^{n+1/2} - T_{j-1/2}^{n+1/2} = Q_s^{n+1/2} C_s^{n+1/2} - K C_j^{n+1/2} V_j^{n+1/2} \quad (7-12)$$

where

T is the transport through the box walls  
j is the grid point number  
n is the time level

The advection-dispersion equation can then be written in discrete form as:

$$T_{j+1/2}^{n+1/2} = Q_{j+1/2}^{n+1/2} C_{j+1/2}^* - A_{j+1/2}^{n+1/2} D_{j+1/2}^{n+1/2} \frac{C_{j+1}^{n+1/2} - C_j^{n+1/2}}{\Delta x} \quad (7-13)$$

where

$Q_{j+1/2}^{n+1/2}$  is the discharge at the right wall of the box ( $m^3/s$ )

$A_{j+1/2}^{n+1/2}$  is the cross sectional area of the right wall ( $m^2$ )

$D_{j+1/2}^{n+1/2}$  is the dispersion coefficient ( $m^2/s$ ) given by equation (7-15)

$C_{j+1/2}^*$  is an upstream interpolated concentration given by equation (7-14)



$$C_{j+1/2}^{n+1} = 1/4(C_j^{n+1} + C_j^n + C_{j+1}^{n+1} + C_{j+1}^n) - \min\left[\frac{1}{6}\left(1 + \frac{C_R}{2}\right), \frac{1}{4\delta}\right](C_{j+1}^n - 2C_j^n + C_{j-1}^n) \quad (7-14)$$

The last term in Equation (7-14) originates from the Neumann stability analysis, see the Technical Reference Manual pp AD 21-28.

The dispersion coefficient is in the model calculated as:

$$D_{j+1/2}^{n+1/2} = a \cdot \left| \frac{Q_{j+1/2}^{n+1/2}}{A_{j+1/2}^{n+1/2}} \right|^b \quad (7-15)$$

where a and b are calibration constants.

### 7.2.1 The Accuracy of the Numerical Scheme

Taylor expansions are used to ensure that the scheme has a third order accuracy by expanding the Taylor series to the third order. Elimination of the third order truncation error makes it possible to simulate concentration profiles with steep fronts. In general the third order terms are associated with phase errors and wiggles in the scheme while the second order terms lead to numerical diffusion. The Taylor expansions together with the Neumann stability analyses are given in the Technical Reference Manual pp. AD 18-29.

The result of the Neumann stability analysis, ie the phase and the amplitude portrait of the numerical scheme can be used to evaluate the accuracy of the numerical scheme. The phase and the amplitude portrait for the situation with pure advection are shown in Figure 7.5. and Figure 7.6. The stability criterion is expressed in terms of the convective Courant number, defined as:

$$Cr = \frac{|u| \cdot \Delta t}{\Delta x} \quad (7-16)$$

From the amplitude portrait it can be seen that the scheme is very accurate even for large Courant numbers. From the phase portrait it can be observed that the scheme is very accurate for Courant numbers smaller than 1.0. For Courant number larger than two with a large grid spacing numerical dispersion is present. Hence, if the advection-dispersion model has been calibrated for conditions with Courant numbers larger than one then the time step should not be changed during the following analyses even though the scheme is still stable. Even if the scheme is stable there are some restrictions on the selection of the time step,  $\Delta t$ , and the grid size,  $\Delta x$ .

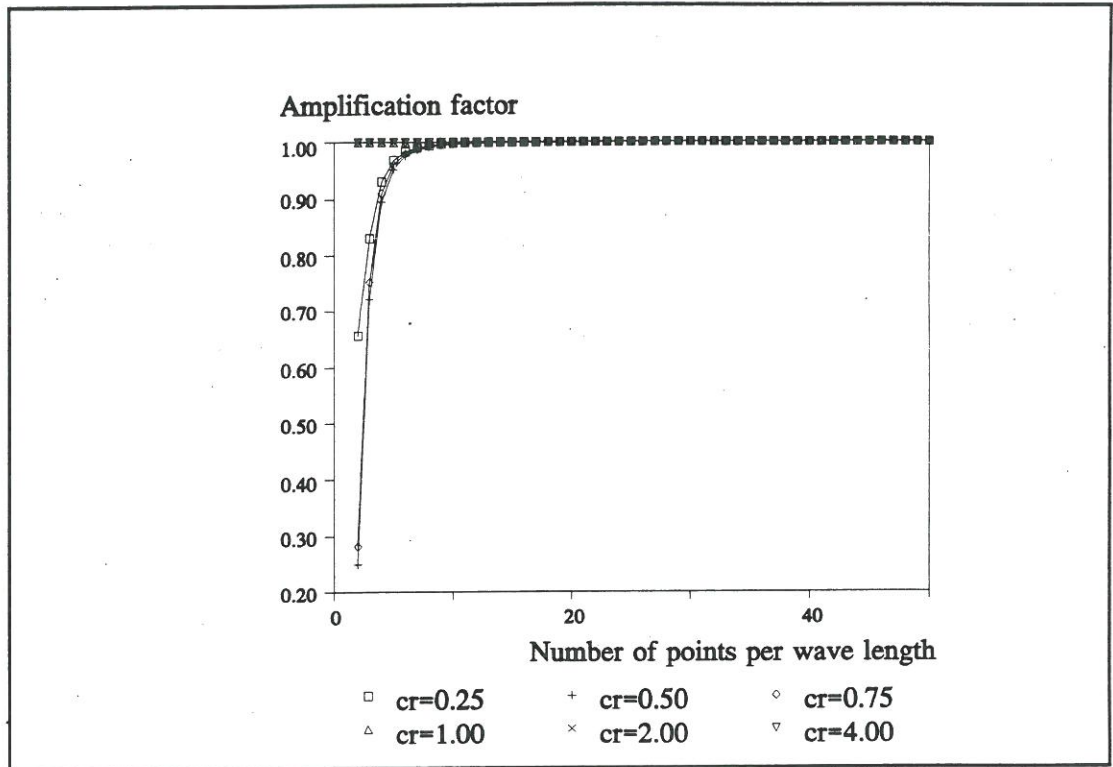


Figure 7.5. The amplitude portrait of the advection-dispersion scheme for the case without dispersion.

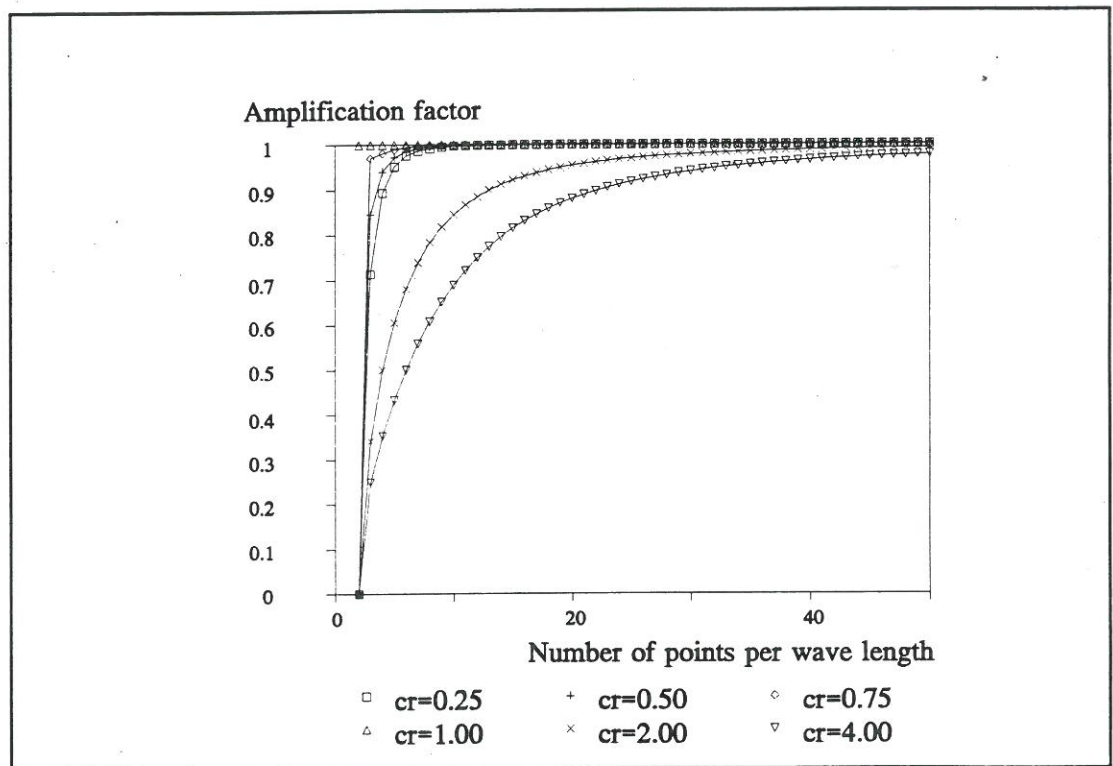


Figure 7.6. The phase portrait of the advection-dispersion scheme for the case without dispersion.

Another dimensionless number used to describe the properties of the numerical scheme is the Peclet number (Pe), defined as:

$$Pe = \frac{|u| \cdot \Delta x}{D} \quad (7-17)$$

The Peclet number is associated with numerical oscillations, wiggles, which grow or decay spatially with a wave length of  $2\Delta x$ . In a diffusion free scheme which is stable in the von Neumann sense, wiggles are likely to occur when large gradients in the concentration are present. The general criterion for the absence of wiggles is:

$$Pe \leq 2 \quad (7-18)$$

A traditional way of eliminating wiggles from the numerical scheme is by use of an upstream centring of the numerical scheme but this introduces numerical diffusion into the scheme. Alternatively the wiggles can be removed by use of the n-1 time step in the computations.

### 7.3 Test of the Applicability of the Advection-Dispersion Scheme to Sewers

In order to test the practical applicability and the implementation of the advection-dispersion model, the basic components of the model have been tested for flow conditions in sewers. Some of the tests are given below and in Appendix B.

#### 7.3.1 Test of Propagation for Pure Advection with a Courant Number = 1.0

The purpose of the test is to show that the pure advection transport of a concentration peak is correct. The test model contains a 30 km long pipe. The hydrodynamics of the test is a steady state with:

water level	= 1.0 m
discharge	= 1.0 m <sup>3</sup> /s
velocity	= 1.0 m/s

The model has a grid spacing of 600 m and the model is run with a time step of 600 s, which gives a Courant number,  $C_r = 1.0$ . The initial condition in the advection-dispersion calculation is a triangle shaped concentration peak with a peak value of 10 000 mg/m<sup>3</sup>. The model is run for 600 minutes (60 time steps). The results of the simulation can be seen in Figure 7.8. It can be seen that the concentration peak propagates with a propagation velocity of 1 m/s and that the peak does not change shape. From the mass balance in Figure 7.9, it can be seen that the simulation is mass conservative.

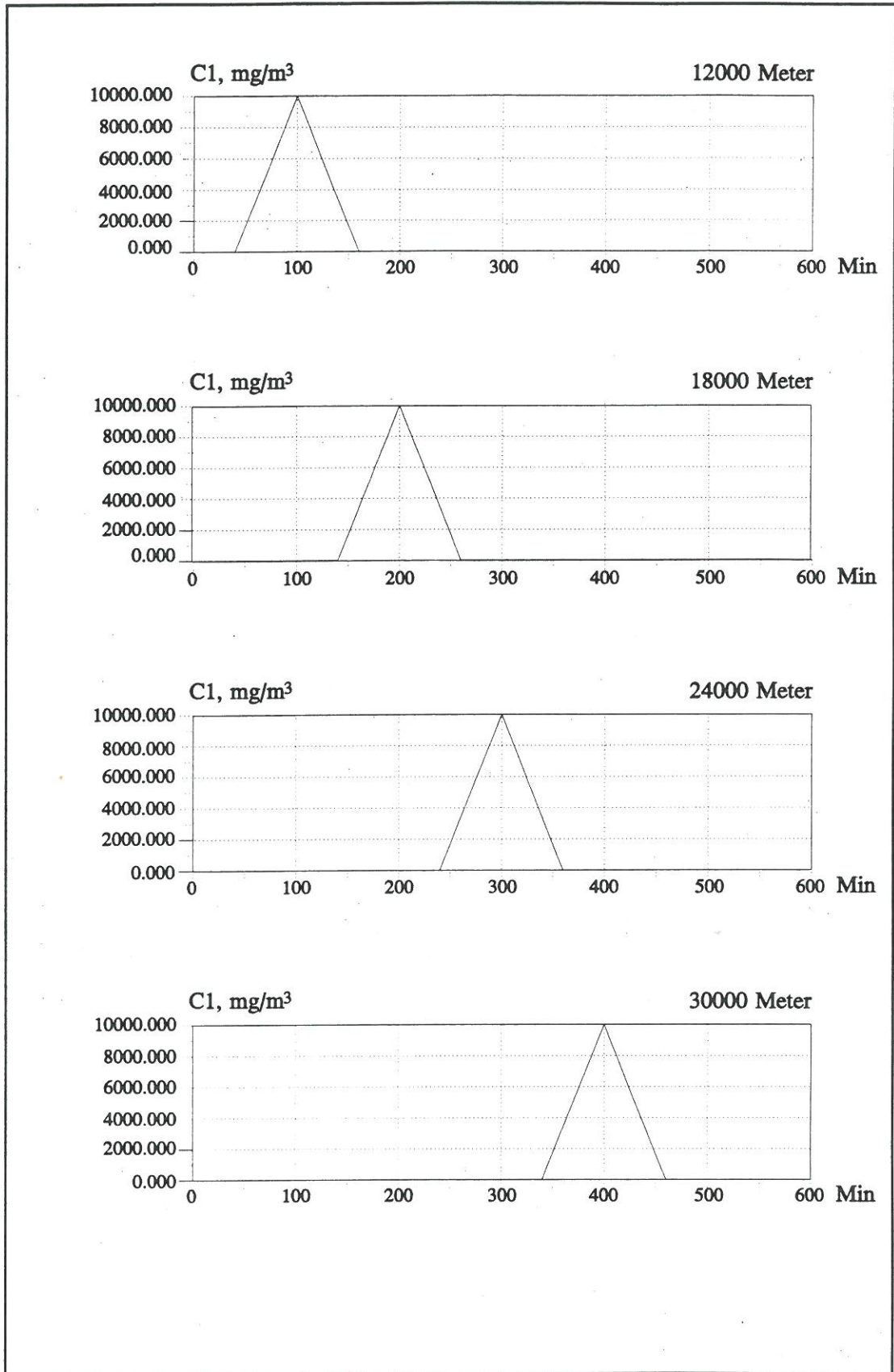


Figure 7.7. Routing of the concentration peak with a Courant number,  $Cr = 1.0$ .

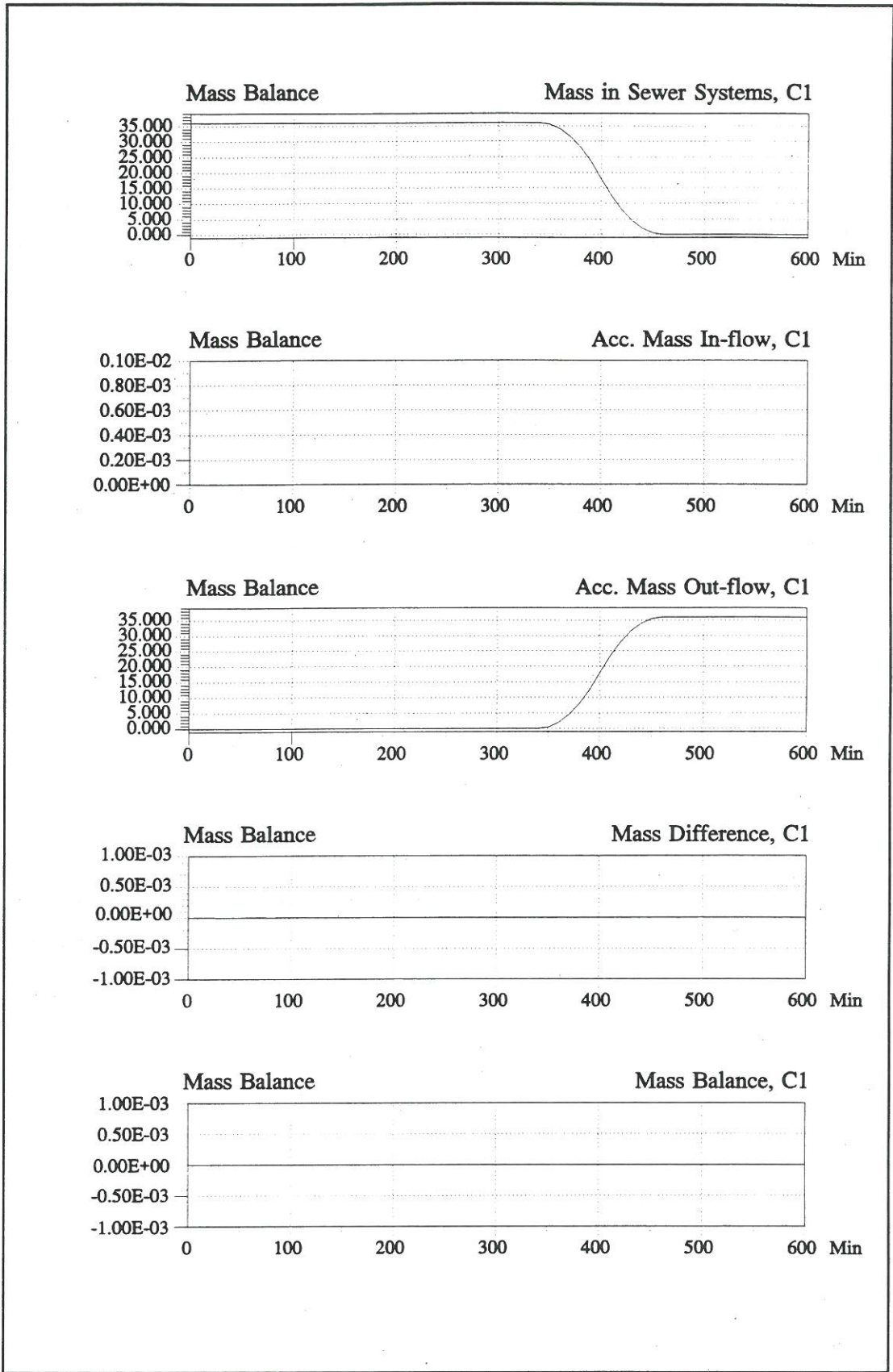


Figure 7.8. The mass balance for the simulation.

### 7.3.2 Propagation Test for pure Advection through a Single Pipe

The purpose of the test is to show that the pure advection transport of a concentration peak is correct for a Courant number,  $C_r$ , not equal to 1. The test model contains a 2.0 km long pipe. The hydrodynamics of the test is a steady state with:

water level               = 0.35 m  
discharge                 = 1 m<sup>3</sup>/s  
velocity                  = 4.038 m/s

The model has a grid spacing of 30.30 m and the model is run with a time step of 1 s, which gives Courant number,  $Cr = 0.13$ .

The initial condition in the advection-dispersion calculation is zero concentration in the pipe. A concentration peak with the shape as half a sinus curve is routed through the pipe. The peak can be seen in Figure 7.9. The model is run for 15 minutes with a time step of 1 second.

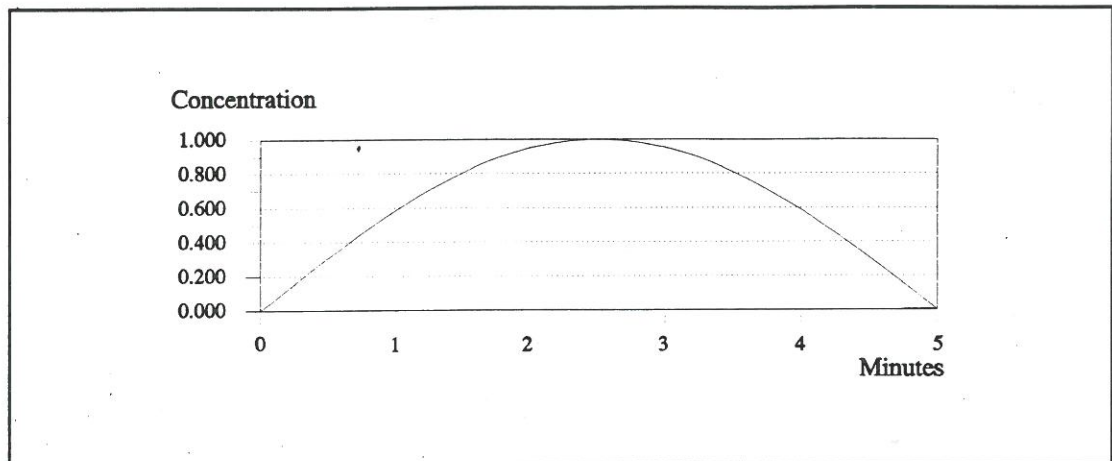


Figure 7.9. The upstream concentration boundary condition.

The time step of 1 second is selected in order to get an accurate estimate of the travel time of the peak. The Courant criteria gives a time step of 7.5 seconds. The travel time of the peak is taken as the difference in time between the occurrence of the concentration peak at the upstream end and the occurrence at the downstream end of the pipe. Hence, the travel time for the peak in the model is:

$$t_{propagation} = 10 \text{ min } 45.5 \text{ s} - 2 \text{ min } 30.5 \text{ s} = 495 \text{ s} \quad (7-19)$$

and the theoretical propagation time is:

$$t_{\text{theoretical}} = \frac{L_{\text{pipe}}}{u} = \frac{2000 \text{ m}}{4.038 \text{ m/s}} = 495.3 \text{ s} \quad (7-20)$$

It can be seen there is a good agreement with the simulated propagation time of the concentration peak and the theoretical propagation time. The results of the simulation can be seen in Table 7.1.

Min:Sec	Concentration	
	Upstream	Downstream
2:21	0.997	0.00000
2:22	0.998	0.00000
2:23	0.999	0.00000
2:24	1.000	0.00000
2:25	1.000	0.00000
2:26	1.001	0.00000
2:27	1.001	0.00000
2:28	1.002	0.00000
2:29	1.002	0.00000
2:30	1.002	0.00000
2:31	1.002	0.00000
2:32	1.002	0.00000
2:33	1.002	0.00000
2:34	1.001	0.00000
2:35	1.001	0.00000
2:36	1.000	0.00000
2:37	1.000	0.00000
2:38	0.999	0.00000
2:39	0.998	0.00000
.	.	.
10:41	0.00000	0.998
10:42	0.00000	0.999
10:43	0.00000	0.999
10:44	0.00000	0.999
10:45	0.00000	1.000
10:46	0.00000	1.000
10:47	0.00000	0.999
10:48	0.00000	0.999
10:49	0.00000	0.999

Table 7.1. Time series of concentration at the upstream and the downstream end of the pipe.

### 7.3.3 Propagation Test for Pure Advection through Multiple Pipes

The hydrodynamics are the same as in the previous test. The model is the same as in the previous test except that 9 manholes with an equal spacing are inserted instead of one long single pipe. The distance between the manholes is 200 m. The delay on the propagation of the concentration peak from a manhole can be estimated as:

$$t_{manhole} = \frac{V_{manhole}}{q} = \frac{0.35 m \pi 0.5 m^2}{1 m^3/s} = 0.27 s \quad (7-21)$$

where

$V_{manhole}$  is the volume of the manhole  
 $q$  is the discharge through the manhole.

The total propagation time for the concentration peak is then given as:

$$T = t_{pipe} + \sum_{i=1}^{i=9} t_{manhole} = 495.3 + 2.4 = 497.7 s \quad (7-22)$$

The results from the simulation can be seen in Table 7.2. The propagation time found from the simulation is:

$$t_{simulation} = 10 \text{ min } 48 \text{ s} - 2 \text{ min } 30 \text{ s} = 498 \text{ s} \quad (7-23)$$

Thus it can be seen that there is a good agreement between the theoretical and the simulated propagation time.



Min:Sec	Concentration	
	Upstream	Downstream
2:20	0.997	0.00000
2:21	0.998	0.00000
2:22	0.999	0.00000
2:23	1.000	-0.00000
2:24	1.000	-0.00000
2:25	1.001	-0.00000
2:26	1.002	-0.00000
2:27	1.002	-0.00000
2:28	1.002	-0.00000
2:29	1.002	-0.00000
2:30	1.002	-0.00000
2:31	1.002	-0.00000
2:32	1.002	-0.00000
2:33	1.002	-0.00000
2:34	1.002	-0.00000
2:35	1.001	-0.00000
2:36	1.001	-0.00000
2:37	1.000	-0.00000
2:38	0.999	-0.00000
2:39	0.998	0.00000
2:40	0.997	0.00000
10:40	0.00000	0.996
10:41	0.00000	0.997
10:42	0.00000	0.998
10:43	0.00000	0.998
10:44	0.00000	0.999
10:45	0.00000	0.999
10:46	0.00000	0.999
10:47	0.00000	0.999
10:48	0.00000	1.000
10:49	0.00000	0.999
10:50	0.00000	0.999
10:51	-0.00000	0.999
10:52	-0.00000	0.999
10:53	-0.00000	0.998
10:54	-0.00000	0.998
10:55	-0.00000	0.997

Table 7.2. The time series of concentration at the upstream and the downstream end of a multiple pipe system.

#### 7.3.4 Verification of the Mass Balance

The purpose of the test is to show that the advection-dispersion scheme is mass conservative. The test model and the boundary conditions are the same as the model used to test the propagation time for a concentration peak for a single pipe.

The total mass in the concentration peak is found by integration of the input curve for the concentration to be:

$$M = \int_0^{\pi/2} \sin\left(\frac{2\pi t}{T}\right) dt = 190.986 \quad (7-24)$$

where

M is the mass, (kg)  
T is the period, (s)

The total mass routed into the model is found by numerical integration of the inflow hydrographs with the same time step as used in the simulation.

$$M_{in} = \sum_{i=1}^{i=N} Q_b^{i+1/2} \cdot c_b^{i+1/2} = 190.970 \quad (7-25)$$

where

index  $q_b$  is the discharge at the boundary, (m<sup>3</sup>/s)  
 $c_b$  is the concentration at the boundary, (arbitrary unit)

The mass routed through the model is found by numerical integration of the outflow to be:

$$M_{out} = \sum_{i=1}^{i=N} Q_{j-1/2}^{i+1/2} \cdot c_{j-1/2}^{i+1/2} = 190.942 \quad (7-26)$$

where

j is the last grid point in the model  
i is the time step  
N is the time required for the entire mass to be routed out of the system

There is relatively little deviation in the mass of  $1.5E^{-4}$  compared to the mass routed into the model. It can be concluded that the simulation is mass conservative within the accuracy of the applied numerical methods.

### 7.3.5 Mass Balance Test for a Peak routed through Multiple Pipes

The purpose of the test is to show that the advection-dispersion scheme is mass conservative. The test model and the boundary conditions are the same as the model used to test the propagation time for a concentration peak for a multiple pipe system.

The mass into the system is:

$$M_{in} = 190.970$$

The mass flowing out of the system is found by numerical integration, by use of formula (7-26) to be:

$$M_{out} = 190.939$$

There is relatively little deviation in the mass of  $1.6E^{-4}$  compared to the mass routed into the model. It can be concluded that the simulation is mass conservative within the accuracy of the numerical methods applied.

### 7.3.6 Mixing Test for three Pipes flowing into a Manhole

The purpose of the test is to test for the correct mixing at a manhole. The model setup consists of three identical pipes, A-D, B-D, C-D flowing into a manhole. From the manhole a single pipe, D-OUT, routes the flow to the outlet. A plan plot of the model is shown in Figure 7.10.

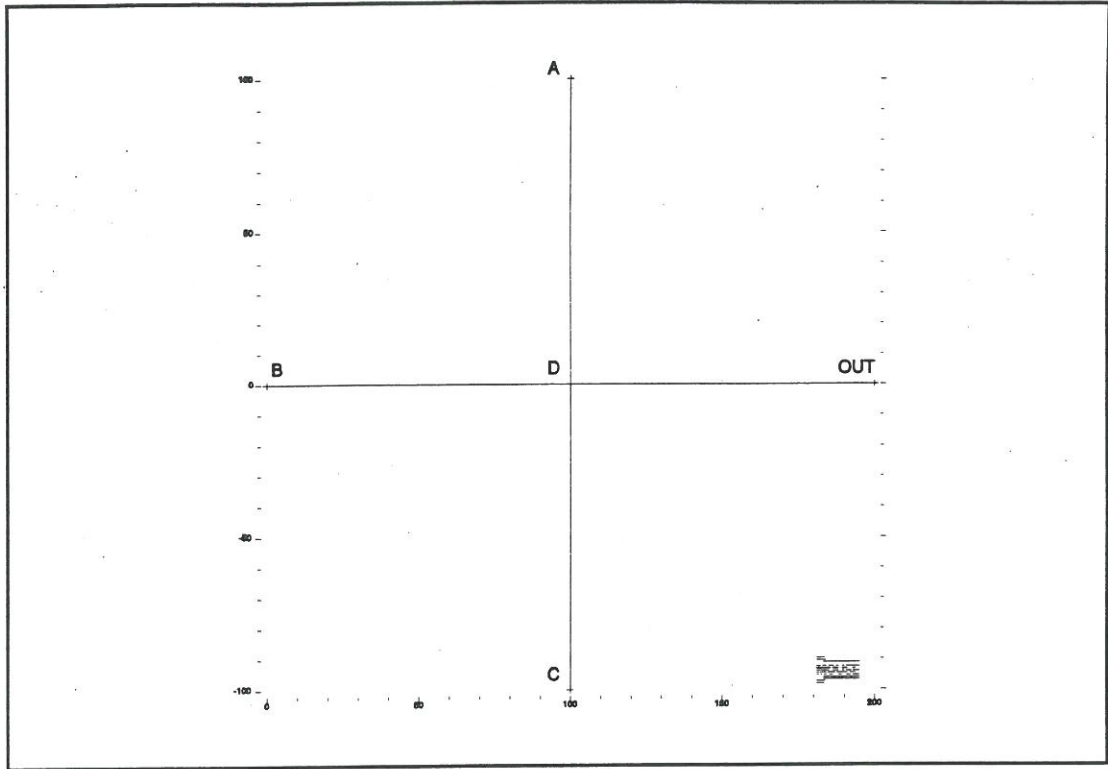


Figure 7.10. A horizontal plot of the model setup.

The hydrodynamics are constant discharges of  $0.1 \text{ m}^3/\text{s}$  in the pipes, A-D, B-D and C-D. A constant concentration of  $10 \text{ g/m}^3$  has been assigned to the flow in pipe A-D and B-D and a constant concentration of  $20 \text{ g/m}^3$  has been assigned to the pipe C-D. The concentration in the manhole should be  $13.333 \text{ g/m}^3$ . A plot of the time series of concentration in manhole D, can be seen in Figure 7.11 and a table with the time series can be seen in Table 7.3. It can be seen that the model mixes the flow correctly at a manhole.

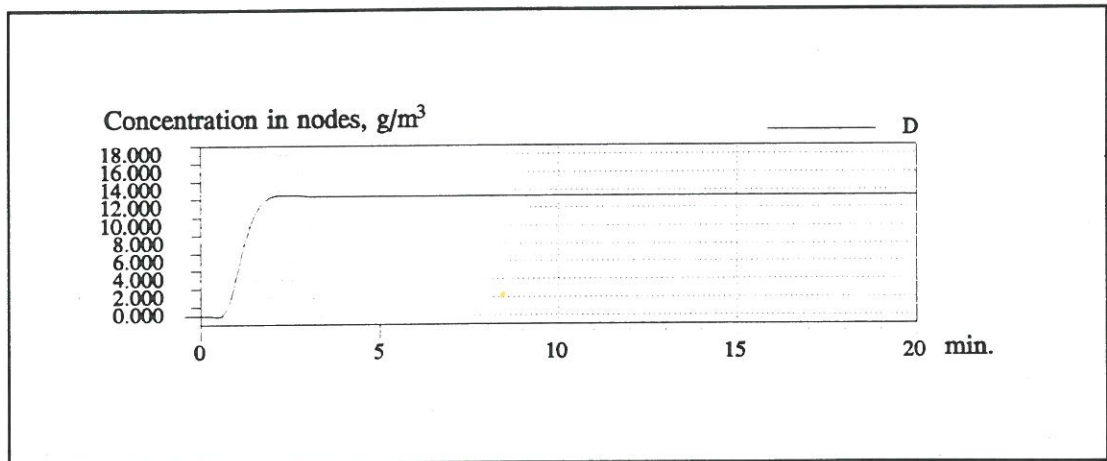


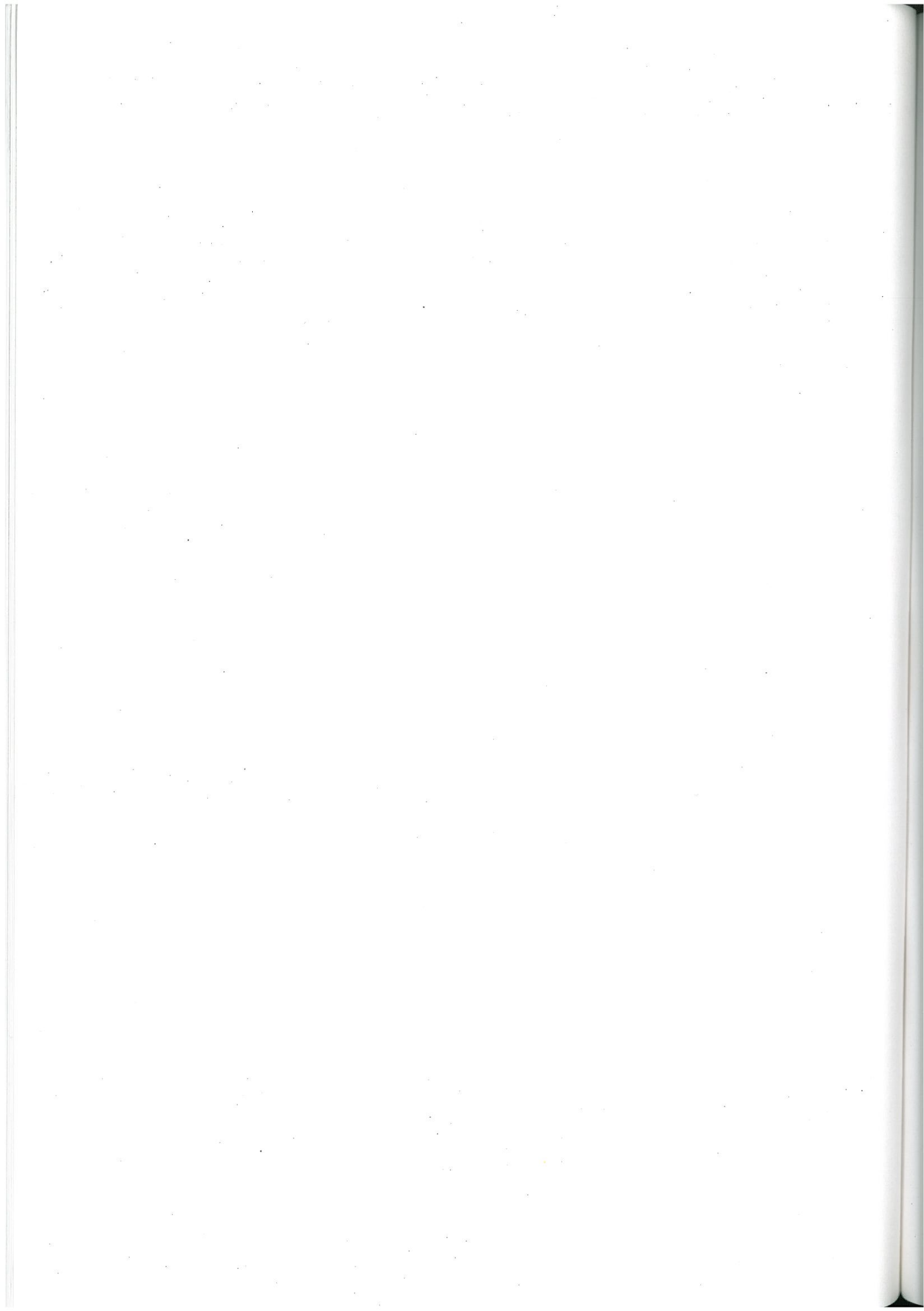
Figure 7.11. The time series of concentration in manhole D.

Min:Sec	Concentration g/m <sup>3</sup>
0:00	0.00000
0:05	0.00028
0:10	-0.0024
0:15	-0.014
0:20	-0.063
0:25	-0.130
0:30	-0.145
0:35	-0.016
0:40	0.343
0:45	0.978
0:50	1.891
0:55	3.039
1:00	4.347
1:05	5.728
1:10	7.095
1:15	8.374
1:20	9.516
1:25	10.489
1:30	11.287
1:35	11.917
1:40	12.398
1:45	12.754
1:50	13.010
1:55	13.188
4:00	13.329
4:05	13.330
4:10	13.330
4:15	13.331
4:20	13.331
4:25	13.332
4:30	13.332
4:35	13.333
4:40	13.333
4:45	13.333

*Table 7.3. The time series of concentration in manhole D.*

#### **7.4 Summary of the Test of the Applicability of the Advection-Dispersion Scheme to Sewers**

From the stability analyses of the numerical scheme and the tests for the mass balance and the propagation time it can be concluded that the advection-dispersion model can be applied for the routing of dissolved matter in simple theoretical sewer systems with a good performance and accuracy.



## **8 DESCRIPTION OF THE SEDIMENT TRANSPORT MODELS**

The transport of sediment particles is based on a numerical solution of the continuity equation for bed sediment. The numerical modelling of the sediment transport continuity equation is based on a finite difference scheme. In this chapter the accuracy of the numerical finite difference scheme in the modelling system is discussed together with an evaluation of the applicability of the scheme to sewer systems. Further, the special modelling approaches for the conditions where no theory is presently available are discussed.

### **8.1 Modelling of Non-Cohesive Sediments in Sewers**

At present, no theories exist for many of the physical processes related to sediment transport in sewers. In order to describe and model the sediment transport for the full range of conditions found in sewer systems, it has been necessary during this study to develop special mathematical formulations for the bed shear stress and the sediment transport. A list of the processes where special mathematical formulations have been developed is given below:

- the transport of dissolved sediments and sediment particles through structures
- the critical bed shear stress for non-uniform non-cohesive sediment
- the critical bed shear stress for sediment particles on a rigid bed
- the critical bed shear stress for the conditions ranging from a pipe without sediment deposits to a pipe with a full deposited sediment bed
- the sediment transport of non-uniform sediments
- the sediment transport for the conditions ranging from a pipe without sediment deposits to a pipe with a full deposited sediment bed

#### **8.1.1 Sediment Transport at Structures**

The description of the sediment transport at structures in sewer systems is very important, as the structures are designed either to trap sediments or to transport the sediments through the structure without sedimentation. Very often the combined sewer overflows, eg the circular weir or the swirl separator, are designed to prevent the sediment particles being discharged to the receiving waters. In the present study the structures in the sewer system are divided into three groups:

- manholes
- overflow structures
- basins

The formulations implemented in the model are general and they have to be adjusted for each individual structure in the sewer system.

## Sediment Transport through a Manhole

The sediment transport in manholes is routed straight through the manhole without any deposition. This is done as the level of turbulence in manholes is high and hence it is assumed that the sediment is transported in suspension. Further, very limited laboratory and field data are available to predict deposition, if any, in manholes. The sediment transport from a manhole is distributed according to the ratio of the out flowing discharges. A pre-defined distribution of the sediment transport out of a manhole can also be specified to take into account different levels of the outflow pipes. The distribution is giving the coefficients and exponents ( $K$  and  $n$  values) in the following relationship:

$$S_3 = \frac{K_3 \cdot Q_3^{n_3}}{K_3 Q_3^{n_3} + K_4 Q_4^{n_4}} (S_1 + S_2) \quad (8-1)$$

where

- $Q_i$  is the discharge in pipe  $i$ , ( $m^3/s$ )
- $S_i$  is the sediment transport in pipe  $i$ , ( $m^3/s$ )
- $K_i$  calibration constant for pipe  $i$
- $n_i$  calibration constant for pipe  $i$

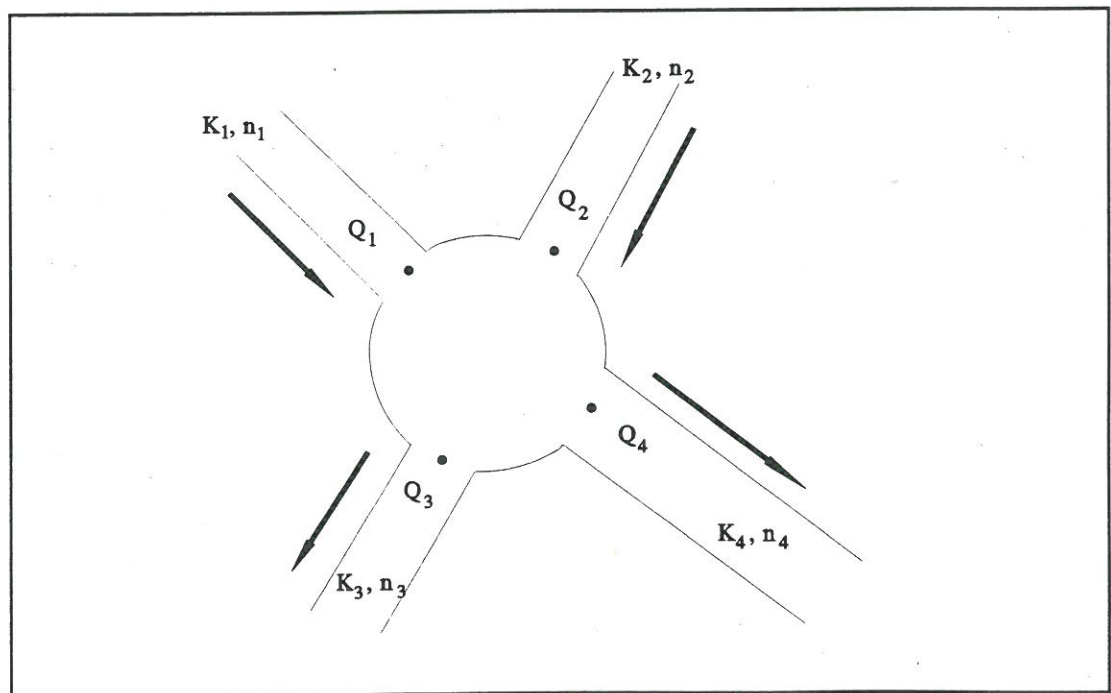


Figure 8.1. The distribution of the sediment transport through a manhole.



## Sediment Transport through an Overflow Structure

The overflow structure is an important part of the sewer system as this structure determines the amount of water and pollutants discharged to the receiving waters. Information is often available concerning the efficiency of the overflow structure, eg from design experiments, hence, accurate information can be specified for this structure. The sediment transport past an overflow structure can be modelled in three different ways:

- $S_{\text{weir}} = (1 - \text{Eff}) \cdot S_{\text{Total into weir}}$ ,  
the reduction factor is constant through out the whole simulation
- $S_{\text{weir}} = (1 - \text{Eff}(Q)) \cdot S_{\text{Total into weir}}$ ,  
the reduction factor is a function of the discharge flowing into the weir
- $S_{\text{weir}} = (1 - \text{Eff}(w/u)) \cdot S_{\text{Total into weir}}$ ,  
the reduction factor is given as the expression below:

$$\text{Eff}\left(\frac{w}{u}\right) = 1 - K \cdot \text{Exp}\left(-\left(\frac{w/u - \mu}{\sqrt{2} \cdot \sigma}\right)^2\right) \quad (8-2)$$

where

$K$ ,  $\mu$  and  $\sigma$  are dimensionless variables given as:

$$\begin{aligned} K &= k_1 \cdot Q_{\text{out}}/Q_{\text{in}} + k_2 \\ \mu &= \mu_1 \cdot Q_{\text{in}}/(Q_{\text{in}} - Q_{\text{out}}) + \mu_2 \\ \sigma &= \sigma_1 \cdot Q_{\text{in}}/(Q_{\text{in}} - Q_{\text{out}}) + \sigma_2 \end{aligned} \quad (8-3)$$

where

$k_1$ ,  $k_2$ ,  $\mu_1$ ,  $\mu_2$ ,  $\sigma_1$  and  $\sigma_2$  are calibration constants.

Equation (8-3) has been found for the central weir and the swirl separator by Sørensen (1991):

The central weir:

$$\begin{aligned}
 K &= -140.697 \cdot Q_{out}/Q_{in} + 133.86 \\
 \mu &= -2.308 \cdot Q_{in}/(Q_{in} - Q_{out}) + 3.17 \\
 \sigma &= 1.617 \cdot Q_{in}/(Q_{in} - Q_{out}) - 0.27
 \end{aligned}
 \tag{8-4}$$

and for the swirl separator:

$$\begin{aligned}
 K &= -79.782 \cdot Q_{out}/Q_{in} + 133.54 \\
 \mu &= -5.015 \cdot Q_{in}/(Q_{in} - Q_{out}) + 3.92 \\
 \sigma &= 2.659 \cdot Q_{in}/(Q_{in} - Q_{out}) - 0.22
 \end{aligned}
 \tag{8-5}$$

### Sediment Transport through a Basin

The sediment transport through basins/tanks is important as basins are often used in the (re-)design of sewer systems. The purpose of the tank may be for storage or for reduction of the combined sewer over flows. The flow pattern in basins/tanks are often very complex. In the modelling system sediment can be removed from basins according to the formula (EPA, 1986):

$$E = 1 - \left(1 + \frac{1}{n} \frac{w}{Q/A}\right)^{-n}
 \tag{8-6}$$

where

E is the sediment trap efficiency  
w is the fall velocity, (m/s)  
Q is the discharge into the tank, (m<sup>3</sup>/s)  
a is the surface area of the basin, (m<sup>2</sup>)  
n is calibration factor, ie a turbulence constant indicating the settling performance of the basin:

n = 1 for poor performance,  
n = 3 for good performance,  
n > 5 very good performance,  
n = ∞ ideal performance.

Equation (8-6) is recommended by the Environment Protection Agency, USA, in 1986. It is a general formula for the removal of sediments under quiescent and dynamic flow conditions. The sediments removed by Equation (8-6) are taken out of the computations. Hence, no update of the bed level takes place for the deposited sediment in basins and it is not possible to re-suspend this sediment.

### 8.1.2 Sediment Transport through a Pump

The sediment transport through a pump taken from the source node of the pump. The amount of sediment transported through the pump is determined according to the ratio of the out flowing discharges from the source node of the pump, see Equation (8-1). The sediment transport is then added to the destination node of the pump without a time lag, ie it is the boundary condition for the destination node.

## 8.2 Special Formulations for Modelling of Sediment Transport in Sewers

In order to model the full range of sediment transport conditions in pipes it has been necessary to develop special formulations where little or no knowledge is available today. The range the special formulations cover is the critical range from a full deposited sediment bed to the conditions where no sediment deposits are present in the pipe.

### 8.2.1 The Critical Bed Shear Stress for Non-Uniform Non-Cohesive Sediments

Real sewer sediments are often non uniform and the description of the sediment transport processes is much more complex than for the case of uniform sediments. When the bed shear stress is much larger than the critical bed shear stress the use of a single representative grain size may be acceptable, otherwise it is necessary to model more sediment fractions to get an accurate description of the sediment transport.

When non-uniform sediments are present the smaller particles are sheltered by larger particles and therefore transported at another rate. The larger particles are exposed to larger fluid dynamic forces compared to the same sized particles in a uniform sediment and hence they are transported at a greater rate. Subsequently at low values of the bed shear stress the coarse fraction might not move at all and an armouring of the bed might take place. A consequence of these phenomena is that the critical bed shear stress predicted by Shields (1936) has to be modified.

The criterion for the threshold of movement,  $\theta_c$ , ("a" in the Ackers and White model) is modified to allow for the hiding of finer particles and the greater exposure of larger particles as well as the mutual interference between particles of different size. The critical bed shear stress can be modified eg by applying Egiazaroff's (1965) correction factor:

$$\theta_{ci} = \theta_c \left[ \frac{\ln(19)}{\ln\left(\frac{19d_i}{d_{med}}\right)} \right]^2 \quad (8-7)$$

where

$\theta_{ci}$  is the dimensionless critical bed shear stress for fraction: i  
 $\theta_c$  is the dimensionless critical bed shear stress for uniform sediment  
 $d_i$  is the representative grain size for fraction: i  
 $d_{med}$  is the average grain size of the total sediment sample

### 8.2.2 The Critical Bed Shear Stress for a Pipe with negligible Sediment Deposits

The critical bed shear stress for a pipe without sediment deposits has many similarities to the critical bed shear stress for non-uniform non-cohesive sediments. The roughness from the pipe can be correlated to one particular grain fraction while the actual sediment can be taken as a second grain fraction. Many experiments have been carried out eg Novak and Nalluri (1984) and Suki and Baker (1991). They concluded that the critical shear stress is a function of the grain size and the concentration, although at present no mathematical description exist which is applicable for a general numerical model. Hence, it has been decided to adopt the Egiazaroff's (1965) correction factor for the calculation of critical bed shear stress when no sediment deposit is present in the pipe.

### 8.2.3 The Critical Bed Shear Stress for a Pipe with a thin Layer of Sediment

A transition zone exists for the critical bed shear stress between the case of a pipe with a full deposited sediment bed and a pipe without a sediment deposit. As no knowledge is available today for the critical bed shear stress in this zone, it was decided to make a linear variation of the critical bed shear stress from the critical bed shear stress for a full deposited bed to the critical bed shear stress in a pipe without sediment deposits in this zone. For further information see the Technical Reference Manual p ST 75.

### 8.2.4 The Critical Bed Shear Stress for Adhesive Sediments

In sewers adhesive forces may exist between the particles in the sediment deposits. The critical bed shear stress has been found to be much larger for particles with adhesive properties than given by the Shields criterion, see Section 4.5.4. It has been shown that when the critical bed shear stress has been exceeded for sediment with adhesive properties they are transported as non-cohesive sediment particles, (Nalluri and Alvarez, 1990).

The adhesive forces depend on various different parameters such as the time since the deposition, the chemical and biological process in the sewer and the sediment characteristics. Insufficient data exist to verify a model which describes the development of the adhesive forces between sediment particles. Hence, the development of adhesion between sediment particles is at present not represented in the modelling system.

In the model it is possible to give the variation of the critical bed shear stress in the initial sediment deposits in the sewer system. It is possible to assign a critical bed shear stress both to cohesive and non-cohesive sediments. A variation of the critical bed shear stress in sediment deposits is described by Ashley (1993). Whilst only erosion occurs the critical bed shear stress is calculated according to the function given for the critical bed shear stress for the adhesive sediments given in equations (8-8) and (8-9). If deposition occurs the critical bed shear stress is set equal to the Shields critical bed shear stress, and Shields critical bed shear stress will be used for as long as the depth of the sediment deposit is larger than the maximum depth to which the initial sediment deposit has been eroded. The formulation of the critical bed shear stress is given in the "if statement" below:

If the actual sediment depth is larger than the maximum depth to which erosion has occurred then

$$\theta_c = \theta_{c \text{ from Shields}} \quad (8-8)$$

else

$$\theta_c = \theta_{bot} + (\theta_{top} - \theta_{bot}) \cdot \left( \frac{y_{sediment}}{y_{initial \ depth}} \right)^{FAC} \quad (8-9)$$

where

$\theta_{bot}$	is the critical bed shear stress at the bottom of the pipe
$\theta_{top}$	is the critical bed shear stress at top of the initial sediment deposit
$y_{sediment}$	is the actual depth of the sediment deposit, (m)
$y_{initial \ depth}$	is the initial depth of the sediment deposit, (m)
FAC	is a calibration factor which specifies the shape of the variation of the critical bed shear stress,

The depth of the initial sediment deposits is taken relative to the bottom level of the pipe.

### 8.2.5 The Sediment Transport in a Pipe without Sediment Deposits

For non-cohesive sediments transported by use of the continuity equation for bed sediments, the sediment transport is zero when no sediment is present in the pipe.

For fine sediments transported by use of the advection-dispersion equations the sediment transport is only dependent on the sediment layer if erosion occurs, otherwise the transport of fine sediments is independent of the thickness of the sediment layer in the pipe.

### 8.2.6 Sediment Transport in Pipes with a thin Layer of Sediment

A transition zone exists for the non-cohesive sediment transport between the case of a pipe with a full deposited sediment bed and a pipe without a sediment deposit. Few laboratory experiments have been carried out in this regime (Perrusquía, 1993 and Kleijwegt, 1992b). From these preliminary experiments it is not possible to establish a general relationship for the sediment transport in a pipe with a thin layer of sediments. Hence, a modelling approach has been made to describe this phenomenon:

If the sediment depth is less than the height of an equilibrium sand dune under similar flow conditions then the sediment layer is classified as thin. In this case the calculation of the sediment transport is modified in the following way:

If  $\frac{\text{Dune height}}{\text{Sediment depth}} < 0.5$  then

$$Sed_{\text{reduction factor}} = 2 \cdot \left( \frac{\text{Dune height}}{\text{Sediment depth}} \right)^2 \quad (8-10)$$

else

$$Sed_{\text{reduction factor}} = 1 - \left( 1 - \frac{\text{Dune height}}{\text{Sediment depth}} \right)^2$$

$$S = Sed_{\text{reduction factor}} \cdot S_{\text{full transport capacity}} \quad (8-11)$$

The equations (8-10) - (8-12) describe the reduction in the sediment transport due to the fact that the sediment depth in the pipe is less than the bed load transport layer (the equilibrium dune height). The reduction factor is shown as a function of the sediment depth over the equilibrium dune height in Figure 8.2.

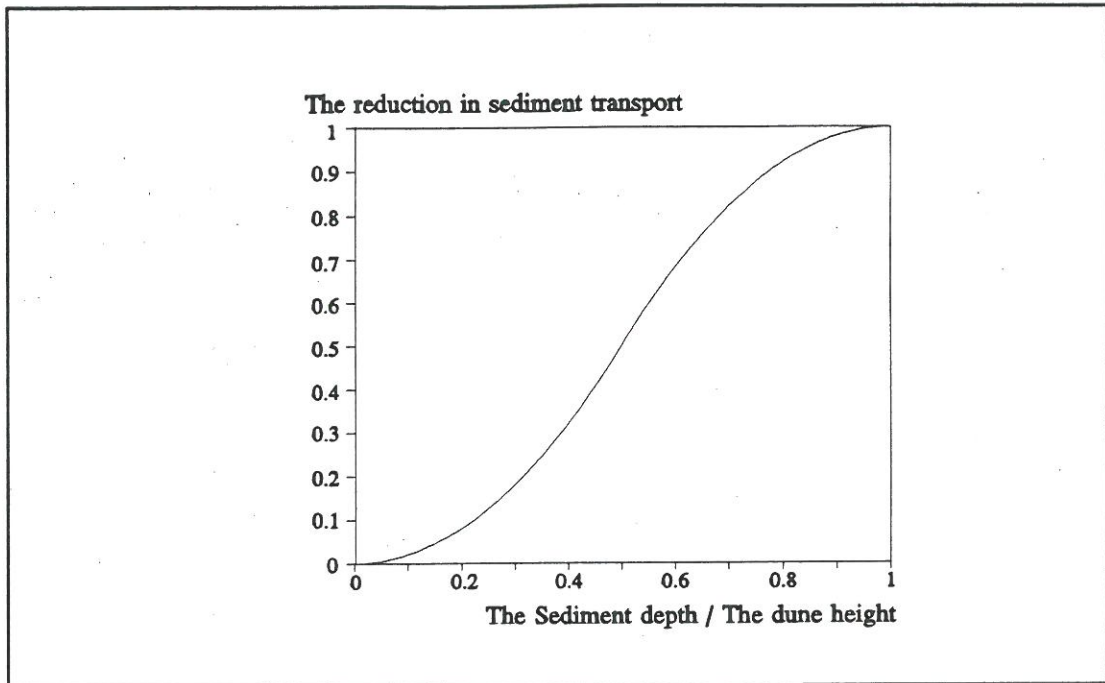


Figure 8.2. The reduction factor for the sediment transport as a function of the sediment depth over the dune height.

### 8.3 The Non-Cohesive Sediment Transport Scheme

A tradition exists for modelling of the non-cohesive sediment transport by use of the Preissmann scheme eg Lyn (1987) and Cunge (1976). When the sediment transport is modelled by use of a Preissmann scheme two possibilities exist:

- an implicit scheme which solves both the hydrodynamic equations, ie the continuity and the momentum equation together with the sediment transport continuity equation. Hence, the amount of sediment eroded/deposited is taken into account in the hydrodynamic continuity equation. An example of a this type of scheme is given in Correia et al. (1992).
- an implicit scheme which solves the hydrodynamic equations first, ie the continuity and the momentum equation. The results from the solution of these equations (water depth, velocity, etc) are then used as input to the solution of the sediment transport continuity equation. The results in terms of changes in bed level and resistance number are then used for updating the conditions for the hydrodynamic module.

An example of a scheme which solves both the hydrodynamic equations and the sediment transport continuity equation at the same time is given in Lyn and Goodwin (1987). A scheme which solves the hydrodynamic equations and the sediment transport continuity equation alternating can be applied when the change in bed level is insignificant compared to the water depth. Correia et al. (1992) compares the two type of schemes and find no difference in the accuracy of the schemes. The present

model uses the scheme which solves the hydrodynamic equations and the sediment transport continuity equation alternating. This approach has been tested for the conditions in sewer systems, see Section 8.4.4. This scheme has the advantage that it is fast to execute. It may eg be chosen only to run the sediment transport model for every 6-10th time the hydrodynamic model is executed. This can be done as the time scale of the sediment transport is much larger than the hydrodynamic time scale.

### 8.3.1 Characteristics of the Sediment Transport Scheme

The movable bed model for non-cohesive sediments is the numerical solution of the continuity equation for sediment transport. The continuity equation for sediment yields:

$$W \cdot \frac{\partial S}{\partial x} + (1 - \epsilon) \cdot \frac{\partial Z}{\partial t} = 0 \quad (8-12)$$

The sediment continuity equation is solved by use of a Preissmann Scheme, see Figure 8.3.

$$(1 - \epsilon) \left[ (1 - \psi) \frac{W \Delta z_j^{n+1}}{\Delta t} + \psi \frac{W \Delta z_{j+1}^{n+1}}{\Delta t} \right] + \quad (8-13)$$

$$\theta \frac{S_{j+1}^{n+1} - S_j^{n+1}}{\Delta x} + (1 - \theta) \frac{S_{j+1}^n - S_n^j}{\Delta x} = 0$$

where

W	is the flow width (m)
$\Delta z^{n+1}$	is the change in bed level (m)
$s_n^j$	is the sediment transport rate per unit width ( $m^2/s$ )
$S_n^j$	is $W \cdot s_n^j$
$\epsilon$	is the porosity of the sediment
$\psi$	is the space centring coefficient ( $0.5 \leq \psi \leq 1$ )
$\theta$	is the time centring coefficient ( $0.5 \leq \theta \leq 1$ )



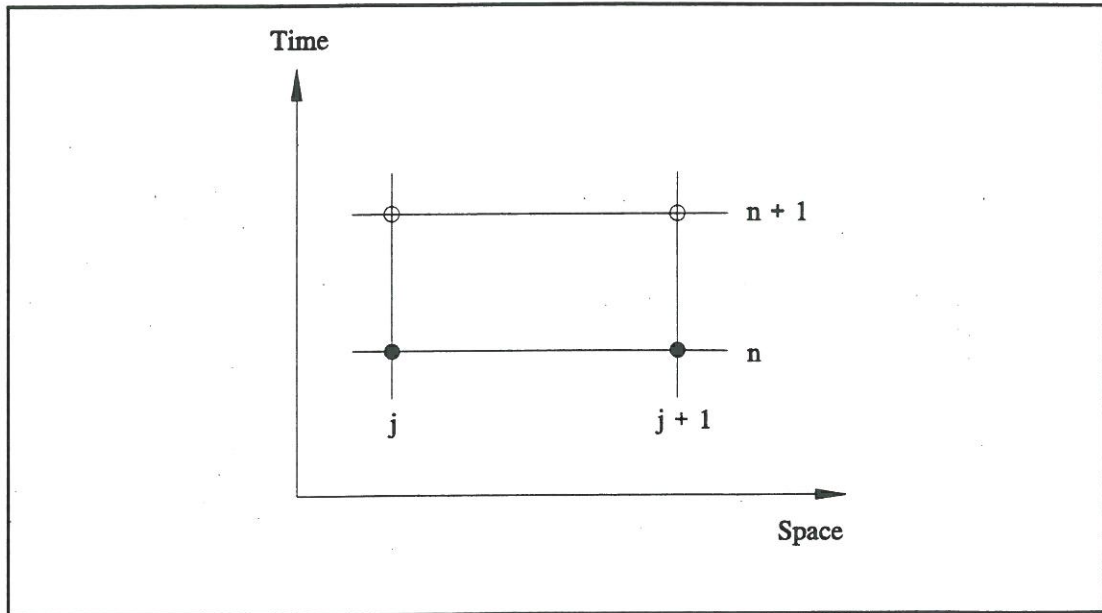


Figure 8.3. The Preissmann scheme.

The transport at  $t = (n+1)\Delta t$  is approximated by

$$S_j^{n+1} = S_j^n + \left( \frac{\partial s}{\partial U} \frac{\partial U}{\partial z} + \frac{\partial s}{\partial Y} \frac{\partial Y}{\partial z} \right) \Delta z_j^{n+1} \quad (8-14)$$

$\partial U/\partial z$  and  $\partial Y/\partial z$  are by default calculated from a back water curve assuming locally steady flow. In the case of strongly unsteady flow  $\partial Y/\partial z$  and  $(\partial U/\partial z) \cdot (Y/U)$  will normally be close to -1 and 1, respectively. Hence, it is also possible to select:

$$\frac{\partial Y}{\partial z} = -1 \text{ and } \frac{\partial U}{\partial z} \frac{Y}{U} = +1 \quad (8-15)$$

$\partial s/\partial U$  and  $\partial s/\partial Y$  can be obtained by numerical differentiation:

$$\frac{\partial s}{\partial U} \approx \frac{s(U+\Delta U, Y) - s(U, Y)}{\Delta U} \quad (8-16)$$

and

$$\frac{\partial s}{\partial Y} \approx \frac{s(U, Y+\Delta Y) - s(U, Y)}{\Delta Y} \quad (8-17)$$

### 8.3.2 The Boundary Conditions for the Continuity Equation for Bed Sediment

The unknown variable in the finite difference scheme is the bed level,  $z$ . This becomes evident by substituting Equation (8-15) into Equation (8-13). Due to this the boundary conditions should therefore preferably be given in terms of bed level variations. However, a sediment transport boundary condition can be given. In this case the difference between the transport specified at the boundary and the calculated transport at the first in-flow point in the model is assumed to erode/deposit at the boundary according to a one point continuity consideration:

$$S_{BND}/W - (S_j^n + \alpha \Delta z_j^{n+1}) = \frac{\Delta x}{\Delta t} (1-\epsilon) \Delta z_j^{n+1} \quad (8-18)$$

where  $\alpha$  is given as:

$$\alpha = \left( \frac{\partial s}{\partial U} \frac{\partial U}{\partial z} + \frac{\partial s}{\partial Y} \frac{\partial Y}{\partial z} \right)_j \quad (8-19)$$

### 8.3.3 The Stability of the Preissmann Scheme Applied to the Continuity Equation for Bed Sediment

The continuity equation for non-cohesive sediment transport is solved by use of an implicit Preissmann scheme. The Preissmann scheme is well suited for the solution of hyperbolic problems with only one characteristic. The condition for numerical stability of the generalized Preissmann scheme was found by use of Fourier series by Lyn and Goodwin (1987):

$$\frac{(\phi - 0.5)}{C_r} + (\theta - 0.5) \geq 0 \quad (8-20)$$

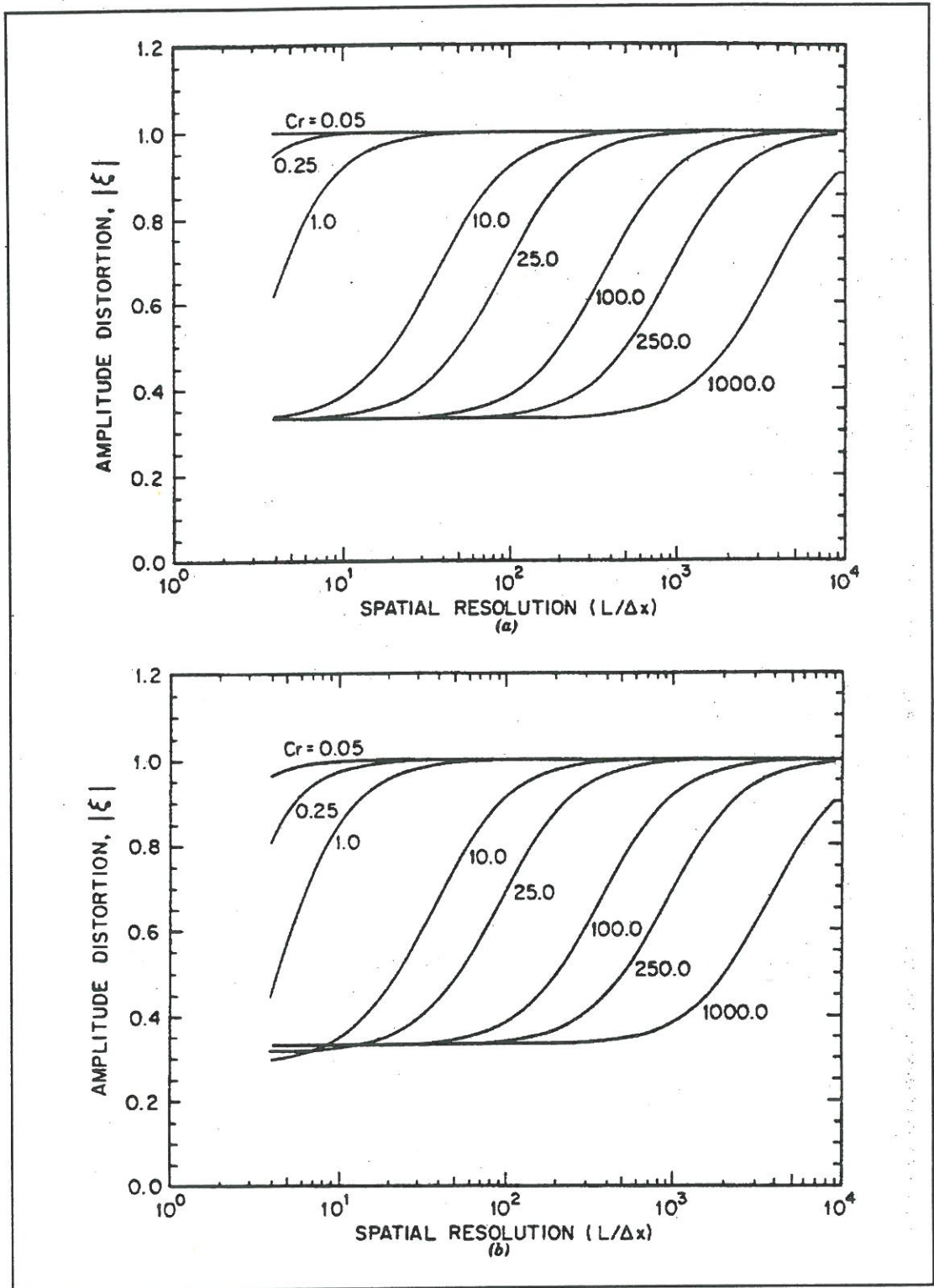


Figure 8.4. The amplitude portrait for the non-cohesive sediment transport scheme. Top: time centring,  $\theta = 0.75$ , and a space centring,  $\psi = 0.5$ ; bottom: time centring,  $\theta = 0.75$ , and a space centring,  $\psi = 0.75$ , from Lyn and Goodwin, 1987.

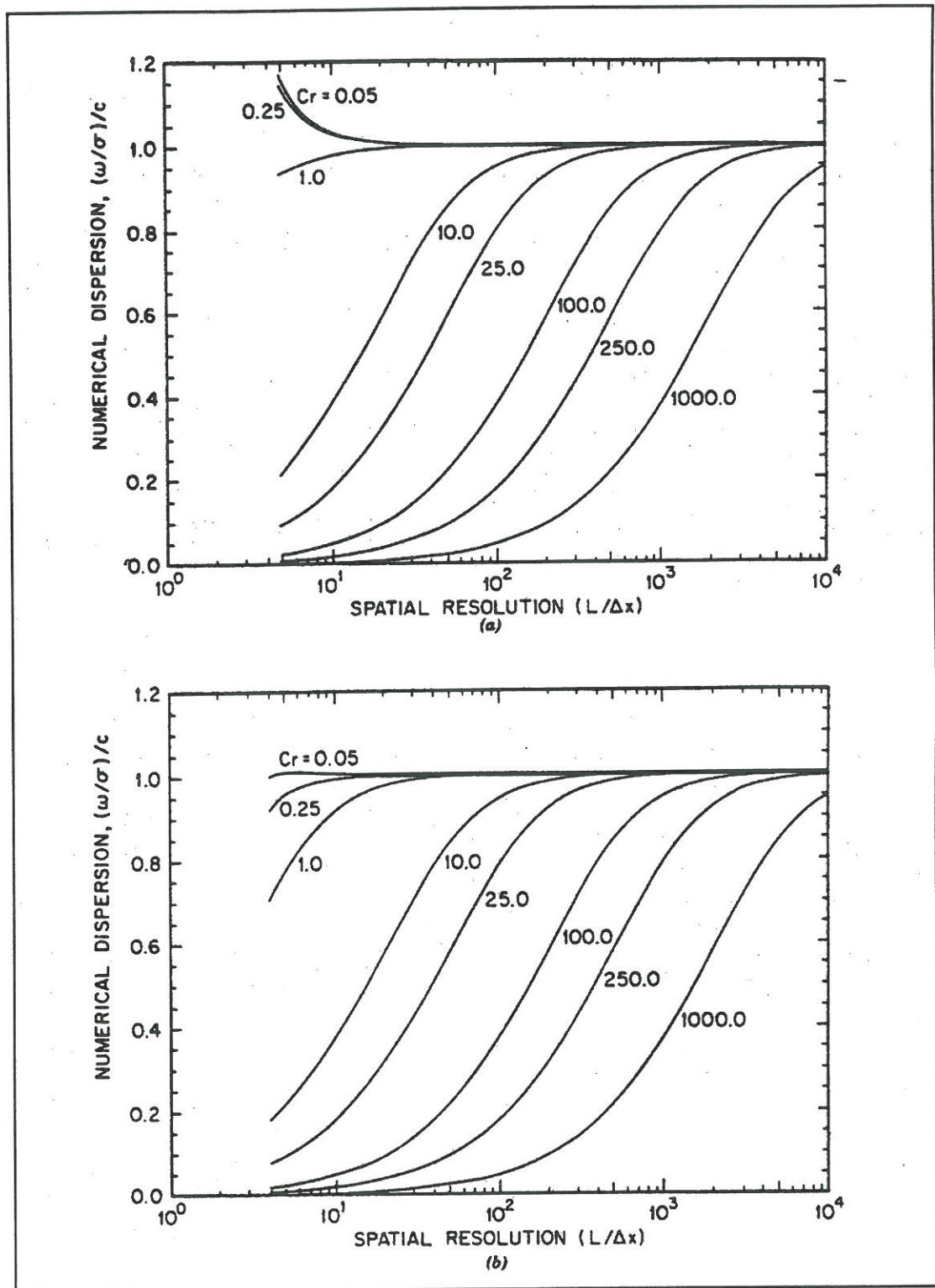


Figure 8.5. The phase portrait for the non-cohesive sediment transport scheme. Top: time centring,  $\theta = 0.75$ , and a space centring,  $\psi = 0.5$ ; bottom: time centring,  $\theta = 0.75$ , and a space centring,  $\psi = 0.75$ , from Lyn and Goodwin, 1987.

The Preissmann scheme has a drawback because at small Courant numbers it generates short wave oscillations (wave length  $2\Delta x$ ). Lyn and Goodwin (1987) showed that it is necessary to centre the scheme forward in space in order to remove numerical oscillations in the bed level, see Figure 8.6.

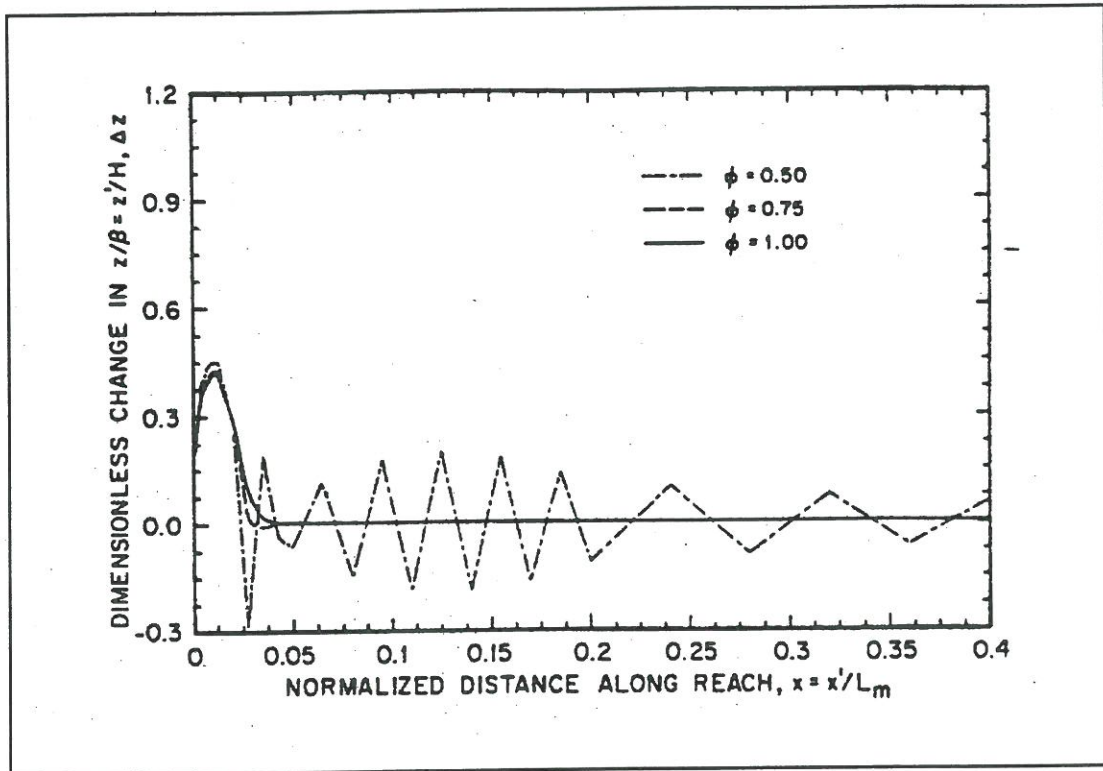


Figure 8.6. Effect of variation in spacial weighting factor,  $\phi$ , on bed oscillations, from Lyn and Goodwin, 1987.

The oscillations can be damped by forward centring the scheme in space ie by using a large value of  $\psi$ , eg 0.75-1.0, but this implies that the scheme is non-centred in space and the second order accuracy is lost and numerical dispersion is introduced at high Courant numbers. This is an acceptable approach if numerical dispersion can be tolerated. If numerical dispersion cannot be tolerated then it is necessary to apply bed Courant numbers larger than unity and  $L/dx > 10$ . Correia and Krishnappan (1991) conclude that the inaccuracies from the numerical scheme are of minor importance compared to the uncertainties from the prediction of the bed resistance and the sediment transport. The sediment transport Courant number  $Cr_b$  (Cunge and Perdreau, 1973) for the bed wave can be calculated as:

$$(8-21)$$

By use of eg the Engelund-Hansen sediment transport formula, see the Technical Reference Manual pp ST-30, Equation (55), the sediment transport Courant number can be approximated by:

$$Cr_b = 5 \frac{\Delta t}{\Delta x} \frac{s}{Y} \frac{1}{1-\epsilon} \quad (8-22)$$

This implies that the movable bed model can run with a much larger time step than the hydrodynamic model. Often the time step will be limited only by the ability to resolve the boundary conditions and the hydrodynamic flow conditions together with the disturbance from the updating of the bed level, which should be sufficiently small in order not to introduce instabilities in the hydrodynamics. A time step in the order of 6-10 times the time step in the hydrodynamic calculation can be suggested for flow conditions which not is very unsteady.

## 8.4 Test of the Applicability of the Sediment Transport Scheme to Sewers

Selected tests are used to evaluate the applicability of the Preissmann scheme to modelling of sediment transport in sewers. The tests are focused on the mass balance and the propagation time in the numerical scheme.

### 8.4.1 Test of Sediment Transport Formulae

The sediment transport formulae implemented in the sediment transport model have been tested against analytical solutions. A summary of the tests is given below. For further details please refer to Appendix C.

The four sediment transport formulae have been verified for steady state hydrodynamic conditions. Only the basic calculations are given below. For further information on the sediment transport formulae, please refer to the Technical Reference Manual. The hydrodynamics used to verify the sediment transport formulae are:

water level	= 1.0 m
discharge	= 1.0 m <sup>3</sup> /s
velocity	= 1.0 m/s
slope	= 6.26E-4
grain size, d <sub>50</sub>	= 0.30 mm

	Analytical bed suspended total			MOUSE bed suspended total		
	(l/s)	(l/s)	(l/s)	(l/s)	(l/s)	(l/s)
Ackers-White	-	-	0.210	-	-	0.210
Engelund-Hansen	-	-	0.305	-	-	0.305
Engelund-Fredsøe*	0.097	0.396	-	0.097	0.394	-
van Rijn	0.032	0.106	-	0.032	0.106	-

\*The small deviation in the suspended load calculated from the analytical solution and MOUSE originates from the fact that the analytical calculation is based on a chart.

It can be seen that the sediment transport models implemented in MOUSE are in agreement with the theoretical calculation of the sediment transport from the four sediment transport formulae. It should be noted that these four well established sediment transport formulae give quite different results for this simple test case with steady state hydrodynamics. The maximum difference is found between the Engelund-Fredsøe and the van Rijn formula where the Engelund-Fredsøe formula gives a factor of 3.6 times more sediment transport than the van Rijn formulation.

#### 8.4.2 Test of the Mass Balance for Non-Cohesive Sediment

The purpose of the test is to show that the mass balance is correct for the non-cohesive sediment transport model. The simulation was carried out with the following data:

a circular pipe with a length of : 1000 m  
 pipe width : 10 m  
 sediment depth in the pipe : 1.0 m  
 grain diameter : 0.1 mm

upstream boundary conditions:  
 discharge : 10 m<sup>3</sup>/s  
 sediment discharge : 0.0 l/s

downstream boundary conditions:  
 water level : 1.5 m

After a time all the sediment should be washed out of the pipe and the amount of sediment washed out should be equal to the initial mass of sediment in the pipe. An extract of the time series for the mass balance for the simulation can be seen in Table 8.1. The initial sediment mass in the pipe was 7040767 kg and the mass routed out of the pipe was 7038563 kg, this gives a deviation of 0.031 %, which is satisfactory.

Min:Sec	Mass in Sewer system Kg	Outflow From Sewer system Kg	Error in Mass balance Kg	Relative error in Mass balance
0:00	7040767	0.00000	0.00000	0.00000
30:00	6917979	139392	16604.3	0.0024
4050:00	17848.3	7023879	960.113	0.00014
4080:00	15896.8	7026062	1192.28	0.00017
4110:00	14081.5	7028123	1437.97	0.00020
4140:00	12743.6	7030005	1981.64	0.00028
4170:00	11421.5	7031680	2334.93	0.00033
4200:00	10114.7	7033156	2504.40	0.00036
4230:00	8823.07	7034440	2496.34	0.00035
4260:00	7546.09	7035538	2316.79	0.00033
4290:00	6283.52	7036455	1971.54	0.00028
4320:00	5035.12	7037198	1466.19	0.00021
4350:00	3800.76	7037772	806.200	0.00011
4380:00	2580.52	7038183	-2.915	-0.00000
4410:00	1374.87	7038437	-955.358	-0.00014
4440:00	195.763	7038537	-2033.94	-0.00029
4470:00	0.00000	7038563	-2203.69	-0.00031
4500:00	0.00000	7038563	-2203.69	-0.00031

Table 8.1. Time series of the mass balance for the simulation.

#### 8.4.3 Test of the Interaction between the Hydrodynamic Model and the Sediment transport Model

The alternating solution of the hydrodynamic equations and the sediment transport continuity equation can be evaluated by use of the mass balance for non-cohesive sediment, see Appendix C, Section C.4. The simulation for the mass balance was carried out with a time step of 1 minute. Hence, the average erosion per time step for the pipe in the example in Appendix C, Section C.4 can be calculated as:

$$\Delta Z_{\text{time step}} = \frac{\text{sediment depth}}{\text{no. time steps}} = \frac{1.0 \text{ m}}{4500} = 0.2e-3 \text{ m/time step} \quad (8-23)$$

As the water depth during the simulation is 1.0 m, it can be seen that the change in bed level per time step is small compared to the water depth.

#### 8.4.4 Propagation Test for a Sand Wave

The purpose of the test is to show that the propagation time for a sand wave is correct in the non-cohesive sediment transport model. It is not possible to make this



test without hard-coding the information concerning the sediment transport, otherwise steady state hydrodynamic conditions cannot be achieved due to the interaction between the hydrodynamic model and the movable bed model. The test is based on the graded sediment transport model. The test consists of a mixing wave propagation in the active transport layer. The initial percentages in the active transport layer were:

sediment fraction no. 1 : 60 %  
 sediment fraction no. 2 : 40 %

The boundary conditions to the model are a percentage of the sediment fraction no. 1 of 40 % and a percentage of the sediment fraction no. 2 of 60 %. A sediment wave will now propagate through the system changing the percentages of the sediment fractions in the transport layer.

The simulation was carried out with the following data (hard coded):

sediment transport	1.0 m <sup>3</sup> /s
change in bed level	0.0 m
width of the pipe	1.0 m
thickness of transport layer	1.0 m
grid spacing	40 m

The result of a simulation with a time centring,  $\theta = 0.5$ , and a space centring,  $\psi = 0.5$ , can be seen in Figure 8.7 and Table 8.2. From Figure 8.7 it can be seen that strong oscillations are present in the simulation.

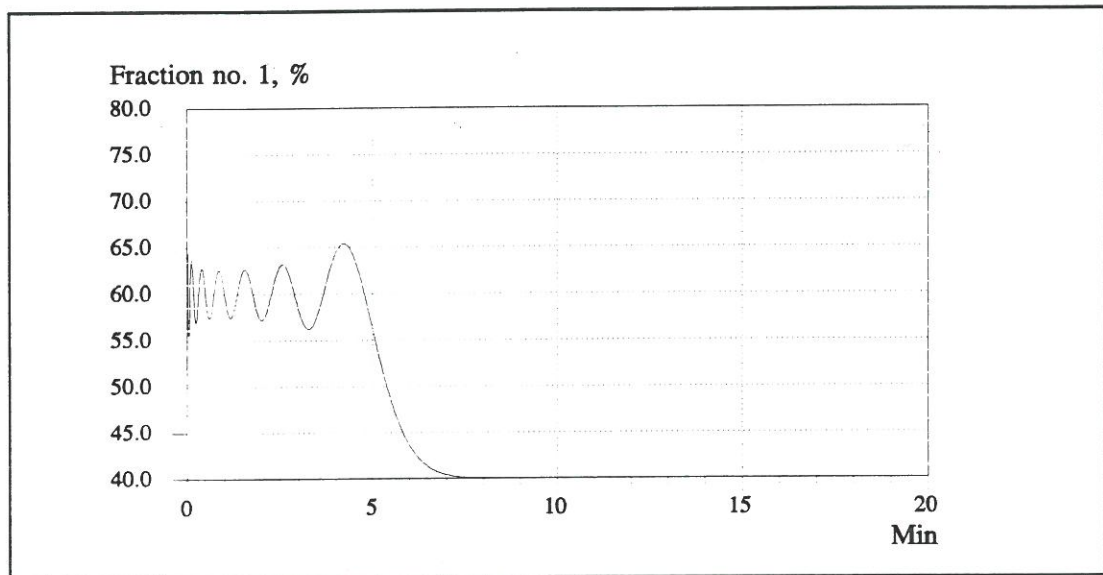


Figure 8.7. The percentage of sediment fraction no. 1 in the transport layer at 520 m from the upstream boundary. Time centring,  $\theta = 0.5$ , and a space centring,  $\psi = 0.5$ .

Min:Sec	Sediment fraction no. 1 in the active layer %
0:00	60.000
0:01	64.367
0:02	55.603
0:03	55.594
.	.
.	.
8:33	40.007
8:34	40.007
8:35	40.006
8:36	40.006
8:37	40.006
8:38	40.005
8:39	40.005
<b>8:40</b>	<b>40.005</b>
8:41	40.005
8:42	40.005
8:43	40.004
8:44	40.004
8:45	40.004
8:46	40.004

Table 8.2. The percentage of sediment fraction no. 1 in the transport layer at 520 m from the upstream boundary. Time centring,  $\theta = 0.5$ , and a space centring,  $\psi = 0.5$ .

The transport time for the bed wave at distance 520 m from the upstream boundary can be calculated as:

$$t_{propagation} = \frac{L W D_t}{S} = \frac{520m \ 1m \ 1m}{1m^3/s} = 520s \quad (8-24)$$

where

- L is the distance from the upstream boundary, (m)
- W is the width of the pipe
- S is the sediment transport
- D<sup>t</sup> is the thickness of the transport layer, (m)

From Table 8.2 it can be seen that after 520 s the percentage of sediment fraction no. 1 in the transport layer is 40.005 %, ie 99.98 % of the mixing is completed.

The Preissmann scheme can be centred forward in time and space to avoid the numerical oscillations. A simulation was carried out with a time centring,  $\theta = 0.75$ , and a space centring,  $\psi = 0.75$ , the results of the simulation can be seen in Figure 8.8 and Table 8.3. From Figure 8.8 it can be seen that the oscillations have been completely removed. The consequence of the forward centring of the scheme is an

introduction of numerical dispersion. From Table 8.3 it can be seen that after 520 sec. the percentage of sediment fraction no. 1 in the transport layer is 40.239 %, ie 98.8% of the mixing is completed. Hence, the propagation time of the wave is still satisfactory, though numerical dispersion has been introduced in the scheme. As dispersion also will be present in the physical transport process of the sediment, the numerical dispersion can be considered as a positive effect in the scheme.

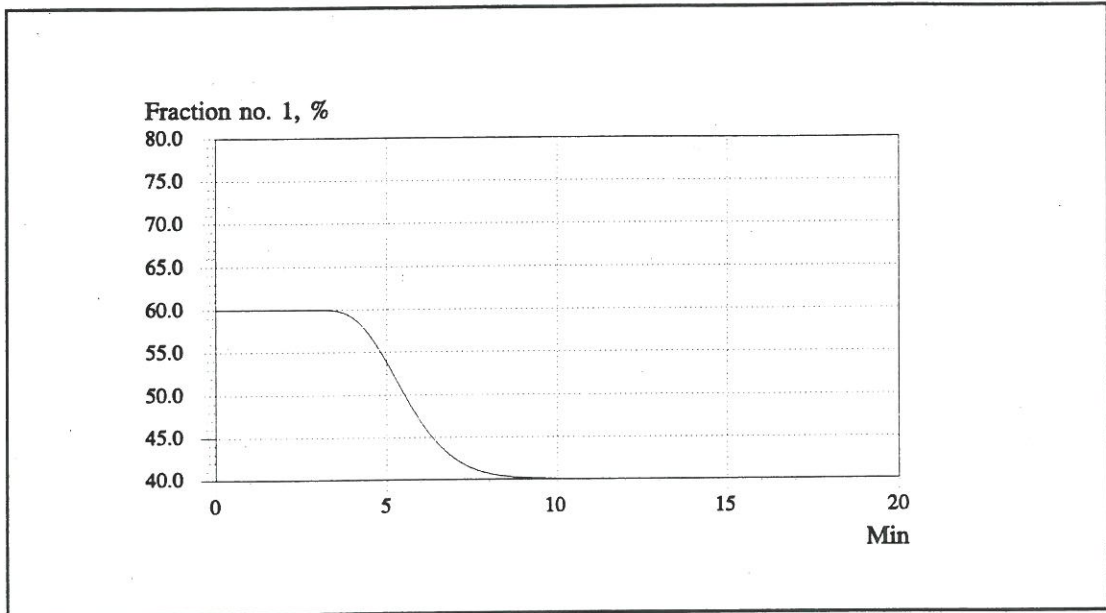


Figure 8.8. The percentage of sediment fraction no. 1 in the active transport layer at 520 m from the upstream boundary. Time centring,  $\theta = 0.75$ , and a space centring,  $\psi = 0.75$ .

Min:Sec	Sediment fraction no. 1 in the active layer %
0:00	60.000
0:01	60.000
0:02	60.000
0:03	60.000
.	
.	
8:30	40.309
8:31	40.301
8:32	40.293
8:33	40.286
8:34	40.279
8:35	40.272
8:36	40.265
8:37	40.258
8:38	40.251
8:39	40.245
<b>8:40</b>	<b>40.239</b>
8:41	40.233
8:42	40.227
8:43	40.221
8:44	40.215
8:45	40.210
8:46	40.204
8:47	40.199
8:48	40.194

*Table 8.3. The percentage of sediment fraction no. 1 in the transport layer at 520 m from the upstream boundary. Time centring,  $\theta = 0.75$ , and a space centring,  $\psi = 0.75$*

## 8.5 Summary of Modelling of Non-Cohesive Sediments in Sewers

From these tests it can be concluded that the propagation time for a sediment wave and the mass balance are represented correctly in the non-cohesive sediment transport model and that the numerical scheme can be used for practical application of sediment transport modelling in sewers. Further, without a significant loss of accuracy the numerical scheme can be centred forward in time and space in order to achieve a solution without numerical oscillations.

## 9 AN EXAMPLE OF AN APPLICATION OF THE ADVECTION-DISPERSION MODEL

The objective with this application was to investigate the capability of the advection-dispersion model to simulate the transport of dissolved matter in sewer systems. If the model is capable of simulating the transport of dissolved matter it is also capable of simulating the transport of fine organic sediments, ie sediments transported in the mode of wash load.

### 9.1 Application of the Advection-Dispersion Model

The advection-dispersion model was applied to a wastewater gravity sewer at Dronninglund, Denmark. The sewer is a concrete pipe, approx. 5 km long, with 70 manholes and a slope of 2.72 ‰. The pipe diameter is 500 mm and the diameter of the manholes is 1.0 m. Further, there is no infiltration to the sewer. The data for the modelling of the gravity sewer were taken from a Ph.D study on "Transformation of organic matter in a gravity sewer", Raunkjær (1994). The longitudinal profile of the sewer can be seen in Figure 9.1. The advection-dispersion model for the sewer was subsequently used for the modelling of water quality in the sewer (Garsdal et al., 1994).

The hydrodynamic data available for calibration of the advection-dispersion model were water levels recorded at the inlet to the sewer system and at the outlet from the sewer system on the 30th September 1991. By use of estimated velocities the water level at the inlet was converted into discharges. In addition the residence time was measured at three manholes along the pipe.

The hydrodynamic model was calibrated for this event by changing the Manning number to match the residence time, ie the Manning number was calibrated based on the advection-dispersion model. The advection-dispersion model was validated against similar data for seven other events, see Table 9.1. The result of the validation can be seen in Figure 9.2, where the observed and the simulated residence time are plotted for all the events.

Date	Discharge at inlet [l/s]
September 30, 1991	9.3 - 16.7
September 10, 1992	11.6 - 16.7
September 17, 1992	8.3 - 17.3
September 22, 1992	11.6 - 17.7
March 25, morning, 1992	22.5 - 32.6
March 25, afternoon, 1992	18.9 - 25.9
April 1, morning, 1992	22.1
April 1, afternoon, 1992	21.3

Table 9.1. Discharges for the Dronninglund-Asaa gravity sewer. From Garsdal et al. (1994).

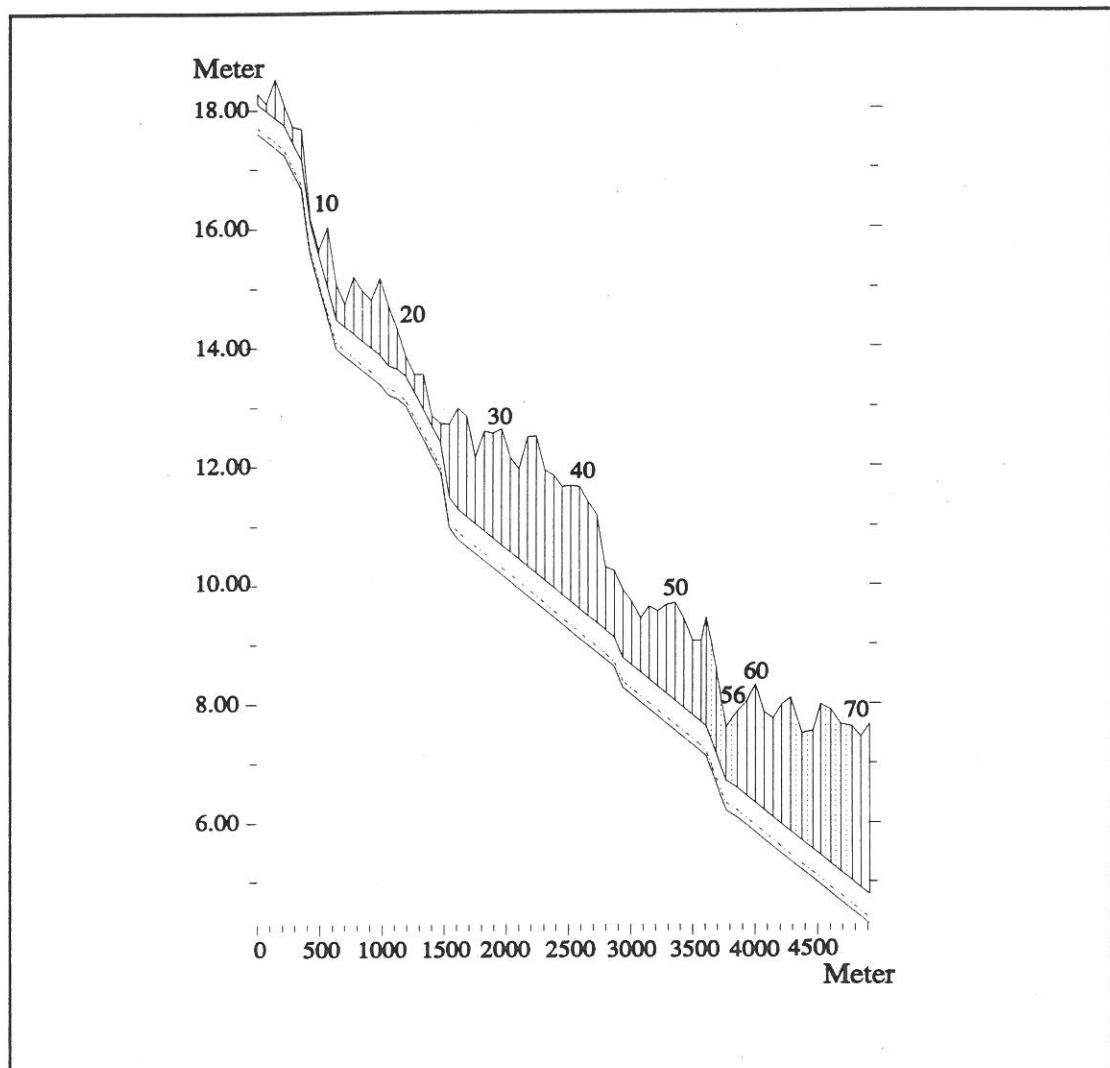


Figure 9.1. The longitudinal profile of the sewer system.

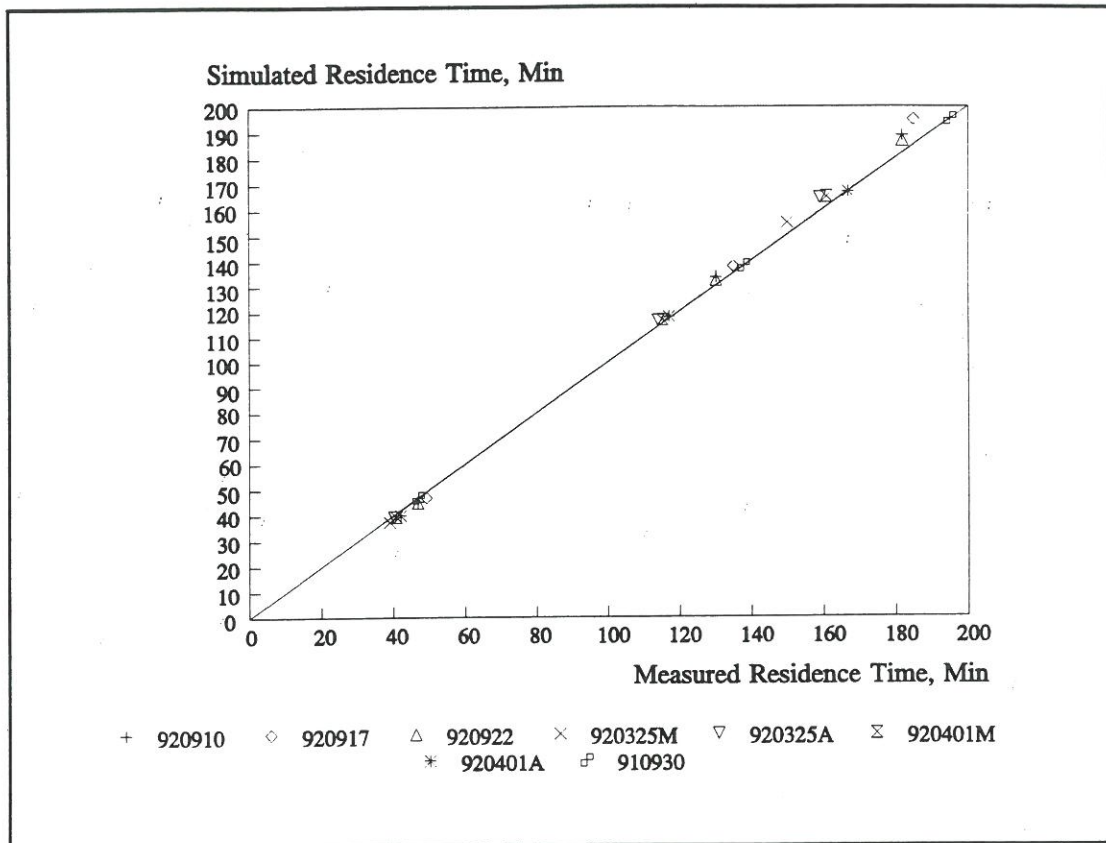


Figure 9.2. The observed and simulated transport times for dissolved matter in the gravity sewer. From Garsdal et al. (1994). The data are taken from Raunkjær (1993). Index M indicates that the measurement is taken in the morning, index A indicates the measurement is taken in the evening.

The advection-dispersion model was calibrated against a Rhodamine spectrum measured on the 30th of September 1991. Due to a lack of data the calibration is rather uncertain and a theoretical dispersion coefficient cannot be calculated. The dispersion coefficient in the advection-dispersion model was changed until a reasonable fit was achieved between the residence time of the simulated the peak and that of the measured peak at manhole number 56. A good match was achieved for a dispersion coefficient,  $D=1.5 \text{ m}^2/\text{s}$ . The simulated concentration peak can be seen in Figure 9.3. The experiment with Rhodamine was only carried out once, hence the dispersive term in the advection-dispersion model is only calibrated, not validated. From Equation (7-6) the theoretical dispersion coefficient can be found for the average flow conditions in the pipes. The dispersion coefficient was found to be  $0.2 \text{ m}^2/\text{s}$ . The theoretical dispersion coefficient is smaller than the calibrated dispersion coefficient, but it is still in the same order of magnitude. However, it must be expected that the theoretical dispersion coefficient is smaller than the dispersion coefficient in the real sewer system as the theoretical dispersion coefficient neglects the dispersion from the manholes and the variation of the pipe diameter and the pipe slope in the sewer system. If vertical gradients are present in the concentration of the dissolved matter the dispersion and the travel will subsequently be increased. For the theoretical evaluation of the importance of vertical gradients in the concentration profile see Chapter 6, pp 6-7 - 6-9.

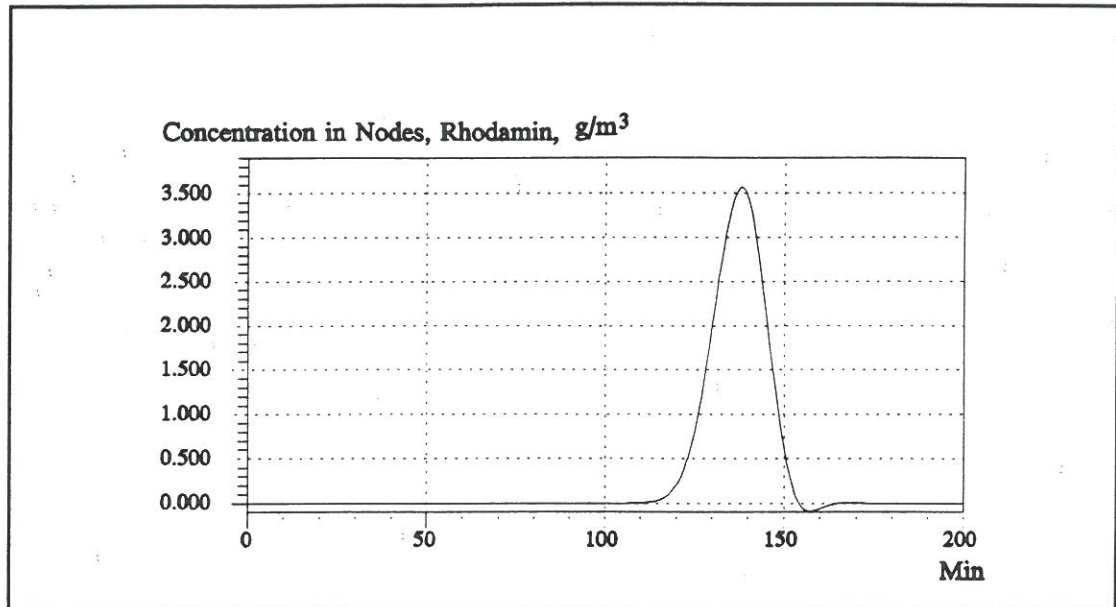


Figure 9.3. The simulated concentration peak at manhole number 56 for the event of the 30th of September 1991.

## 9.2 The Dispersion Processes in Sewer Systems.

The dispersion term in the advection-dispersion equations is important if a pulse of dissolved matter is routed through the sewer system. In order to judge the importance of the dispersion, the advection-dispersion model was run without dispersion and with the dispersion increased by 100% compared to the calibrated model. The results of the simulations are shown in Figure 9.4. From Figure 9.4 it can be seen that the simulation without dispersion produces significant wiggles and that the concentration peak is approx. twice as high as for the calibrated peak. Further, it can be seen that the increase in dispersion reduces and broadens the peak and that the dispersion reduces the wiggles significantly. It can be concluded that the dispersion has an effect on the transport processes in sewer systems and that the transport of dissolved matter which is fully mixed in the water can be modelled accurately by the use of an advection-dispersion model provided that an appropriate dispersion coefficient is chosen.



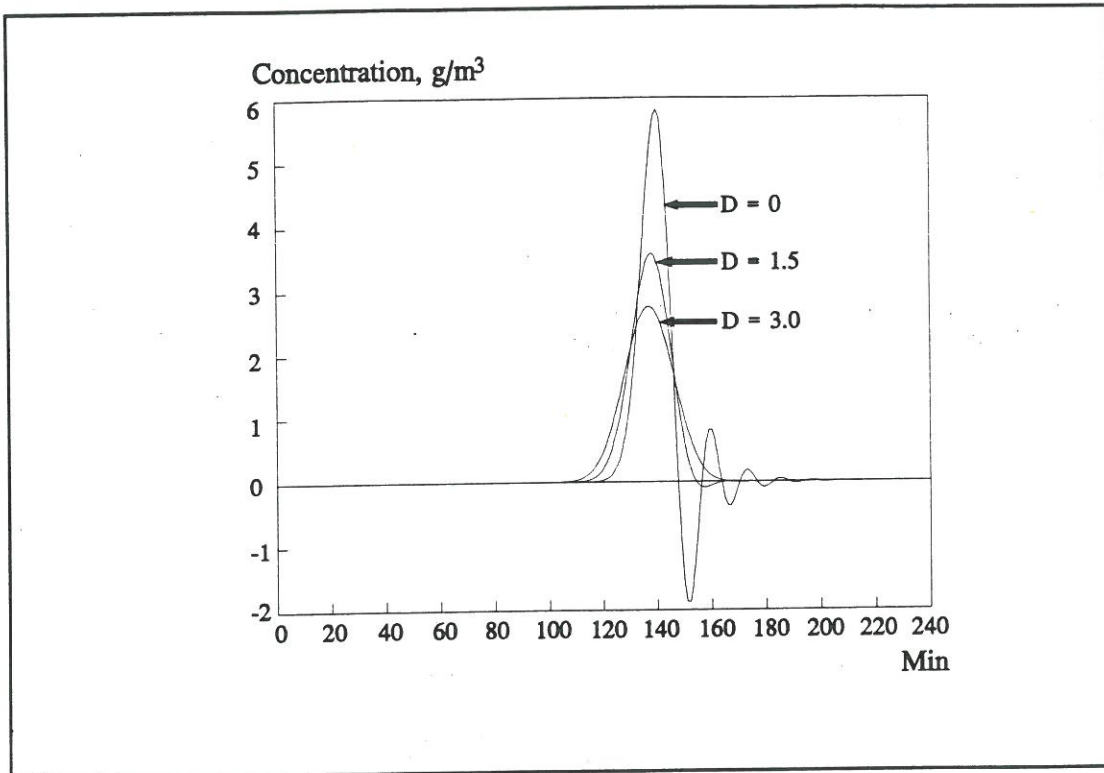


Figure 9.4. The simulated concentration peak at manhole number 56 for pure advection ( $D = 0.0 \text{ m}^2/\text{s}$ ) plotted with simulations carried out with a dispersion coefficient of  $D = 1.5 \text{ m}^2/\text{s}$  and  $D = 3.0 \text{ m}^2/\text{s}$ .

### 9.3 The Dispersion from Manholes.

The transport across a manhole is modelled by assuming that the incoming volume of water mixes instantaneously with the water in the manhole. Hence, dispersion is introduced when the water passes through a manhole. In order to investigate the effect on the concentration peak from the manholes two simulations were carried out with different sizes of the manholes:

- the diameter of the manholes was decreased by 50%
- the diameter of the manholes was increased by 100%

The results of the simulations are shown in Figure 9.5. From Figure 9.5 it can be seen that a change in the diameter of the manholes in the model changes both the arrival time of the peak and the size and shape of the peak. If the diameter of the manhole is reduced by 50% it can be seen that the peak becomes slightly larger and arrives 10 minutes earlier. If the size of the manhole diameter is increased by 100% the peak is reduced by 20-30% and delayed by approx. 20 minutes. This sensitivity analysis was carried out for low flow conditions where the pipes were running approx. 20% full. It may be expected that the situation is aggravated further when the pipes becomes surcharged.

It can be concluded that the manholes have a significant impact on the routing of dissolved matter in sewer systems. Hence, it is necessary to have accurate information on the geometry of the manholes and to have a knowledge of the dispersion coefficient in order to model the transport of dissolved matter in sewer systems by use of the advection-dispersion equations.

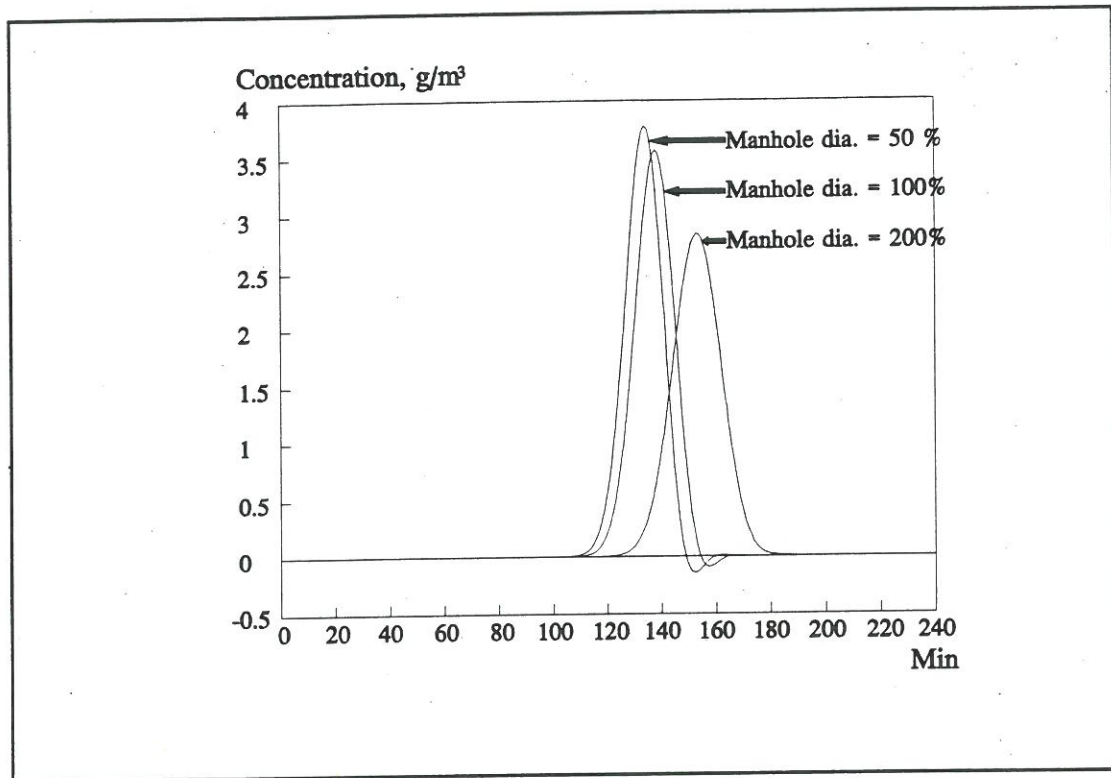


Figure 9.5. The simulated concentration peak at manhole number 56 for manholes with 50%, 100% and 200% of the real manhole diameter. Dispersion coefficient,  $D = 1.5 \text{ m}^2/\text{s}$ .

## 10 EXAMPLES OF APPLICATIONS OF THE SEDIMENT TRANSPORT MODEL

The sediment transport model has been applied to two catchments: the sewer system of Gothenburg, Sweden and the sewer system of Ljubljana, Slovenia. Both of the applications have been carried out with a minimum of data concerning the sediment in the sewer systems.

### 10.1 The Rya catchment, Gothenburg, Sweden

The Rya catchment has a daily load of approx. 793,000 person equivalents including industrial waste water. The mean daily flow was 321,000 m<sup>3</sup>/d in 1991. The flow capacity of the full secondary treatment is 518,000 m<sup>3</sup>/d (6 m<sup>3</sup>/s). Flow exceeding this capacity only receives primary treatment.

The sediment transport model was applied in conjunction with an existing hydrodynamic MOUSE model of the pipe system (Gustafsson et al., 1993). The pipe system consists of a 120 km tunnel in bed rock with cross-section areas from 6 m<sup>2</sup> to 18 m<sup>2</sup> and slope varying from 0.07 to 0.1%. The hydrodynamic model has been calibrated and verified against water levels and discharges at the sewage treatment plant. The calibration of the hydrodynamic model for a storm in November 1992, can be seen in Figure 10.1.

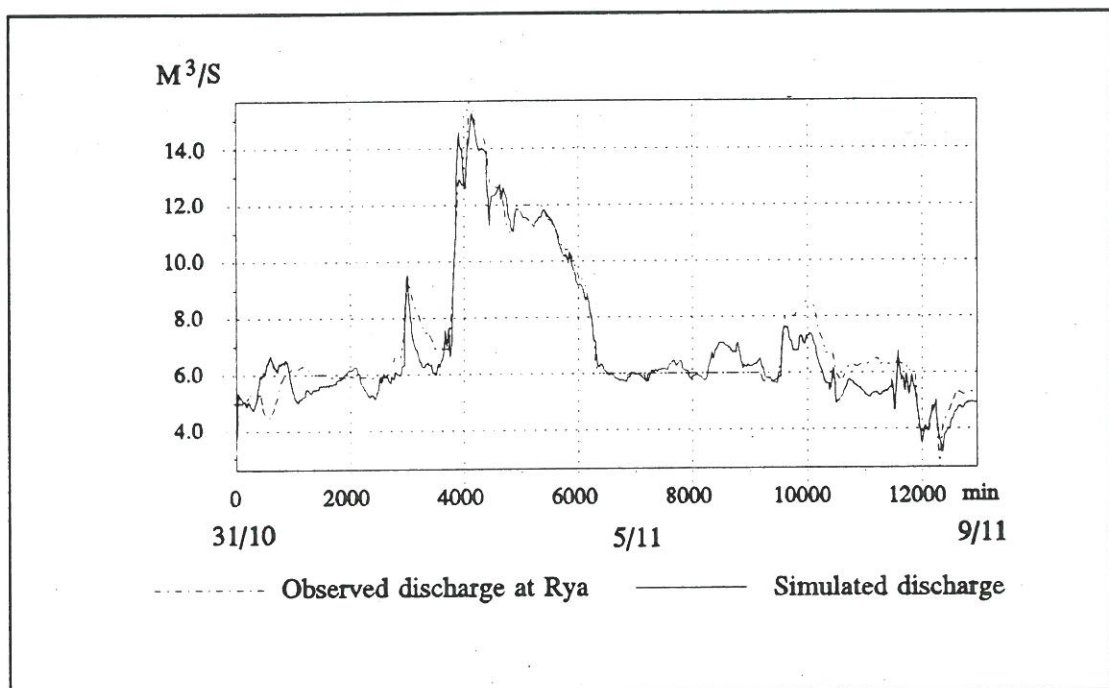


Figure 10.1. The observed and simulated discharges at the Rya sewage treatment plant in November 1992.

Only few data are available for the setup and calibration of the sediment transport model for this event. The only available data were the accumulated mass of fine and coarse sediments (wet<sup>1</sup>) at the sewage treatment plant. The time series of accumulated sediments can be seen in Figure 10.2.

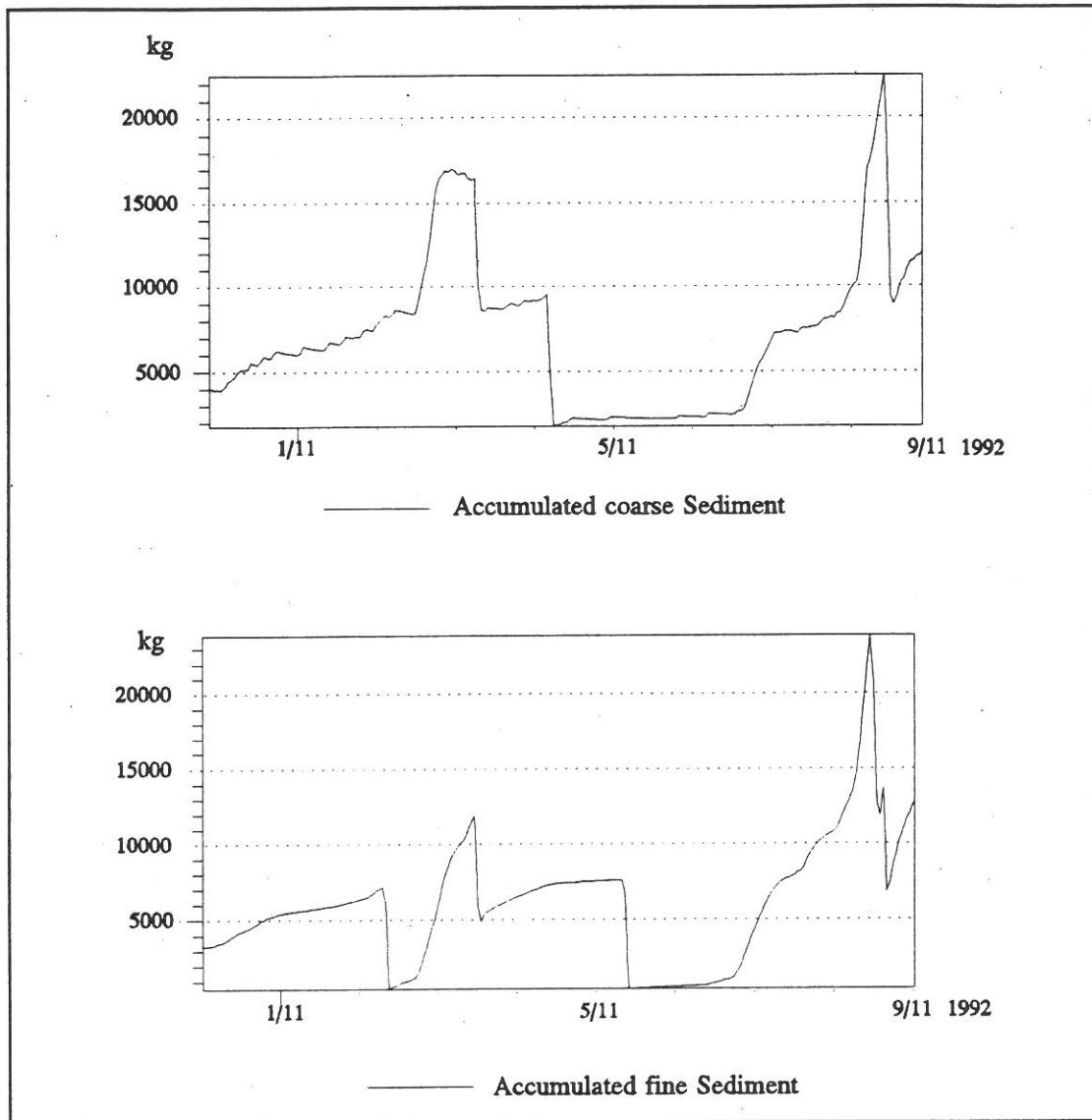


Figure 10.2. Time series of accumulated wet sediments at the Rya sewage treatment plant for the fine and the coarse sediment fractions.

<sup>1</sup> The term "wet" covers the fact that it takes some time for the water to drain from the containers with the sediments.

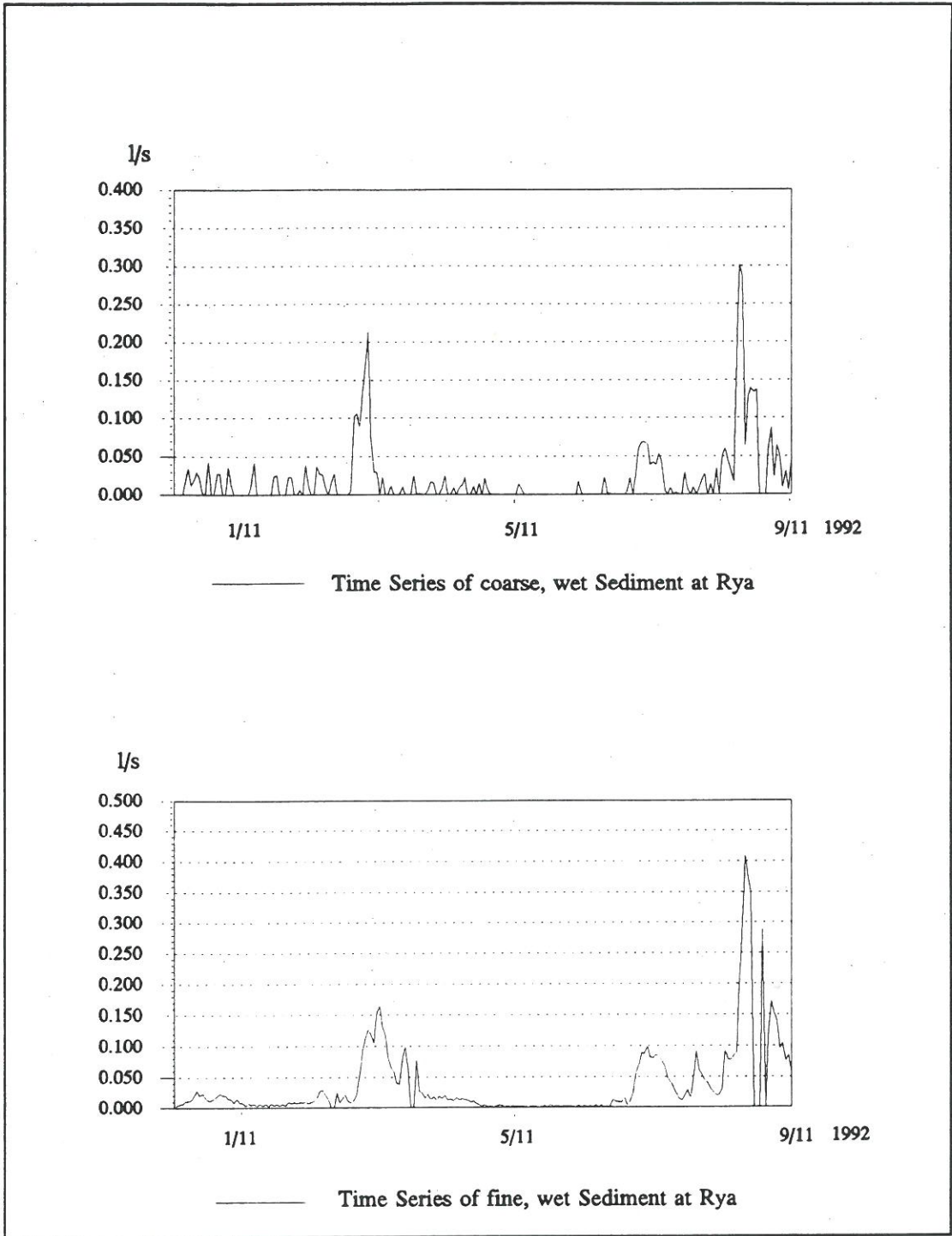


Figure 10.3. Time series of sediment transport (wet) at the Rya sewage treatment plant for the fine and the coarse sediment fractions.

The incoming sediment to the sewage treatment plant is divided into fine and coarse sediment by sieves. The sediment transport is calculated from the mass of three containers placed on scales. The large drops in the time series for the accumulated sediment transport are due to a full container having been replaced by an empty container. The small drops in the curve for the accumulated mass is due to draining of water from the containers. The time series of accumulated mass for the coarse and fine fraction were converted into time series of sediment transport into the treatment plant. These time series are rather uncertain as they are based on accumulated wet sediment. The time series can be seen in Figure 10.3.

At present, little information is available on the density and the grain size of the fine and the coarse sediment fractions, nor is information available on the sediment properties in the sewer system, eg sediment depths in the tunnel system. Due to the sparse data it was decided to make the sediment transport model as simple as possible, and only to evaluate the sediment transport capacity of the flow. This is obviously a rather simple approach as it assumes unlimited supply of sediments to the sewer system, it neglects the influence on the sediment transport of a limited amount of sediment available in the sewer system and it disregards the time of travel for the sediment within the sewer system. As no data were available, the data used in the simulation were the default values found for sewer systems in the U.K. (Crabtree et al. 1993). The fine fraction was taken to be Type C sediment with the properties:

density : 1727 kg/m<sup>3</sup>  
grain size : 0.3 mm

The coarse fraction was taken to be Type A sediment, ie sand, with the properties:

density : 2492 kg/m<sup>3</sup>  
grain size : 1.0 mm

Based on personal communication with people working at the sewage treatment plant the sediment depth in the system was assessed to be 5-10% of the pipe diameter and it was confirmed that large amounts of sand arrive at the treatment plant during periods with heavy rain. All the data used in the simulation are consequently rather uncertain. Hence, no attempt was made to calibrate the sediment transport model as the lack of information did not justify a calibration. The Engelund-Hansen model was used for the simulation. The results of the simulations, ie the sediment transport in the pipe at the Rya treatment plant, can be seen in Figures 10.4 and 10.5.

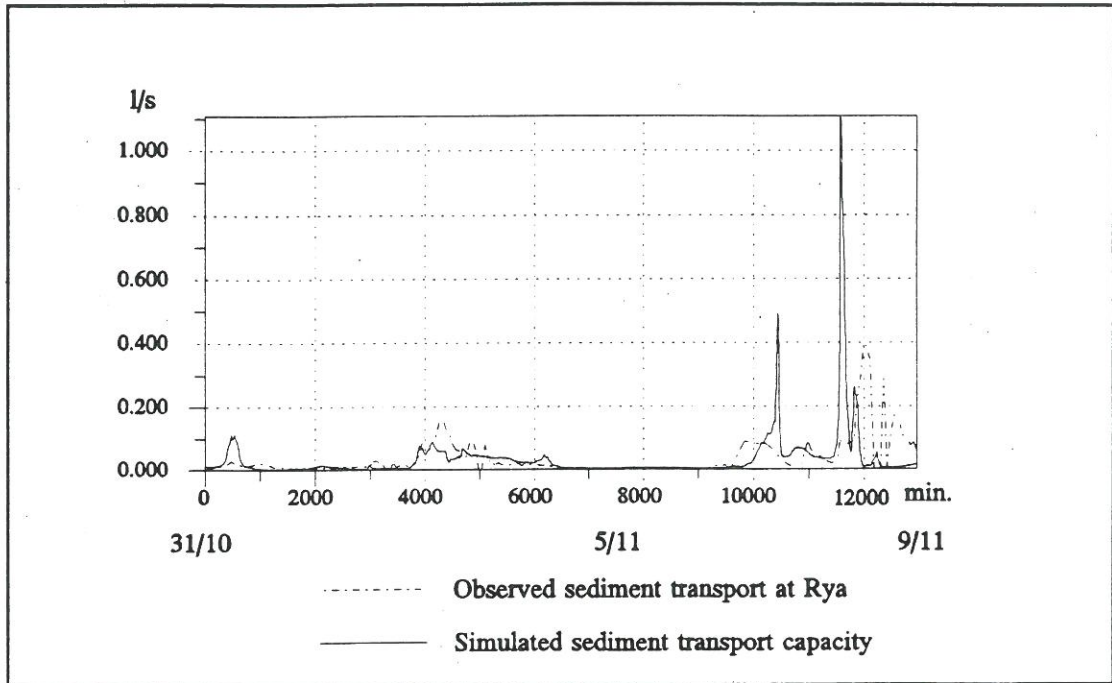


Figure 10.4. The observed sediment transport of the fine sediment (wet sediments) and simulated sediment transport capacity at the Rya sewage treatment plant in November 1992.

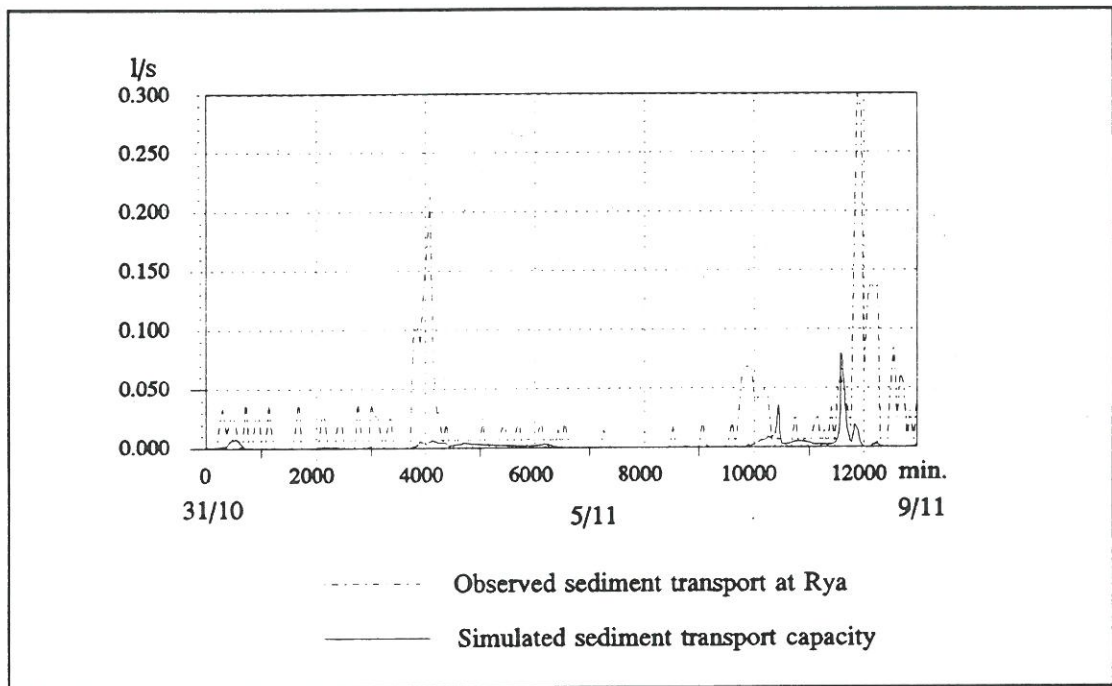


Figure 10.5. The observed sediment transport of the coarse sediment (wet sediments) and simulated sediment transport capacity at the Rya sewage treatment plant in November 1992.

From Figure 10.4 it can be seen that the model predicts sediment transport for the fine fraction when sediment transport was recorded at the sewage treatment plant. Further, it can be seen that the sediment transport capacity simulated for the fine fraction follows the trend of the sediment inflow at the treatment plant very well during the first 9000 minutes of the simulation. During the last part of the simulation it seems as if there is a time lag between the sediment inflow and simulated sediment transport capacity and the magnitude of the simulated sediment transport is not correct. Further, it can be observed that there is a correlation between the performance of the hydrodynamic model and the sediment transport model. In short the deviations between the observed and the simulated sediment transport may be explained as:

- incorrectly assumed sediment properties
- the transport time of the sediments being neglected in the simulation
- only a limited supply of sediment being available in the pipe system
- the fact that the model simulates dry sediment mass while the sediment inflow measured at Rya is wet sediment
- discrepancies between the simulated and the observed discharge at the sewage treatment plant during this period

From Figure 10.5 it can be seen that the simulated transport capacity for the coarse sediment is well below the recorded sediment transport at the treatment plant, although it still follows the trend of the sediment transport measured at the treatment plant. If the time series for the fine and the coarse sediment inflow to the sewage treatment plant are compared, it can be seen that they are of the same order of magnitude. Hence, the assumed properties for the coarse sediment must be wrong, as the coarse sediment cannot have both a significantly higher mass and a significantly larger grain size compared to the fine sediment fraction. This is due to the fact that an increase in both of these properties would reduce the sediment transport. It can be concluded that the density of the coarse fraction has to be less than or equal to the density of the fine fraction or the grain size of the coarse fraction should be reduced. A simulation was carried out where the density of the coarse sediment was changed to the same density as for the fine sediment, ie  $1727 \text{ kg/m}^3$ . The result of the simulation can be seen in Figure 10.6. It can be seen that the simulated results are now of the same order of magnitude as the observed sediment transport at Rya, and the simulation follows the same pattern as for the fine sediment.

The results from the modelling of the fine and the coarse sediment fractions are not perfect. The results of the simulation can probably be improved if more data on the sediment properties become available, eg sediment size, density and sediment depth in the pipe system. The modelling of the sediment transport capacity for the fine and the coarse fractions can be used to indicate whether sediment transport will take place and give an idea of the magnitude of the transport at the sewage treatment plant.



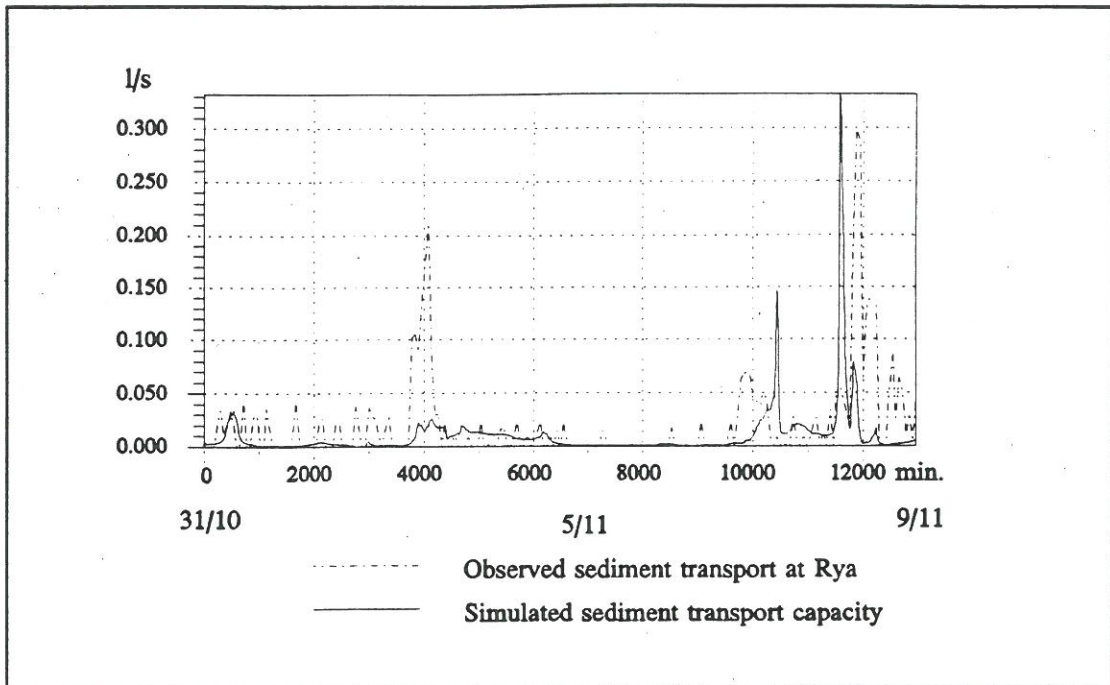


Figure 10.6. The observed sediment transport of the coarse sediment (wet sediments) and simulated sediment transport capacity of the sediment with a grain size of 1.0 mm and a density of  $1727 \text{ km/m}^3$  at the Rya sewage treatment plant in November 1992.

The model could have been usefully employed during the period after the storm in November 1992, when a period occurred without sediment transport to the treatment plant, due to deposition of sediment in the tunnel system during the storm<sup>2</sup>. The lack of sediment inflow gave a lower efficiency of the treatment plant. Several regulation strategies were unsuccessfully tried to increase the sediment transport to the sewage treatment plant during the days after the storm, until the 7/11 when two valves were opened. Large amounts of sediment started to flow to the treatment plant, see Figure 10.2, and during the following day approx 64 tons (eight containers) of sediment arrived at the treatment plant. It can be seen from Figures 10.4 and 10.6 that the model did not predict the sediment transport during this event very accurately but the model could have been used to evaluate whether or not the outcome of a regulation strategy would have resulted in sediment inflow to the treatment plant. The model could also have been used to estimate the magnitude of the sediment transport at the sewage treatment plant.

<sup>2</sup> The sediment deposited during the storm due to severe back water at the sewage treatment plant.

## 10.2 The Ljubljana catchment, Slovenia

At present, the MOUSE modelling package is used to develop a master plan for the city of Ljubljana - the capital of Slovenia. One of the objectives of the master plan is to evaluate the effect from the combined sewer overflows on the water quality of the Ljubljanica river and subsequently to reduce the load of pollutants from the sewer system to the river. The Ljubljana catchment has an area of 4,000 ha and a daily load of approx. 240,000 person equivalents including industrial waste water. A horizontal plot of the Ljubljana sewer system can be seen in Figure 10.7.

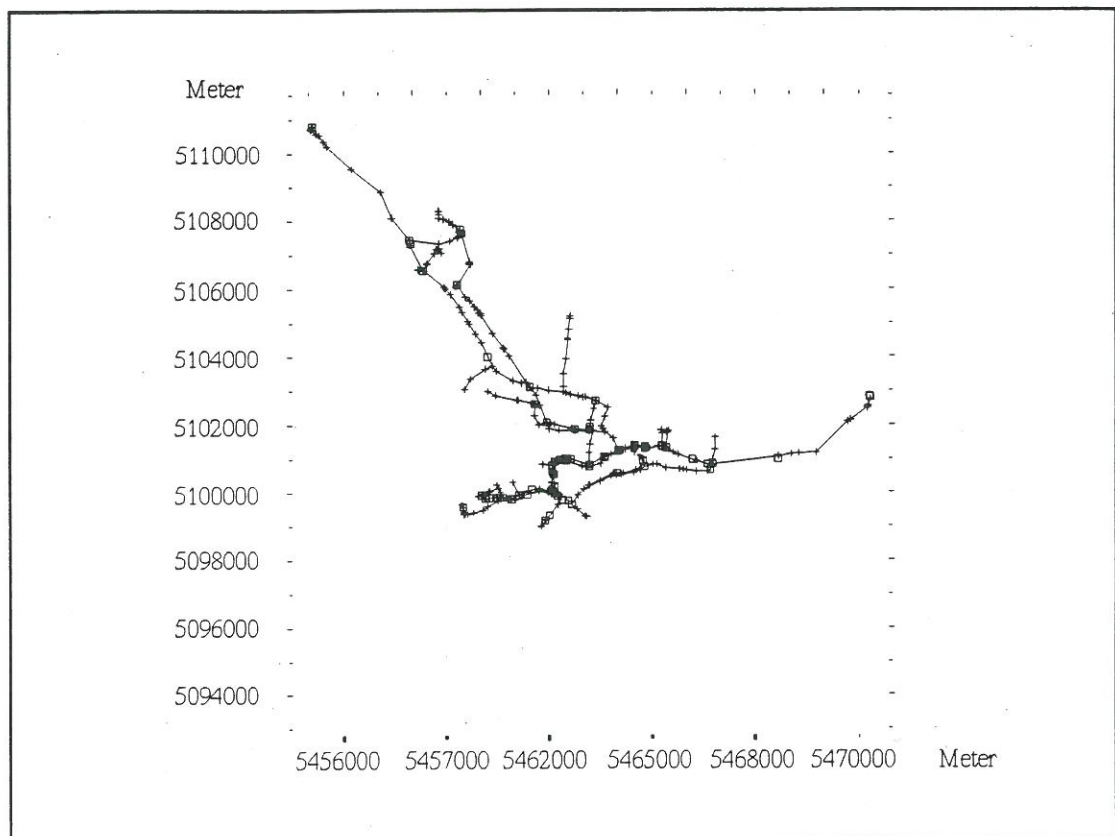


Figure 10.7. Horizontal plot of the Ljubljana sewer system.

A collector (A2) from the Ljubljana model has been used to test performance of the sediment transport model for prediction of the erosion and the deposition pattern. The sewer is used to check the dynamic development of the sediment deposits in a real sewer. Further, the sediment transport model with a movable bed is used to predict the locations of sediment deposits and to evaluate the effects from the sediment deposits on the combined sewer overflow volumes.

For the present application a calibrated and verified hydrodynamic MOUSE model exists for the sewer system of Ljubljana. The hydrodynamic model of the Ljubljana sewer system has been calibrated and verified against water levels and discharges measured at 17 locations in the sewer system. The measurements for the calibration of the hydrodynamic model were made during the autumn of 1994. Examples of the calibration results can be seen in Figure 10.8.

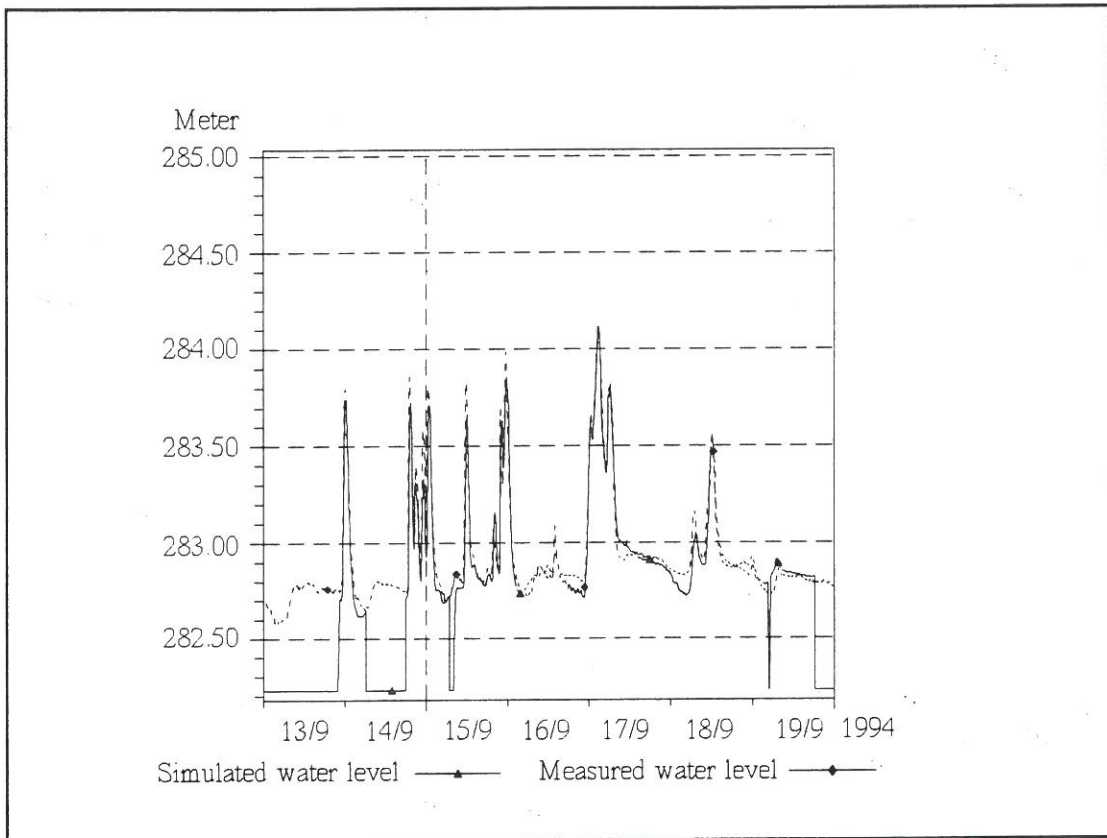
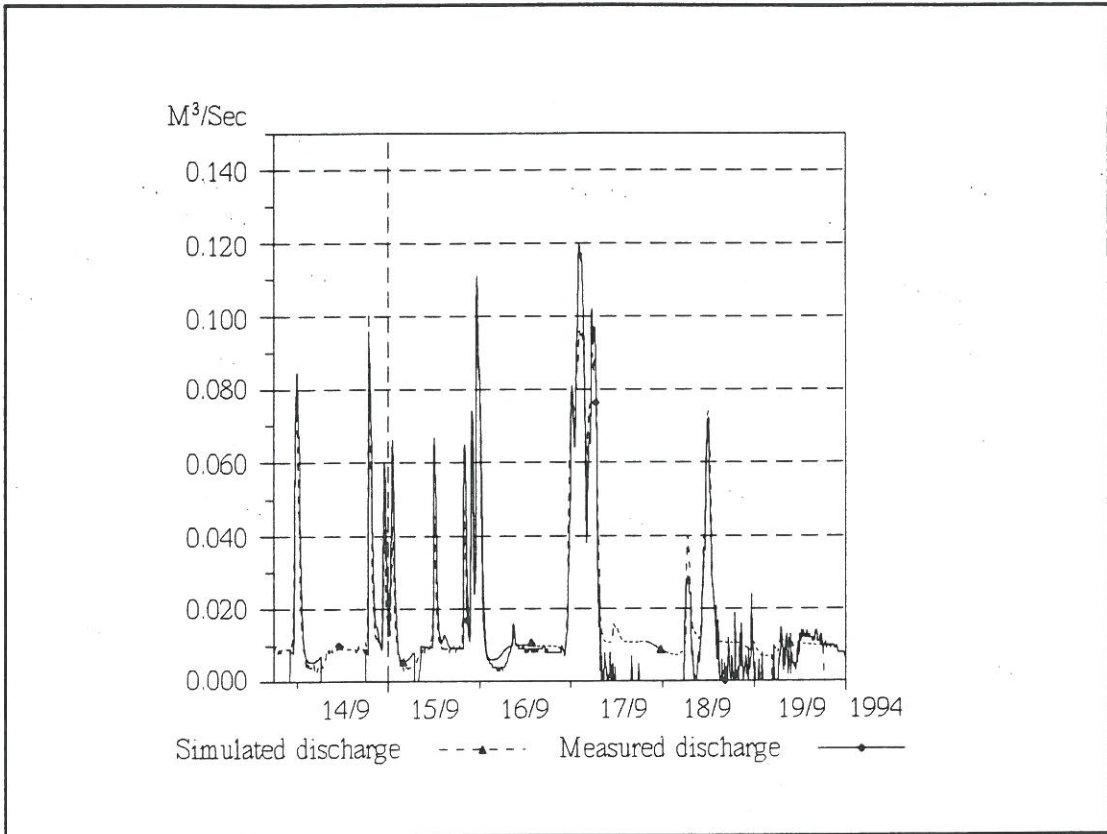


Figure 10.8. Examples of calibration results for the Ljubljana sewer system, (Gustafsson et al., 1995).

### **10.2.1 Evaluation of the Erosion/Deposition Pattern in the A2 Collector**

A general problem in the modelling of sediment transport in sewer systems is that usually only few field data are available and they are difficult and expensive to collect. Further, it should be noted that the hydrodynamic model should be well verified as the sediment transport is a highly non-linear function of the hydrodynamic parameters. In the present application, modelling of the sediment transport has been carried out with a minimum use of field data concerning the sediment. The method used to predict the locations of the sediment deposits in the sewer system is based on calculations performed by use of a morphological sediment transport model with update of the bed level. The advantages in the present method are:

- the locations with deposition/erosion can directly be identified,
- the method takes the physical routing of the sediment into account,
- the method includes factors such as sediment availability,
- the method can be used without much knowledge of the sediment characteristics.

However, it should be noted that the present method may predict sediment deposits at locations where no sediment sources are present. Furthermore, it must be recalled that factors such as bricks, bad junctions, setting of pipes, spatial variability of sediment characteristics and the presence of sediment sources may lead to local flow conditions which are not described accurately in the present study, which again may affect the sediment transport computations.

The A2 collector in Ljubljana was selected as it has a large variation in the geometry, ie the collector has manholes with a shift in levels between the inlet and the outlet pipe, steep and flat pipes and pipes with a negative slope. The test of the capability of the model to reproduce to erosion/deposition pattern consisted of two tests:

- a layer of 1 cm sediment was put into the A2 collector and one week of dry weather flow conditions was simulated without any sediment supply,
- for dry weather flow conditions a 150 minutes time series of sediment wash off was routed into a manhole in the A2 collector. The A2 collector was without any sediment deposits at the beginning of the simulation. The simulation covered one week of dry weather flow conditions.

### **10.2.2 Simulation of the Development of the Sediment Deposits with an Initial Sediment depth of 1 cm and no Sediment Supply**

The model was initialised with a sediment depth of 1 cm in all of the pipes. The model was run for one week with dry weather flow conditions. Since, the time scale for the sediment transport is many times larger than the time scale for the hydrodynamic model, a very small grain size 0.1 mm together with a small density of the sediment ( $1300 \text{ kg/m}^3$ ) were selected for the simulation in order to make the sediment pattern develop faster. The locations which had a significant increase in the

sediment depth compared to the initial conditions were considered to be prone to have sediment deposits. The longitudinal profile with sediment depths in the A2 collector after 30 minutes of simulation can be seen in Figure 10.9. From this figure it can be seen that there is a significant deposition just downstream of section A2082-A2076. This deposition is due to the heavy erosion just upstream, where the pipe is very steep and there is a large difference in the invert levels between the inlet and the outlet pipe. The large drop between the inlet and the outlet means that for dry weather flow conditions, critical flow exists at the inlet to the manhole; hence large velocities are present and erosion occurs. Further, it can be seen from the figure that erosion happens very fast in pipes with steep slopes and at locations with critical depth, eg at upstream of a manhole with a drop.

The sediment depths in the A2 collector after seven days of simulation with dry weather flow can be seen in Figure 10.10. It can be observed that only few locations have a significant deposition and that the sediment deposits all are at locations with large negative slopes. Especially it may be noted that the sediment deposited initially at location A2076, has now been eroded; hence the location at A2076 is not prone to have sediment deposits.

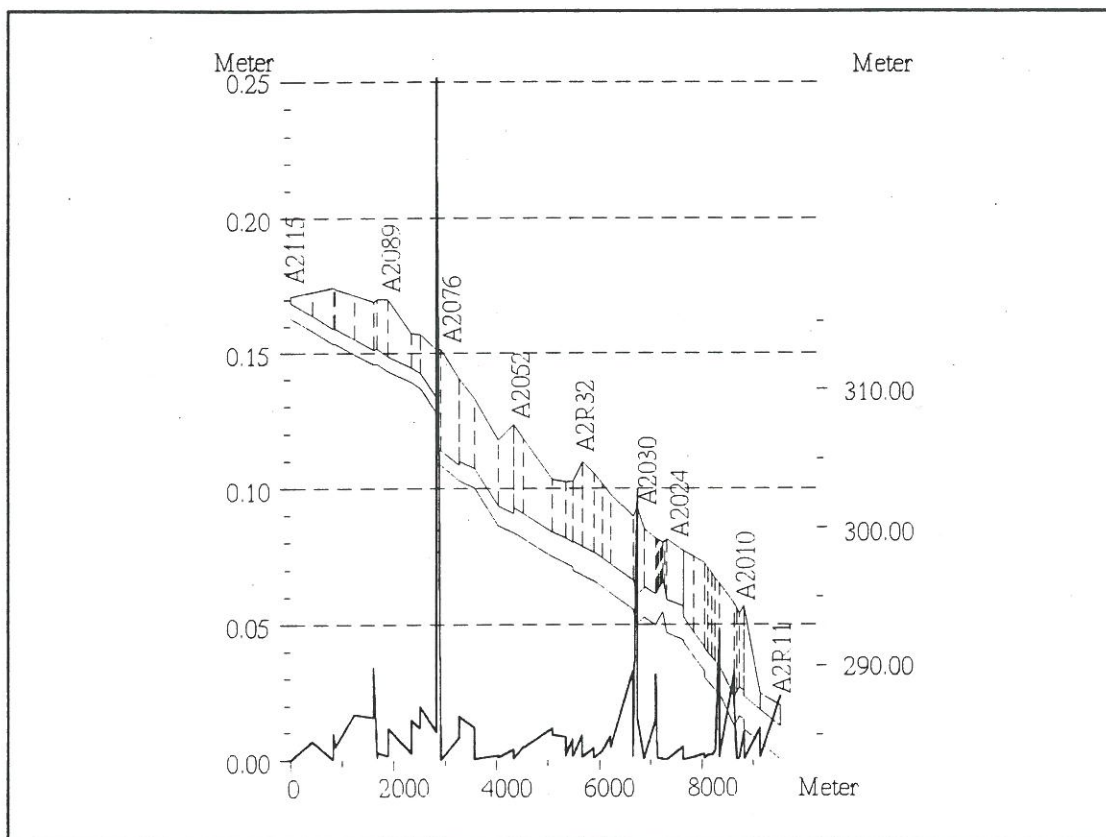


Figure 10.9. The longitudinal profile of sediment depths in the A2 collector in Ljubljana sewer system after 30 minutes of simulation.

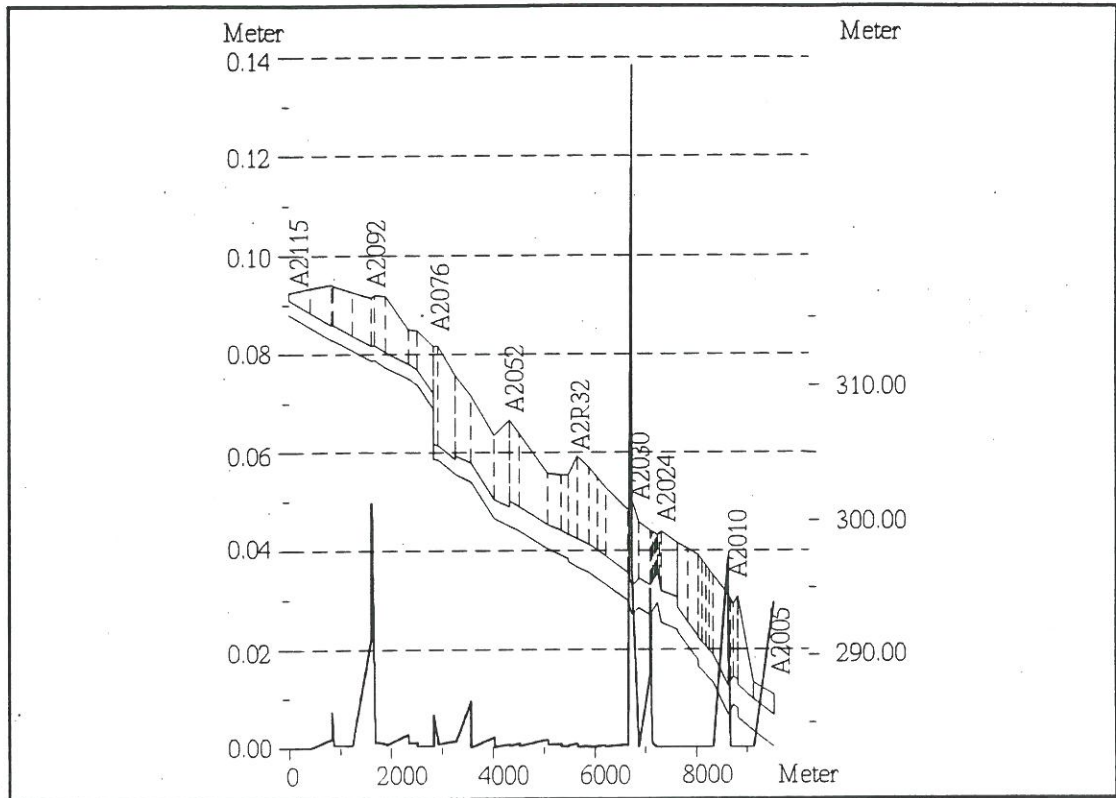


Figure 10.10. The longitudinal profile of sediment depths in the A2 collector in Ljubljana sewer system after 7 days of simulation.

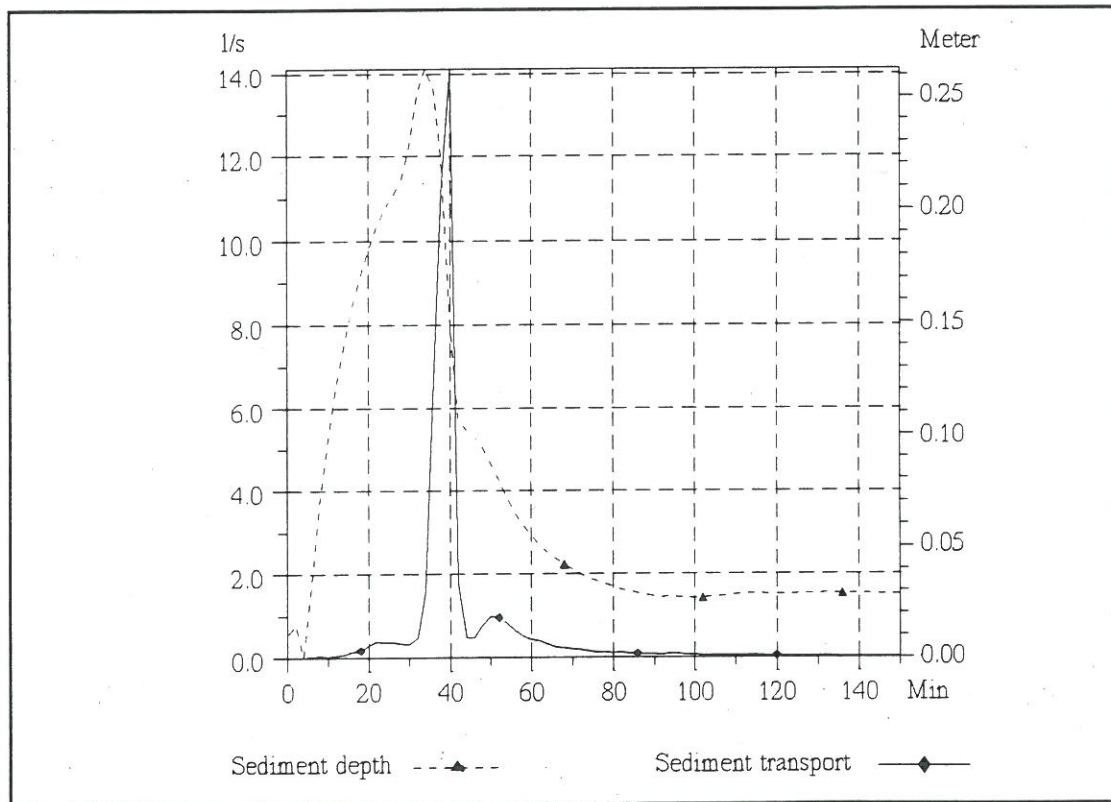


Figure 10.11. The dynamic time series of sediment depth and sediment transport just downstream of manhole 2076.

The dynamic time series of sediment transport and the sediment depth at location A2076 can be seen in Figure 10.11. This figure shows that initially deposition occurs due to large sediment input from the upstream pipe. Later, when the sediment from the upstream pipe has decreased, then the sediment deposit is eroded. The test shows that the sediment pattern which develops in the model corresponds to what should be expected.

### 10.2.3 Prediction of Locations with Sediment Deposits in the Ljubljana Sewer System

In order to further test the functionality of the sediment transport model, the complete model for the Ljubljana sewer system was run with various storms and with various sediment characteristics with the aim to predict where sediment deposits exist in the sewer system. The simulations by use of the model was preceded by a field trip with site inspections to the locations where sediment deposits were predicted by the model. In total six sites of the Ljubljana sewer system were inspected during February 1995.

Based on the experience from the simulation with the A2 collector, the complete MOUSE model for the Ljubljana sewer system was analysed to find locations which would have sediment depositions. Simulations both with dry weather conditions and rain storms with return periods of 0.1 and 1.0 year were carried out. However, the simulation results were also judged together with the initial conditions and the geometrical layout of the sewer system; ie a section downstream of a steep pipe was not considered to be prone to have sediment deposits if erosion occurred at the end of the simulation.

Based on the simulations five locations were selected for inspection during a field trip. The locations were selected so that they were spread over the sewer system and the locations should represent different hydraulic conditions. The locations (A-E) were:

- location A a pipe which goes into the Ljubljanica river,
- location B a pipe which is located downstream of a steep section and where the following pipe has a negative slope,
- location C a pipe located in a part of the sewer system which has mild slopes,
- location D a pipe which is exposed to back water effects,
- location E an overflow structure.

A field trip was made to the Ljubljana sewer system on the 21/2-95 after three days of moderate rain. No detailed measurement were made of the sediment deposits found in the sewers, ie the sediment depth and the sediment characteristics, eg density and size were only visually estimated.

The visit to the sewer system gave the following results:

- location A was not inspected due to high water in the river. However, the people in the maintenance department could confirm the presence of sediment in this pipe,
- at location B, a very thin layer of small stones was observed,
- at location C, a layer of 10-15 cm sediment was observed. The sediment was mainly sludge mixed with sand. The area was cleansed on a regular basis every third year,
- at location D, a layer of approx. 15 cm sediment was observed. The sediment was black with sand with a grain size of approx. 1 mm as the dominant sediment type,
- at location E, a layer of approx. 25 cm sediment was present in the pipe passing the overflow structure. The sediment was mainly gravel with a grain size of approx. 2.5 mm. The area was cleansed on regular basis every year.

Further, the manhole A2093 was inspected during the field trip. Here no sediment deposits were observed at all; which is in agreement with the simulation results.

#### **10.2.4 Simulation of the Development of the Sediment Deposits without any Initial Sediment Deposits and a Time Varying Sediment Supply**

Based on the maximum sediment transport rates from the previous test, the time series of sediment transport just downstream of manhole A2076 was selected as input for the present test. The time series can be seen in Figure 10.12. The time series of sediment was routed into the A2 collector and the model was run for one week of dry weather flow. The deposition pattern can be seen in Figures 10.13 - 10.15. From these figure it can be seen that the sediment initially deposits just downstream of the manhole where the sediment is entered into the pipe. This is due to the fact the sediment transport capacity of the flow is less than the sediment coming into the system. After the injection of sediment has stopped the sediment is slowly transported through the system, and the sediment tends to deposit at the following locations, see Figure 10.14:

- downstream of steep pipes,
- at locations where the pipe diameter is increased and hence the velocity is decreased,
- at locations with a mild or a negative slope.

The sediment is transported until it reaches locations where the bed shear stress is smaller than the critical bed shear stress; and hence the sediment deposits, see Figure 10.15.



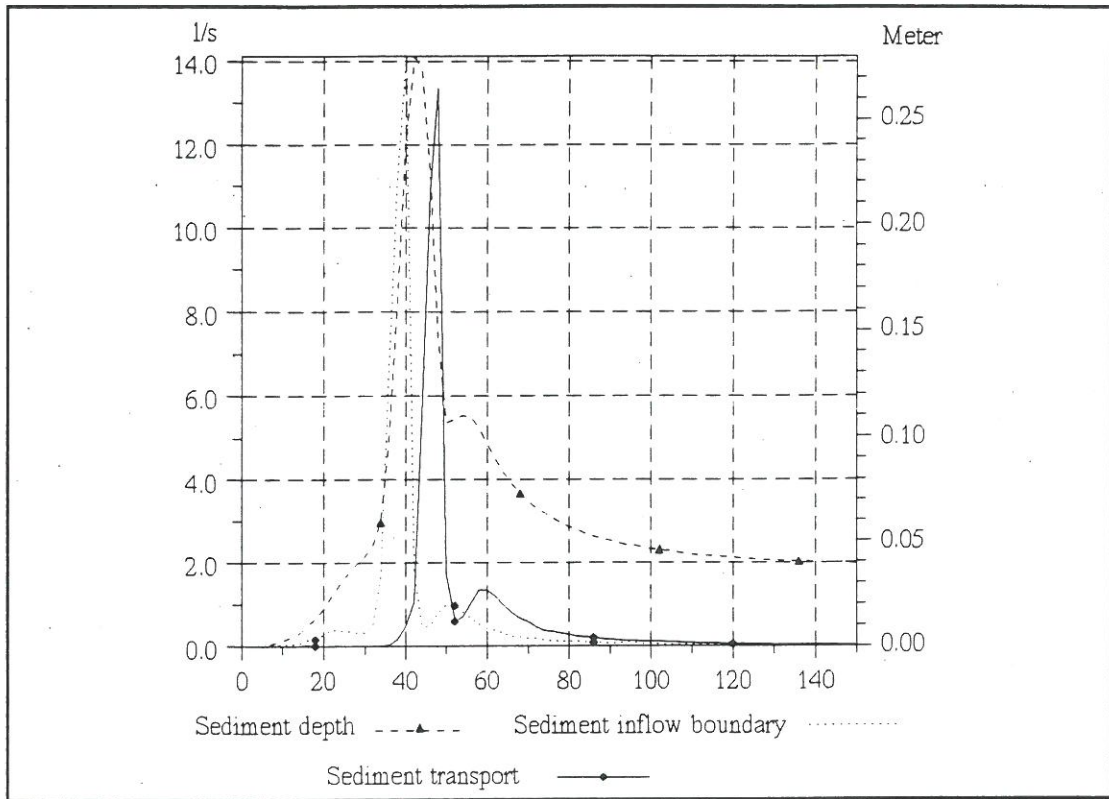


Figure 10.12. Time series of inflow sediment transport, sediment depth and computed transport just downstream of manhole A2076.

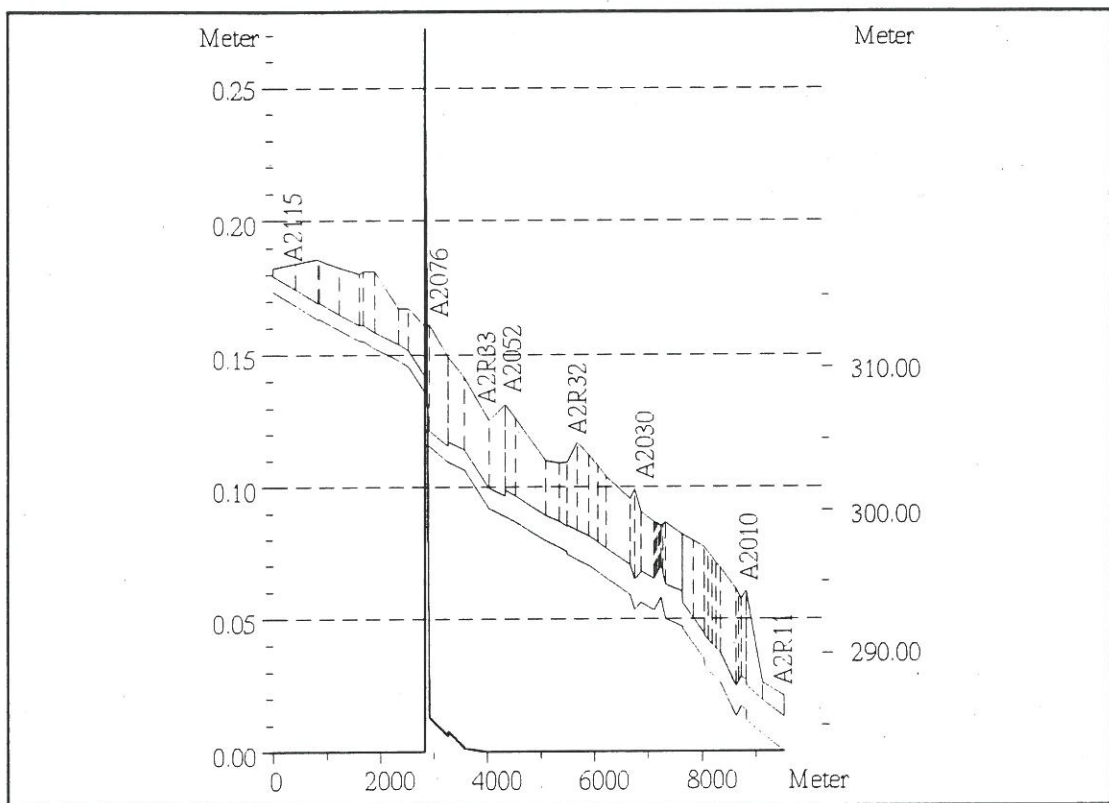


Figure 10.13. The longitudinal profile of the sediment depths in A2 sewer after 44 minutes of simulation.

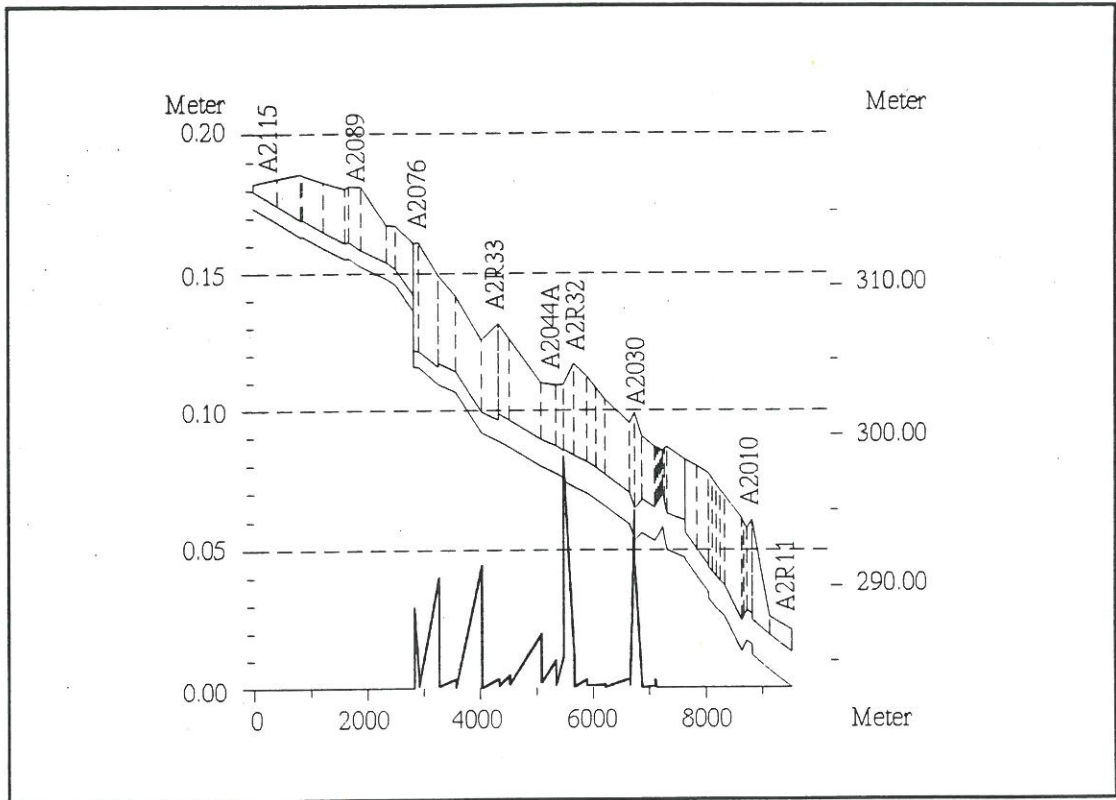


Figure 10.14. The longitudinal profile of the sediment depths in A2 sewer after 6 hours and 40 minutes of simulation.

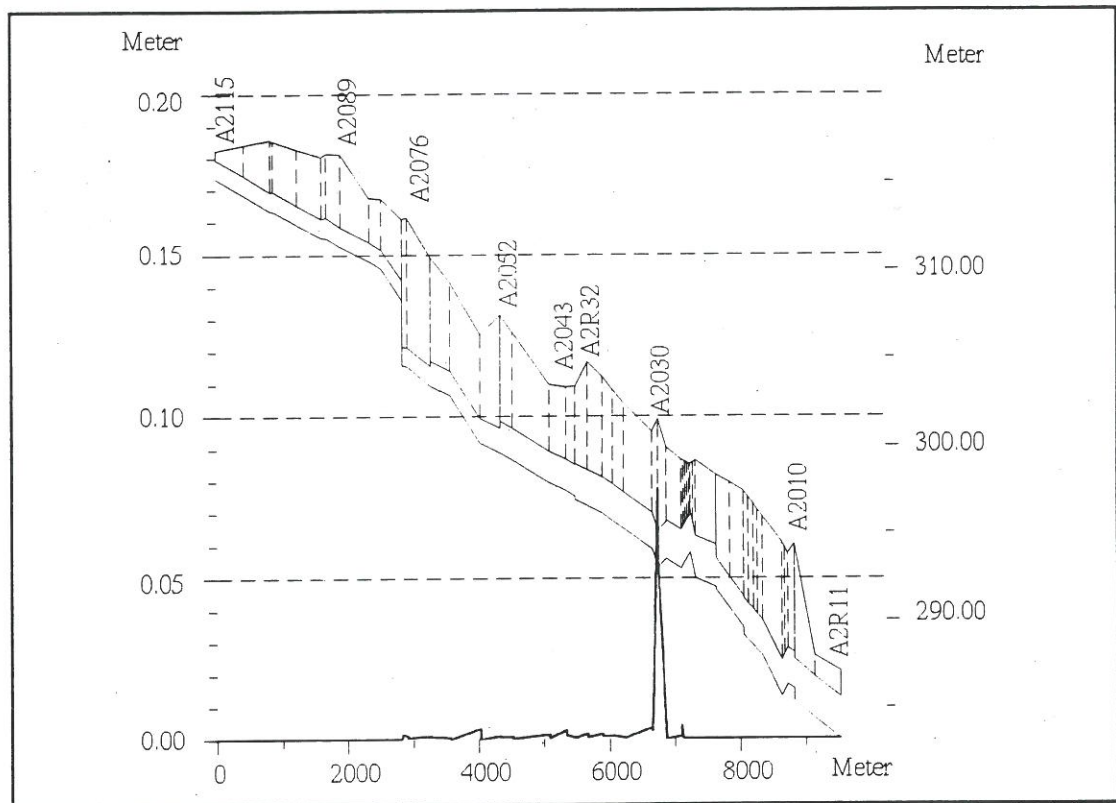


Figure 10.15. The longitudinal profile of the sediment depths in A2 sewer after 7 days of simulation.

As the present method based on a sediment transport model with a movable bed seems to have a good capability of predicting the locations with sediment, future studies could try to establish a standard procedure for the use of this sediment transport model for prediction of locations which are likely to have sediment deposits. Further, it would be interesting to try to evaluate the local criteria<sup>1</sup> for self cleansing conditions in sewers.

### 10.2.5 Effects from Sediment Deposits on the Hydraulic Capacity of the Ljubljana Sewer System

During September-October 1994 another field survey was carried out for selected overflow structures of the Ljubljana sewer system. The primary purpose of this survey was to inspect the overflow structures, in order to evaluate the effect from the sediment deposits at these structure on the flow volume out of the system during rain. The overflow structures were inspected by the companies: Vodovod-Kanalizacija and Hidroinzeniring. At eight overflow structure sediment deposits were observed and the sediment depth measured. The sediment depths at the overflow structures are presented in Table 10.1.

Name of the location	Node name in the model	Sediment depth (cm)	Overflow volume with sediment deposits	Overflow volume without sediment deposits	Reduction of the overflow in %
Zidovska	A0R24	20	1803.4	1930.1	-7.0
Svabiceva	R27-2	5	119.9	111.0	7.4
Ziherlova	R28	20	1421.8	1427.2	-0.3
Vrhovnikova	A6R41	10	579.8	551.8	4.8
Gostilnicarska	A6R42	15	322.3	316.0	2.0
Jamova	A6R43	5	20.9	9.3	55.6
Opekarska	A0R47	5	33.5	36.6	-9.3
Opekarska	A0R48	10	290.1	290.8	-0.2

Table 10.1. Report of sediment locations at overflow structures carried out by Vodovod-Kanalizacija and Hidroinzeniring during September and October 1994. Overflow volumes for the structures with and without sediment deposits.

The sediment transport model was run with and without the sediment deposits in the sewer system for a rain event with a return periods of 1 year. The sediment data were estimated for the field survey: grain size 2 mm and density 2650 kg/m<sup>3</sup>. A time series of the overflow volumes for the overflow structure A6R43 can be seen in

---

These are often based on either the flow velocity or the maximum bed shear stress for dry weather flow.

Figure 10.16. This figure shows that the overflow volumes are increased when sediment deposits are present in the sewer. This is what should be expected. However, the overflow volumes are reduced, eg at structures AOR24, R28 and AOR47, due to the fact that less water flows to this structure as more water is spilled out of the sewer system upstream of the structure due to sediment deposits.

The simulated overflow volumes with and without sediment deposits for the rain with a return period of 1 year can be seen in Table 10.1. In this table only data for the eight structures with sediment deposits are shown; in total there is 75 structures in the MOUSE model. From the table it can be seen that a strong relation exists between the overflow structures in the sewer system of Ljubljana.

In the near future water quality data will also be collected at selected overflow structures, in order to investigate the temporal variation of the concentration of the pollutants in the overflowing water.

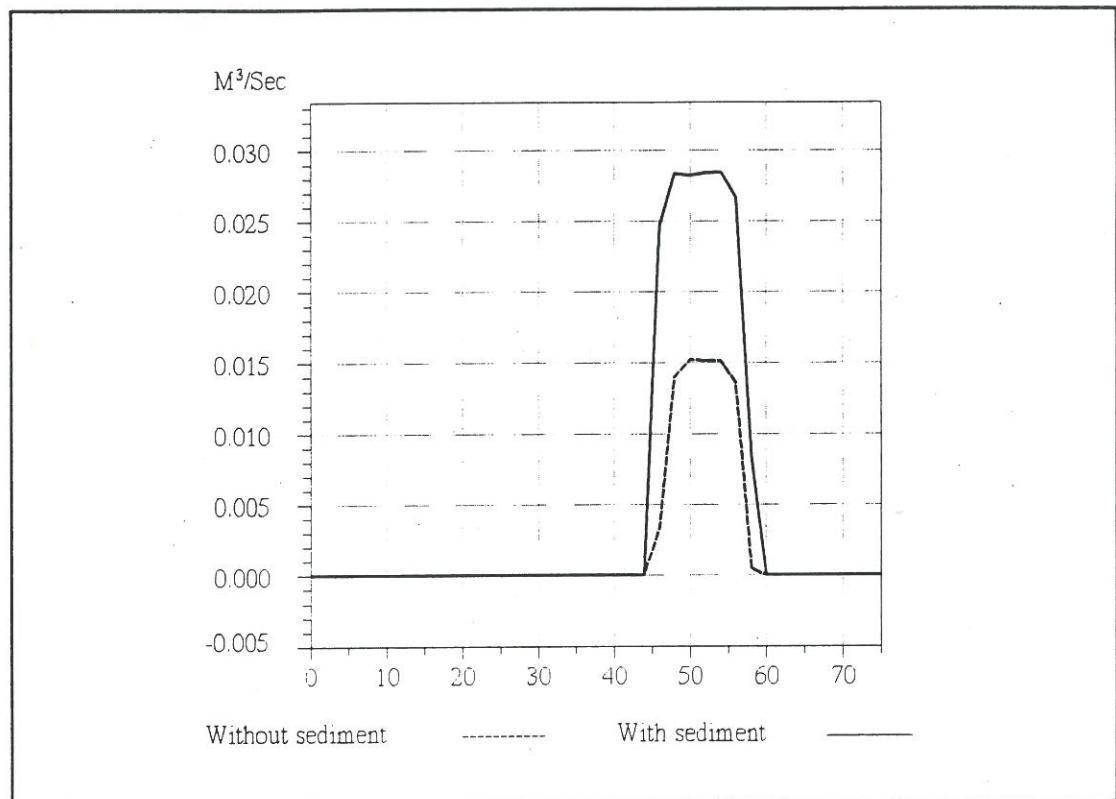


Figure 10.16. Time series of overflow for a storm with a return period of 1 year with and without sediment deposits at the overflow structure A6R43.

## 11 CONCLUSION

### 11.1 Summary of Goals and Objectives

The objective of the study was to collect the existing knowledge on sediments in sewer systems, and based on this knowledge make a mathematical model for the description of the transport of sediments in sewer systems from the source to the sewage treatment plant. The model describes the physical processes involved in transport, erosion and deposition for the hydraulic conditions and sediment characteristics found in sewer systems. The result of the study is an engineering tool, built into the MOUSE system, which can be used to evaluate the performance of sewer systems with respect to the hydraulic capacity, the transport of particles and the transport of dissolved matter. During the process of building the model it has become evident where further research is needed in order to model more accurately the transport processes in sewer systems.

### 11.2 The Selected Modelling Approach

The transport models have been based on the MOUSE system, which has been successfully applied to describe the flow in sewer systems without sediment deposits. It is important that the sediment transport model is based on a well verified and validated hydrodynamic model as the sediment transport is a highly non-linear function of the flow velocity.

A problem in applying a deterministic model for the sediment transport in sewer systems is that often very few or no sediment transport data are available, eg the sediment depth in the pipe system. In addition, not all of the physical processes in sewer systems have continuous mathematical formulations applicable for numerical modelling, eg no single description exists for the critical bed shear stress covering the range from a pipe without sediment deposits to a pipe with a full deposited sediment bed. Further, uncertainties from the hydrodynamic model are carried directly into the transport model, hence the results from a deterministic transport model can not be expected to be as accurate as from the hydrodynamic model. Hence, if no sediment data is available for calibration of the sediment transport model, very large uncertainties will be present in the results from the sediment transport computations. The uncertainties will be much larger than the uncertainties in the hydrodynamic computations, as the sediment transport often is related to the velocity to the power 3-5. Even though large uncertainties may be present in the results from the sediment transport model, the modelling of sediment transport gives the possibility for analyses of the sediment transport in the sewer system and enables the comparison of different management strategies for the sewer system to be made together with providing the opportunity of gaining a better understanding of the transport processes in sewers.

## 11.3 **Résumé of Results Achieved**

A mathematical modelling system has been developed which describes the transport processes of sediments and dissolved matter from the source to the sewage treatment plant. The modelling system has been built into the MOUSE system, hence it constitutes a general modelling tool which contains most of the knowledge applicable today for mathematical modelling of sewer systems. The modelling system constitutes a frame work which can easily be updated as new knowledge on the processes in sewer systems becomes available. The modelling system has been verified against hand calculations and the capability to predict the hydraulic capacity for pipes flowing part full has been validated. The system consists of the three models types which describe the physical transport processes concerning particles and dissolved matter in sewers. The models in the system are:

- a surface model
- a sediment transport model with a moveable bed
- an advection-dispersion model

Due to a lack of data only a few aspects of the models have been compared to field and laboratory data. The evaluation of the sediment transport model showed that the model in pipes flowing part full gave good results for:

- prediction of the hydraulic capacity in pipes with sediment deposits
- prediction of the bed shear stress from sediment deposits
- prediction of the bed load transport in pipes

The evaluation of the advection-dispersion model showed that the model for pipes running part full can accurately simulate the transport time for dissolved matter, and that it is necessary to include both the transport by advection and the transport by dispersion in order to describe the transport processes.

### 11.3.1 **The Hydraulic Capacity in Pipes with Sediment Deposits**

The model was compared to experiments from Chalmers University of Technology (Perrusquía et al, 1976). The model gave a good prediction of the hydraulic capacity for a pipe flowing part full with a uniform sediment layer in the pipe.

### 11.3.2 **The Bed Shear Stress**

It was concluded that the resistance from bed forms must be included in order to estimate the bed shear stress in sewers with non-cohesive sediment deposits. The four theories for prediction of the bed shear stress implemented in the modelling system were compared to the experiments by Perrusquía et al. (1986). Generally the prediction of the bed shear stress is better with the four theories than the prediction of the bed shear stress based on the grain friction, which underestimates the bed shear stress. From a conservative point of view it can be recommended to use the Englund-Hansen model for the prediction of the dimensionless bed shear stress in

the range 0.03-0.45. This model gives a better estimate of the bed shear stress than the estimate based on the skin friction only and the Engelund-Hansen model does not overestimate the bed shear stress.

#### **Ackers-White**

The model gives good estimates of the bed shear stress, except for dimensionless bed shear stresses in the range 0.06-0.1, where the model overestimates the bed shear stress.

#### **Engelund-Hansen**

The model gives good estimates for small bed shear stresses, but it has a tendency to underestimate the dimensionless bed shear stresses larger than 0.3.

#### **Engelund-Fredsoe**

The model gives good estimates of the dimensionless bed shear stresses in the range 0.03-0.1. For large bed shear stresses there is a large scatter present in the prediction of the bed shear stress. The model gives a good estimate of the bed form height but it has a tendency to underestimate the bed form length. This may explain why the model has a tendency to overestimate the bed shear stress for dimensionless bed shear stresses in the range 0.03-0.1.

#### **van Rijn**

The model gives good estimates of the bed shear stress, except for dimensionless bed shear stresses in the range 0.05-0.1, where the model overestimates the bed shear stress. The model overestimates both the bed form height and the bed form length, but as an increase in the bed form height increases the bed shear stress and an increase in the bed form length decreases the bed shear stress, the errors from the estimation in the bed forms are levelled out. The calculation of the length of the bed forms in the van Rijn formulae is based on a fixed relationship with the water depth. This is not a good principle in sewers as a unique relation does not exist between the bed shear stress and the water depth due to the fact that both the pipe walls and the sediment contribute to the average flow resistance.

### **11.3.3 The Sediment Transport**

The prediction of the sediment transport is sensitive to the prediction of the bed shear stress and the critical bed shear stress. Hence, an accurate prediction of the bed shear stress is necessary in order to give a good estimate of the sediment

transport. The four sediment transport formulae implemented in the modelling system: Ackers-White, Engelund-Hansen, Engelund-Fredsøe and van Rijn were compared to the experimental data by Perrusquía (1990, 1991, 1992).

When the sediment formulae were calibrated, all the formulae give satisfactory results for the prediction of the bed load transport in a pipe flowing part full when they were compared to the capability of predicting sediment transport in rivers/flumes. If no sediment transport data are available and the transport mode is bed load then it is recommended to use the Engelund-Fredsøe and the van Rijn formulae (for grain sizes  $< 2.0$  mm).

The capability of the formulae to predict the suspended load was not evaluated due to a lack of data. It was concluded that the existing formulations for suspended load in the Engelund-Fredsøe and the van Rijn formulae probably have to be modified for full flowing pipes due to the change in velocity profile when the pipe is flowing full. For the moment the suspended load transport formulations from rivers have been implemented in the model, but the formulations can probably be adjusted to the conditions in sewer systems by use of a calibration factor.

#### **Ackers-White**

The performance of the model is not good for the prediction of the sediment transport without calibration. When the model is calibrated, the performance is acceptable. The model is very sensitive to the critical bed shear stress within the range of the experimental data.

#### **Engelund-Hansen**

The prediction of the sediment transport by the model is not good without calibration either for the case with or without prediction of the bed shear stress. When the model is calibrated the performance is good. The performance of the model is slightly poorer when the model itself predicts the bed shear stress compared to when the model uses the observed bed shear stress as input to the sediment transport calculation.

#### **Engelund-Fredsøe**

The prediction of the sediment transport by the model is acceptable without calibration both for the case with and without prediction of the bed shear stress. When the model is calibrated the performance is better. The performance of the model is a little poorer when the Engelund-Fredsøe resistance predictor is applied for calculation of the bed shear stress compared to when the model uses the observed bed shear stress as input to the sediment transport calculation. The model is sensitive to the critical bed shear stress within the range of the test data.



## **van Rijn**

The model has an acceptable prediction of the sediment transport without calibration. The performance of the model can not be improved by calibration of the model. If the 2.5 mm fraction is taken out of the test data the model has a good performance and it can be further improved by calibration. This may be due to the fact that the van Rijn formulae have not been validated by van Rijn for grain fractions larger than 2.0 mm. If a calibration is carried out for the 2.5 mm grain fraction only, the performance of the model is good. The model is very sensitive to the criteria for the critical bed shear stress within the range of these experimental data.

### **11.3.4 Application of the Advection-Dispersion Model**

The model was applied to a gravity sewer in Dronninglund, Denmark. The advection-dispersion model predicted well the transport times and the dispersion in the sewer.

### **11.3.5 Application of the Sediment Transport Model**

The model was applied to the Rya-catchment in Gothenburg and the Ljubljana sewer system in Slovenia. The knowledge of the sediment characteristics in the Rya-catchment was very sparse, hence default values, (Crabtree et al. 1993) for the sediment properties were assumed and only the sediment transport capacity at the inflow point to the Rya treatment plant was evaluated. The model predicted sediment transport when sediment transport was recorded at the Rya sewage treatment plant. The results in terms of sediment transport capacity follow the trend of the sediment mass observed at the sewage treatment plant, but the results are not very accurate. The modelling results can presumably be improved if knowledge concerning the sediment depths in the pipe system and more information on the sediment characteristics become available.

The application of the sediment transport model with a movable bed to the sewer system of Ljubljana demonstrated that the model is capable of reproducing the dynamics of the erosion and sedimentation processes in sewers. The model was used to predict the locations of sediment deposits in the sewer system. Based on model simulations five sites were selected for inspection. Four of these sites were inspected during a field trip, and they all had sediment deposits. Finally, the effects of the sediment deposits on the combined sewer overflows were evaluated. At the most upstream overflow structures the overflow is increased when sediment deposits are present. Further, it was concluded that a strong interaction exists between the overflow structures in the Ljubljana sewer system.

### 11.3.6 Verification of the Modelling System

The modelling system was verified against analytical solutions. The verification showed that the surface model, the advection-dispersion model and the sediment transport model are mass conservative and that the transport times are correct within the models. Further, it can be concluded that the models are applicable to the transport processes for the flow conditions in sewer systems.

## 11.4 Recommendations for further Work

There is still discussion as to which physical processes take place in sewer systems, eg the discussion on fluid sediment, see Chapter 4. As it is necessary to have a concise knowledge of the processes in sewer systems before they are modelled, it is necessary to collect sediment transport and hydraulic data from real sewer systems in order to evaluate the importance of each of the physical processes. With such knowledge the modelling effort can be concentrated on the important phenomena, eg during storm conditions probably only a limited supply of sediments will be present in the pipes compared to the sediment transport capacity of the flow. At present, the sediment transport formulations for a limited supply of sediments not can be evaluated due to a lack of data.

Field measurements and further laboratory experiments with graded sediment and suspended load transport are needed in order to evaluate the ability of the model to represent these phenomena. Further, the model should be validated against data from a real sewer system, and the modelling system should be updated as new knowledge becomes available.

### 11.4.1 The Bed Shear Stress

At present, it is widely accepted that the side wall elimination procedure can be used to find the bed shear stress for pipes flowing part full. It is necessary to study the limits of the applicability of the sidewall elimination procedure for full flowing pipes and for different pipe shapes with different sediment depths.

In order to describe when sediment starts to deposit a formulation of the critical bed shear stress for a pipe with little sediment or no sediment deposits is necessary. At present laboratory experiments do exist, Novak and Nalluri, 1975, but no general mathematical formulation has yet been made for the critical bed shear stress as a function of the grain size, the pipe roughness and the sediment concentration. Further, only a sensitive iterative procedure is available for the bed friction when isolated bed forms are present in the pipes, Kleijwegt, 1993. Further, when pipes are flowing full, it has been shown that dunes form, Kleijwegt, 1993. As the dunes in rivers often interact with the free surface and this condition can not be fulfilled in pipes running full, the formulations for the dimensions of the bed forms for pipes running full probably have to be revised. Hence, a general physically based continuous formulation is needed for the bed shear stress ranging from conditions without sediment in the pipe to conditions with a fully developed sediment bed.

#### **11.4.2 The Sediment Transport**

If the side wall elimination procedure is applicable to find the bed shear stress in sewers and if no scale effects exist then existing bed load formulae based on data from flumes can be used to describe the bed load transport in sewers with a full deposited bed.

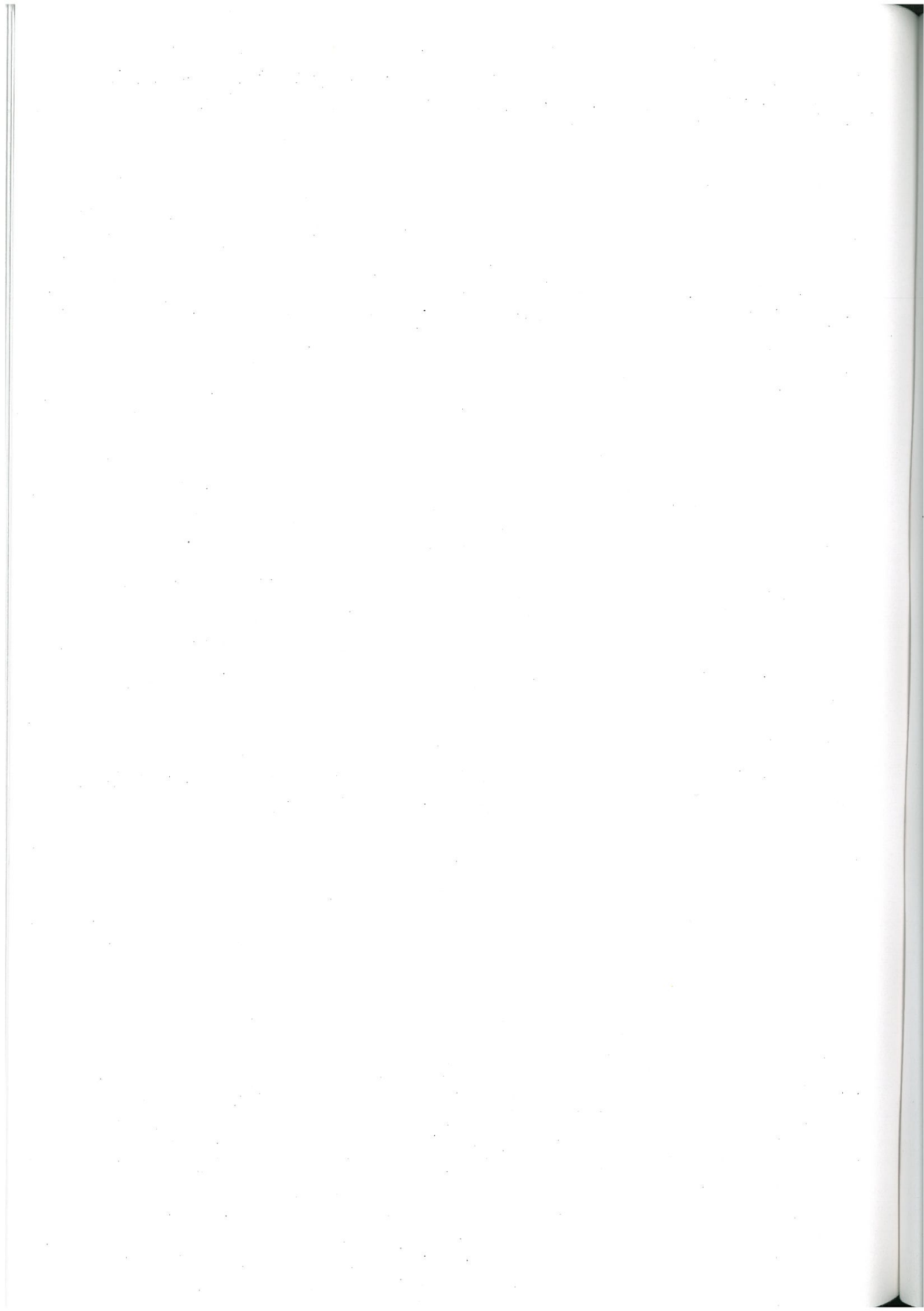
Knowledge of the concentration profiles over the cross-section area in full running pipes are needed in order to calculate the suspended load transport in sewers. This is because the sediment transport formulations for suspended load in rivers have to be modified when they are applied to the flow taking place in a full running pipe due to the change in velocity profile. The suspended load transport formulation can easily be modified when knowledge concerning the concentration profiles over the cross-section area in full running pipes becomes available.

The conventional sediment transport formulations for rivers have to be modified when they are applied to sewers with a limited supply of sediments, as these formulae assume an unlimited supply of sediments from the bed. At present, no physical formulation exists for the sediment transport in sewers with isolated bed forms. A method which takes a limited amount of sediment into account has been implemented in the modelling system, but it has not been validated as few data exist for these conditions. Hence, a general continuous physically based formulation is needed for sediment transport ranging from conditions without sediment in the pipe to conditions with a fully developed deposited sediment bed.

The transport of dissolved matter and sediment transported in the mode of wash load are influenced by the mixing process in the manholes. At present very limited data are available on this process. Experiments concerning this process are necessary to evaluate whether the implemented formulation is sufficiently accurate.

#### **11.4.3 Basins, Structures and Pumps**

One of the most common solutions to reduce the combined sewer overflows is to build retention basins. An evaluation of the modelling system with respect to the descriptions of transport and deposition of sediments in structures/basins is necessary, in order to evaluate the overall applicability of the modelling system to problems related to combined sewer overflows. Finally, the capability of the modelling system should be evaluated against field data for the special transport conditions in connection with pumps in sewer systems.



## 12 REFERENCES

- Ackers, P. and White, W.R. (1973): Sediment Transport: New approach and analysis. *Journal Hydraulics Division* 99(HY11):2041-2060.
- Ammentorp, H. C., Olesen, K. W., Mark, O. (1992): Flood Control Modelling, CWC/DHI Cooperation on Flood Control Modelling. Volume IV, Danish Hydraulic Institute, Denmark.
- Ariathurai, R., MacArthur, R.C. and Krone, R.B. (1971): Mathematical model of Estuarial Sediment Transport. Department of Civil Engineering, University of California at Davis.
- Ashley, R. M. (1993): Cohesive Sediment Erosion and Transport in Sewers. Scottish Hydraulics Study Group 1993 Symposium on sediment transport, Edinburgh. Cap. 4:1-11
- Ashley, R. M., Wotherspoon, J.J., Coghlan, B.P. and McGregor, I. (1992): The Erosion and Movement of Sediments in Combined Sewers. *Water Science and Technology* 25(8):101-114.
- Ashley, R. M., Arthur, S., Coghlan, B.P. and McGregor, I. (1993): Fluid Sediment Movement and First Flush in Combined Sewers. Sixth International Conference on Urban Storm Drainage, Niagara 1:875-883.
- Butler, D., Xiao, Y., Karunaratne, S.H.P.G., Thedchanamoorthy, S. (1994): The Gully Pot as a Physical, Chemical & Biological Reactor". Specialized International Conference: The Sewer as a Physical, Chemical & Biological Reactor. Aalborg, Denmark.
- Coerria, L.R.P., Krishnappan, B.G. and Graf, W.H. (1992): Fully Coupled Unsteady Mobile Boundary Flow Model. *Journal of Hydraulic Engineering* 118:476-494.
- Coerria, L.R.P. and Krishnappan, B.G. (1991): Numerical Modelling of Unsteady Sediment Transport. *Environmental Hydraulics* 1:639-643.
- Crabtree, R. W. (1988): A classification of combined sewer sediment types and characteristics. WRc Engineering, ER 324E.
- Crabtree, R., Gent, R. and Spooner, S. (1993): MOUSE TRAP: Specification of Pollutant and Sediment Characteristic Default Values. WRc Engineering, UC 1950.
- Deigaard, R. (1980): Longitudinal and transverse sorting of grain sizes in alluvial rivers. Series Paper 26, Institute of Hydrodynamics and Hydraulic Engineering, Technical University of Denmark.
- Egiazaroff, V. I. (1965): Calculation of Nonuniform Sediment Concentrations. *Journal Hydraulics Division* 91(1):225-247.

Einstein, H. A. (1942): Formulas for the transportation of bed load. Transactions **107**:561-577.

Engelund, F. A. and Hansen, E. (1967): A monograph on sediment transport in alluvial streams. Teknisk Forlag, Copenhagen, Denmark.

EPA (1986): Methodology for Analysis of Detention Basins for Control of Urban Runoff Quality. U.S. Environmental Agency, EPA440/5-87-001.

Fredsøe, J. (1984): Sediment Transport in current and Waves. Prog. Rep. 49, Institute of Hydrodynamics and Hydraulic Engineering, Technical University of Denmark.

Fredsøe, J. and Deigaard, R. (1992): Mechanics of Coastal Sediment Transport. Advance Series on Ocean Engineering - Volume 3, Wold Scientific.

Garsdal, H., Mark, O., Dørge, J., Jepsen, S-E. (1994): MOUSE TRAP: Modelling of Water Quality Processes and the Interaction of Sediments and Pollutants in Sewers. Specialized International Conference: The sewer as a Physical, Chemical & Biological Reactor. Aalborg, Denmark.

Guymer, I. and O'Brian, R. (1994): The Effects of Manholes on the Travel and Retention Times of Solutes in Sewer Systems. Specialized International Conference: The Sewer as a Physical, Chemical & Biological Reactor. Aalborg, Denmark.

Gustafsson, L-G., Lumley, D., Persson, B. and Lindeborg C. (1993): Development of a Catchment Simulator as an On-Line Tool for Operating a Wastewater Treatment Plant. Sixth International Conference on Urban Storm Drainage, Niagara 2:1508-1513.

Gustafsson L. G et al. (1995) *Ljubljana Sewerage Master Plan. Summary activity 1-5*. Internal report Danish Hydraulic Institute, Denmark.

Huber, W. and Dickinson, E. (1988): Storm Water Management Model, Version 4: User's Manual. Environmental Research Laboratory, U.S. Environmental Protection Agency, Athens, Georgia 30613, USA.

Ichiki, A., Yamada, K. and Nakade, Y. (1993): Study on Quantification and Management of Runoff Pollutants from Non-point Sources in Urban Area. Sixth International Conference on Urban Storm Drainage, Niagara 1:537-542.

Kleijwegt, A. R. (1992): On sediment transport in Circular sewers with non-cohesive deposits. Communication on hydraulic and geotechnical engineering, Faculty of Civil Engineering, Delft University of Technology Report no. 92 - 1.

Kleijwegt, A. R. (1992): Sewer sediment models and basic knowledge. Water Science and Technology **25**(8):123-130.

Kluesener, J.W. and Lee, G.F. (1974): Nutrient loading from a separate storm sewer in Madison, Wisconsin. J. WPCF **46**(5):920-936.

Laplace, D. (1991): Dynamique du Depot en Collecteur D'Assainissement. Seram Société d'exploitation du Réseau d'Assainissement de Marseille, Marseille Cedex, France.

Lindberg, S. and Jørgensen, W. T. (1986): MOUSE -Modelling of Urban Storm Sewer Systems. International Symposium on Comparison of Urban Drainage Models with Real Catchments, Dubrovnik.

Lindberg, S., Nielsen, J.B., and Carr, R. (1989): An Integrated PC-Modelling System for Hydraulic Analysis of Drainage Systems. WATERCOMP '89, The first Australian Conference on Technical Computing in the Water Industry, Melbourne.

Lyn, D.A. and Goodwin, P. (1987): Stability of a General Preissmann Scheme. Journal of Hydraulic Engineering 113(1):16-28.

Morrison, G. M., Revitt, D.M. and Ellis, J.B. (1994): The Gully Pot as a Biological Reactor. Specialized International Conference: The sewer as a Physical, Chemical & Biological Reactor. Aalborg, Denmark.

Nalluri, C. and Alvarez, E. (1990): The Influence of Cohesion on Sediment Behaviour in Pipes and open Channels. Department of Civil Engineering, University of Newcastle upon Tyne.

Nalluri, C. and El-Zaemey, A. K. S. (1993): Sediment Transport over Deposited Beds in Sewers. Sixth International Conference on Urban Storm Drainage, Niagara 1:631-637.

Novak, P. and Nalluri, C. (1975): Sediment Transport in Smooth Fixed Bed Channels. Journal of Hydraulics Division 101(HY9):1139-1154.

Novak, P. and Nalluri, C. (1984): Incipient motion of sediment particles over fixed beds. Journal of Hydraulic Research 22(3):181-197.

O'Brian, R.T. (1993): Longitudinal Dispersion of Solutes in Urban Drainage Systems. Fourth European Post graduate Workshop on Urban Runoff-Sewer Systems, Treatment Plants and Receiving Waters, Aalborg University, Denmark.

O'Brian, R.T. and Mark, O. (1995): Modelling of Dispersion of Solutes in Manholes. In prep.

Pedersen, F. B.. (1977): Prediction of Longitudinal Dispersion in Natural Streams. Series Paper 14. Institute of Hydrodynamics and Hydraulic Engineering, Technical University of Denmark.

Pedersen, F. B. and Mark, O. (1990): Head Losses in Storm Sewer Manholes: Submerged Jet Theory. Journal of Hydraulic Engineering, Vol. 116, No. 11.

Perrusquía, G. S.(1990): Sediment in sewers, Research leaves in England. Chalmers University of Technology, Gothenborg, Sweden. Report Series B:52.

- Perrusquía, G. S. (1991): Bed Load Transport in Storm Sewers. Stream Traction in Pipe Channels. Chalmers University of Technology, Gothenborg, Sweden. Report Series A:22.
- Perrusquía, G. S. (1992): Sediment Transport in Pipe Channels. Chalmers University of Technology, Gothenborg, Sweden. Report Series B:55.
- Perrusquía, G. S., Lyngfelt, S., Sjöberg, A. (1986): Flödeskapacitet hos avloppsledningar delvis fyllda med sediment. Chalmers University of Technology, Gothenborg, Sweden. Report series B:48.
- Perrusquía, G. S., Petersen, O. and Larsen, T. (1994): Hydraulic Resistance in Part-full Pipes with Composite Roughness. Specialized International Conference: The Sewer as a Physical, Chemical & Biological Reactor. Aalborg, Denmark.
- Perrusquía, G. S. and Mark, O. (1995): Prediction of Locations with Sediment Deposits in Sewers. Submitted for: International Conference on Sewer Solids - Characteristics, Movement, Effects and Control. University of Abertay Dundee.
- Raudkivi, A. J. (1990): Loose Boundary Hydraulics. 3rd Edition, Pergamon Press.
- Raunkjær, K. (1993): Characterization and Transformation of Wastewater Organic Matter in Sewer Systems. Aalborg University, Denmark.
- Rijn, L. C. van (1984a): Part I: Bed Load Transport. Journal of Hydraulic Engineering 110(10):1431-1456.
- Rijn, L. C. van (1984b): Part II: Suspended Load Transport. Journal of Hydraulic Engineering 110(11):1613-1641.
- Rijn, L. C. van (1984c): Part III: Bed Forms and Alluvial Roughness. Journal of Hydraulic Engineering 110(11):1733-1754.
- Ristenpart, E., Ashley, R., Uhl, M. (1994): Fluid Sediment and Particulate Transport in Combined sewers. Specialized International Conference: The Sewer as a Physical, Chemical & Biological Reactor. Aalborg, Denmark.
- Rouse, H. (1939): Experiments on the Mechanics of Sediments in Suspension. Proc. 5th Intern. Congr. Appl. Mech., Cambridge, Mass.
- Shields, A. (1936): Anwendung der Ähnlichkeitsmechanik und Turbulenzforschung auf die Geshiebebewegung. Mitt. Preuss. Versuchsanstalt für Wasser, Erd und Schiffbau, no. 26, Berlin.
- Svensson, G. (1987): Modelling of Solids and Metal Transport from small Urban Watersheds. Chalmers University of Technology, Gothenborg, Sweden.
- Sørensen, M. S. (1991): Stofseparation I Overløbsbygværker. Aalborg University, Denmark.



Taylor, G.J. (1954): The dispersion of matter in turbulent flow through a pipe. Proceedings Royal Society London 223 A:446-468.

Vanoni, V.A. (1946): Transportation of Suspended Sediment by Water. Transactions 111.

Vanoni, V.A. and Brooks, N. (1957): Laboratory Studies of Roughness and Suspended Load of alluvial Streams. Final Report No. 68, Sedimentation Laboratory, California Institute of Technology, Pasadena, California.

Verbanck, M. (1992): Field Investigations on Sediment Occurrence and Behaviour in Brussels Combined Sewers. Water Science and Technology 25(8):71-82.

Verbanck, M. (1994): Capturing and releasing settleable solids - the significance of dense undercurrents in combined sewers. Specialized International Conference: The Sewer as a Physical, Chemical & Biological Reactor. Aalborg, Denmark.

White, W.R., Paris, E. and Bettess, R. (1979): A new generation method for predicting the frictional characteristics of alluvial streams. Hydraulic Res. Station, Wallingford, Report No. IT 187.

**NUMERICAL MODELLING APPROACHES  
FOR SEDIMENT TRANSPORT  
IN SEWER SYSTEMS**

**APPENDICES**

**APPENDIX A VERIFICATION OF THE SEDIMENT PROCESSES IN THE SURFACE MODEL . . . . . A-1**

- A.1 Test of the Sediment Build-up Functions . . . . . A-1
- A.2 Test of the Amount of Sediment Mass washed off the Surface . . . . . A-4
- A.3 Test of the Sediment wash-off Formulation . . . . . A-7
- A.4 Test of the Transport Capacity for the Coarse Grain Sediment Fraction . . . . . A-9

**APPENDIX B VERIFICATION OF THE SEDIMENT TRANSPORT PROCESSES IN THE ADVECTION-DISPERSION MODEL . . . . . B-1**

- B.1 Test of Independency of the Flow Direction in the Pipe . . . . . B-1
- B.2 Test of the Interaction between the Hydrodynamic Model and the Advection-Dispersion Model . . . . . B-5
- B.3 Test of the Dispersion in a Single Pipe . . . . . B-8

**APPENDIX C VERIFICATION OF THE SEDIMENT TRANSPORT PROCESSES IN THE SEDIMENT TRANSPORT MODEL . . . . . C-1**

- C.1 Test of the Sediment Transport Formulae: Ackers-White, Engelund-Hansen, Engelund-Fredsøe and van Rijn . . . . . C-1
  - C.1.1 The Ackers-White Sediment Transport Model . . . . . C-1
  - C.1.2 The Engelund-Hansen Sediment Transport Model . . . . . C-3
  - C.1.3 The Engelund-Fredsøe Sediment Transport Model . . . . . C-4
  - C.1.4 The van Rijn Sediment Transport Model . . . . . C-8
  - C.1.5 Summary . . . . . C-10
- C.2 Test of Independency of the Flow Direction in the Pipe . . . . . C-11
- C.3 Test of the Formulation for Graded Sediment . . . . . C-12

**APPENDIX D SENSITIVITY ANALYSIS OF THE INFLUENCE OF THE CRITERION FOR THE INITIATION OF MOTION ON THE SEDIMENT TRANSPORT . . . . . D-1**

- D.1 The Ackers-White Sediment Transport Model . . . . . D-1
- D.2 The Engelund-Fredsøe Sediment Transport Model . . . . . D-2
- D.3 The van Rijn Sediment Transport Model . . . . . D-4

**APPENDIX A**

**Verification of  
the Sediment Processes  
in the Surface Model**

## A VERIFICATION OF THE SURFACE MODEL

The following tests have been carried out to verify the sediment processes in the surface model:

- test of the sediment build-up functions
- test of the amount of sediment mass washed off the surface
- test of the sediment wash-off formulation
- test of the transport capacity for the coarse sediment fraction.

### A.1 Test of the Sediment build-up Functions

The purpose of the test is to show that the linear and the exponential build-up functions are correct.

#### The linear build-up Function

The test of the linear build-up function as carried out with the following data:

surface area	:	1 ha
time since last storm	:	0 days
build-up rate	:	40 kg/ha/day
maximum amount of mass on the surface	:	100 kg/ha

A simulation was carried out without any wash-off. The result of the simulation can be seen in Figure A.1 and an extract of the results can be seen in Table A.1. The theoretical build-up time is given as:

$$t_{\text{build-up}} = \frac{\text{Maximum surface mass}}{\text{build-up rate}} = \frac{100 \text{ kg}}{40 \text{ kg/day}} = 2.5 \text{ days} = 3600 \text{ min.} \quad (\text{A-1})$$

It can be seen that the theoretical build-up time corresponds to the build-up time in the simulation.

Min:Sec	Mass on the surface, kg
0:00	0.00000
5:00	0.139
10:00	0.278
15:00	0.417
20:00	0.556
25:00	0.694
.	.
.	.
3550:00	98.611
3555:00	98.750
3560:00	98.889
3565:00	99.028
3570:00	99.167
3575:00	99.306
3580:00	99.444
3585:00	99.583
3590:00	99.722
3595:00	99.861
3600:00	100.000
3605:00	100.000
3610:00	100.000
3615:00	100.000
3620:00	100.000
3625:00	100.000

Table A.1. An extract of the results for test of the linear build-up function.

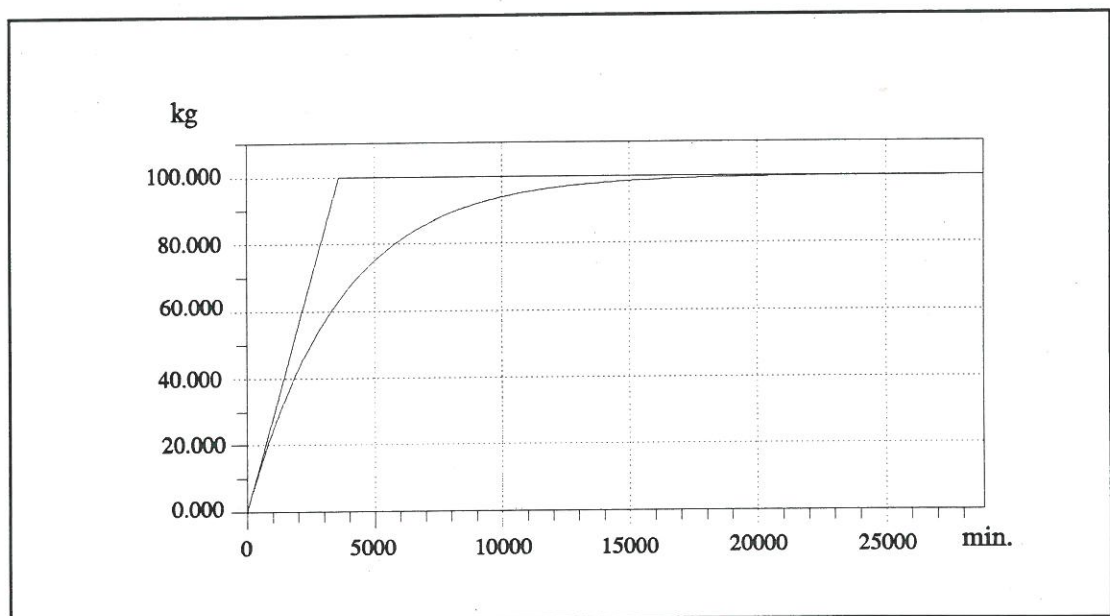


Figure A.1. The linear and the exponential build-up function. Maximum amount of mass on the surface = 100 kg and build-up rate 40 kg/ha/day.

## The exponential build-up Function

The test of the exponential build-up function was carried out with the data:

surface area	:	1 ha
time since last storm	:	0 days
build-up rate	:	40 kg/ha/day
maximum amount of mass on the surface	:	100 kg/ha

A simulation was carried out without any wash-off. The result of the simulation can be seen in Figure A.1 and an extract of the results can be seen in Table A.2. The theoretical build-up function is given as:

$$\text{Surface mass} = \text{Maximum surface mass} \cdot \left[ 1 - e^{-\frac{dt \cdot \text{Maximum surface mass}}{\text{build-up rate}}} \right] \quad (\text{A-2})$$

where

dt is the time step in the calculation.

Hence, after 2.5 the mass on the surface should days be:

$$\text{Surface mass} = 100 \text{ kg} \cdot \left[ 1 - e^{-2.5 \text{ days} \frac{100 \text{ kg}}{40 \text{ kg/day}}} \right] = 63.212 \text{ kg} \quad (\text{A-3})$$

From Table A.2 it can be seen that the model corresponds to the analytical calculation for the exponential build-up of mass on the surface.

Min:Sec	Mass on the surface, kg
0:00	0.00000
5:00	0.139
10:00	0.277
15:00	0.416
20:00	0.554
25:00	0.692
30:00	0.830
35:00	0.968
40:00	1.105
45:00	1.242
3560:00	62.801
3565:00	62.853
3570:00	62.904
3575:00	62.956
3580:00	63.007
3585:00	63.058
3590:00	63.110
3595:00	63.161
<b>3600:00</b>	<b>63.212</b>

Table A.2. An extract of the results from the test of the exponential build-up function.

## A.2 Test of the Amount of Sediment Mass washed off the Surface

The purpose of the test is to show that the mass balance is correct for the surface.

The test was carried out with the following data:

surface area	:	1 ha
time since last storm	:	2.5 days
maximum mass on the surface	:	100.0 kg
build-up rate	:	40.0 kg/ha/day
rain intensity	:	8.0 $\mu\text{m/s}$

The results of the simulation can be seen in Figure A.2 and Table A.3. It can be seen that the initial mass on the surface is washed off after three minutes. However, during the simulation mass continues to build up at a rate of  $40 \text{ kg/ha/day} = 4,6 \cdot 10^{-4} \text{ kg/s}$ . The total mass available for wash-off during the simulation is:

$$\text{Mass} = 100 \text{ kg} + (20 - 1.5) \cdot 60 \text{ s} \cdot \frac{40 \text{ kg/s}}{24 \cdot 3600} = 100.514 \text{ kg} \quad (\text{A-4})$$

It can be seen from Table A.3 that the mass balance is correct for the build-up/wash-off on the surface.



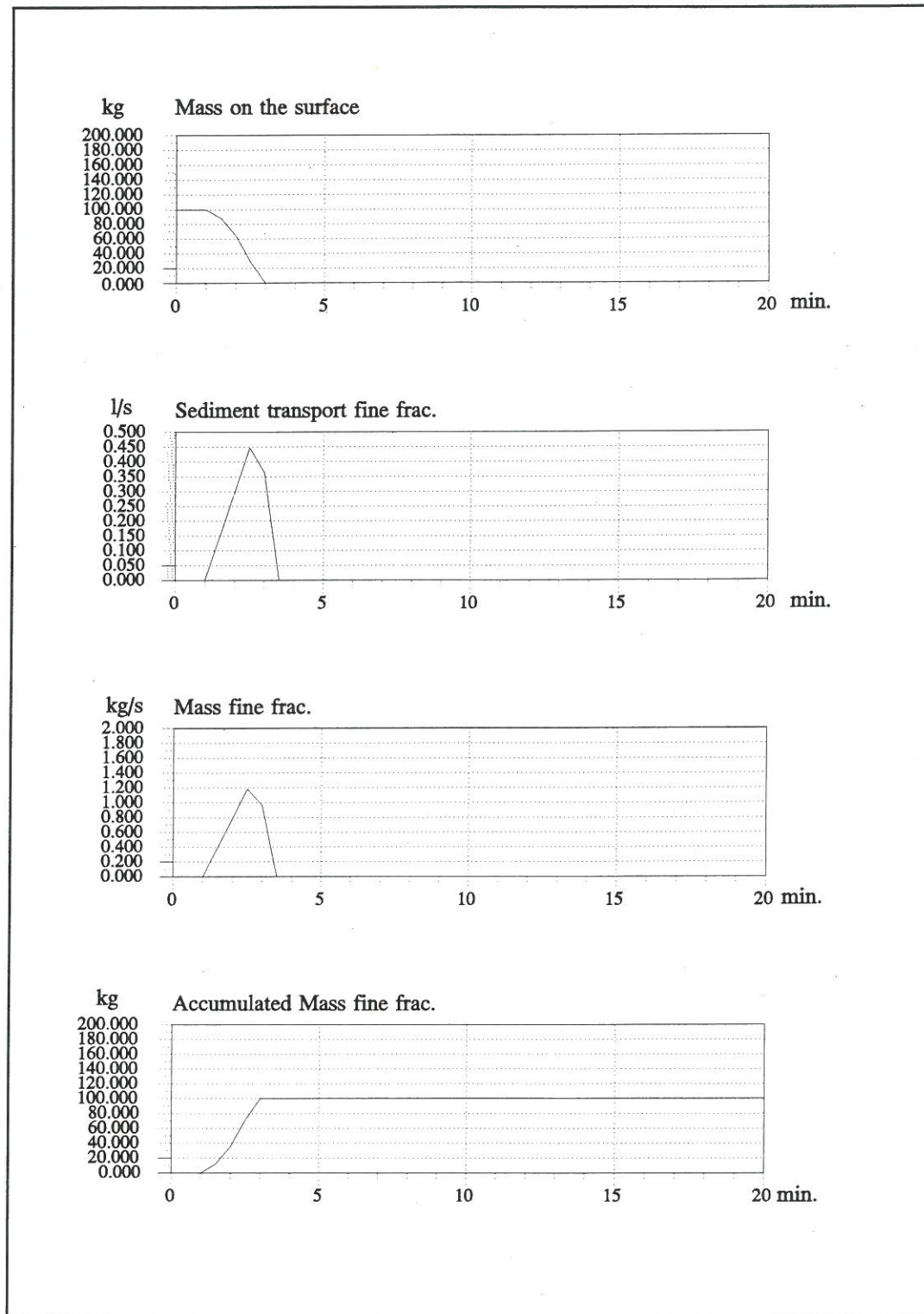


Figure A.2. Time series for the mass of the fine sediment fraction on the surface (kg), sediment transport (l/s), mass transported (kg/s) and the accumulated mass washed-off the surface.

Min:Sec	Mass on the surface, kg
0:00	100.000
0:30	100.000
1:00	100.000
1:30	88.137
2:00	64.424
2:30	28.847
3:00	0.00000
3:30	0.00000
4:00	0.00000
.	
.	
.	

Min:Sec	Sediment transport fine fraction, l/s
0:00	0.00000
0:30	0.00000
1:00	0.00000
1:30	0.149
2:00	0.298
2:30	0.448
3:00	0.363
3:30	0.00017
4:00	0.00017
.	
.	
.	

Min:Sec	Mass fine fraction, kg/s
0:00	0.00000
0:30	0.00000
1:00	0.00000
1:30	0.395
2:00	0.791
2:30	1.186
3:00	0.962
3:30	0.00046
4:00	0.00046
.	
.	
.	

Min:Sec	Accumulated Mass fine fraction, kg
0:00	0.00000
0:30	0.00000
1:00	0.00000
1:30	11.863
2:00	35.590
2:30	71.181
3:00	100.042
3:30	100.056
4:00	100.069
4:30	100.083
5:00	100.097
.	
.	
.	
19:00	100.486
19:30	100.500
20:00	100.514

Table A.3. An extract from the time series for the mass of the fine sediment fraction mass on the surface (kg), sediment transport (l/s), mass transported (kg/s) and the accumulated mass washed-off the surface.

### A.3 Test of the Sediment wash-off Formulation

The purpose of the test is to show that the wash-off from the rainfall generated erosion is correct.

The test was carried out with the following data:

surface area	:	1 ha
time since last storm	:	11.0 days
maximum mass of the surface	:	9999.99 kg
build-up rate	:	999.99 kg/ha/day
rain intensity	:	8.0 $\mu\text{m/s}$
power in wash-off equation	:	2.0
detachment rate	:	0.0010

The results of the simulation can be seen in Table A.4 and Figure A.3. The equation for the detachment generated by the rainfall is:

$$V_{sr} = D_r \left( \frac{i_r}{i_d} \right)^2 LW(1-\epsilon)A_s = 0.001 \left( \frac{8 \mu\text{m/s}}{25.4 \text{mm/h}} \right)^2 \cdot 10000 \text{m}^2 \cdot (1-0.35)0.90 = 2.089 \cdot 10^{-3} \text{t/s} \quad (\text{A-5})$$

where

$V_{sr}$	sediment volume detached by the rain per unit of time ( $\text{m}^3/\text{h}$ )
$D_r$	coefficient for rainfall generated detachment (m/h)
$i_r$	rainfall intensity (mm/h)
$i_d$	rainfall intensity constant (25.4 mm/h)
L	length of the catchment (m)
W	width of the catchment (m)
$\epsilon$	porosity of the sediment
$A_s$	fraction of surface area covered with sediment (90 %)

It can be seen that the amount of washed off sediment is the same for the simulation and the hand calculation.

Min:Sec	Sediment transport fine fraction, l/s
0:00	0.00000
0:30	0.00000
1:00	0.00000
1:30	0.149
2:00	0.298
2:30	0.448
3:00	0.597
3:30	0.746
4:00	0.895
4:30	1.045
5:00	1.194
5:30	1.343
6:00	1.492
6:30	1.641
7:00	1.791
7:30	1.940
8:00	2.089
8:30	2.089
9:00	2.089
9:30	2.089
<b>10:00</b>	<b>2.089</b>

*Table A.4. An extract from the time series for the wash-off of the fine sediment fraction (l/s).*

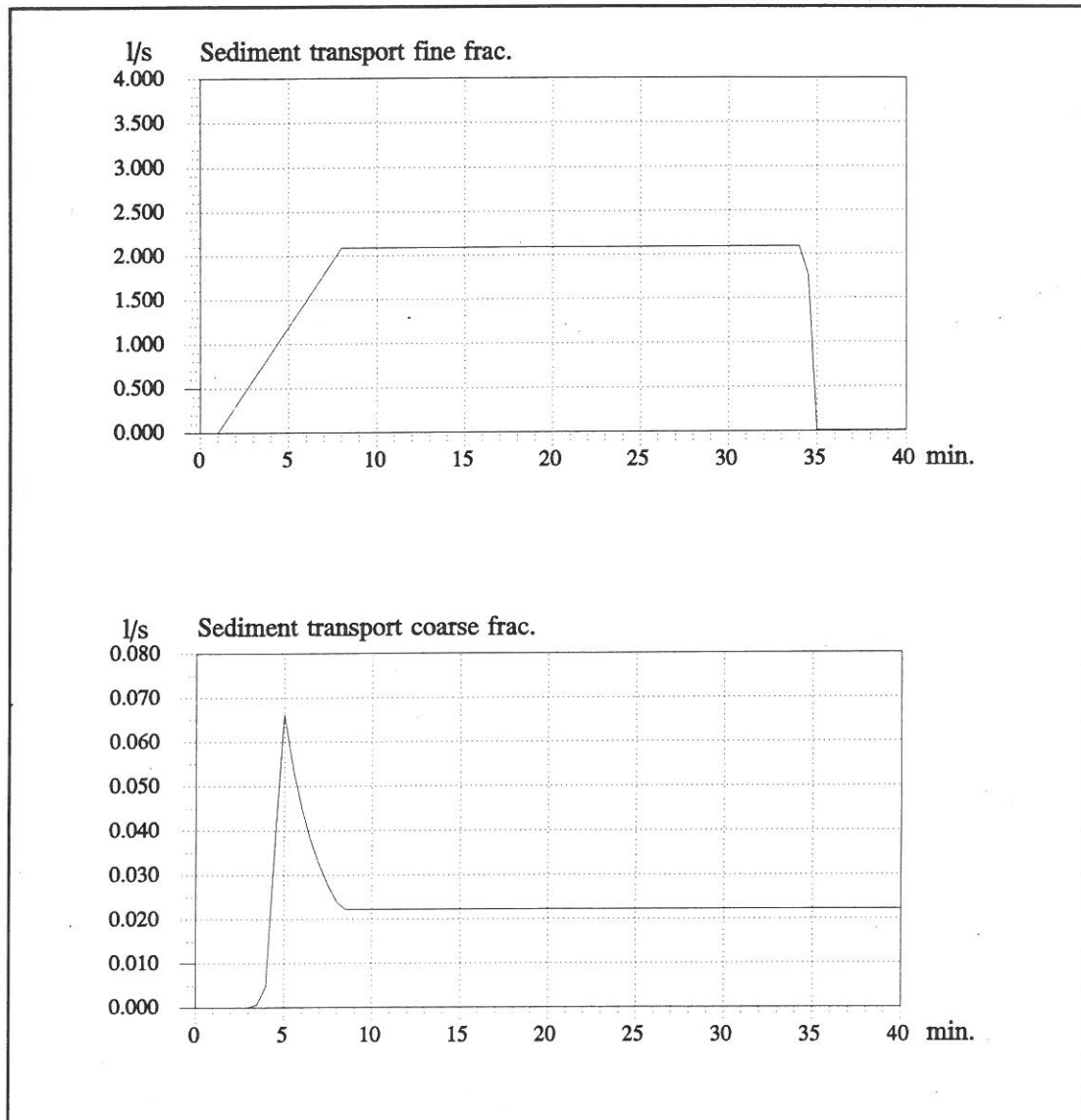


Figure A.3. The sediment transport for the fine and the coarse fraction.

#### A.4 Test of the Transport Capacity for the Coarse Grain Sediment Fraction

The purpose of the test is to show that the calculated van Rijn transport capacity for the coarse grain fraction is correct. The data are the same as in the previous test. The wash-off by rainfall is: 2.089 l/s. The sediment transport capacity of the flow is calculated from the van Rijn theory. The calculation is based on the data in the previous test and the following data, (not all of these data are standard input/output from MOUSE):

grain size	:	0.1 mm
density	:	2650 kg/m <sup>3</sup>
porosity	:	0.35
Manning number	:	53.0 m <sup>1/3</sup> /s
water depth	:	3.36 mm
velocity	:	0.12 m/s
dim.less critical bed shear stress	:	0.056
surface width	:	180 m

The sediment transport capacity is calculated using the procedure described in the section on the verification of the van Rijn sediment transport model, see APPENDIX C. The sediment transport capacity is calculated to be:  $2.22 \cdot 10^{-5}$  m<sup>3</sup>/s. Since the sediment transport capacity calculated by the van Rijn model is less than the rate of detached sediment, the sediment transport is set equal to the sediment transport capacity. The sediment transport of the coarse fraction calculated by the model is 0.022 l/s which is in agreement with the hand calculation. The results of the simulation can be seen in Table A.5.

Min:Sec	Sediment transport coarse fraction, l/s
0:00	0.00000
0:30	0.00000
1:00	0.00000
1:30	0.00000
2:00	0.00000
2:30	0.00000
3:00	0.00000
3:30	0.00069
4:00	0.0049
4:30	0.038
5:00	0.066
5:30	0.054
6:00	0.045
6:30	0.038
7:00	0.032
7:30	0.028
8:00	0.024
8:30	0.022
9:00	0.022
9:30	0.022
<b>10:00</b>	<b>0.022</b>

Table A.5. An extract from the time series for the wash-off of the coarse sediment fraction (l/s).

**APPENDIX B**

**Verification of  
the Transport Processes in  
the Advection-Dispersion Model**

## **B VERIFICATION OF THE ADVECTION-DISPERSION MODEL**

Selected test cases are used to verify the advection-dispersion model. The test cases are:

- test of independency of the flow direction in the pipe
- test of the interaction between the hydrodynamic model and the advection-dispersion model
- test of the dispersion in a single pipe

### **B.1 Test of Independency of the Flow Direction in the Pipe**

The purpose of the test is to show that the calculation of concentrations by the advection-dispersion model is independent of the flow direction in a pipe. The test setup consists of two pipes between the manholes A, B and OUT. A longitudinal profile of the model is shown in Figure B.1. The hydrodynamic boundary conditions are given by a time series of discharge and the advection-dispersion boundary conditions by a time series of concentration. The time series are shown in Figure B.2. The test setup is first run with positive flow in the pipe A-B. In the second run the direction of the flow in pipe A-B is reversed. Hence, the discharges in this pipe will now be negative but with the same numerical values as in the first simulation. The results of the simulation can be seen in Figure B.3. The concentrations in the first grid point in pipe B-OUT, plotted in Figure B.4, are independent of the flow direction in the upstream pipe. It can be seen that the concentrations are the same for both cases.



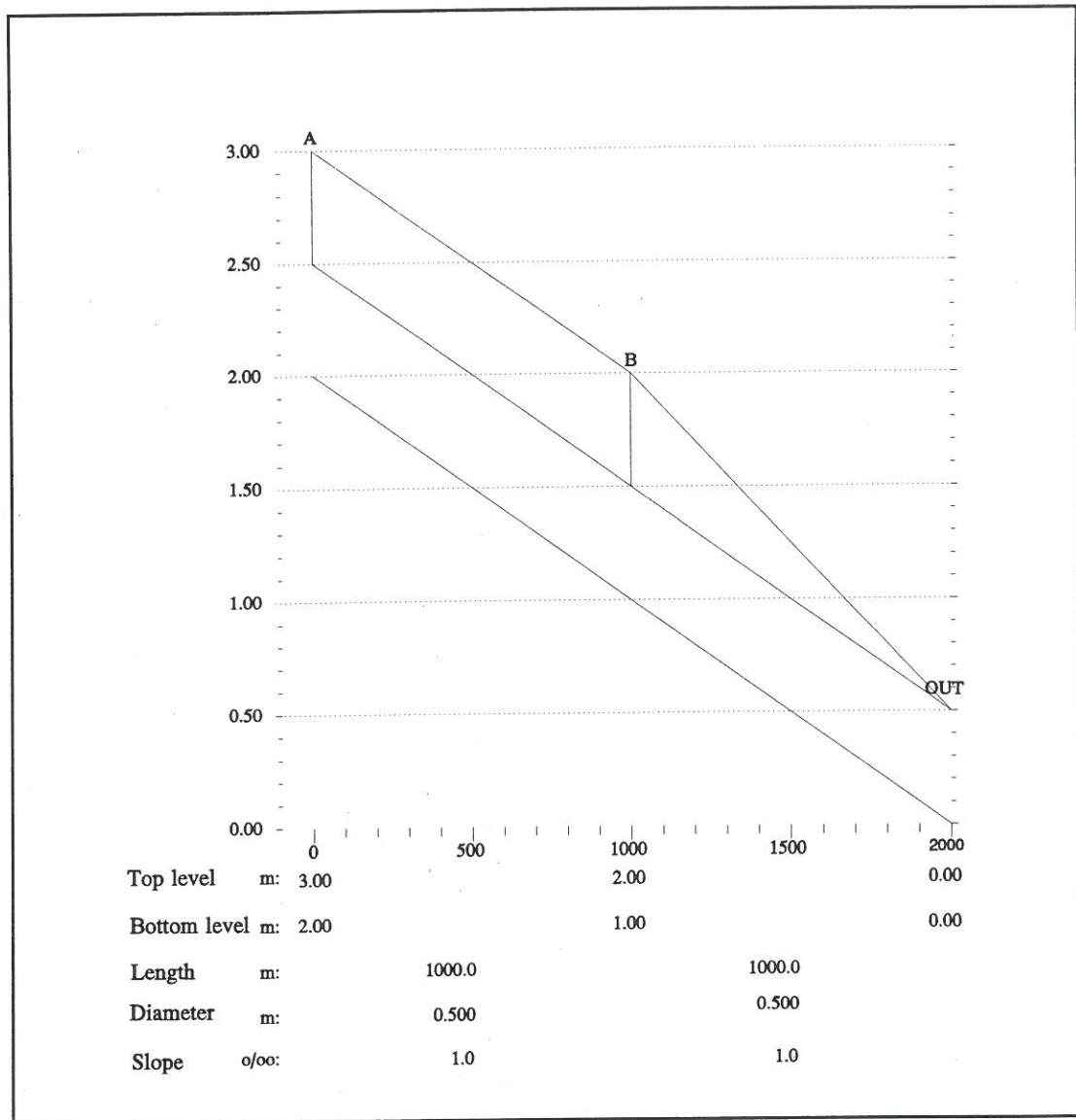


Figure B.1. Longitudinal profile of the test setup.

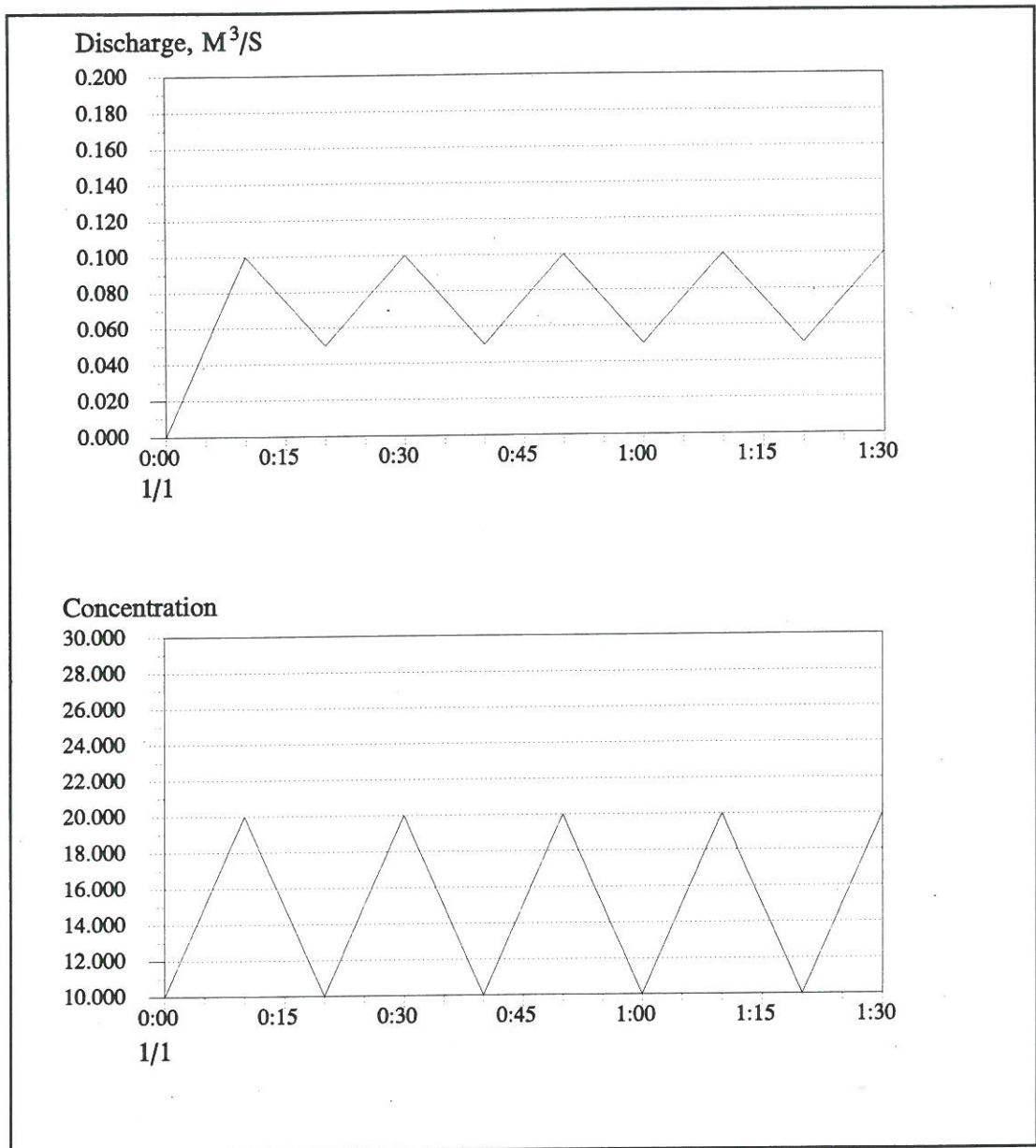


Figure B.2. Boundary conditions for the test.

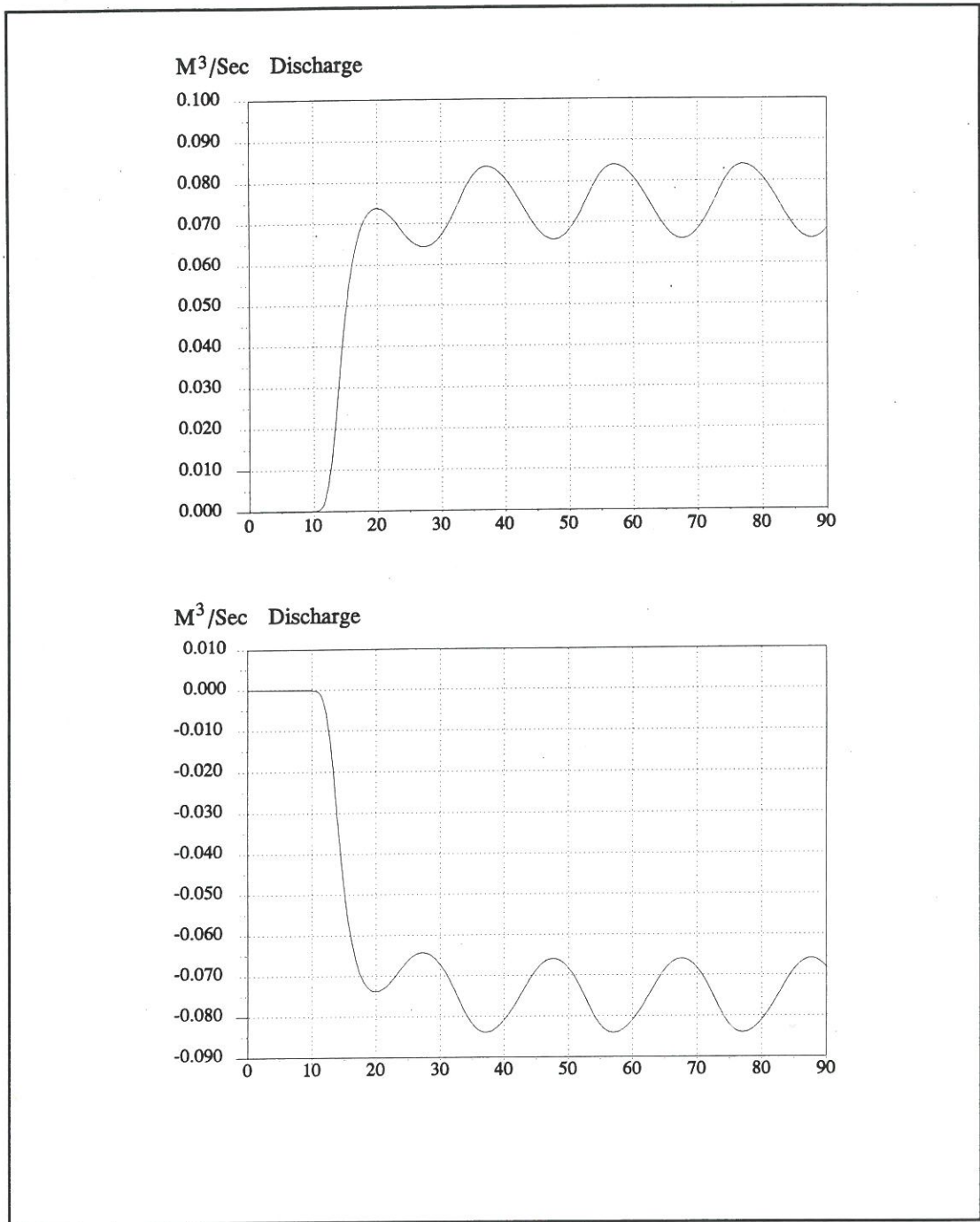


Figure B.3. The simulated time series of discharge in pipe A-B.

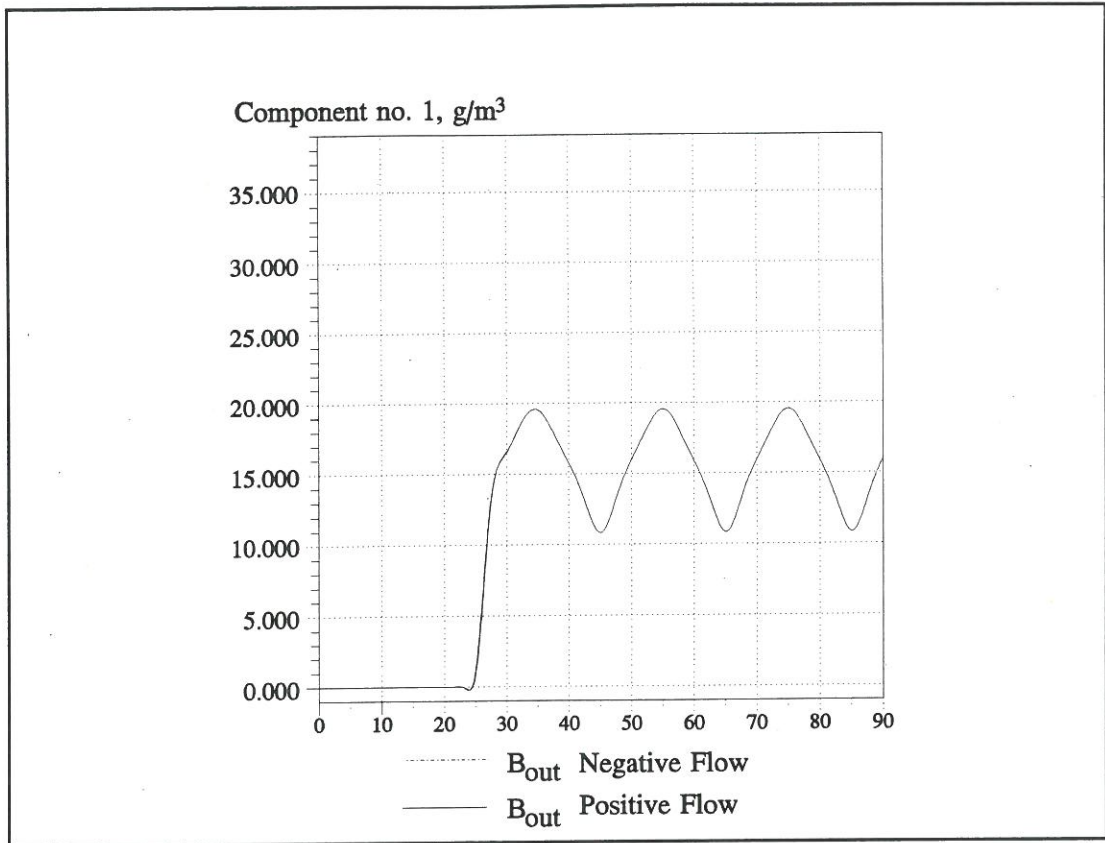


Figure B.4. The simulated time series of concentration in pipe A-B.

## B.2 Test of the Interaction between the Hydrodynamic Model and the Advection-Dispersion Model

The purpose of the test is to show that the transfer of variables between the hydrodynamic model and the advection-dispersion model is consistent, ie strongly unsteady hydrodynamics do not influence the advection-dispersion simulation in a situation with constant concentration input. The test model contains a single horizontal pipe, which is open at the upstream end and closed at the downstream end. A longitudinal profile can be seen in Figure B.5. The hydrodynamic boundary condition is a tidal variation at the upstream end and a closed boundary at the downstream end. The boundary conditions for the advection-dispersion model are an initial concentration of  $10 \text{ g/m}^3$  in the pipe and a constant concentration of  $10 \text{ g/m}^3$  at the upstream boundary. The concentration should be exactly  $10 \text{ g/m}^3$  everywhere in the pipe during the simulation. The time series of the water level and the concentration in the middle of the pipe can be seen in Figure B.6. It can be seen that the concentration is  $10 \text{ g/m}^3$  and constant.

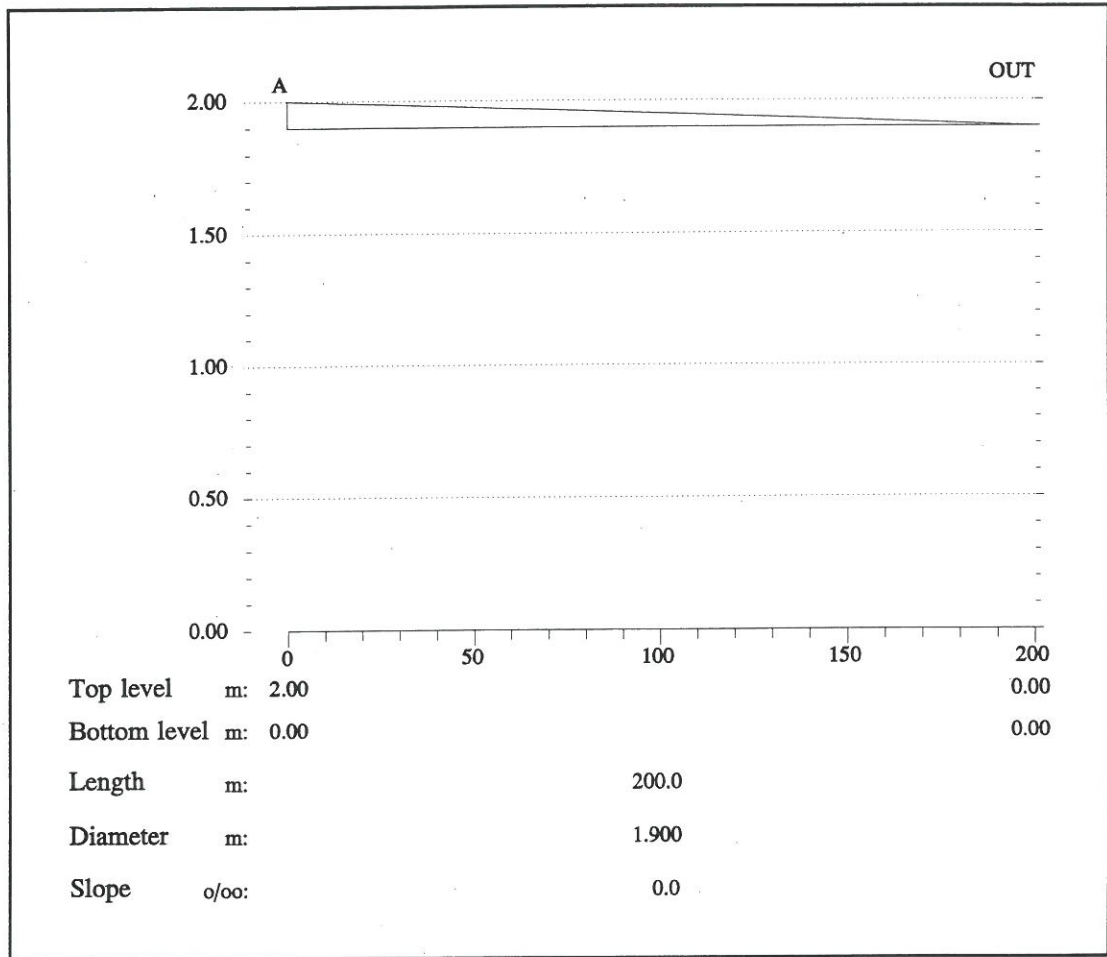


Figure B.5. Longitudinal profile of the test setup.

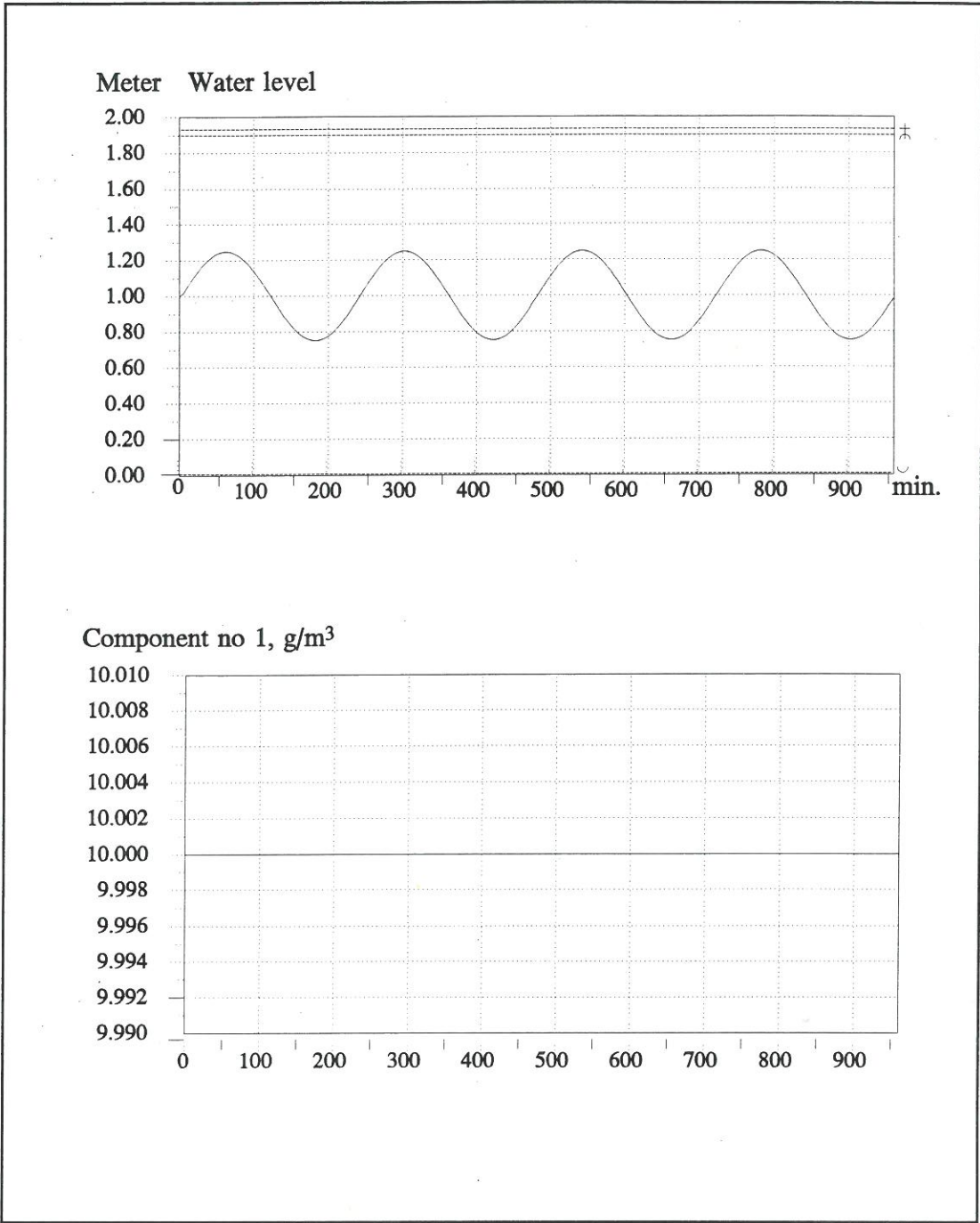


Figure B.6. Time series of water level and concentration in the middle of the pipe.

### B.3 Test of the Dispersion in a Single Pipe

The purpose of the test is to show that the transport by pure dispersion is correct.

Data:

pipe length	: 1000 m
dx	: 1 m
Dispersion coefficient	: 2 m <sup>2</sup> /s
Initial conditions	: The concentration is zero everywhere except for x = 500 m where the concentration is 200 g/m <sup>3</sup>
Hydrodynamic	:
flow area	: 1 m <sup>2</sup>
water level	: 1 m <sup>2</sup>
discharge	: 0.0 m <sup>3</sup> /s
slope	: 0.0 %

The analytical solution to a pulse injection can be expressed as:

$$c(x,t) = \frac{\frac{m}{A}}{\sqrt{4\pi Dt}} e^{-\frac{(x-ut)^2}{4Dt}} \quad (\text{B-1})$$

where

m is the mass, kg

A is the flow area, m<sup>2</sup>

x is the distance from the injection point, m

t is the time, s

u is the velocity, m/s

D is the dispersion coefficient, m<sup>2</sup>/s.

The time series of concentration calculated from both the analytical solution and the model at a point 10 m from the injection point can be seen in Figure B.7. It can be seen from Figure B.7. that there is good agreement between the analytical solution and the solution calculated by the model. The concentrations at a distance 10 m upstream and 10 m downstream of the injection point have been plotted in Figure B.8. From Figure B.8 it can be seen that the dispersion propagates symmetrically from the injection point.

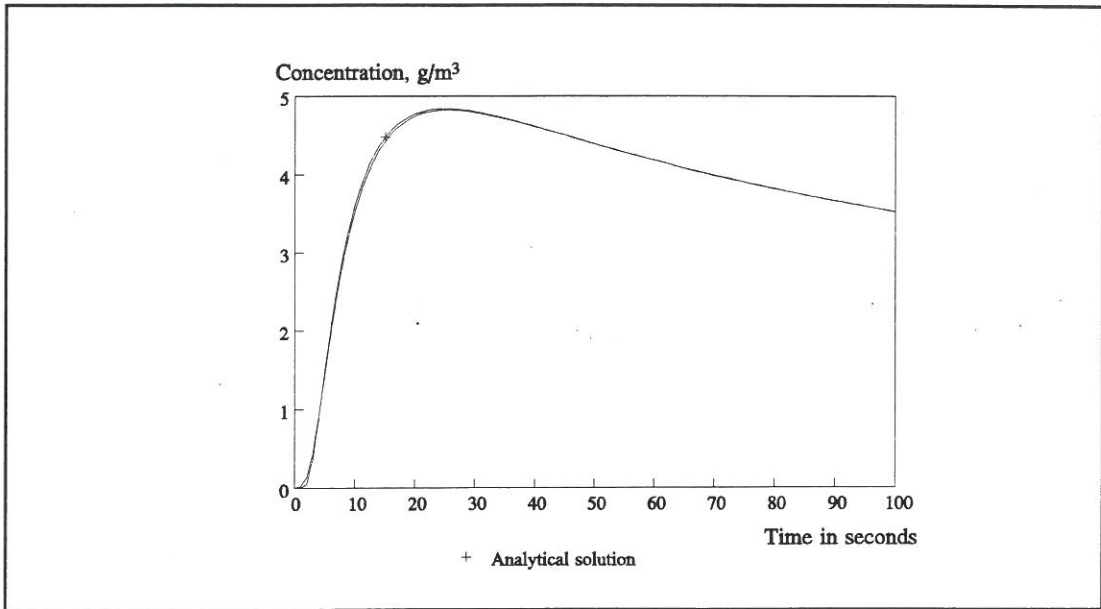


Figure B.7. Time series of concentration calculated from the analytical solution, +, and by the model 10 m from the injection point.

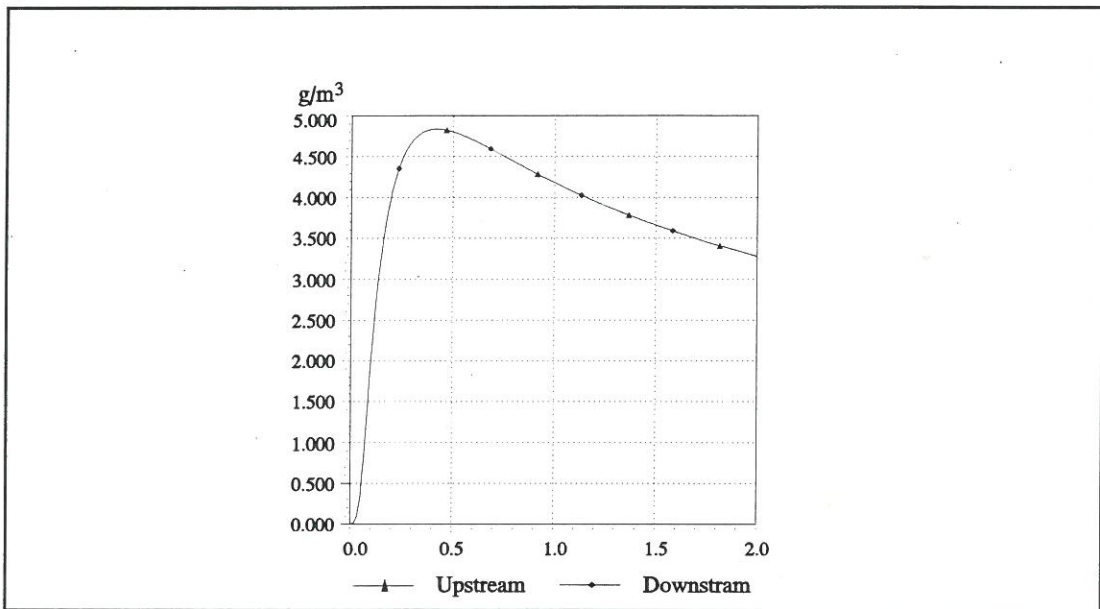


Figure B.8. Time series of concentration calculated 10 m upstream and 10 m downstream from the from the injection point.



**APPENDIX C**

**Verification of  
the Sediment Transport Processes  
in the Sediment Transport Model**

## C VERIFICATION OF THE SEDIMENT TRANSPORT MODEL

Selected test cases have used to verify the sediment-transport model. The test cases are:

- test of the sediment transport formulae: Ackers-White, Engelund-Hansen, Engelund-Fredsøe, van Rijn
- test of independency of the flow direction in the pipe
- test of the formulation for graded sediment

### C.1 Test of the Sediment Transport Formulae: Ackers-White, Engelund-Hansen, Engelund-Fredsøe and van Rijn

The four sediment transport formulae have been verified for steady state hydrodynamic conditions. Only the basic calculations are given below. For further information on the sediment transport formulae, please refer to the Technical Reference Manual. The hydrodynamics used to verify the sediment transport formulae are:

water level	= 1.0 m
discharge	= 1.0 m <sup>3</sup> /s
velocity	= 1.0 m/s
slope	= 6.26E-4
dimensionless bed shear stress	= 0.056
grain diameter, d <sub>50</sub>	= 0.30 mm

#### C.1.1 The Ackers-White Sediment Transport Model

The Ackers-White sediment transport formulation gives the sediment transport, mass flux per unit mass flow rate as:

$$X = \frac{G_{gr} \cdot s \cdot d}{Y} \left( \frac{U}{U_f} \right)^n = 5.56E-4 \quad (C-1)$$

The parameters in the Ackers-White sediment transport formulation are given below:

$$D_{gr} = d \left[ \frac{g(s-1)}{v^2} \right]^{1/3} = 7.5888 \quad (C-2)$$

$1 < D_{gr} < 60$  (Transitional grain size):

The transition exponent,  $n$ , is:

$$n = 1.0 - 0.56 \log D_{gr} = 0.5071$$

The value of  $F$  at nominal initial motion,  $A$ , is:

$$A = \frac{0.23}{\sqrt{D_{gr}}} + 0.14 = 0.2235 \quad (\text{C-3})$$

The coefficient,  $C$ , in the sediment transport function equation (C-8) is:

$$\begin{aligned} \text{Log}(C) &= 2.86 \text{Log} D_{gr} - (\text{Log} D_{gr})^2 - 3.53 \\ &\quad \downarrow \\ C &= 0.1632 \end{aligned} \quad (\text{C-4})$$

The exponent,  $m$ , in the sediment transport function, equation (C-8) is:

$$m = \frac{9.66}{D_{gr}} + 1.34 = 2.6129 \quad (\text{C-5})$$

The friction velocity,  $u_f$ , is:

$$U_f = \sqrt{gYI} = 0.0783 \quad (\text{C-6})$$

$F_{gr}$  is the general sediment mobility number calculated as:

$$F_{gr} = \frac{U_f^n}{\sqrt{gd(s-1)}} \cdot \left( \frac{U}{\sqrt{32} \log \left( \frac{10Y}{d} \right)} \right)^{1-n} = 0.7978 \quad (\text{C-7})$$

The dimensionless sediment transport rate,  $G_{gr}$  is:

$$G_{gr} = C \left( \frac{F_{gr}}{A} - 1 \right)^m = 0.1921 \quad (\text{C-8})$$

The sediment transport, mass flux per unit mass flow rate is:

$$X = \frac{G_{gr} \cdot s \cdot d}{Y} \left( \frac{U}{U_f} \right)^n = 5.56E-4 \quad (\text{C-9})$$

The sediment transport rate is:

$$S = \frac{X}{s} = 0.210 \text{ l/s} \quad (\text{C-10})$$

The corresponding value calculated by MOUSE is:

$$S = 0.210 \text{ l/s} \quad (\text{C-11})$$

### C.1.2 The Engelund-Hansen Sediment Transport Model

The Engelund-Hansen formula reads:

$$\Phi = \frac{0.1}{f} \theta^{5/2} \quad (\text{C-12})$$

The friction factor,  $f$ , is given as:

$$f = \frac{2gYI}{u^2} = 0.0122 \quad (\text{C-13})$$

The dimensionless bed shear stress,  $\theta$ , is given as:

$$\theta = \frac{DI}{(s-1)d} = 1.2626 \quad (\text{C-14})$$

The sediment transport is then:

$$S = \frac{0.1}{f} \theta^{5/2} \sqrt{(s-1)gd^3} = 0.305 \text{ l/s} \quad (\text{C-15})$$

The corresponding value calculated by MOUSE is:

$$S = 0.305 \text{ l/s} \quad (\text{C-16})$$

### C.1.3 The Engelund-Fredsøe Sediment Transport Model

The dimensionless bed load transport is calculated as:

$$\Phi_b = \frac{9.3 \cdot \pi}{6} (\sqrt{\theta'} - \sqrt{1/2} \sqrt{\theta_c}) = 4.6494 \quad (\text{C-17})$$

The various parameters are calculated below:

The friction velocity,  $u_f$ , is:

$$u_f = \sqrt{gYI} = 0.0783 \quad (\text{C-18})$$

The dimensionless bed shear stress,  $\theta$ , is:

$$\theta = \frac{u_f}{(s-1)gd} = 1.2626 \quad (\text{C-19})$$

From the  $\theta-\theta'$  relation  $\theta'$  it is found that:

$$\theta' = \theta = 1.2626 \quad (\text{C-20})$$

The number of surface particles per unit area which move is  $p/d$  where  $p$  is the probability for the particles to move:

$$p = \left\{ 1 + \left( \frac{\pi/6 \beta}{\theta' - \theta_c} \right)^4 \right\}^{-1/4} = 0.9984 \quad (\text{C-21})$$

where  $\beta$  is the dynamic friction coefficient, approx. equal to 0.65.

The bed load transport can now be found as:

$$q_b = \Phi_b \cdot \sqrt{(s-1)gd^3} = 0.097 \text{ l/s} \quad (\text{C-22})$$

The corresponding bed load transport calculated by MOUSE is:

$$q_b = 0.097 \text{ l/s}$$

The suspended load,  $q_s$ , is found as the integral of the current velocity,  $u(y)$ , and the concentration of suspended sediment,  $c(y)$ :

$$q_s = \int_a^Y cu \, dy \quad (\text{C-23})$$

where  $a$  is the thickness of the bed layer which can be approximated by  $2 \cdot d_{50}$ .

With known bed concentration,  $c_b$ , and settling velocity,  $w$ , the integral in Equation (C-23) can for instance be evaluated by use of the diagram presented by Deigaard (1980), see Figure C.1. The parameters in the diagram are:

$$\frac{d}{Y} = 0.3E-3 \quad (\text{C-24})$$

and

$$z = \frac{u_f}{\kappa w} = 1.4019 \quad (\text{C-25})$$

and

$$\frac{\Phi_s}{c_b \sqrt{\theta}} \quad (\text{C-26})$$

where

Z is the Rouse number

$c_b$  is the concentration at the bed

$\Phi_s$  is the dimensionless suspended load transport

w is the settling velocity of the suspended material given by:

$$w = \frac{10 \cdot v}{d} \left[ \sqrt{1 + \frac{0.01 \cdot (s-1) g d^3}{v^2}} - 1 \right] = 0.0439 \quad (\text{C-27})$$

The bed concentration,  $c_b$ , at a distance  $y = 2 \cdot d$  from the bed is given as:

$$c_b = \frac{0.65}{(1 + 1/\lambda_b)^3} = 0.2808 \quad (\text{C-28})$$

The linear concentration,  $\lambda_b$ , is related to  $c_b$  by:

$$\lambda_b = \sqrt{\frac{\theta - \theta_c - \pi/6 \beta p}{0.027 \cdot S \cdot \theta}} = 3.0976 \quad (\text{C-29})$$

From the diagram, the parameter for the suspended load can be found to be:

$$\frac{\Phi_s}{c_b \sqrt{\theta}} = 60 \quad (\text{C-30})$$

which gives the suspended load:

$$q_s = 60 \cdot c_b \cdot \sqrt{\theta} \cdot \sqrt{(s-1)gd^3} = 0.396 \text{ l/s} \quad (\text{C-31})$$

The corresponding suspended load transport calculated by MOUSE is:

$$q_s = 0.394 \text{ l/s}$$

It can be seen there is a small deviation in the suspended load calculated from the analytical solution and the calculation carried out by MOUSE. This is expected as the analytical calculation is based on a chart.

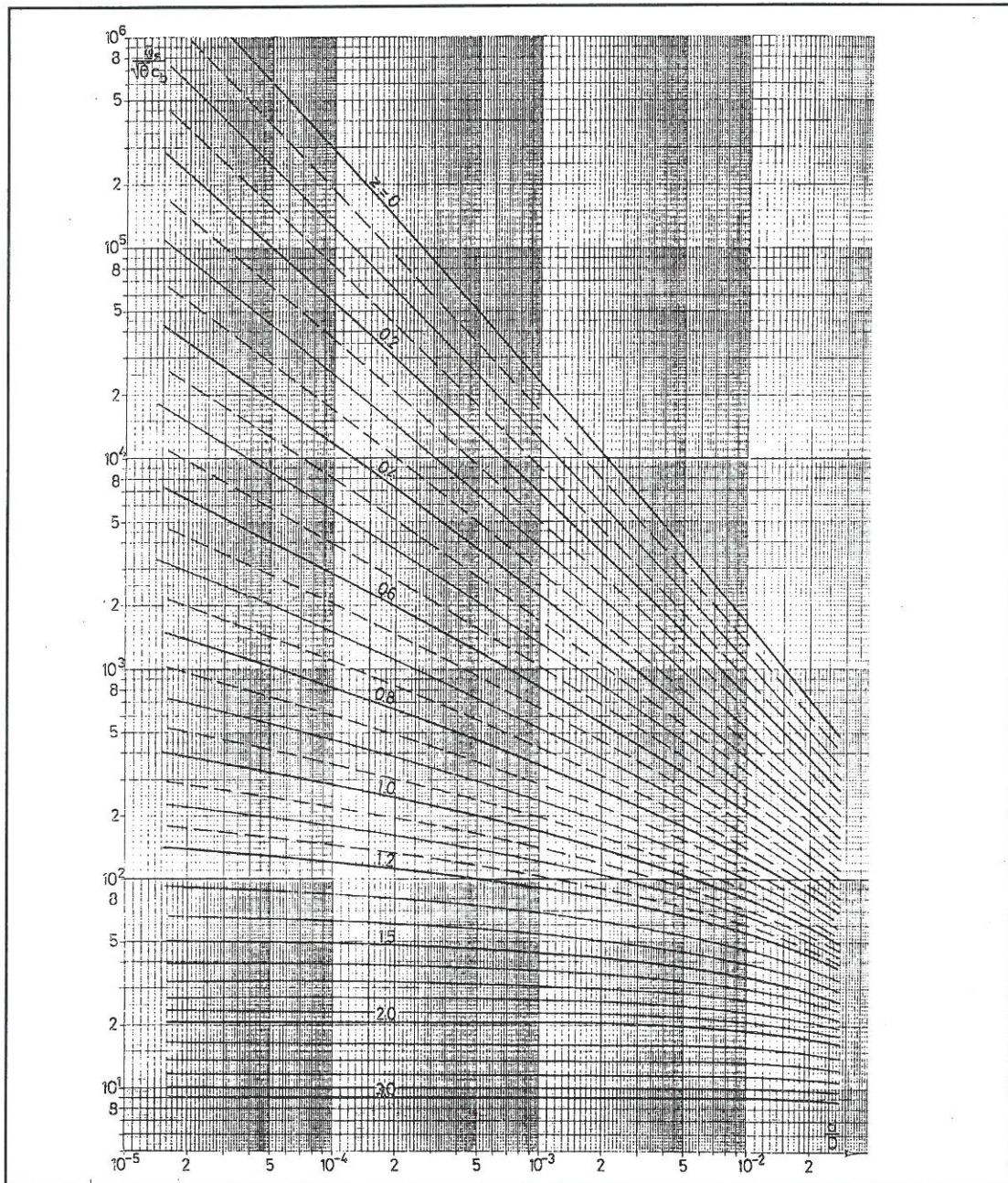


Figure C.1. Chart for calculation of suspended load in the Engelund-Fredsoe formula, (Deigaard 1980).



#### C.1.4 The van Rijn Sediment Transport Model

The bed load transport is calculated as:

$$\Phi_b = \frac{0.053 T^{2.1}}{D_*^{0.3}} \quad (\text{C-32})$$

or in a dimensionless form:

$$\frac{q_b}{\sqrt{(s-1)gd^3}} = \frac{0.053 T^{2.1}}{D_*^{0.3}} \quad (\text{C-33})$$

The various parameters in the van Rijn formula are calculated below:

The dimensionless particle diameter,  $D_*$ , is given as:

$$D_* = d \left[ \frac{(s-1)g}{v^2} \right]^{1/3} = 7.5888 \quad (\text{C-34})$$

The critical bed shear velocity,  $u_{f cr}$ , is given by:

$$u_{f cr} = \sqrt{\theta_c (s-1)gd} = 0.0165 \quad (\text{C-35})$$

and the effective bed shear velocity,  $u_f'$ , is:

$$u_f' = \frac{u\sqrt{g}}{C'} = 0.0455 \quad (\text{C-36})$$

where  $C'$  is the Chézy coefficient related to grain roughness given by:

$$C' = 5.75\sqrt{g} \text{ Log} \left( \frac{12R_b}{k_s} \right) = 68.8304 \quad (\text{C-37})$$

and  $R_b$  is the hydraulic radius related to the bed, here  $R_b = 1$  meter. van Rijn assumed the grain roughness height,  $k_s$ , of a plane movable bed to be  $3 \cdot d_{90}$ . In formula (C-37)  $k_s$  has been approximated by  $2 \cdot d$ . The dimensionless transport stage parameter,  $T$ , can now be calculated as:

$$T = \frac{(u_f')^2 - (u_{f cr}')^2}{(u_{f cr}')^2} = 6.6146 \quad (\text{C-38})$$

The bed load transport is now found from equation (C-33) to be:

$$q_b = 0.032 \text{ l/s}$$

The corresponding bed load transport calculated by MOUSE is:

$$q_s = 0.032 \text{ l/s}$$

The computation of suspended load transport is based on the solution of the integral:

$$q_s = \int_a^y c u dy \quad (\text{C-39})$$

van Rijn calculates the suspended load to be:

$$q_s = F u Y c_a \quad (\text{C-40})$$

The various parameters are calculated below. The calculation of the suspended load is based on the computation of a reference concentration determined from the bed load transport. The reference concentration,  $c_a$ , is given as:

$$c_a = 0.015 \frac{d_{50}}{a} \frac{T^{1.5}}{D_*^{0.3}} = 4.168E-3 \quad (\text{C-41})$$

with the minimum roughness height,  $a$ , given as:

$$a = 0.01 Y = 0.01 \text{ m} \quad (\text{C-42})$$

The suspension number,  $Z$ , is calculated as:

$$Z = \frac{w}{\beta \kappa u_f} = 0.8607 \quad (\text{C-43})$$

$\beta$  is a ratio of the sediment diffusion and fluid diffusion coefficient calculated as:

$$\beta = 1 + 2 \left[ \frac{w}{u_f} \right]^2 = 1.6290 \quad (\text{C-44})$$

$Z'$  is the modified suspension number given as :

$$Z' = Z + \psi = 1.0695 \quad (\text{C-45})$$

where the overall correction factor,  $\psi$ , represents all additional effects (volume occupied by particles, reduction of fall velocity and damping of turbulence).  $\psi$  is given as:

$$\psi = 2.5 \left[ \frac{w}{u_f} \right]^{0.8} \left[ \frac{c_a}{c_o} \right]^{0.4} = 0.2088 \quad (\text{C-46})$$

where  $c_o = 0.65$ , is the maximum bed concentration.

The correction factor for suspended load,  $F$ , is given as:

$$F = \frac{\left[ \frac{a}{Y} \right]^{Z'} - \left[ \frac{a}{Y} \right]^{1.2}}{\left[ 1 - \frac{a}{Y} \right]^{Z'} [1.2 - Z']} = 0.0254 \quad (\text{C-47})$$

The suspended load can now be calculated as:

$$q_s = FuYc_a = 0.106 \text{ l/s} \quad (\text{C-48})$$

The corresponding suspended load transport calculated by MOUSE is:  $q_s = 0.106$  l/s.

### C.1.5 Summary

The sediment transport models implemented in MOUSE are in agreement with the theoretical calculation of the sediment transport from the four sediment transport formulae. It must be noticed that these four well established sediment transport

formulae give quite different results for this simple test case with steady state hydrodynamics. The maximum difference is found between the Engelund-Fredsoe and the van Rijn formula where the Engelund-Fredsoe formula gives a factor of 3.6 times more sediment transport than the van Rijn formulation.

## C.2 Test of Independency of the Flow Direction in the Pipe

The purpose of the test is to show that the sediment transport calculation is independent of the flow direction in the pipe. The simulation was carried out with the following data:

a square pipe with a length of	: 1000 m
pipe width	: 10 m
sediment depth in the pipe	: 1.0 m
grain diameter	: 0.1 mm

upstream boundary conditions:

discharge	: 10 m <sup>3</sup> /s
constant bed level of	: 2.0 m

downstream boundary conditions:

water level	: 1.5 m
-------------	---------

The simulation was first carried out with flow in the positive direction of the pipe, secondly the positive direction of the flow was reversed in the pipe and the simulation was carried out again. The results of the simulation can be seen in Figure C.2. It can be seen that the sediment transport in the middle of the pipe has the same numerical value but with the opposite sign. Further, the development of the bottom level is exactly the same for the two simulations. It can be concluded that the sediment transport calculation is independent of the flow direction.

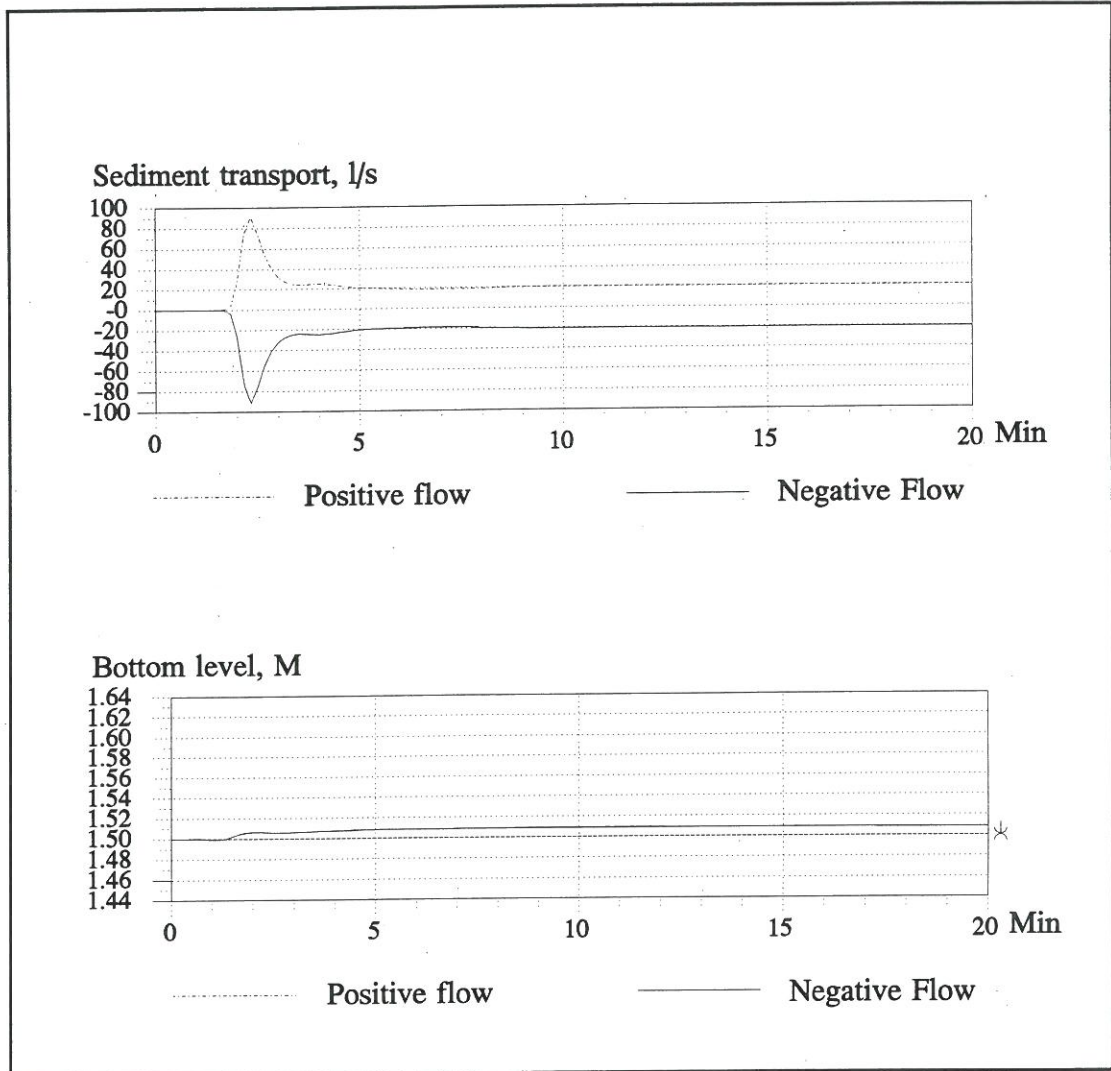


Figure C.2. The sediment transport and the bed level for simulations with a different definition of the positive flow direction in a pipe.

### C.3 Test of the Formulation for Graded Sediment

The purpose of the test is to show that the calculation of the sediment transport with the graded sediment transport model is correct. The simulation is carried out with two sediment fractions where both of the sediment fractions have the same grain diameter. The sediment transport and the morphological changes should be exactly the same as in the previous test with uniform sediment. The data for the simulation are the same as in the previous test plus the following data:

Sediment data:

Grain sizes:

Fraction no. 1 : 0.1 mm

Fraction no. 2 : 0.1 mm

The active layer:

Fraction no. 1 : 40 %

Fraction no. 2 : 60 %

The passive layer:

Fraction no. 1 : 40 %

Fraction no. 2 : 60 %

Upstream boundary conditions:

a constant bed level of 2.0 m, with 40 % of fraction no.1 and 60 % of fraction no. 2.

The results of the simulation can be seen in Figures C.3 and C.4. It can be seen that the total sediment transport and the changes in bed level are exactly the same as for uniform sediment. Further, it can be seen from Figures C.3 and C.4, that the composition of the bed does not change and that the sediment transport of fraction no.1 is 40 % of the total sediment transport and the sediment transport of fraction no. 2 is 60 % of the total sediment transport. It can be concluded that the graded sediment transport model calculate the transport for the individual fractions correctly.

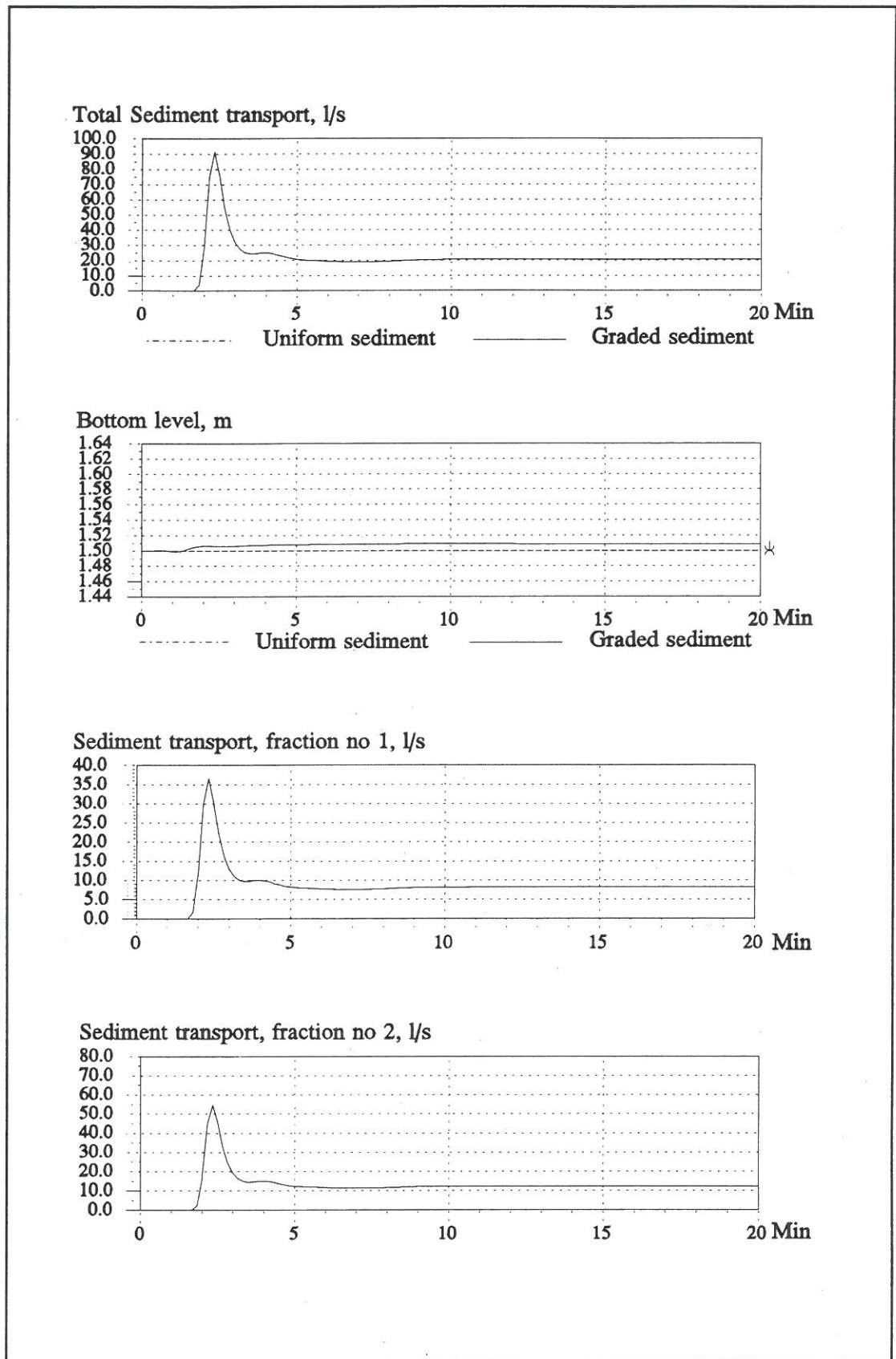


Figure C.3. Comparison between the graded sediment transport model and the sediment transport model with uniform sediment.

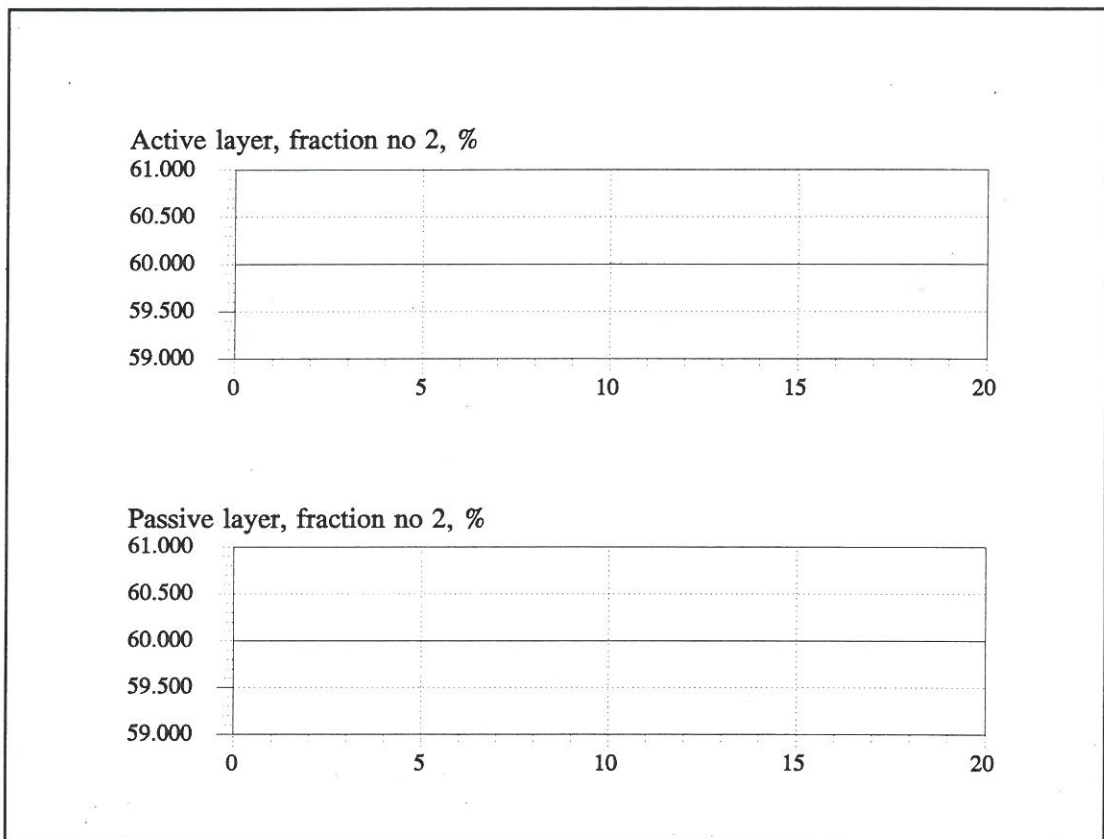
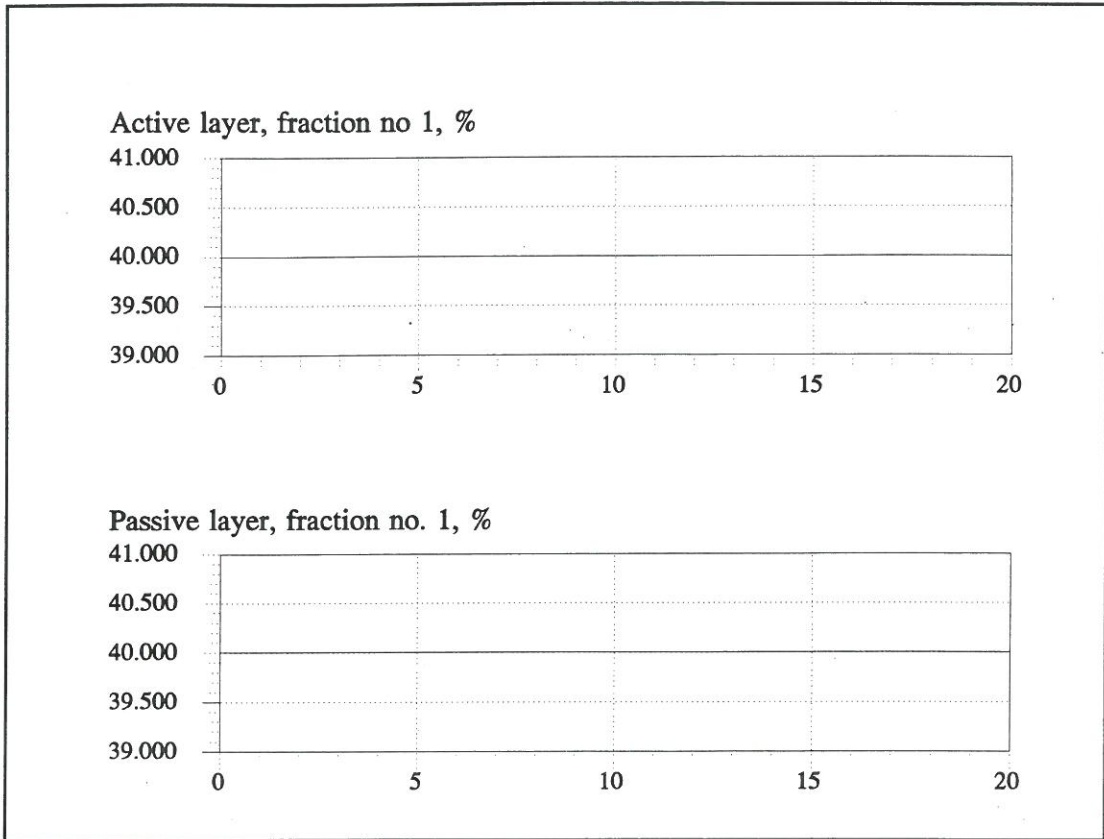


Figure C.4. The percentages of the sediment fractions calculated by the graded sediment transport model.



**D. SENSITIVITY ANALYSIS OF THE INFLUENCE OF THE  
CRITERION FOR THE INITIATION OF MOTION**

**APPENDIX D**

**Sensitivity Analysis of the Influence  
of the Criterion for the Initiation  
of Motion on the Sediment Transport**

## **D SENSITIVITY ANALYSIS OF THE INFLUENCE OF THE CRITERION FOR THE INITIATION OF MOTION ON THE SEDIMENT TRANSPORT**

As the experimental data were in the range close to the critical bed shear stress and the Ackers-White, the Engelund-Fredsoe and the van Rijn theory give the sediment transport as a function of the criteria for the initiation of motion a sensitivity analysis was carried out to investigate the sensitivity of the sediment transport predicted by these theories as a function of the criteria for the initiation of motion. The sensitivity analysis show that the Engelund-Fredsoe and the van Rijn formulae give 1.5-3 times more sediment transport for a decrease in the critical bed shear stress of 10 %. The Ackers-White formula gives approximately 4 times more sediment transport for a decrease of 10 % in the critical bed shear stress.

### **D.1 The Ackers-White Sediment Transport Model**

The sensitivity analysis was carried out on the critical mobility number: "a". It was found from the paper by Ackers and White, 1973, that the variation of "a" could be as much as 10%. A 10% reduction in the criterion for the initiation of motion gave 1.5 -110 times higher sediment transport rates with an average of 4 times when the extreme cases were neglected. The sediment transport with a 10% reduction in "a" is shown in Figure D.1. It can be seen that a much better agreement between the measured and the simulated sediment transport rates is achieved when the criterion for initiation of motion, "a", is reduced by 10%.

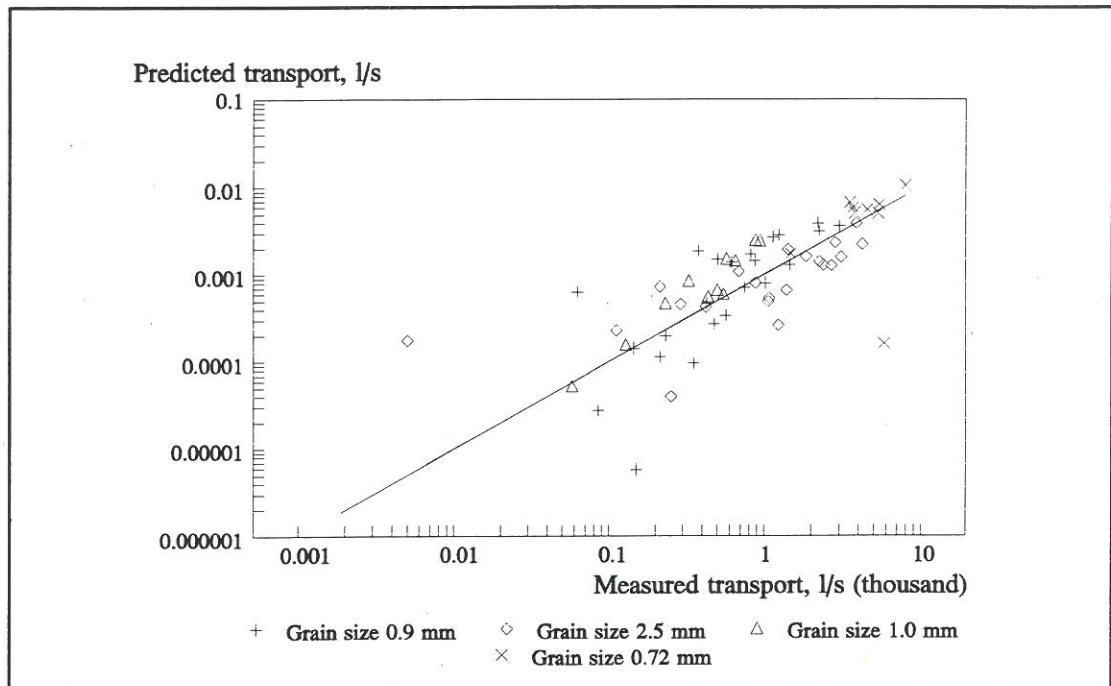


Figure D.1. The sediment transport simulated by the Ackers-White theory with a 10 % reduction in the criterion for initiation of motion.

## D.2 The Engelund-Fredsoe Sediment Transport Model

The sensitivity analyses were carried out on the critical bed shear stress which was reduced by 10%. The 10% reduction of the critical bed shear stress gave up to 23 times more sediment transport with an average of 1.2 - 2 times when the extreme cases were neglected. The sediment transport rates for the theory with and without prediction of the bed shear stress with the reduced critical bed shear stress can be seen in Figure D.2 and D.3. It can be seen that the sediment transport rates in both cases generally are overestimated.

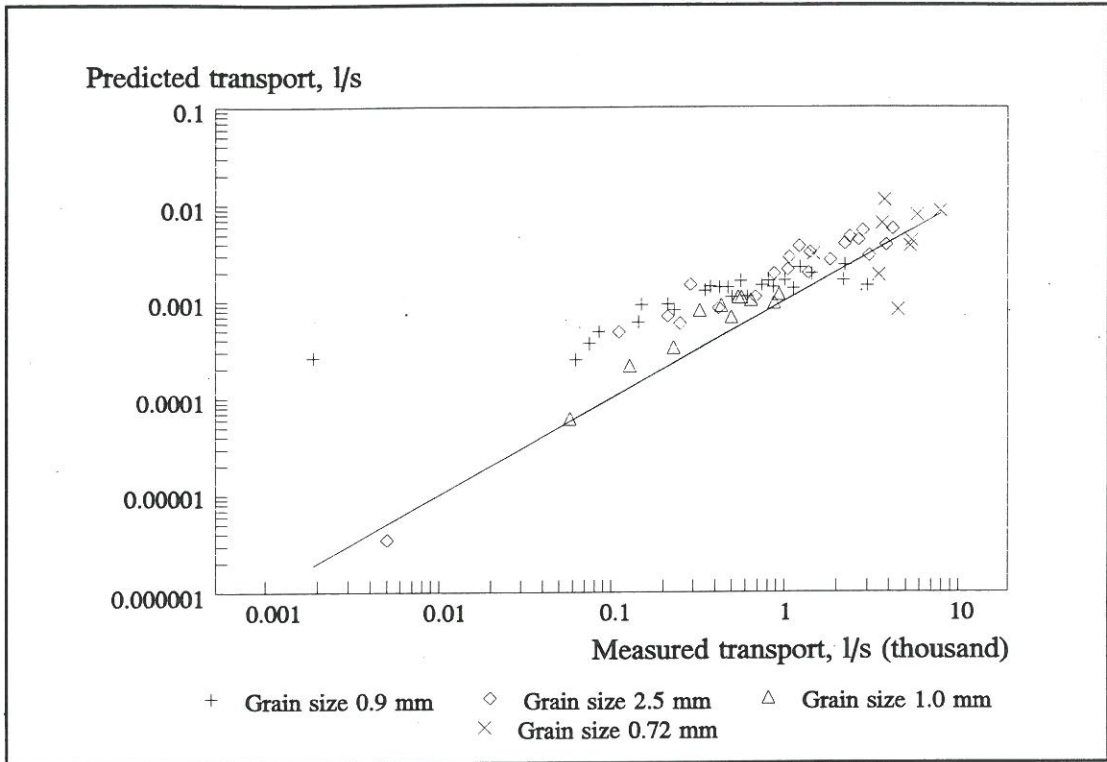


Figure D.2. The sediment transport *without* prediction of the bed shear stress predicted by the Engelund-Fredsøe formula with a 10% reduction in the critical bed shear stress.

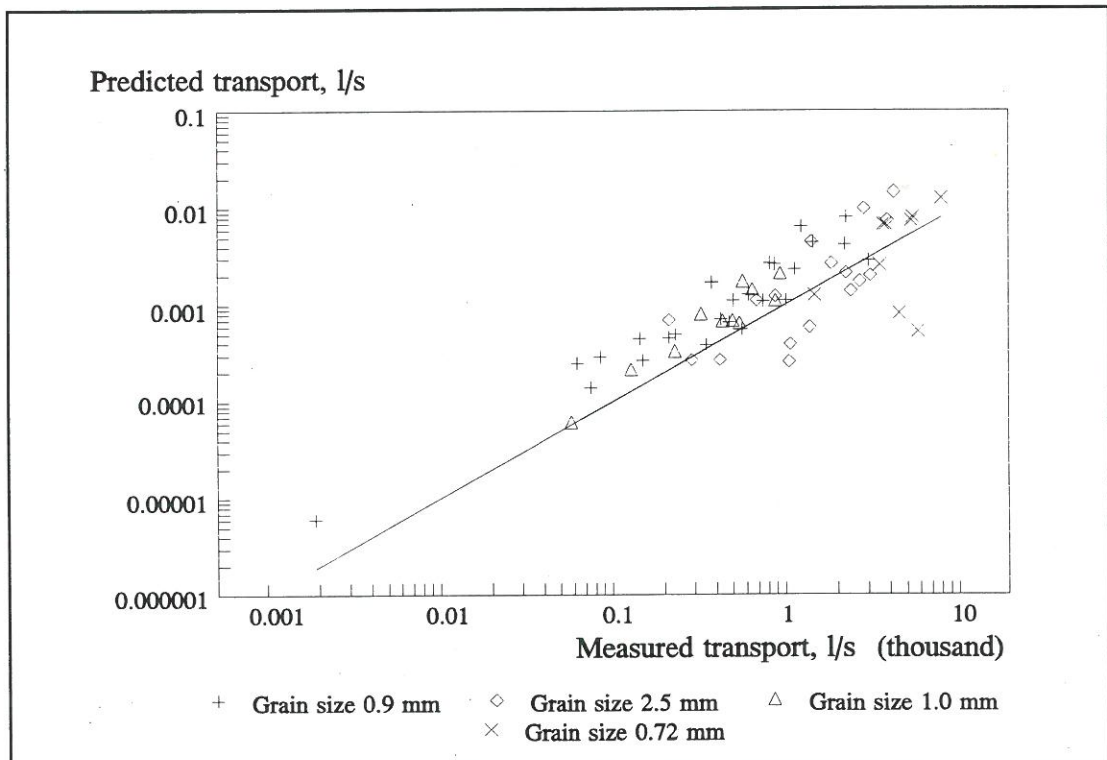


Figure D.3. The sediment transport *with* prediction of the bed shear stress predicted by the Engelund-Fredsøe formula with a 10% reduction in the critical bed shear stress.

### D.3 The van Rijn Sediment Transport Model

The sensitivity analysis was carried out on the critical bed shear stress which was reduced by 10%. The sediment transport based on the reduced critical bed shear stress can be seen in Figure D.4. The sensitivity analysis showed that the sediment transport on the average was increased by a factor of 1.5 - 3. The sediment transport rates are overestimated for the small grain sizes and the sediment transport rate for the 2.5 mm grain size is closer to the observed values but is still underestimated.

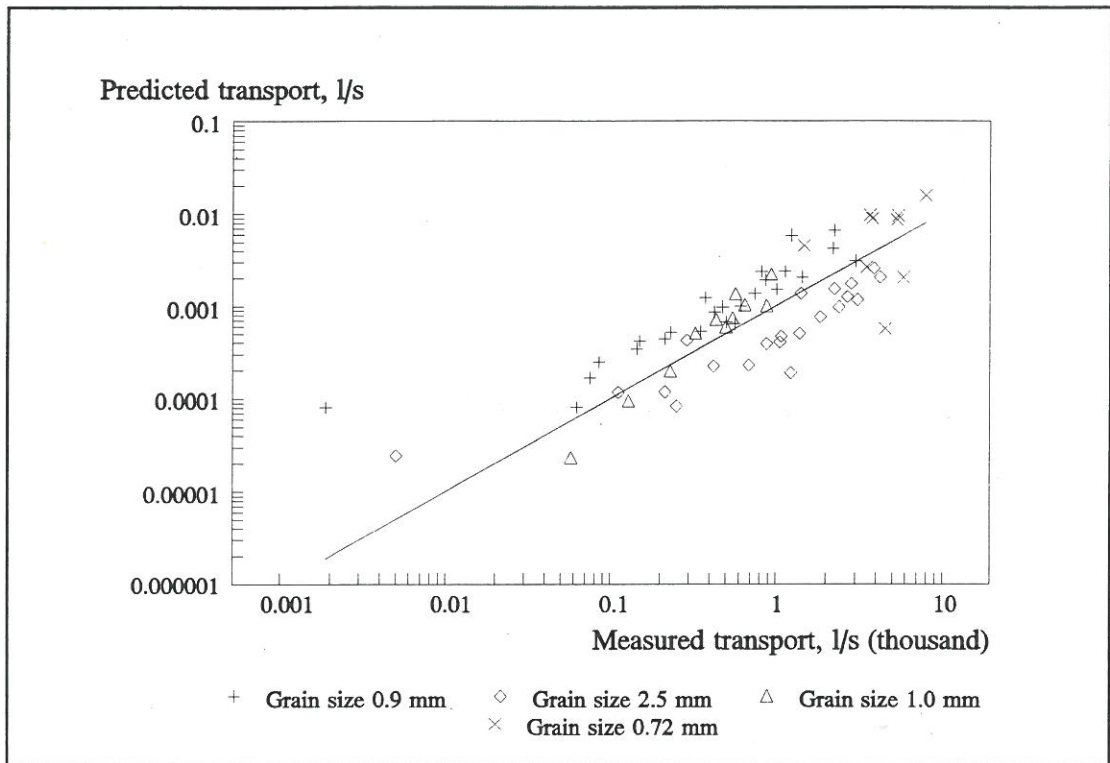


Figure D.4. The sediment transport predicted by the van Rijn formula with a 10% reduction in the critical bed shear stress.